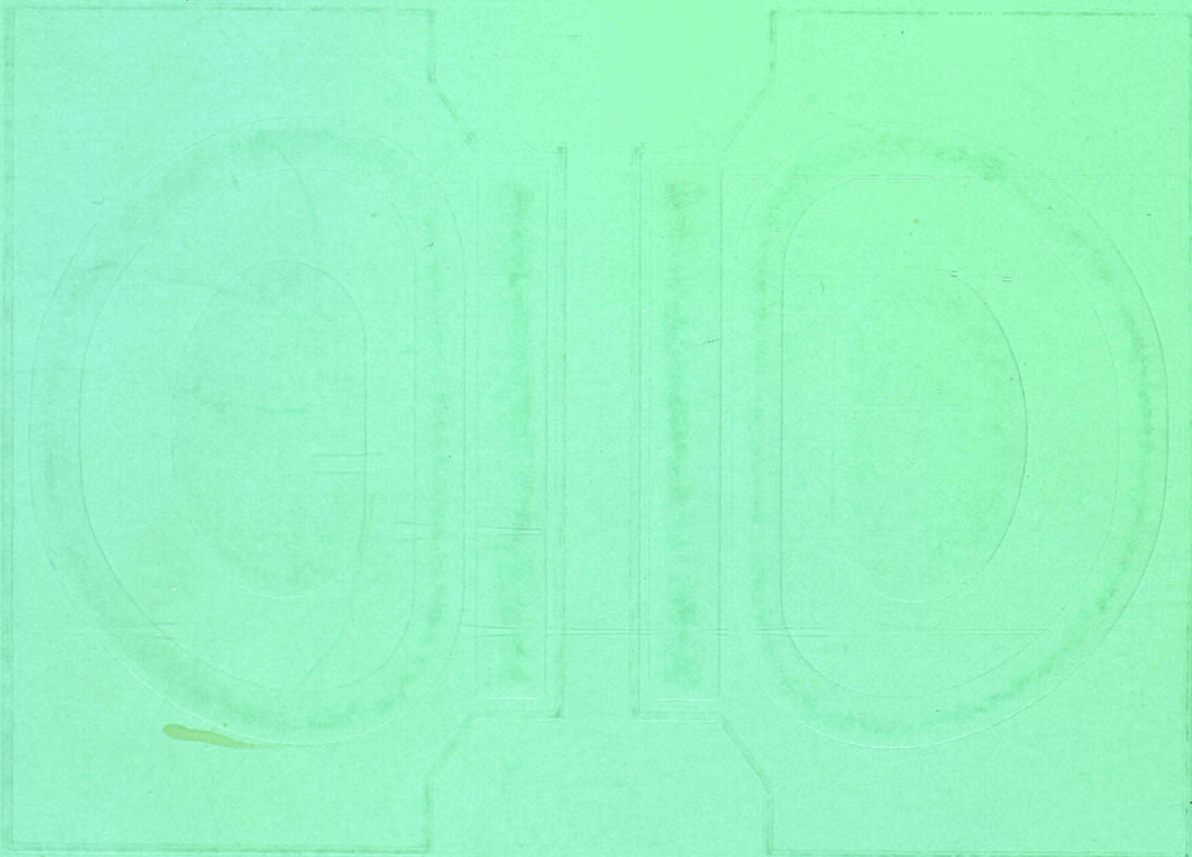


JOINT EUROPEAN TORUS

JET

**JET
JOINT
UNDERTAKING**

**PROGRESS
REPORT 1984**



MI 50676

33

✓
EUR 10223 EN
EUR-JET-PR2

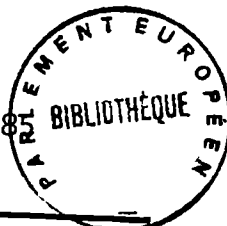
JET JOINT UNDERTAKING

PROGRESS REPORT 1984

Num Doc. 30.382

PARL. EUROP. Biblioth.
N.C. EUR [✓] 10223
C1.

SEPTEMBER 1985



PARL. EUROP. Biblioth.
N.C. EUR
CL

*This document is intended for information only and
should not be used as a technical reference.*

EUR 10223 EN (EUR-JET-PR2) September 1985
Editorial work on this report was carried out by B.E. Keen and P. Kupschus
The preparation for publication was undertaken by
the Documentation Service Units, Culham Laboratory.

© Copyright ECSC/EEC/EURATOM, Luxembourg 1985.
Enquiries about copyright and reproduction should be addressed to:
The Publications Officer, JET Joint Undertaking, Abingdon, Oxon. OX14 3EA, England

Printed in England

Contents

Introduction, Background and Report Summary	1
Summary of Technical and Scientific Achievements during 1984	5
– Introduction	5
– Technical Achievements	5
– Scientific Results	8
JET – Operations and Development	13
– Introduction	13
– Operations and Development Directorate	16
– Torus Division	18
– Power Supply Division	39
– Control and Data Acquisition System (CODAS) Division	49
– Neutral Beam Heating Division	55
– Radio Frequency Heating Division	68
– Fusion Technology Division	81
JET – Scientific	91
– Introduction	91
– Scientific Directorate	95
– Experimental Division 1	100
– Experimental Division 2	121
– Theory Division	140
Appendices	153
1 Task Agreements	153
2 Articles, Reports and Conference Papers Published, 1984	155

Foreword

This second JET Progress Report covers the first full year of JET's operation. It provides a more detailed account of JET's scientific and technical progress throughout 1984 than that contained in the JET Annual Report. However, it is anticipated that it will interest a wider scientific and technical audience than the members of the Joint Undertaking. Therefore, its presentation is aimed not only at specialists and experts engaged in nuclear fusion and plasma physics, but also at a more general scientific community.

To assist in meeting these general aims, the Report contains a brief summary of the background to the Project, describes the basic objectives of JET and the principal design aspects of the machine. A further section sets out an overview of progress on JET during 1984 and a survey of scientific and technical activities during the year sets these advances in their general context. The body of the report describes in more detail the activities of the Operation and Development Department in operating and maintaining the tokamak and in developing equipment to enhance the machine for full performance and of the Scientific Department in specifying, procuring and operating the diagnostic equipment, and in executing the experimental programme and interpreting results.

1984 saw further considerable achievements for the Project in the first full year of operation. The major objective was to reach and then consolidate the design performance of the machine in its basic configuration with ohmic heating only. This objective was more than fulfilled. Plasma currents of up to 3.7MA were obtained for several seconds within overall pulse lengths of 15 seconds. Plasma temperatures of 3 keV, densities of $3.5 \times 10^{19} \text{ m}^{-3}$ and a record energy confinement time of 0.8 seconds were achieved. These results established JET as the leading tokamak in the world. The performance of the machine is now being extended,

principally by the addition of neutral beam and radio frequency heating systems. During a scheduled shutdown period in late 1984, the first radio frequency antenna/generator units were installed and commissioned successfully. Further diagnostic systems were also introduced during this shutdown.

The year inevitably brought some problems. The level of impurities in the plasma was higher than anticipated; steps were taken to reduce this level by coating the inside of the vacuum vessel with carbon. Also, unexpected vertical disruptions of the plasma occurred, one of which was of particular concern as it resulted in substantial forces being transmitted to the vacuum vessel which, if repeated, could cause serious damage to the vessel. Modifications to the vessel supports and to feedback control systems have since been introduced. Furthermore, the neutral beam heating programme suffered delays due to welding problems with some highly stressed components. Following design changes to certain high heat load dissipating elements, the assembly of the first beamline system was brought close to completion.

The successful construction of the device and the encouraging results obtained to date are a tribute to the dedication and skill of all who work on the Project. They also reflect the continuous and growing co-operation and multi-faceted assistance received from the Associated Laboratories and from the Commission of the European Communities. They support the confidence and guidance given to the management of the project by the JET Council, JET Executive Committee and JET Scientific Council.

I have no doubt that with such devotion from all sides, the Project will face the many problems and challenges that will be encountered in the future with confidence.

P. H. Rebut
September 1985

Dr Hans-Otto Wüster

During the final preparation and printing of this Report, it was with shock, great sadness and regret that the Project learned of the sudden and untimely death, on 30th June 1985, of Dr Hans-Otto Wüster, the Director of the JET Joint Undertaking. His contribution to the formation and success of the Project to this date was immense. His energy, leadership and infectious enthusiasm were qualities recognised by all of the members of JET and the tributes to his memory which have come from all over the world bear testimony to this. Fusion in Europe and the world has lost a great man, but, above all, everyone within the JET Project has lost a great friend.

In June 1978, Hans-Otto joined JET as its Director, from CERN in Geneva. The Project has brought together the skills of staff from twelve nations and required leadership of outstanding qualities—diplomatic, technical and political. In retrospect, it is difficult to accept that anyone was better equipped to

provide these talents. It was his leadership and tremendous enthusiasm and drive which have contributed substantially to JET's pre-eminent position in the fusion world. Although latterly, JET became the whole centre of his life, he carried a huge pride in the concept of Europe and its embodiment in JET and CERN.

He will be sadly missed by his many friends inside and outside the Project. He will be remembered for his strong managerial style—generous with praise, scornful of bureaucracy and forceful in debate. He seemed to know everyone by name and treated each one as an individual. He was a big man in every way with a personality to match. He will be missed for many reasons, not least for his loud deep resonant bass voice echoing along the corridors.

The greatest tribute that we can pay to his memory is to strive with renewed vigour to ensure that JET continues to be the world's leading fusion experiment.

Introduction, Background and Report Summary

Introduction

Following the formal start of the Operation Phase of the JET Project in June 1983, it was decided to produce an annual JET Progress Report which should provide a more detailed account of JET's scientific and technical activities than that which was provided in the JET Annual Report. The first JET Progress Report (EUR-JET-PR1) described activities and advances up to the end of 1983. This second Report (EUR-JET-PR2) describes progress made to the end of 1984, and, again, concentrates mainly on scientific and technical activities in the Operations and Development Department (ODD) and the Scientific Department.

For completeness, this chapter contains a brief summary of the background to the Project. It describes the basic objectives of JET and the principal design aspects of the machine. In addition, the Project Team structure is included, within which the activities and responsibilities for machine operation are carried out and in which the scientific programme is executed.

Background

Objectives of JET

The Joint European Torus (JET) is the largest single project of the nuclear fusion research programme of the European Atomic Energy Community (EURATOM). The project was designed with the essential objective of obtaining and studying plasma in conditions and with dimensions approaching those needed in a fusion reactor. The studies are aimed at:

- a) investigating plasma processes and scaling laws, as plasma dimensions and parameters approach those necessary for a fusion reactor;
- b) examining and controlling plasma-wall interactions and impurity influxes in near-reactor conditions;
- c) demonstrating effective heating techniques, capable of approaching reactor temperature in JET, in the presence of the prevailing loss processes (particularly, RF and Neutral Beam Heating processes);
- d) studying alpha-particle production, confinement and subsequent plasma interaction and heating produced as a result of fusion between deuterium and tritium.

Two of the key technological issues in the subsequent development of a fusion reactor should be faced for the first time in JET. These are the use of tritium and the application of remote maintenance and repair techniques. The physics basis of the post-JET programme will be greatly strengthened if other fusion experiments currently in progress are successful. The way should then be clear to concentrate on the engineering and technical problems involved in progressing from an advanced experimental device like JET to a prototype power reactor.

Basic JET Design

To meet these overall aims, the basic JET apparatus was designed as a large tokamak device with overall dimensions of about 15m in diameter and 12m in height. A diagram of the apparatus is shown in Fig.1 and its principal parameters are given in Table.I. At the heart of the machine, there is a toroidal vacuum vessel of major radius 2.96m having a D-shaped cross-section 2.5m wide by 4.2m high. During operation of the machine, a small quantity of gas (hydrogen, deuterium or tritium) is introduced into the vacuum chamber and is heated by passing a large current (up to 3.8MA during the initial phase, and up to 4.8MA during the full design phase) through the gas. This current is produced by transformer action using the massive eight-limbed magnetic circuit, which dominates the apparatus (see Fig.1). A set of coils around the centre limb of the magnetic circuit forms the primary winding of the transformer with the hot gas or 'plasma' acting as the single turn secondary. Subsequently, additional heating of the plasma will be provided by injecting beams or energetic neutral atoms into the system and by the use of high power radio frequency waves.

The plasma is confined away from the walls of the vacuum vessel by a complex system of magnetic fields, in which the main component, the toroidal field, is provided by 32 D-shaped coils surrounding the vacuum vessel. This field, coupled with that produced by the current flowing through the plasma, forms the basic magnetic field for the tokamak confinement system, which

provides a field at the centre of 2.8T in the initial phase, rising to 3.45T during the full design phase. The poloidal coils, positioned around the outside of the vacuum vessel, shape and position the plasma in operation.

Initial experiments have been undertaken using hydrogen and deuterium plasmas, but in the later stages of the operation, it is planned to operate with deuterium-tritium plasmas, so that fusion reactions can occur.

In order to reach conditions close to those relevant to a fusion reactor, a plasma density of 10^{20}m^{-3} at a temperature of 10keV would be needed. Even with a current of 4.8MA in JET, this would be inadequate to provide the temperature required using ohmic heating alone. Consequently, additional heating will be required and two main systems will be added to JET over the coming years, as follows:

- Injection into the plasma of highly energetic neutral atoms (Neutral Injection heating) and
- Coupling of high power electromagnetic radiation to the plasma (Radio Frequency (RF) heating).

The total power into the plasma will increase in discrete steps up to 25MW.

Project Team Structure

To undertake machine operation and to execute the scientific programme during the Operations Phase of the Project, the Team Structure adopted for management purposes was divided between three Departments, as follows:

- (i) Operation and Development Department;
- (ii) Scientific Department;
- (iii) Administration Department.

The main duties of the Administration Department have been described in previous JET Annual Reports. This Report concentrates on the scientific and technical progress made in the Scientific and the Operation and Development Departments during 1984. The responsibilities of these Departments are described below.

J
E
T
EUROPEAN
TORUS

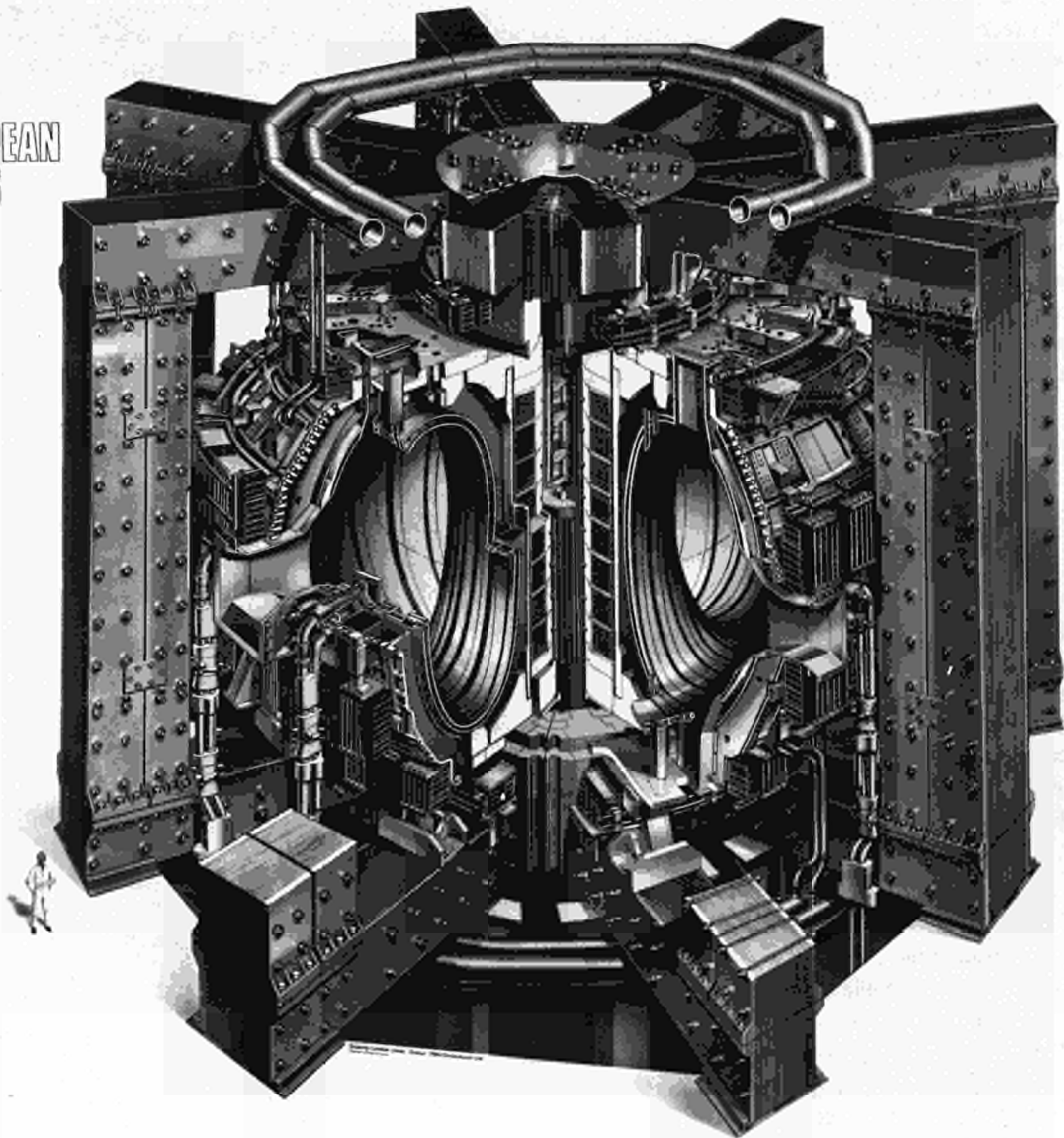


Fig.1: Diagram of the JET Tokamak

Table 1: Principal JET Parameters.

Parameter	Value
Plasma minor radius (horizontally), a	1.25m
Plasma minor radius (vertically), b	2.10m
Plasma Major radius, R_0	2.96m
Plasma aspect ratio, R_0/a	2.37
Plasma elongation ratio, $e=b/a$	1.68
Flat top pulse length	10s
Toroidal magnetic field (plasma centre)	3.45T
Plasma current, circular plasma	3.2MA
D shaped plasma	4.8MA
Volt-seconds available	34Vs
Toroidal field peak power	380MW
Poloidal field peak power	300MW
Additional heating power (in plasma)	25MW
Weight of vacuum vessel	108t
Weight of toroidal field coils	384t
Weight of iron core	2800t

Operation and Development Department

The Operation and Development Department is responsible for the operation and maintenance of the tokamak and for developing the necessary engineering equipment to enhance the machine to its full performance. The Department contains six Divisions:

- (1) Torus Division, which is responsible for the operation of the Torus, including the creation and training of the operating team and the organisation and execution of maintenance work in the Torus Hall and Basement. The Division also organises major shutdowns for the installation and commissioning of new equipment and for development work necessary for improvement of sub-systems integrated into the JET device (vacuum system, baking and cooling plants, limiters, first wall, etc.).
- (2) Power Supply Division, which is responsible for the design, installation, operation, maintenance and modification of all power supply equipment needed by the Project.
- (3) Control and Data Acquisition System Division (CODAS), which is responsible for the implementation, upgrading and operation of computer-based control and data acquisition systems for JET.
- (4) Neutral Beam Heating Division, which is responsible for the construction, installation, commissioning and operation of the neutral injection system, including development towards full power operation of the device. The Division also participates in studies of the physics of neutral beam heating.
- (5) Radio Frequency Heating Division, which is responsible for the design, construction, commissioning and operating the RF heating

system during the different stages of its development to full power. The Division also participates in studies of the physics of RF heating.

- (6) Fusion Technology Division, which is responsible for the design and development of remote handling methods and tools to cope with the requirements of the JET device, and for maintenance, inspection and repairs. Tasks also include design and construction of facilities for the handling of tritium.

Scientific Department

The Scientific Department is responsible for definition and execution of the experimental programme, the specification, procurement and operation of diagnostic equipment and interpretation of experimental results. The Department contains three Divisions:

- (1) Experimental Division 1 (ED1), which is responsible for specification, procurement and operation of approximately half the JET diagnostic systems. ED1 undertakes electrical measurements, electron temperature measurements, surface and limiter physics and neutron diagnostics.
- (2) Experimental Division 2 (ED2), which is responsible for specification, procurement and operation of the other half of the JET diagnostic systems. ED2 undertakes all spectroscopic diagnostics, bolometry, interferometry, the soft X-ray array and neutral particle analysis.
- (3) Theory Division, which is responsible for prediction by computer simulation of JET performance, interpretation of JET data and the application of analytic plasma theory to gain an understanding of JET physics.

The Divisions are also involved in:

- Execution of the experimental programme.
- Interpretation of results in collaboration with appropriate Divisions and the Operations and Development Department.
- Making proposals for future experiments.

Report Summary

Chapter 1 of this Report provides a brief introduction and some background information relevant to the Report. Chapter 2 sets out an overview of progress on JET during 1984 and, with a survey of scientific and technical achievements during 1984, sets these advances in their general context.

In Chapter 3, the activities and progress within the Operation and Development Department are set out; particularly relating to its responsibilities for the operation and maintenance of the tokamak and for developing the necessary engineering equipment to enhance the machine to full performance. This is

described in detail for each Group within the Divisional structure of this Department.

In Chapter 4, the activities and progress within the Scientific Department are described; particularly, relating to the specification, procurement and operation of diagnostic equipment; definition and execution of the programme; and the interpretation of experimental results. Again, this is set out in detail within the Group structure of the Department.

Summary of Technical and Scientific Achievements during 1984

Introduction

In order to provide an overview of progress on JET and to set these advances into context, a summary of technical and scientific achievements during 1984 is included. The main details of this progress is included in later chapters described within the sections on activities of each individual Division.

During 1984, a major technological aim was to reach and then to consolidate the full performance of the operational equipment, and this was generally achieved. A further aim was to improve equipment, where operational experience had shown it to be necessary or advantageous. The major scientific aim was to continue the promising ohmic heating campaign of 1983 in establishing operating conditions for clean hydrogen and deuterium plasmas suitable for the additional heating studies of later phases. Important elements of this work involved studies of conditions necessary to achieve stable control of plasma position, size and shape; to control the influx of impurities; and to determine the conditions for disruption-free discharges. Implicit in this programme was extension of machine performance towards the highest possible currents and fields consistent with freedom from hard disruptions.

JET was in operation as a Tokamak for 17 weeks during 1984. The remaining time was devoted to modifying the machine and to commissioning. Overall, about 500 plasma pulses were fired, of which the majority had plasma currents in excess of 1MA.

Technical Achievements

Vacuum Systems

The number of new systems directly connected to the main Torus vacuum increased considerably during the year. In January, the high vacuum rotary valve was welded to the port at Octant No.8, to isolate the box containing the neutral injector heating system from the main Torus. The valve is of a novel design and provides a large aperture by means of cylindrical rotor.

Many new diagnostics were also installed, and wherever possible, these were connected to the torus through conventional gate valves. In October, the first

two RF antennae and their pumping systems were also installed. By the year's end, there were about 200 sealed and 150 welded flanges for attaching equipment to the vessel. These numbers illustrate the complexity of the vacuum system and the difficulties associated with leak testing. Even so, leak testing and repairing did not delay the operating programme.

The procedure used to restore clean vacuum conditions after a shutdown, involving assembly work inside the vessel, has become a well established and effective routine. The vessel is first carefully cleaned and washed using high pressure water jets. Following drying by mild baking under vacuum, the final wall conditioning for plasma operation relies on full baking and glow discharge cleaning. The vessel is baked by circulating hot gas through the interspace of the double-walled structure. This process out-gasses the walls to ensure high vacuum conditions. During 1984 operations, the baking plant was used routinely to keep the vessel at a temperature between 200 and 300C, using a temporary blower and nitrogen as a heat carrying gas.

During the October shutdown, a new blower with a single stage radial turbo-compressor was installed to operate with helium to heat the vessel up to a temperature of 500C. Helium is not activated by neutrons and can be easily cleaned from contaminants, such as tritium, which may permeate through the first wall, in the active phase.

Glow discharge cleaning has proved to be a simple and yet powerful means to satisfactory restore wall conditions for plasma operation. By the end of the year, the effectiveness of glow discharges was further increased when two more electrodes were installed increasing the number of RF assisted electrodes to four.

Initially, it was decided that the tiles protecting the vacuum vessel bellows should also be made of Inconel. There are now indications that better plasma performances might be achieved, if only low-Z materials face the plasma. Consequently, it was decided to replace the Inconel tiles by graphite tiles on the inboard side of the vessel, where the most severe plasma-wall interactions take place. During the October shutdown, nearly one thousand tiles were fitted to cover the inboard wall over a 2m height.

Studies, originating from the vertical instability that occurred during Pulse No.1947, revealed that the vacuum vessel could potentially be subjected to large vertical forces during a disruption. With the existing

vessel supports these forces could have reached a dangerous level at plasma currents in excess of 4MA. Additional mechanical supports were fitted to restrain the vessel and damp the rocking motion set up by the vertical forces. These new supports include rigid vertical struts to link all main horizontal ports to the lower limbs of the magnetic circuit, and hydraulic dampers to connect all 16 main vertical ports to the mechanical structure.

The gas introduction system, which establishes the gas (hydrogen or deuterium) pressure for initiation of the discharge, and then provides the additional gas required to achieve the specified plasma density, uses fast valves which empty prefilled calibrated reservoirs into the vessel, and dosing valves which are computer controlled and bleed gas according to programmed waveforms. Feedback control of these dosing valves was introduced in September, whereby the gas feed is automatically controlled to achieve a specified plasma density.

Power Supplies

The peak electrical power required for JET during operational pulses can exceed 900MW. There are five principal loads, although their peaks are not simultaneous: the toroidal magnetic field with requirements up to 600MW, the ohmic heating circuit up to 300MW, the plasma position control up to 150MW, neutral injection up to 80MW, and RF heating up to 60MW.

As there are limits on the power that may be drawn directly from the grid, the base power for the toroidal magnetic field coils and for the ohmic heating circuit is provided by two large flywheel generators. Each of these identical vertical shaft generators is capable of delivering 400MW of peak power and 2600MJ of energy. Each rotor, weighing 775t, is accelerated between pulses by a 8.8MW pony motor to 225rpm. During operation, the rotor windings are energised, the rotational energy of the flywheel is converted into electrical energy and the rotor slows down to half speed. The AC power from each generator is converted to DC power by diode rectifiers before delivery to the loads.

During the Summer session, the maximum design value of the toroidal magnetic field of 3.45T was reached with a flat-top of several seconds. In order to achieve this performance, the full energy output of the toroidal flywheel generator was required together with the two toroidal field static units operating at full power. Since that time, the toroidal field busbars and coil system has been used routinely at the full design value, during which the power supplies have delivered the full design value current of 67kA with a flat-top time of 10s. The energy of 5000MJ delivered per pulse has been close to the maximum design value of 5500MJ. Instrumentation channels which monitor temperatures and displacements indicated that all systems were behaving in accordance with calculations.

The ohmic heating circuit was commissioned up to 60kA of premagnetisation current and 100kA of slow rise and flat top currents. Plasma currents up to 3.7MA for several seconds were produced with the full toroidal

magnetic fields of 3.45T. About 75% of the total available flux swing has been used, as larger plasma breakdown voltages would lead at present to early plasma disruptions. Modifications are being studied to allow the use of the full flux swing and to permit plasma currents of 5MA.

Operational experience on JET has suggested the need for certain modifications and improvements to the toroidal and poloidal field power supplies. On the flywheel generators, an AC reverse current braking system now reduces the braking time to about 20 minutes. New installations include a lubricating oil purification system, oil cooling on the thrust bearing pads, a new tachometer driving system, and a fire fighting system for each generator pit. In addition, the earthing switches on the ohmic heating circuit have been modified to allow braking of the higher than expected remanence current of the generators, and a number of modifications have been introduced in the control systems of the AC/DC conversion systems, (e.g. the bandwidth of the radial field amplifier has been increased from 60 to 150Hz, to cope better with vertical plasma instabilities).

Neutral Beam Heating System

During the early phases of the additional heating programme, hydrogen beams will be injected at 80keV with a beam pulse length of 10s. The total beam power into the Torus will be around 15MW, with 10MW in the full energy beam component. The power will be provided from sixteen beam sources each with an extracted positive ion beam current of 60A, arranged in two systems of eight sources. For the later phases of the programme, the system will be modified to inject 160keV deuterium beams with an extracted beam current of 30A per source.

The development of the beam sources was a joint venture between JET, the Euratom-CEA Association, Fontenay-aux-Roses, France and the Euratom-UKAEA Association, Culham Laboratory, U.K. During 1984, the ten sources so far manufactured were tested and found satisfactory.

Two problems required further development and were successfully solved. First, the mixture of atomic and molecular ions measured in the beams from prototype sources gave unacceptably low full-energy and unacceptably high-fractional energy beam components. Joint development by Culham Laboratory and JET of an internal magnetic filter resulted in a proton fraction of 84% and a plasma uniformity of $\pm 8\%$ over the extraction area, which fully met requirements. Second, the focussing of 260 beamlets through an electrode system measured during tests was different from the design value and could have led to destructive beam power loadings on certain beamline components. This was corrected by re-drilling the apertures in one electrode of every source. In the meantime, the method of computation has been improved and now matches the test results. In preparation for deuterium beam injection, a spare beam source was successfully modified at Fontenay-aux-Roses

Laboratory and subsequently operated with deuterium beams of 160keV beam energy and 37A ion current during 5s pulses.

After passing through the neutraliser, the remaining ion beam fractions are magnetically deflected and dumped in various types of beam dumps. The neutralised beams are tailored by beam scrapers for entrance through the torus port. All these components are designed for quasi-stationary thermal power loadings of 100MW Im_2 . During thermal and pressure tests, certain beam dumps produced from a chromium-zirconium copper alloy, developed cracks adjacent to electron-beam welds. The necessary design changes and repairs of these components have delayed the assembly of the beamline system.

The cryopump was delivered in 1984 installed in the neutral injector box and successfully tested on the JET site. The helium refrigerator was also installed and commissioning started.

Installation of the first injection system on the torus has progressed. The high power beam scrapers in the torus duct, the rotary valve to isolate the torus and injector vacuum system, and the fast shutter have been installed and successfully leak-tested. The cryopump has also been installed as well as the neutralisers and most of the beam sources, including all supply systems.

A neutral injector Testbed, including power supplies for two beam sources, has been set up in the JET Hot Cell, and beam operation started in early 1984. So far, it has been used to commission the system of power supplies and beam sources with their controls as well as the diagnostics, data acquisition and data analysis system. Long pulse operation of a beam source at full parameters has been achieved. Prior to installation on the torus, the beamline system will be commissioned in the Testbed, but will be limited to operation of the beam sources for one quadrant.

All nine outdoor high voltage grid power supply modules, four for each beamline and one for the testbed, have been successfully tested on a dummy load. The four modules for the first beamline have been commissioned on a dummy load with their protection systems. Two of the protection systems for the second beamline have been delivered and two more are under manufacture. All eight PINI auxiliary power supply units for the first beamline and two for the testbed have been delivered on site and installed. Six of the ten units have been fully commissioned on a dummy load. The units for the second beamline are still under manufacture.

The eight SF6-insulated transmission lines, which will carry the power to the first beamline from the J1 North Wing to the Torus Hall, have been installed and tested up to 260kV DC, well above the maximum operating voltage of 80kV in hydrogen and 160kV in deuterium.

The first SF6 tower, interfacing the transmission lines and other services to the PINI's, has been installed and tested in the Torus Hall. The main components of the second tower have been delivered and its snubbers have been fully tested and installed.

Radio Frequency Heating System

The Radio Frequency (RF) heating system, radiates energy from antennae located on the walls of the vacuum vessel, and power is coupled into the plasma at a frequency (25-55MHz) corresponding to an ion cyclotron frequency of one of the ion species in the plasma. The wide frequency band chosen for JET allows the RF system to be operated with the various mixes of ion species required in the different phases of the scientific programme. Ultimately, ten RF generators will be installed, producing 30MW of power required.

During 1984, attention was devoted to the construction and testing of the first two antenna-generator systems, which were installed during the shutdown at the end of 1984. Experiments on a complete unit aimed at measuring the antenna losses started before the end of the year. At the same time, the design of equipment required for the second stage of the RF programme was completed and the major contracts placed.

The first generator unit was received and installed on site. The prototype driver, which delivers 200kW, has been connected to an antenna and fully commissioned in remote operation. Early plasma experiments on coupling and matching have started. The prototype unit has demonstrated full power operation over the entire bandwidth during long pulses (20s) and will be operated on the second antenna early in 1985 as soon as remote controls and instrumentation are commissioned. All eight generators necessary for the first two stages of the RF programme are expected to be on site at the beginning of 1986.

Two prototype antennae (one dipole and one quadrupole configuration) have been installed in JET. A graphite limiter frame is used to protect the screen. A third antenna of the same design is presently under construction and will be installed in mid-1985. The central conductors of the third antennae will be of the type that gives the better results during the first half of 1985.

The RF Testbed has been operated since August 1983 at CEA Fontenay by a joint CEA-JET team. All critical items have been systematically and separately tested. The complete antenna and vacuum transmission line assembly was tested with the nominal RF pulse length at full reactive power (45kW, 1.5kA), and behaved as expected.

Remote Handling

Some remote handling is expected to be needed inside the vessel from mid-1986 and full remote handling both inside and outside the vessel from the end of 1989. The philosophy remains that all remote handling of JET components will be performed fully remotely by end effectors carried into position by transporters, each carrying special or general purpose tools. The most sophisticated of the end effectors will be the force-feedback servomanipulators. Support vehicles will carry and interconnect the various elements.

A system has been established whereby remote handling procedures, describing the planned operations,

are required before the design of a component is released for manufacture. This system is being applied retrospectively to most components already fitted. Each remote handling procedure will eventually certify that a physical check has been made to ensure that the component is fitted as drawn and that the procedure is feasible. The procedures will be used to establish remote handling operating schedules used in the control room, verified by mock-up simulations.

The articulated boom capable of carrying a 1t load inside the vacuum vessel was delivered to JET in October 1984, and is almost fully commissioned. It will be used for mock-up tests and will assist in the hands-on in-vessel operations during the shutdown in June 1985.

Tritium Handling

During 1984, the detailed duties of the tritium handling system were decided and the interfacing conditions to other JET systems defined. Concepts and flow diagrams were developed for the integration of the gas supply and vacuum systems of the neutral injection and torus into a closed gas recycling loop with the tritium handling plant. The tritium recycling system will reprocess and separate the gases into hydrogen isotope fractions ready for re-use in plasma pulses or for reconditioning the torus in a closed loop glow discharge cleaning mode. It will also provide for the removal of impurities.

The diagnostic design of long lead-time equipment, particularly for the cryogenic processing of the gases, was well underway at the end of 1984. Design options for certain key components such as the accumulation panels and the cryotransfer pumps were under construction and will be performance tested in a special test-rig early in 1985. The test will allow optimisation of the equipment for its performance, control, reliability and consumption of cryogenics. Suitable engineering codes for the design of plant equipment and interconnecting piping under various thermal cycling conditions have been identified. Stress analysis on thermally cycled components and piping will be applied to guarantee a high degree of reliability.

Diagnostic Systems

During the year, a number of new diagnostics were brought into operation on JET, as follows:

- (a) Single Point Thomson scattering system (for T_e and n_e);
- (b) Multi-channel Far-Infrared Interferometer (partly) (for $\int n_e(r)ds$);
- (c) Microwave Reflectometer (Prototype system) (for n_e profiles and fluctuations);
- (d) X-Ray Pulse Height Spectrometer (Provisional system) (Plasma purity monitor and T_e (axis)).
- (e) Soft X-Ray Monitor (Provisional System) (MHD instabilities and location of rational surfaces);
- (f) Electron Cyclotron Emission Spatial Scan (Partly operational) (for T_e (r,t));

- (g) Limiter Surface Temperature (monitor surface temperature);
- (h) Neutral Particle Analyser Array (partly) (T_i profile);
- (i) VUV Broadband Spectroscopy (Impurity survey).

Scientific Results

Plasma Optimization

Much attention has been devoted to optimization of plasma in the ohmic heating phase, in which studies have been undertaken on the four phases: start-up, current rise, flat-top and termination. Considerable attention was applied to the elimination of stray fields during start-up. For typical JET conditions, avalanche build up is inhibited at stray field levels which are less than 1% of those required to maintain equilibrium later in the pulse. A major source of stray fields has been small currents flowing in the radial and vertical field windings and considerable care has been taken with their control at start-up. This has been a particular problem at low toroidal fields.

Once ionisation is complete, the plasma temperature begins to rise with current. As a consequence, the conductivity increases and the magnetic fields penetrate the plasma more slowly. A current skin starts to form on the outside, which is highly unstable and the current is redistributed in a series of internal rearrangements of the plasma. These rearrangements increase the interaction of the plasma with the limiters and chamber wall, and interaction brings in such impurities as carbon, oxygen, nickel and chromium, which cool the plasma. The cooling clamps the electron temperature at such a low value that the plasma current is prevented from increasing. The metallic impurities cool the centre of the plasma, thereby making it locally more resistive and so exacerbating the formation of the current skin. The rearrangements become more and more violent until there is a major disruption. Therefore, it is important to avoid these effects by operating the machine to prevent current skin formation. If the rate of plasma current increase is small enough, the current can penetrate resistively and skin formation can be avoided. However, the characteristic time for current penetration is typically as long as the toroidal field pulse, so this had to be made faster. Two techniques were used successfully in JET to enhance this current penetration: increasing the plasma aperture and ramping the toroidal field as the plasma current increases. In both cases, the current was effectively carried into the plasma centre even when formed at the edge.

Special recovery procedures were required following a major disruption. Whilst disruptions were rare during operation with routine settings, some were inevitably caused by exploration of new operating regimes. The main effect of such disruptions was to increase the impurity content of subsequent discharges, causing

difficulties in start-up. Recovery has been accomplished by using a low prefill pressure, to avoid cooling of the discharge by impurities, and low plasma currents to minimise the effects of a further disruption.

During the current rise and flat-top periods, gas is bled into the vessel to increase the plasma density. However, a certain proportion of the density arises from the desorption of gas from the limiters. After glow discharge cleaning, the operating range can be quite restricted, because of the density increase due to desorption. This effect rapidly becomes less important during a session as the stored gas is removed by plasma pulses. The maximum density is set by the disruption limit, which is proportional to the plasma current, except near resonant q values, and also depends on the impurity content. The current control settings on JET are such that it is not possible to drive the plasma current down. The driving voltage is removed at the end of the flat-top and the plasma current is allowed to decay resistively, over a period of about 10s, which the plasma density usually follows. However, in pulses that have a high density in the flat-top, the density often pauses in the decay so that the high density limit can be exceeded and a disruption occurs. As yet, no means has been found of combatting this effect.

Plasma Position and Current Control

Three feedback control systems have been used for plasma current and radial position control and for the stabilisation of the vertical position. A fourth system has been prepared for the control of the elongation ratio of the plasma cross-section. During most of the 1984 operating periods, the plasma current was controlled by preprogramming the excitation voltage of the poloidal flywheel generator according to a simplified simulation model of JET. This mode of operation was satisfactory, but a current feedback system was successfully introduced in September, as it provided a more convenient way of achieving current pulses with constant flat-top. The control error was less than 5%, which can be further reduced by auxiliary pre-programming.

An unexpected phenomenon occurred during attempts (Pulse No.1947) to increase the elongation and the plasma current to the design values of 1.6 and 5MA, respectively. When the elongation exceeds about 1.2, the plasma is unstable against vertical displacements and is maintained in the central position by the feedback system which applies a radial magnetic field correction in response to any vertical displacement. In general, this system worked well with plasma elongations up to 1.4 and plasma currents (I_p) of 3.7MA. However, in one discharge with $I_p = 2.6$ MA and an elongation of 1.7, the feedback system was switched off by a protection system for the amplifier. The plasma moved rapidly downwards a distance of about 1m without significant reduction in current. This was followed by a typical disruption with rapid current quench and movement of the plasma towards the inner (smaller major radius) section of the wall. The unexpected feature was that large forces of about 200t were transferred to the vacuum vessel causing

rapid displacement of about 1cm and a permanent reduction in the mean major radius of the vessel by 1mm. A tentative explanation is that poloidal currents flowed through the plasma and the rigid sectors transferring the full destabilising force on the plasma to the vessel. This explanation has not yet been proven by direct measurement of the associated magnetic fields.

In view of the potential risks to the vessel, the campaign to take the current towards 5MA was suspended until the vessel mounting system was improved and the full implications understood. During the shutdown at the end of 1984, new restraints were fitted to the large ports to resist vertical motion of the vacuum vessel together with hydraulic dampers to control torsional movements. The stabilisation circuit has since been studied in greater detail, and temporary improvements of the feedback circuitry were implemented. Preparations were made to increase the voltage range of the power source by a factor of two and its response speed by a factor of two or three. As a precaution, Tokamak operation was restricted to plasmas with elongation ratios of less than 1.5. In 1985, it is hoped to increase the performance level in cautious steps towards 5MA.

The radial position control uses the measured difference in the poloidal flux between the limiter and the desired inboard position of the limiter magnetic surface (equivalent to the plasma boundary) as a feedback control signal for the power source of the vertical field coil. The inboard position may be varied during the pulse by preprogramming, (e.g. to build up the plasma starting from a small initial radial diameter). This system has worked satisfactorily, but has been extended by doubling the voltage range of the vertical field power source in order to cope more easily with large amplitude perturbations, such as disruptions. In addition, a system for the independent control of the plasma elongation ratio has been prepared, and this was partially commissioned in December.

Impurities and Radiation Losses

Impurities in the plasma have been studied by visible and VUV spectroscopy, and from bolometer and soft X-ray signals. Visible spectroscopy is essentially restricted to lines of neutral atoms and low ionisation stages, providing information on sources and local influxes of impurities. Measurements in the VUV spectrum are more suitable for deriving impurity concentrations in the plasma, though, in the case of light impurities, the analysis is limited to the plasma edge, since these elements are fully stripped in the interior.

Oxygen, carbon, metals from the wall material (nickel, chromium, iron), chlorine and molybdenum were identified as the main impurities in the plasma. Chlorine is believed to have been introduced when washing the torus with detergent. The carbon limiters are the obvious source of carbon, though there is also a substantial carbon influx from the vessel walls. The walls also seem to play a dominant role for oxygen and chlorine impurities. Metals are deposited on the limiter surfaces in

the course of operation (for wall material) or during manufacturing (in the case of molybdenum). Subsequently, limiter sputter is the main source of metals in the plasma.

Metal densities increased with plasma current and decreased with electron density, while the light impurities were relatively insensitive to these plasma parameters and depended more on the state of the vacuum vessel and size and elongation of the plasma. These facts led to the usual decreasing tendency of Z_{eff} with electron density during an experimental campaign. The lowest values at the end of a campaign were $Z_{\text{eff}} \sim 2-3$. An inverse correlation of light impurities and metals was observed throughout.

During 1984, there were two main campaigns to clean the plasma and reduce Z_{eff} : a period of 12,000 pulse-discharge-cleaning pulses; and repetitive carbonisation of the vessel walls. In the first case, some reduction of oxygen and chlorine was noted and the molybdenum fraction in the plasma decreased. However, at electron densities of $2 \times 10^{19} \text{m}^{-3}$ the radiated power was still about 90% of the ohmic power and Z_{eff} was 4-5. Carbonisation reduced the metal content of the immediately following pulses by about x5, but the metals recovered after removing the carbon layer or after a day's ageing. Oxygen and chlorine decreased gradually during the carbonisation campaign, while the carbon fraction in the plasma increased. Thus, the radiated power as low as 40% for $n_e = 2 \times 10^{19} \text{m}^{-3}$ and a considerable heat load on the limiters was observed.

Operation at higher electron densities ($> 3 \times 10^{19} \text{m}^{-3}$) led to higher radiated power before and after carbonisation, 100% and 80% respectively. High density pulses were always dominated by light impurities and their radiation profiles were hollow. Quite frequently, poloidal asymmetries were observed in the radiation, starting in the horizontal midplane near the inner wall and growing in poloidal direction. Eventually, a radiation mantle formed around the plasma leading to a shrinking of the minor radius and a disruption. Due to the reduction of oxygen and chlorine during the carbonisation period, the total radiation was lower and the values of Z_{eff} reduced to 2.5, consisting of about 2% C, 1% O, 0.05% Cl, and 0.015% metals. The density limit was somewhat higher for the cleaner plasmas and it is hoped to increase it by removing the remaining oxygen fraction.

Plasma Boundary Phenomena

The JET plasma is surrounded by material surfaces, notably the Inconel vacuum vessel walls and the carbon limiters. The interaction of the plasma with these surfaces is the source of impurities, which contaminate the plasma and which exert a considerable influence on the plasma behaviour. Whilst the basic physics processes involved, such as sputtering, are well understood, the complex cocktail of processes, which occurs in JET, is less well known.

A picture of these interactions in JET has been built up from combined data from spectroscopic measurements of the edge plasma, from probes inserted into the edge

plasma and from examining surfaces exposed in JET. Samples were also taken and analysed from the carbon tiles on the limiters, the Inconel protection plates lining the vacuum vessel wall, and from the body of a diagnostic probe which was exposed to the edge of the plasma during a sequence of tokamak discharges.

These data have shown that there are many processes by which metallic impurities enter the plasma, and many which redistribute the impurities on surfaces surrounding the plasma. Analysis showed that the metals (nickel, chromium and iron) are taken from the Inconel walls and deposited on the carbon limiter. The analysis also showed molybdenum on the limiter surface, which was inadvertently deposited on the carbon limiter tiles during manufacture. There was a large variation in metals distribution across the tile surface, with maxima at the edges and substantial minima at the centre, with profiles similar to the power flux to the limiter, which raised the temperature in the tile centre to over 1000C. The metal concentrations represented an equilibrium between erosion and deposition. Erosion was stronger in the tile centre where the plasma flux was stronger; deposition was stronger at the edges where the plasma flux was weaker.

The metals on the limiters appeared to be the main source of metal influx into the plasma, except in highly elongated discharges where the plasma was in close contact with the top and bottom of the vacuum vessel wall. The main release mechanism seemed to be sputtering of the metals by oxygen impurity ions. The nickel, chromium and iron reached the limiters by various methods: sputtering of the wall by charge-exchange neutral atoms during tokamak discharges; melting and vaporisation of localised areas of the wall by energetic electrons following plasma disruptions; and sputtering by ions during glow and pulsed discharge cleaning. All of these processes appeared to contribute to the metal deposits seen on the limiter.

During this period of operation, three methods were used to condition the vacuum vessel: glow discharge cleaning in hydrogen; pulsed discharge cleaning; and carbonisation by glow discharge cleaning in hydrogen with 3% methane. The first two methods appeared to be effective at removing lightly bound contaminants such as water vapour, but were less effective at removing oxide layers. Both methods also resulted in the deposition of metals onto the limiter. By contrast, carbonisation, appeared to cover walls and limiter with a fresh layer of carbon, burying the metal contaminants. However, it was not possible to measure the carbon layer depth or its chemical form (e.g. graphite or carbide). Experiments were also carried out on the change-over from tokamak discharges in hydrogen to deuterium. In contrast to experience on some other tokamaks, the change-over in JET was achieved in as few as 5-10 discharges. This is consistent with a simple model of isotope exchange between the plasma and absorbed gas in the wall.

During 1984, JET was operated with four graphite limiters each straight in the poloidal direction of length 80cm, and curved in the toroidal direction with width

40cm. The limiters are fixed to the midplane of the vacuum vessel at its outer circumference on the left hand side of Octants Nos.2,4,6 and 8. The limiters are observed by charge-couple-device infra-red video cameras, which image the limiter surface in a narrow wavelength band in the visible to near infrared. Depending on filters used, this system provides a thermal image at any temperature above 500C. The following results were observed:

- The limiters withstood without damage power loads of up to 1.9MW for a flat-top time of 5s and a discharge duration of over 12s, but under these conditions, the limiter reached over 1500C;
- The scrape-off thickness was measured from the spacing of the maximum heat deposition zone as 15mm, which increased during current rise and fall to about 30mm;
- The thermal load on the limiters was not symmetrical, with the ion side usually 10% hotter, which might be associated with the observation that hydrogen recycling occurred mainly on the ion side;
- Arcing was observed on the limiter during early operations but disappeared during later stages in normal operation. Arcing still occurred during disruptions;
- Hot spots were not normally observed on the limiter surface, though intermittent bright areas were seen at the limiter edges.

The limiters performed well during 1984 operation, and observed damage was only superficial. The limiter load is now close to the design value. With the introduction of additional heating in 1985, the increase in the power load will necessitate installation of additional limiters. A further four graphite limiters are planned for installation in mid-1985, when loads of 4-5MW should be accommodated.

Instabilities and Disruptions

Instabilities pose a threat to increasing the plasma energy content and to maintaining sufficient heat isolation in JET. The main force for driving such instabilities is the inhomogeneity in the distribution of the current, magnetic field and plasma energy. However, such inhomogeneities are inevitable in a toroidally contained fusion plasma and methods must be developed to optimize plasma parameters and locate their limits without disruptions or major instabilities. Studies of such phenomena have been carried out in JET.

Magnetic islands have been observed mainly associated with small m/n numbers (1/1, 2/1, 3/2), except during the start-up phase, when the values of m/n are high. With small radial dimensions, these islands do not pose problems. They enhance the heat-transfer locally, but the thermal isolation between resonant surfaces is still good. However, if the islands grow radially to such dimensions that they overlap, a large heat transfer takes place from the central core to the edge. These disruptions lose the confined plasma energy in a

period of <1 ms, which can be drained and deposited on the limiter (energy-quench phase). Normally, the driving voltage to maintain the plasma current cannot rise sufficiently fast to compensate for the increased resistivity of the cooled plasma, and therefore the current dies quickly (current quench phase). If position equilibrium can still be maintained (soft-disruption), the current quench takes about 0.3s, whilst it can become as short as 0.02s if the position control amplifier reaches saturation voltage (hard disruption).

Investigations have been undertaken on the cause of the current distribution change, so that magnetic islands grow from a modest size to become overlapping. It has been observed in JET (as in other tokamaks) that a density increase beyond a certain limit induces such disruptions (the high density limit). This limit increases with current and to a certain degree with toroidal magnetic field, but reduces with impurity content. A plausible explanation under investigation is that impurities cause radiation losses that are larger in the cold edge than in the hot centre. Increasing the particle content by conventional gas injection from the outside raises the radiation losses relatively more at the outside than in the core. Therefore, the resistivity increases more outside than inside, and so the current density difference across a resonant surface increases, leading to growing island sizes and eventually to a disruption. Consequently, a reduction in impurities should lead to an increased density limit. Fuelling methods which deposit particles in the centre (pellet-injection), should prevent island growth, since density increases would not lead to differential radiation increases. Initial results with pellet-injection, for instance in ALCATOR-C (M.I.T. USA), seem promising.

Energy and Particle Confinement

Both the energy and particle confinement properties of JET have been examined throughout the various phases of 1984 operation. Scans of density, current and toroidal field have been carried out to obtain information on scaling of energy and particle confinement times. These were carried out at constant plasma major and horizontal minor radius but with varying elongation factors (b/a) in the range 1.1 to 1.6.

The energy confinement time τ_E was determined from the relationship

$$\tau_E = 3/2 \int (n_e T_e + n_i T) dV / P_\Omega$$

where P_Ω is the total ohmic input power. The ion deficiency factor is $n_i/n_e = (Z_i + 1 - Z_{\text{eff}})/Z_i$, where Z_i is the charge of the principal impurity. In all calculations, the density profile was that measured by the microwave reflectometer, and the ion temperature was taken from the neutral particle analyser and the neutron yield monitors and spectrometers (in deuterium). τ_E was found to increase with density, in both hydrogen and deuterium plasmas. Improved values of τ_E were found in deuterium, and values up to $\tau_E = 0.7$ s were achieved. Regression analysis has shown a good fit between τ_E and nq_{cyl} .

On a Hugill-Murakami plot of normalized plasma

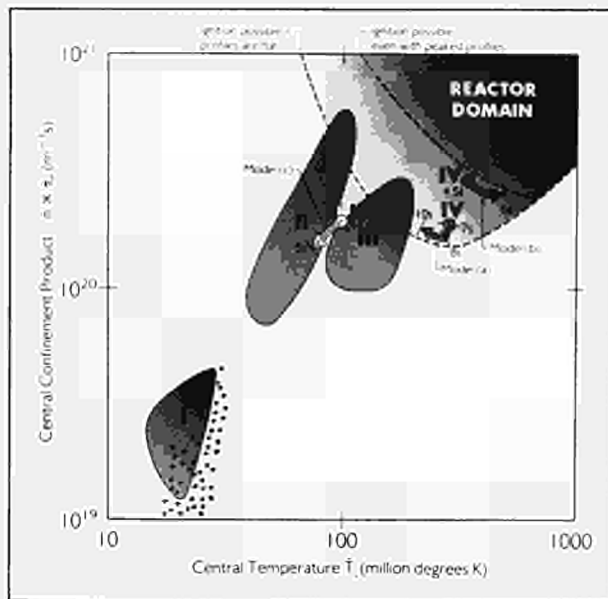


Fig.2: Lawson diagram plot $\langle n_i \tau_E \rangle$ versus central ion temperature T_i . The experimental points show the recently achieved values in JET and the areas marked I, II, III and IV show the regions of parameter space predicted for the various phases of JET operation ($\circ I_p < 3MA$, $\bullet I_p > 3MA$).

current $1/q_{cyl}$ ($=\mu_0 R I_p / 2\pi B_T a b$) versus normalised density nR/B_T , an approximate linear relationship is obtained for all JET data. At a fixed nR/B_T , the maximum current is bounded by low q disruptive instabilities corresponding to q_{cyl} of 2-3, while for a given value of q , there is another type of disruption at the density limit given by $nR/B_T = A/q_{cyl}$ (where A is a constant depending on the purity of the plasma). This gives the relationship $n_{max} \propto \bar{j}$, where \bar{j} is the average current density. If this proportionality is taken together with the relationship $\tau_E \propto n q_{cyl}$, the maximum achievable value for the parameter $\langle n \tau_E \rangle$ is:

$$\langle n \tau_E \rangle_{max} \propto B_T^2 / q_{cyl}$$

However, it should be emphasised that the three dimensional space in B_T , I_p and (b/a) has not been explored uniformly, so the relationship cannot be regarded as fully proven.

A detailed local power balance has been completed for selected shots. It was found that, for the central plasma

region ($r/a < 0.75$), radial transport was dominated by thermal conduction and in the outer region by radiation. The accuracy of measurements did not permit a conclusive determination of whether the main loss channel in the central region was via electrons or ions. If the assumption was made that the ion thermal conductivity, χ_i , was neoclassical, then the electron thermal conductivity, χ_e , was found to scale inversely with density.

The global particle confinement time was determined from the particle balance equation, in which the source of new plasma particles was obtained from H_α measurements along various chords viewing the walls and limiters. The main source of gas in the present series of experiments was the limiter. However the ratio of the gas flux from the walls to the limiter increased as plasma elongation was increased, and as the plasma came closer to the walls. The scaling of the particle confinement time τ_p with density showed a general pattern that, at low densities, τ_p increased with density, whereas at higher densities, τ_p decreased with density, showing that at higher densities the plasma was impervious to neutrals. The effect of the carbonisation of the wall was to reduce τ_p further.

Overall Picture

At the end of 1984 (Phase I), the gross picture showed that plasma currents of up to 3.7MA were obtained for several seconds within overall pulse lengths of 15s, at the full performance toroidal magnetic field of 3.45T. Electron and ion temperatures up to 3 and 2.5keV, respectively were obtained with densities of up to $3.5 \times 10^{19} m^{-3}$ and a record energy confinement time of $\tau_E = 0.8s$.

From the long-term viewpoint of alpha-particle heating and fusion power, the progress of JET is properly measured in the Lawson diagram in which the product of plasma density and energy confinement ($\langle n \tau_E \rangle$) is plotted against the central ion temperature T_i (see Fig.2). The experimental points show the recently achieved values in JET and areas marked I, II, III and IV shown the regions of parameter space predicted for the various phases of JET operation. It can be seen that the best results are obtained at the highest currents and that the predicted results for Phase I have been more than achieved in JET.

JET – Operations and Development

Introduction

The Operation and Development Department was formally brought into existence at the start of the Operations Phase in June 1983 following completion of the Construction Phase. At that time, the Department was made responsible for the operation and maintenance of the machine and for developing the necessary engineering equipment to enhance the machine to its full performance. In undertaking these tasks, the Department is now subdivided into a Directorate and six Divisions:

- (1) Torus Division;
- (2) Power Supply Division;
- (3) Control and Data Acquisition Systems (CODAS) Division;
- (4) Neutral Beam Heating Division;
- (5) Radio Frequency Heating Division;
- (6) Fusion Technology Division.

The present structure to Group Leader level is shown in Fig. 3 and the list of Divisional Staff at 31st December 1984 is shown in Fig. 4.

Summary of Progress

During 1984, operational duties made heavy demands on resources in the Department, particularly on Torus, Power Supply and CODAS Divisions. In addition to specific Control Room activities, the Divisions had to provide on-call staff to perform special functions or repair specific equipment. As well, a number of these tasks (in particular, glow discharge cleaning) could only be carried out outside normal working hours and at weekends, which imposed further heavy demands on staff.

In parallel with these duties, Torus Division was active in preparation and installation of new equipment on the machine, particularly during the shutdowns in January, March and October/November. Major pieces of equipment installed included the high vacuum rotary valve and pumping equipment for the Neutral Injection Beam (at Octant No. 8), the graphite protection tiles on the inward wall of the vacuum vessel, and new mechanical supports for the vacuum vessel. In addition, progress was made on development work for future belt limiters and in experiments to assist the choice of a suitable material (i.e. graphite or beryllium) for these limiters.

Power Supply Division has expended considerable effort in streamlining the control of amplifiers and generators to accomplish the required pulse profiles and assisted substantially in the successful completion of the Ohmic Heating Phase (Phase I) of JET operation. As well, the Division has responsibility for the additional heating power supplies, for which the neutral injection Test-bed was brought to full operation and the RF d.c. power units were completed, during the year.

During the year, CODAS work has concentrated on expanding and consolidating facilities required to further improve efficient operation, and adding and commissioning subsystems designed for the extension to full performance. The computer system has now been extended to 34 computers (from 25).

Neutral Beam Heating Division has brought the NI Test-bed into operation and ion beam sources have been operated at full power and pulse length. Ten beam sources were manufactured and tested successfully. The eight PINIs, each of them individually checked on the UKAEA's Culham Laboratory test beam-line, are now ready for pre-commissioning with their respective power supplies, at short HV pulse length. The Central Support column which carries the main beam-line components, such as magnets, beam dumps and calorimeter is being prepared for a test in the Testbed before being subjected to integrated commissioning at Octant No. 8. The construction of the second neutral injector is advancing.

Radio Frequency Heating Division has had two antennae of different coupling properties installed in the vacuum vessel, and the first power supply and RF generator is ready to operate at the 3MW level. The second unit will be completed in early 1985. All essential components of the transmission line system were conditioned and tested at the RF Testbed at the CEA, Fontenay-aux-Roses Laboratory prior to installation on JET.

For the active phase of JET, Fusion Technology Division are making preparations to cope with later requirements. The articulated boom to handle a one tonne load inside the vacuum vessel has been delivered and is under test. Also a number of important remote handling units - a turret truck, a radio-controlled support vehicle, and two force-feedback servo-manipulators - have been ordered or are under design. The design of the tritium recycling system is well advancing and prototype key components are being manufactured and prepared for testing.

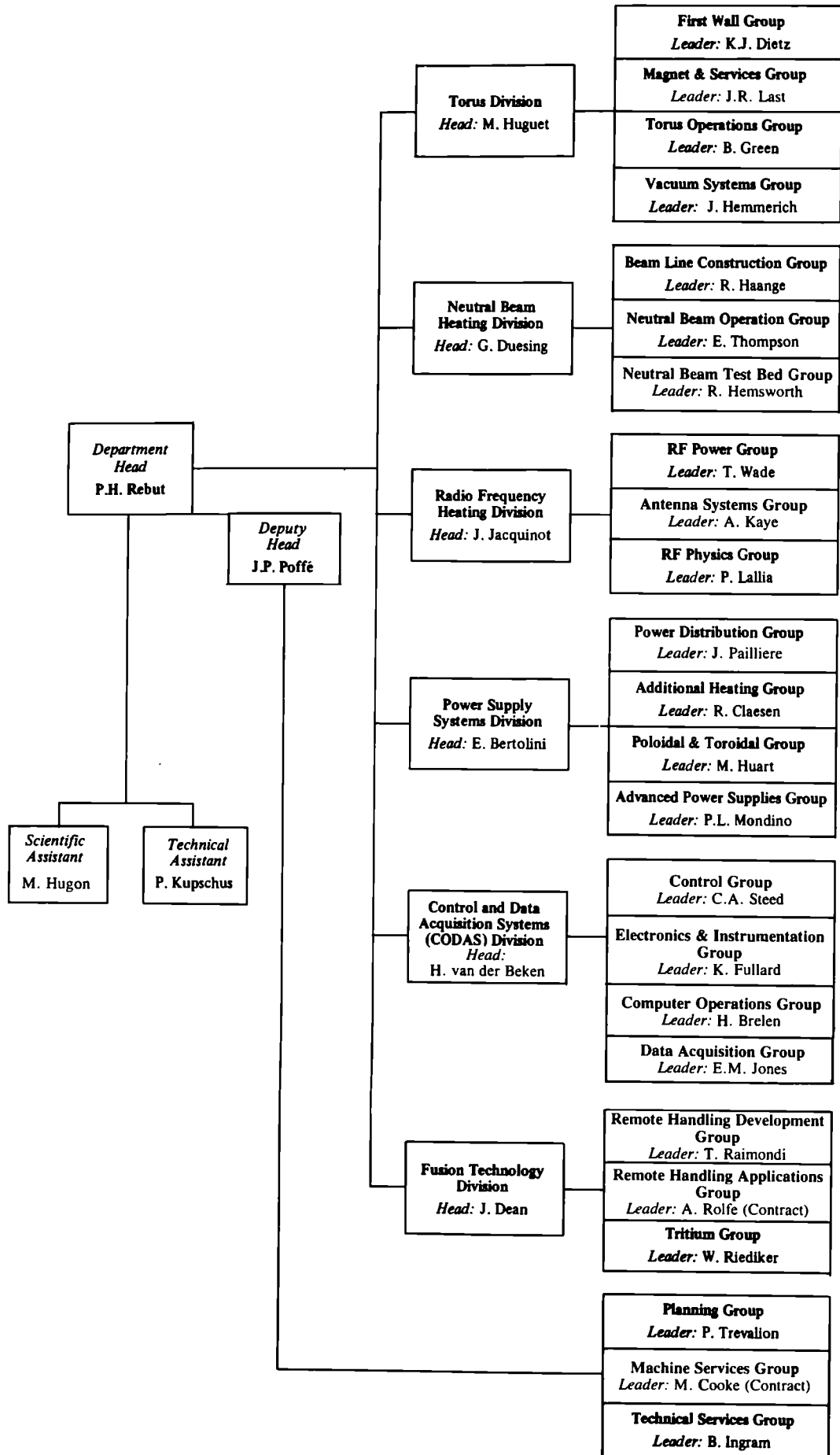


Fig.3 Structure of the Operation and Development Department (December 1984)

Fig. 4: List of Divisional Staff (December 1984)

OPERATION and DEVELOPMENT DEPARTMENT

Head of Department: P.H. Rebut
Deputy Head of Department: J.P. Poffé

DIRECTORATE:

Head: J.P. Poffé

P. Barker	M. Guillet	P. Kupschus	L. Nickesson
D. Carré	Mrs E.D. Harries	D. Lecornet	H. Panissie
Mrs D. Dalziel	Mrs M. Hicks	Mrs H. Marriott	J. Potter
N. Davies	R. Howes	J. McDonald	Miss A. Strange
H. Duquenoy	M. Hugon	J. McGivern	P. Trevalion
G. Edgar	A.H. Humphreys	S. McLaughlin	M. Walravens
Miss M. Fraser	B. Ingram	P. Meriguet	C. Woodward
L. French			

TORUS DIVISION:

Head: M. Huguet

K. Adams	E. Daly	D. Holland	Mrs M. Rydalm
W. Baker	W. Daser	M. Hughes	R.L. Shaw
B. Bignaux	K. Dietz	Mrs I. Hyde	W. Smith
J. Booth	K. Fenton	G. Israel	K. Sonnenberg
A. Boschi	C. Froger	H. Jensen	R. Thomas
D. Cacaut	B. Glossop	H. Key	S. Turley
G. Celentano	K. Grabenstatter	J. Last	E. Usselmann
P. Chuilon	B. Green	P. McCarthy	J. van Veen
A. Conway	N. Green	P. Noll	T. Winkel
D. Cook	L. Grobusch	J. Orchard	M. Young
T. Dale	J. Hemmerich	R. Rigley	J. Zwart

NEUTRAL BEAM HEATING DIVISION:

Head: G. Duesing

H. Altmann	D. Ewers	A. Jones	M. Mead
C. Brookes	H. Falter	T.T.C. Jones	W. Obert
A. Browne	J. Gallacher	D. Kausch	S. Papastergiou
A. Burt	Mrs S. Gerring	E. Kussel	D. Raisbeck
D. Cooper	A. Goede	F. Long	R. Roberts
N. Cowern	R. Haange	J. Lundqvist	D. Stork
Mrs D. Cranmer	R. Hemsworth	D. Martin	E. Thompson
J.F. Davies	H. Hupfloher	P. Massman	Miss D. Vernal
G. Deschamps	F. Hurd	C. Mayaux	M. Watson
A. Dines	J. Jensen		

RADIO FREQUENCY HEATING DIVISION:

Head: J. Jacquinet

H. Acounis	Mrs L. Brookes	G. Jessop	Mrs L. Rowe
R.J. Anderson	M. Bures	A. Kaye	F. Sand
J. Arbez	W.H. Clark	P. Lallia	M. Schmid
G. Bosia	A. Franklin	C. Maradan	T. Wade
M. Brandon	E. Hanley	P. Murray	C. Walker
H. Brinkschulte	R. Horn	J. Plancoulaine	

POWER SUPPLY SYSTEMS DIVISION:

Head: E. Bertolini

Mrs C. Allen	A. Eyrard	A. Moissonnier	A. Santaguistina
U. Baur	H. Fielding	P. Mondino	K. Selin
T. Bonicelli	J. Goff	G. Murphy	S. Shaw
O. Buc	D. Halliwell	Mrs J. Nolan	A. Skinstad
C. Christodoulopoulos	M. Huart	J. Paillère	N. Walker
R. Claesen	A. Keymer	R. Perez-Taussac	C. Wilson
J. Dobbins	V. Marchese	I. Piacentini	G. Wilson
P. Doidge	G. Marcon	C. Raymond	L. Zannelli
B. Eriksson	L.W. Mears		

CONTROL AND DATA ACQUISITION SYSTEMS DIVISION:

Head: H. van der Beken

H. Brelen	S.E. Dorling	Miss K. Mathiä	V. Schmidt
W. Brewerton	K. Fullard	D. Nassi	C.A. Steed
M.L. Browne	Mrs N. Gandy	J.P. Nijman	J. van Montfoort
T. Budd	R.F. Herzog	C.G. Pollard	A. Wallander
P. Card	E.M. Jones	G. Rhoden	J.R. Watkins
A.J. Cleaves	Miss J. Kedward	J. Saffert	I.D. Young
Mrs L.M. Dines			

FUSION TECHNOLOGY DIVISION:

Head: J. Dean

S.J. Booth	E. Gebler	M. Pescatore	J. Schreibermaier
R. Cusack	Mrs M.E. Jones	P. Presle	L. Sonnerup
Mrs M. Daish	P.D. Jones	T. Raimondi	A. Tesini
L. Galbiati	A. Konstantellos	J. Removille	M. Tschudin
A. Galetsas	A. Nowak	W. Riediker	M. Wykes

Operations & Development Directorate

(Division Head: J-P Poffé)

Besides managerial tasks, within the Operations and Development Department, the Directorate is responsible for the provision of a wide range of services to the whole project, such as:

- Technical Services, including civil and mechanical engineering support, workshop services and procurement;
- Machine Services, including cooling water, compressed air, as well as routing of pipes and cables within congested areas;
- Planning and co-ordination services (long and short term), and stores;
- Drawing office and design facilities;
- Quality control.

In addition, an assessment of pellet injection as a potential future method of fuelling/refuelling is being undertaken under the leadership of the Technical Assistant to the ODD Director.

Specific activities of the Directorate Groups are reported in the following paragraphs.

Technical Services Group

(B. Ingram)

This Group provides mechanical support services for the JET machine, auxiliary equipment and diagnostics. The work is organised through three sections with tasks described as follows:

Civil Section

(C. Woodward, P. Barker, J. Gedney, G. Evans)

This section is responsible for building maintenance and enhancements of JET buildings and site facilities. The section provides a design and construction service for the JET Divisions. Civil works projects undertaken during 1984 included structural steelwork and concrete shielding for diagnostic equipment, auxiliary transformer pens, additional office accommodation for 60 persons, a car park for 180 vehicles, an extension to the stores building, structural platforms and sundry office/laboratory partitioning.

Engineering Support, Workshop and Procurement

(J. McDonald, S. McLaughlin, R. Smith)

This section provides close workshop support together with a procurement and manufacturing service. Running contracts exist with local manufacturing firms and together with the Host Laboratory workshop organisation, they have provided facilities for the manufacturing and installation of various items of equipment and plant. The new contactless control system for the 3 tonne post crane on the Tokamak is a typical installation. The section is also responsible for the operation of the Metrology Laboratory and the Statutory

Inspection and Registration of Lifting Equipment and Pressure Vessels.

Engineering manpower support is organised by a contract with a large commercial organisation who provide a base load of skilled manpower for normal maintenance and assembly tasks. During shutdowns (4 months in 1984) the manpower is normally doubled to allow maintenance and installation of equipment on the Tokamak. Such items as RF antennae, NI heating equipment and various diagnostics have been installed.

Building and Mechanical Services Section

(N. Davies, R. Howes)

This section is responsible for general building services maintenance and enhancements. This covers all the heating, air conditioning, cranes and general services. A design and construction service is provided for JET Divisions. Projects undertaken during 1984 included demineralised water system extensions, additional laboratory services together with extra workshop facilities.

Machine Services Group

(M. Cooke)

The Machine Services Group is responsible for the operation and maintenance of the site water distribution system, demineralised cooling water to the Torus and Neutral Injection Testbed, together with the compressed air supply and distribution system. In addition to normal operation, the Group has been examining the uprating of existing services to meet increased demand for additional heating and also to improve the reliability and quality of existing services. Co-ordination of the routing of pipes and cables in the Basement of the Torus Hall is another duty of the Group.

Compressed Air System

(D. Lecornet, P. Butcher)

During 1984, it was decided to increase the capacity of the compressed air system and improve the reliability by the introduction of a further $15\text{m}^3\text{h}^{-1}$ 12bar water cooled air compressor set in the Basement and an additional $10\text{m}^3\text{h}^{-1}$ 10bar air cooled compressor set in the West Wing of Building J1. The introduction of the new compressor sets involved modifications to the supply pipework, and to give better quality air, further air filters and an increased capacity heatless drier were introduced. The air distribution systems were interlinked with pipework and valves to ensure the maximum security of supply. Further multitube air distribution systems were installed to the backs of the limbs of the machine to allow increased air distribution from the solenoid valves in the Basement for the Neutral Injection services on Octants Nos.4 and 8.

Site Water

(L. Nickesson)

The design and construction of an additional fourth cooling water tower was started in 1984, with an

anticipated completion date of May 1985, to give additional water cooling for the summer of 1985. The fourth cooling water tower is an identical unit to the existing three, with an increase in pumping capacity produced by the installation of a fifth cooling water circulating pump. The associated water treatment electrical distribution and instrumentation services were also increased to match this 30% increase in cooling capacity.

Demineralised Water

(L. Nickesson)

Studies were carried out to improve the quality of the demineralised water, in which further filters and treatment would be used to reduce bacteria, in order to improve the conductivity of the water and assist in the reduction of any pipework corrosion. A further mixed bed polishing column was installed in readiness for the demineralised water plant for Octant No.4 Neutral Injection additional heating.

Instrumentation

(P. Butcher)

The classification of the service alarms were re-assessed to give reliability of signals and discrimination for true faults. The control system for the water plant and air distribution systems were re-assessed to suit the increased capacity and associated plant. The pneumatic systems for the Neutral Injection system at Octant No.8 were re-assessed to give local transducers located close to sensing points for better repeatability.

Pipework Systems

(D. Lecornet)

The scope of the stainless steel systems in the Basement were increased to allow the water cooling plant and distribution piping for Octant No.4 Neutral Injection heating. This pipe system was completed mechanically by the end of 1984 and included the installation of penetration plates and new circulating pumps. Additional pipe services for air, nitrogen and vacuum were designed and installed for the Diagnostic Hall with additional services to Octant No.8 Neutral Injection heating including a vacuum line, SF₆ supply gas, nitrogen and water system vents and drains.

Basement Services Coordination

(M. Cooke)

Further studies investigated the capacity of penetration plates and cable tray routes to allow for expansion in later years of diagnostics and RF heating cable requirements. These studies will be extended in 1985 and a new system installed to allow for the necessary expansion of the machine services.

Planning Group

(P. Trevalion, G. Edgar, E. Harries, J. Nicholson, L. French, A.J. Smith, T. Stubbings)

The Group is responsible for the long term technical planning, preparation and monitoring of assembly and installation work. The work is organised and co-ordinated continuously through the formulation and progressing of a weekly work plan. Particular emphasis is given to the assembly and installation activities carried out during planned shut-downs. The group also organises the Duty Officer rota and contributes to the logistics by provision of stores, hired equipment, additional mechanical handling and scaffolding requirements as well as cleaning and clean conditions facilities. During the year, there were three major shut-downs involving a total of eighteen weeks when in-vessel work and the installation of additional heating and new diagnostics systems were carried out. Most of the work was performed by the Main Assembly Contractor (MAC2) workforce, which was doubled (to about 75) during these periods.

The JET Stores and its associated activities has changed its main role from receipt and handling of construction materials and components to one more suited for storage and replenishment of spares. There are about 7000 items stocked and during the year, 4000 deliveries were received including 350km of cable.

Drawing Office and Design Facilities

(H. Duquenoy)

The organisation of the drawing office and a description of the main tasks is given in the following paragraphs.

Mechanical and Electrical Designs

Over 40 Designers and Draughtsmen have completed over 200 major designs, under the supervision of relevant project engineers.

Among the principal designs were:

- Intervention Module for Beryllium operation;
- All remote handling tests;
- Articulated Boom extension;
- Tritium Recycling Plant (started in September 1984);
- Graphite Tiles for inner wall and ports protection of Vacuum Vessel;
- New supports for Vacuum Vessel to withstand Vertical Disruptions;
- Toroidal Belt Limiters;
- Vacuum System for RF Antenna;
- Liquid Helium back-up system; - Services at rear of NI Boxes at Octants Nos.4 and 8;
- Cryotransfer Pump for Tritium;
- Vacuum beam lines between the JET Torus and Diagnostic Hall;
- Interfaces between JET Torus and the Diagnostic produced by the Associations;

- RF Auxiliary Power Supply Transformer and associated switchgear;
- Torus and Basement Power Supplies;
- PINI Power Supplies;
- Public address and intercom system for the whole site.

In addition, development tests and procurement of special equipment have also been carried out by the Drawing Office.

Configuration Control

This section studies geometrical interfaces of designs and systems, checking compatibility with equipment already installed and known future developments. The areas considered are: Torus Hall; Basement including Plant Room; West Wing and J1F and North Trench.

Print Room

Over 10,000 originals are filed in the Print Room and one Photoprinter is covering the printing demand for drawings from the whole project.

Technical Library

The Technical Library provides assistance to all JET personnel who require information from the Technical Engineering and Manufacturing Directories, Books, Catalogues and Standards.

Models

Models of the Torus Hall (1/10 scale), Basement (1/25 scale), West Wing (1/25 scale) are kept updated and are used continuously as essential designer tools.

Quality Control Group

(P. Meriguet, S. Church, J. McGivern, D. Sigournay)

This Unit established and implements policy on Quality Assurance/Quality Control and has three main tasks:

- provides a consultancy service (technical advice and assistance) to all Divisions on all aspects from design to testing through manufacture. In 1984, Quality Control was applied to most of the main mechanical contracts such as:
SF6 Towers, Articulated Boom, In-Vessel Inspection System, Rotary Valves, Water cooling and Compressed air Systems, PINI, PINI Grids, NI Transmission lines, UHV Shutter Actuators, Horizontal X-Ray Camera, RF Antennae, Radiation-cooled Limiters, and Tritium Recycling System.
- ensures that all pressurised equipment associated with the JET Machine has been designed, fabricated and tested in accordance with current national or international standards governing safety and relevant statutory regulations. All vessels are registered and classified and the Unit is responsible for liaison with JET insurers. To date, 70 pressure vessels have been installed on site.

- sets up the Quality Library which is divided into three sections:

- (a) Housing, reviewing and updating all standards (ASME, DIN, ISO, BS, AFNOR...), JET quality procedures and assembly procedures;
- (b) Collecting Contract documentation packages and producing reports after auditing;
- (c) Archiving contract packages and audit reports with location guides.

Multi-Pellet Injection Considerations

(P. Kupschus, K. Sonnenberg, M. Watkins)

For 'deep fuelling or refuelling' of the torus plasma, the injection of pellets of frozen deuterium, or alternatively tritium to beyond the $q=2$ surface at least has been considered. The intention is to introduce particles into the plasma which will not immediately participate in the edge recycling depending on the central particle confinement time, which in turn determines the requirements for the repetition frequency of the pellet injector and for edge pumping. It is anticipated that with this method the central density can be raised independently of processes clamping the edge density and that thermal instabilities might be suppressed. Experiments in recent years on other tokamaks have shown evidence in a number of cases where plasmas have been favourably influenced by pellet injection leading to claims of higher density limits, longer energy confinement times, higher $\langle n\tau_E \rangle$ values and impurity reduction even beyond dilution.

While the assessment of benefits for JET from pellet injection is underway, it is clear that the present state of experience is not sufficient to make firm predictions on plasma performance. However, it seems that JET might need larger pellets (up to 6mm diameter) and higher velocities than those presently available (4mm diameter and about 1.5kms^{-1} , respectively). So far, the best acceleration performance has been produced by pneumatic guns limited by the sound speed of ambient temperature hydrogen used as a driver gas. If hot hydrogen of several thousand degrees was being employed, velocities of up to 10kms^{-1} should be attainable. JET supports a proposal by, and the subsequent Article 14 contract (since July '84) with, the Risø National Laboratory, Denmark to use an arc heated gas gun and is looking for a partner to investigate the adiabatic compression heating method as an alternative.

Torus Division

(Division Head: M. Huguet)

Torus Division is responsible for the operation of the torus, the creation and training of operation teams, the planning of torus operation related activities and the rostering of operations staff. The Division controls and supervises all maintenance and assembly working in the Torus Hall and Basement. In addition, the Division undertakes development work necessary to improve the systems which form the basic JET device (magnets and

controls, vacuum system, baking plant, limiters, first wall, etc.).

The Division is structured as follows:

- The Division Head is assisted by a Senior Physicist who deals with matters related to programme definition which is carried out in close liaison with the Scientific Department. The Senior Physicist is also responsible for plasma control;
- The Torus Operations Group provides and trains operations staff. It also organizes and plans the operation and maintenance work. The Group is also responsible for safety and related activities such as permits-to-work, access control and fire detection and prevention;
- The Magnet Systems Group maintains and operates the coil systems together with all machine instrumentation. It also supervises assembly work in the torus during shutdowns;
- The Vacuum Systems Group is responsible for the vacuum vessel and all associated systems including the pumping system, the bakeout system and the interface with all components connected to the vessel;
- The First Wall Group designs, procures and installs in the machine, the limiters and components for the wall, such as protection tiles. The Group is also responsible for the discharge cleaning system and the gas handling and introduction systems.

During 1984, operational duties have drawn heavily on the resources of the Division. In addition to Session Leaders, Engineers-in-Charge and Control Room operators, the Division has provided on-call staff required to carry out special operations or repair particular equipment. Again this year, tasks related to wall conditioning (especially glow discharge cleaning) have been extremely demanding on staff involved, since these tasks had to be undertaken outside normal working hours and during weekends. As a result, overtime working reached a very high level. The commitment and dedication of these staff was rewarded as few failures were recorded and little operation time was lost due to torus systems.

In 1984, the main operational achievements credited to Torus Division staff were the following:

- The vacuum quality was good throughout and was maintained even after shutdowns when assembly work had taken place inside the vessel;
- Glow discharge cleaning proved to be a most efficient though simple wall conditioning technique. Covering the walls with a carbon layer (carbonisation) yielded encouraging results;
- Plasma control systems including position and current feed-back control were successful;
- The magnet systems operated reliably, up to the maximum design value for the toroidal field system, and above the design value for the ohmic heating coil system.

The Division was also active in the preparation and installation of new equipment on the torus. For this work, three shutdowns took place in January, March and October/November. These were hectic periods for Divisional staff, during which they had to install their own equipment and also interface with other Divisions working on the torus. The assembly work was successful and indeed all scheduled activities were completed on time. However, recommissioning following shutdown periods proved extremely difficult, mainly due to damage inflicted on jumper cables. The identification and repair of damaged cables was a long, difficult and frustrating task.

The major pieces of equipment installed in 1984, included the high vacuum rotary valve and the pumping equipment for the Neutral Injector Box at Octant No.8 (January), the graphite protection tiles on the inboard wall of the vacuum vessel (October), and the new mechanical supports for the vacuum vessel (October). A major improvement of the gas bake-out plant took place in November, with the installation of the new blower with its ancillary equipment. Work was also carried out on the limiters, gas introduction system and poloidal field coils and busbar system. This is described further in the following sections.

In addition to operation duties and assembly work, good progress was made on the development of future machine systems. Graphite protection tiles were designed for installation in 1985. Contracts were placed for the manufacture of the belt limiters and for the blackening of the cooling fins of these limiters. A great deal of effort was invested in the selection of the material for the belt limiter, the choice being between graphite and beryllium. The characterization of beryllium as a limiter material included heat load tests, the use of beryllium in the small Unitor Tokamak at University of Düsseldorf, F.R.G., and a large contract with USDOE's Oak Ridge National Laboratory to use beryllium limiters on the ISX-B machine.

Senior Physicists Activities

(M.L. Browne, M. Huart, H. Niedermeyer*, P. Noll, I. Piacentini, A. Santagiustina, J.R. Watkins)

* EURATOM-IPP Association, IPP-Garching, F.R.G

Plasma Position and Current Control System

The plasma position and current control system (PPCC) was initially described in the 1983 JET Progress Report and this has been further developed in the following aspects:

- The voltage range of the radial position control has been doubled by adding a second thyristor power supply, connected in series with the first one.
- The response speed of the stabilisation circuit for the vertical plasma position has been increased in a provisional way by enhancing the feedback loop gain for frequencies $>80\text{Hz}$. This measure was necessary in order to stabilize plasmas with an elongation ratio $b/a > 1.6$.

- Plasma current feedback control was introduced in September.

Specific studies have been performed on the vertical instability and the performance of the stabilisation circuit. These studies were initiated by an incident where the stabilisation limit was exceeded and the vessel was subjected to large vertical forces.

Apart from this incident, the position and current control system worked satisfactorily and plasmas of different elongation ratios $b/a < 1.6$, different sizes, and with currents up to 3.8MA have been produced.

Radial Position Control

This control system is based upon the measurement of the poloidal flux difference between the limiter radius, R_L , and the desired inboard radius, R_i , of the limiter magnetic surface (plasma boundary). R_i can be varied during the pulse by means of the control function $D\phi_R$ proportional to the plasma/wall distance. The feedback loop is enabled during the premagnetization phase in order to control the initial vertical flux at the start of the plasma pulse. During plasma formation at the beginning of the 'fast rise' phase, the feedback control of the radial position is not fast and sensitive enough to cope with rapid changes of the initial current channel. Therefore, a preprogrammed voltage is used to facilitate gas breakdown and initial current build up.

A reasonable feedback control of the plasma inboard radius R_i (and of its diameter $R_L - R_i$) is obtained from about 0.2s after the start of the discharge. An example is shown in Fig.5. This shows the inboard plasma wall

distance $DXIN$ as a function of time, which reflects the preprogrammed control function $D\phi_R$.

The plasma diameter is made to increase during the current rise. This expanding aperture scenario is applied in order to avoid skin effects and the formation of hollow current profiles during the plasma build up phase. Fig.5 shows also the feedback control error of R_i which is proportional to the flux error signal $DFRH(\delta\Omega_R)$. The feedback control error is typically $< 10^{-2}m$ during the pulse, when $I_p > 0.3MA$. There are systematic errors of a similar order due to imperfections of the electronics (offset voltages), imperfect compensation of toroidal field pick-up in the flux measurement, and due to poloidal field gradients ignored in these measurements.

In 1984, the second poloidal vertical field amplifier (PVFA 3/4), installed as part of the extended performance of JET, has been connected in series with the first amplifier (PVFA 1/2) in order to increase to about $\pm 4kV$ the range of controllable voltage at the vertical field coil. This enhancement was made in anticipation of experiments with large premagnetization and large initial loop voltage. A relatively large negative voltage of the vertical field amplifier is needed to prevent an early rise in vertical field caused by direct connection of the vertical field coil to the ohmic heating circuit. It was thought that a large voltage range would be beneficial for slowing down the speed of current disruptions. However, experiments have shown that large initial loop voltages must be avoided in order to reduce MHD activity during the current rise. Measurements have also been performed on the current quench time in disruptions before and after the increase in voltage range. There is an indication that current quench times increase on average for disruptions which evolve with a moderate speed ($\tau > 0.1s$). However, high current fast disruptions are hardly affected by external circuits, and are mainly limited by eddy currents in the vessel resulting from the plasma current decrease and the inward motion of the plasma. Therefore, it was concluded that the use of the second PVFA for radial position control was unnecessary. It was then decided that one of the two amplifiers would be used as a power source for active control of the plasma shape carried out in late 1984.

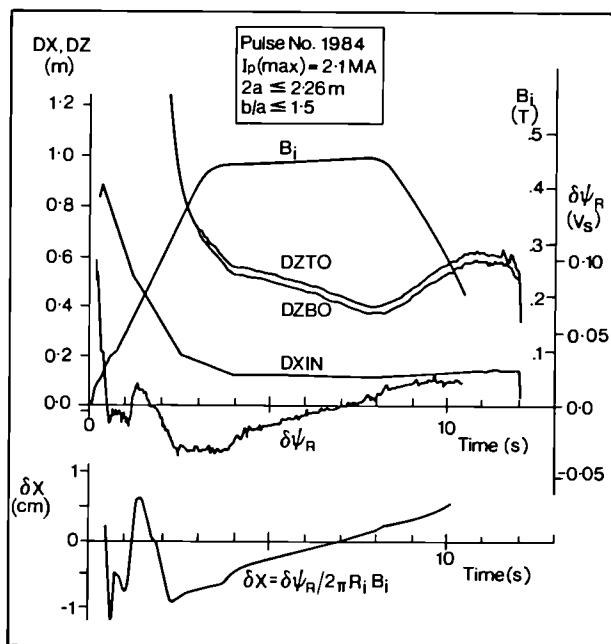


Fig. 5: Plasma/wall distances $DXIN$, $DZTO$, $DZBO$ at the inside, top and bottom, error flux $\delta\psi_R$, magnetic field B_i at the inside, and resulting control error δx of the position of the limiter magnetic surface (plasma boundary);

Stabilisation of the vertical position

Stabilisation limits

The feedback system uses the differential voltage between symmetric positions at radial position $R_m = 2.8m$ and vertical position $Z = \pm 1.7m$, which is derived from a combination of 6 integrated saddle loop and discrete coil signals, after differentiation in a proportional/derivative controller. A minimum feedback loop gain $G_o(\min)$ is required because the vertical plasma position is unstable without feedback, when the plasma elongation ratio $b/a > 1.2$. On the other hand, the loop gain G_o cannot be increased without limits to guarantee stabilisation, because unavoidable delays or phase shifts of the feedback circuit would lead to growing

oscillations of a medium frequency eigenmode. The range of stabilisation is approximately given by:

$$\gamma T_v < G_o < \left[\frac{T_v}{T_A} + \frac{T_v}{T_u} \right] (1 - \gamma T_A)(1 - \gamma T_u)$$

where γ = growth rate without feedback, typically in the range 50...150s for plasmas with elongation ratio $b/a \approx 1.4-1.7$.

T_v = effective vessel time for the penetration of radial poloidal flux (= 3ms).

G_o = voltage open loop gain without plasma (normally set = 1.0).

T_A = step response delay of the poloidal radial field amplifier, in voltage mode. (Experimental tests gave $T_A = 3.5$ ms).

T_u = sum of second order delays in the feedback loop. (e.g. due to the required filters and due to rate limiters, $T_u = 1.5$ ms, typically).

The maximum growth rate which can be stabilized theoretically is $\gamma_m = 1/(T_A + T_u) = 200s^{-1}$, and the loop gain would have to be chosen $G_o(\text{crit}) = T_v \gamma_m = 0.6$. Actually the loop gain is normally set $\approx 1.0 > G_o(\text{crit})$ in order to reduce the amplitude of perturbations in cases $\gamma < \gamma_m$.

The stabilisation has worked satisfactorily for plasmas with elongation ratio $b/a < 1.6$. An example is shown in Fig.5, where the plasma wall distances DZTO, DZBO at top and bottom of the vessel, respectively, indicate that the plasma is stabilized in the vertical direction with a displacement $|\delta Z| < 2$ cm.

Vertical Instability

During Pulse No.1947, the vertical plasma position became unintentionally unstable during the slow current rise, at parameters $I_p = 2.7$ MA and elongation ratio $b/a = 1.68$, before the intended current of $I_p = 3$ MA was reached. The instability started with growing oscillations at an eigenmode frequency, $f \approx 58$ Hz. Eventually the oscillation amplitude of the current in the radial field coil became so large that a protective trip on the radial field amplifier caused the coil voltage to fall to zero. The vertical instability evolved monotonically with an estimated growth rate $\gamma \approx 125s$. The effective current centre of the plasma moved downwards by about 1m. Then, the current decreased to zero within 30ms, and the current centre moved radially inwards as in a disruption.

The vessel experienced large forces as shown in Fig.6. It performed a rocking motion around an apparent rotation centre in the vicinity of the horizontal ports. Estimated deflection amplitudes at the vertical ports were about 1cm. At extended performance with $I_p = 4.8$ MA, such as instability could lead to forces up to 800t on the vessel. The vessel supports would break and the stresses at the vessel would be unacceptably high. Therefore, additional vessel supports were designed to restrain the radial motion of the large vertical ports and to provide a strengthened vertical anchoring at the horizontal ports. Ultimately, additional vertical supports at the 16 vertical

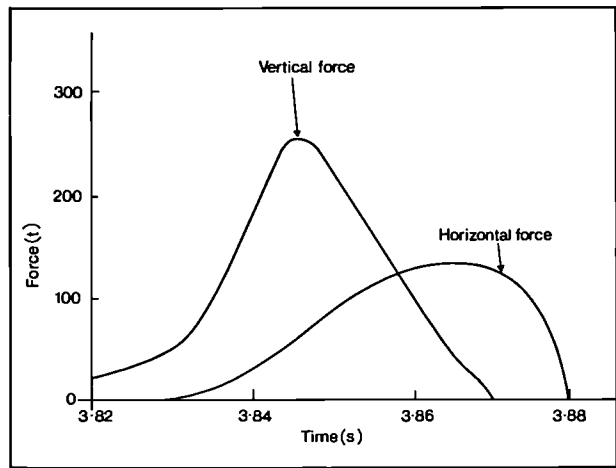


Fig.6: Vessel Forces in Pulse No.1947, ($I_p(\text{max}) = 2.7$ MA);

ports may become necessary, depending on the results of further investigations and stress analysis.

Studies of the vertical instability have been carried out at lower currents $I_p < 1.5$ MA. The instability was initiated by disabling feedback stabilisation at a time $t = 5.05$ s after the start of the discharge. Plasmas with elongation ratios $b/a = 1.24-1.54$ and at minor diameters $2a = 1.9-2.3$ m were made unstable, to explore the effect on the vessel forces and on the instability growth rate. Fig.7 shows an example of the movement of the effective current centre in a pulse with $I_p = 1.42$ MA, $b/a = 1.41$, and $2a = 2.26$ m. The forces on the vessel/plasma system were deduced from the observed growth rate γ , the displacement, and from the induced current in the radial field coil. In this example, the estimated normalized peak force was $F_{zV}/I_p^2 \approx 29t/(MA)^2$.

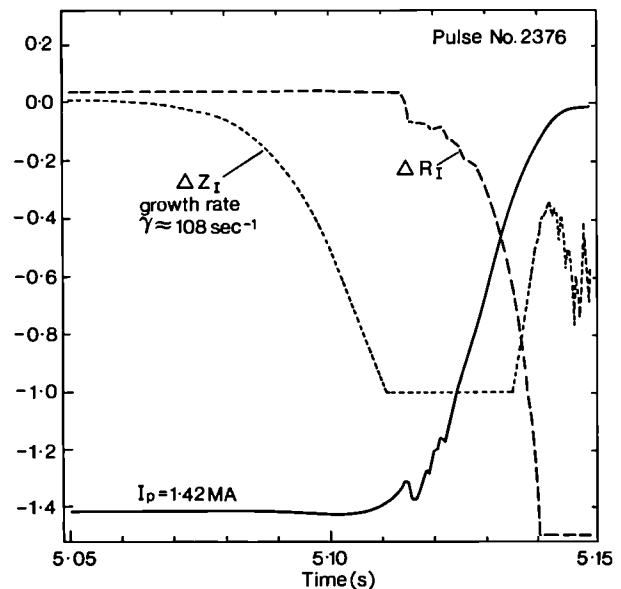


Fig.7: Displacement ΔZ_i , ΔR_i of the current centre in a pulse where the vertical position feedback is disabled at $t = 5.05$ s;

In general, the peak force increased with growth rate γ . The growth rate increased when, for a given structure of the external field, the plasma diameter $2a$ was increased. This could be attributed to the effect of the unsaturated shoulders of the iron circuit at top and bottom of the vessel. The growth rate is also a monotonic function of the quadrupole component of the externally applied magnetic field.

From the experiments performed, it was not possible to derive a reliable scaling law for vessel forces. This difficulty may be related to the observation that apart from the stalling force due to measured toroidal vessel currents, the plasma force balance requires the existence of poloidal currents crossing the plasma and returning through parts of the vessel. These poloidal currents have not been directly measured, and their parametric dependence is unknown. Further experiments with fully size low currents plasmas and low q -values are planned to simulate the behaviour at extended performance.

Test and improvement of the stabilizing circuit

The stabilisation range was tested with plasmas of moderate elongation ratio $b/a \approx 1.4$ and growth rate $\gamma \approx 108s^{-1}$ by application of a square wave perturbation at different voltage loop gains G_0 , and by observation of the damping rate of the excited eigenmode. The estimated stabilisation range was $0.4 < G_0 < 1.5$, for this case. The response characteristics of the radial field amplifier was tested separately and in detail. The step response time of the amplifier is 3.5–4ms, depending on amplitude. A response time $T_A \approx 2ms$ is possible, in principle, but a slower response was selected in order to make continued amplifier operation possible, in the situation that one half of the amplifier was turned into the freewheeling mode during a pulse.

The shortcomings of the stabilisation at large plasma elongations (in particular, the difficulties encountered in Pulse No. 1947) stemmed mainly from the relatively slow amplifier response. A provisional enhancement was obtained by the inclusion of a phase advancing element in the feedback loop, with characteristics $(1 + ST_1)/(1 + ST_2)$, where $T_1 = 1.9ms$, $T_2 = 0.22ms$. For example, previously observed damped oscillations in step response tests at normal loop gain $G_0 = 1$ and for plasmas with elongation $b/a \approx 1.4$ were suppressed. No serious case of vertical instability occurred after this modification. For the future, a genuine reduction of the amplifier response time and of the output voltage range has been planned by addition of a second amplifier unit.

Plasma Current Control

In most experiments, the plasma current was adequately controlled by suitable programming of the exciter control voltage of the poloidal flywheel generator converter. Plasma current feedback control was applied in Autumn 1984, using a proportional/derivative/integral controller for the plasma current error signal. Feedback is enabled during the slow rise and flat top phases, by control of the amplitude limit of the feedback signal. The feedback control is supported by preprogramming. Fig.8 shows

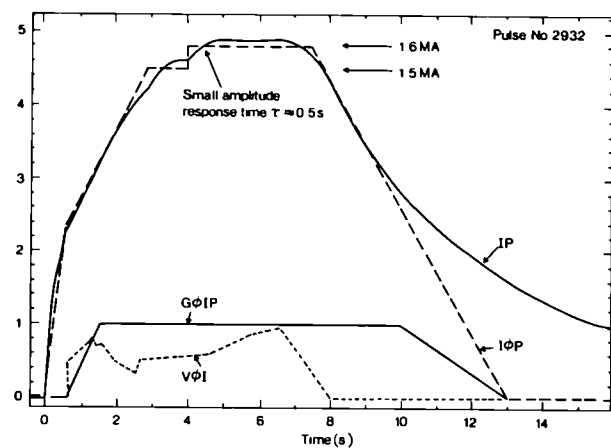


Fig. 8: Plasma current I_P and current reference $I_{\phi P}$ for a test pulse of the current feedback control, where $V_{\phi I}$ is the preprogrammed voltage, and $G_{\phi I P}$ is the function limiting the feedback signal amplitude;

the reference and actual plasma current during a feedback test. The observed small amplitude step response time $t \approx 0.5s$ agrees reasonably well with results from a system model. The control error is typically $< 5\%$, but no optimization has yet been made.

In the case of a disruption and current quench, the error signal increases exponentially and the flywheel generator would become unnecessarily stressed. Therefore the current control system has been linked to the plasma fault protection system (PFPS) in such a way that the preprogrammed control voltage and the feedback voltage are immediately reduced to zero upon detection of a disruption.

Torus Operations Group

(K. Adams, P. Chuilon, C. Conway, D. Cook, T.C. Dale, E. Daly, F. Erhorn, K. Fenton, B. Glossop, B.J. Green, N. Green, M.J. Hughes, H. Key, R. Rigley, R. Saunders, R. Thomas, W. Smith, D. Webberley)

The Torus Operations Groups' main responsibility is to operate the machine and this includes participation in the establishment of both the experimental and commissioning programmes and maintenance of adequate operation records. Outside operation, a team of shift technicians within the Group provides continuous surveillance of JET subsystems and building services. Eleven shift technicians (of a team which will ultimately comprise twelve) were recruited during 1984. The Group prepares and updates the three-week rolling commissioning and operation plan, organises the operations team and prepares system description and operation manuals and emergency procedures. In addition, the Group is responsible for the design, installation and maintenance of the Personnel Safety and Access Control System (PSACS), for the control of access to the Torus Hall and Basement, and for the design, installation and maintenance of the Fire Detection, Alarm and Suppression System (FDASS).

Table II: Time Periods spent in Various Activities

Time Periods Spent in Various Activities					
		1983		1984	
Period Type	Weeks	%	Weeks	%	
Shutdown (S)	9	32.1	21	40.4	
Commissioning (C)	8	28.6	14	26.9	
Tokamak T	11	39.3	17	32.7	
Total	28	100.0	52	100.0	

Table III: Analysis of JET Pulses Achieved

Tokamak Operation Period	1 June–July 1983	2 Oct–Dec 1983	3 March–May 1984	4 June–Aug 1984	5 Aug–Sept 1984
Tokamak Operation days	7	35	30	21	24
Tokamak Pulses	35	182	159	219	192
Commissioning Pulses	35	186	100	30	72
Average number of pulses per day	10	10.5	8.6	11.8	11.1
Average number of tokamak pulses per day	5	5.2	5.3	10.4	8.1
Average number of commissioning pulses per day	5	5.3	3.3	1.4	3.0

Torus Operations

(K. Adams, P. Chuilon, C. Conway, D. Cook, T.C. Dale, E. Daly, K. Fenton, B. Glossop, B.J. Green, N. Green, M.J. Hughes, H. Key, R. Rigley, R. Thomas, W. Smith)

Since the start of the JET operation programme, the periods of activity have been classified as follows (see Fig.9):

- (a) shutdown (S)
- (b) commissioning (C)
- (c) tokamak operation (T)

During shutdown periods, major installation of particular systems (e.g. additional heating systems, protective tiles for the interior of the vacuum vessel, and plasma diagnostic systems) was undertaken. Commissioning periods involved the testing of particular subsystems

sometimes in conjunction with others but never in the fully-integrated, tokamak operation mode. Some commissioning-type activity spilled over into tokamak operation periods, but the aim of this was to ensure reliable machine operation.

The distribution of time among these activities is summarised in Table II. During June 1984, some tokamak operation time was devoted to wall-conditioning by pulse discharge cleaning. The relative increase of shutdown activity in 1984 resulted from the significant work required for vessel preparation for Phase II operation, and that required for installation of RF transmission lines and antennae and the neutral beam injector system at Octant No.8.

The work within each tokamak operation period has been analysed (see Table III) in terms of numbers of JET pulses achieved. It should be noted that not every day of

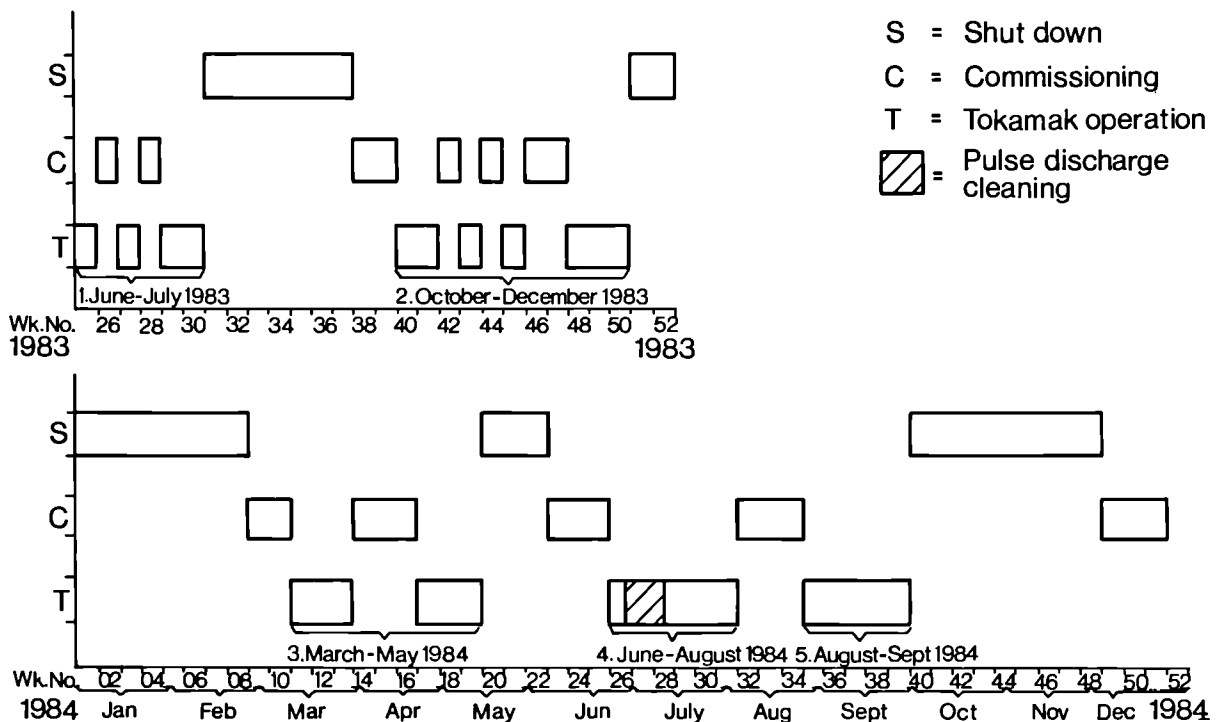


Fig.9: JET Operations Programme 1984

a tokamak operation week (see Table.II) was a tokamak operation day. Two major facts can be seen:

- the relative number of commissioning pulses in these periods has been significantly reduced;
- the average number of tokamak pulses achieved per day has been significantly increased although the number is still not high enough.

Clearly machine reliability must be improved before the projected number of JET tokamak pulses per year can be achieved.

Throughout the operation period, plasma current performance has steadily increased, until by the end of the 1984 operation a maximum current of 3.7MA was achieved. Fig.10 shows progress: early in 1983 most tokamak discharges were under 1MA, but by the end of 1984, most discharges were in the 2-3MA range.

During 1984 operational periods, the daily sessions normally lasted for 7 hours of operation with additional time taken in preparation and close-down (see Table.IV). On some occasions, extended sessions of up to 9 hours were worked. In 1984, there was no tokamak operation at weekends, in contrast to 1983, where some weekend operation had taken place.

During 1984, activities for Operations personnel were well-defined and appropriate procedures developed. Each session programme was defined in a pulse schedule prepared by the Session Leader, the Engineer-in-Charge and the Physicist-in-Charge within the guidelines established by a hierarchy of committees (see Fig.11). The Session Leader is responsible for achieving the programme goals which have been set for the session. The Engineer-in-Charge is responsible for the operation of the machine, for its protection and for the safety of Operations staff (see Fig.12). The Physicist-in-Charge is responsible for ensuring that all diagnostics required are operational and for collecting the relevant plasma measurement results to assist in the evaluation of the session's progress.

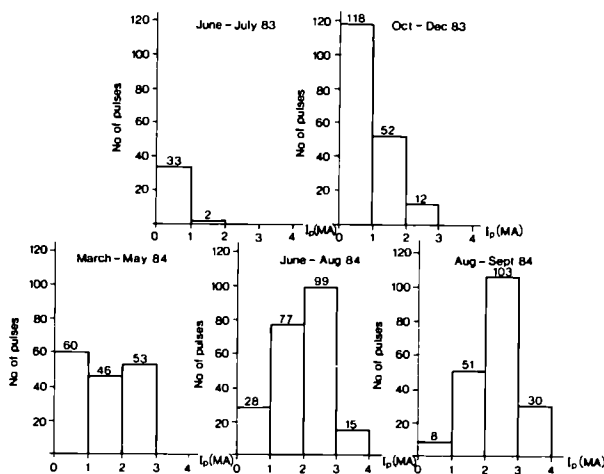


Fig.10: JET Plasma Current - Pulse Distribution 1983/84;

Table IV: Outline Programme for a typical Tokamak Operations Day.

TIME	MAJOR ACTIVITIES
07.45	CODAS: Duty Officer takes over from computer operator shift. Control room (machine and experimental) duty officers commence duty. Start preparation for the day's operation.
08.00	ENGINEER-IN-CHARGE: takes over from the shift technician, checks on status, and initiates the inspection/door closure routine. Operators A and B commence duty.
08.30	POWER SUPPLIES: Operation Engineer and assistant start duty. (On duty staff commence work in power supply areas J5, J4, J3, J1F).
08.45	CODAS test run complete. CODAS Duty Officer hands over the consoles to the Torus Division and Power Supply Division staff on duty. "CODAS READY STATE". Inspection/closure tour complete, and machine brought to the "TORUS READY STATE".
08.45 to 09.30	Pulse schedules for the day finalised. Prepare for the JET Dry Run.
09.30 to 10.00	Complete the JET Dry Run.
10.00 to 17.00	TOKAMAK OPERATIONS
12.45 to 13.15	CODAS & POWER SUPPLIES: Staff change over.
17.00	Session closed. Shutdown routine initiated. Lockup procedures initiated.
17.30	Lockup completed. Session Leader's meeting to discuss the day's results.
18.00	CODAS: Briefing, hand over to computer operators on duty. ENGINEER-IN-CHARGE: Hand over to the shift technicians.

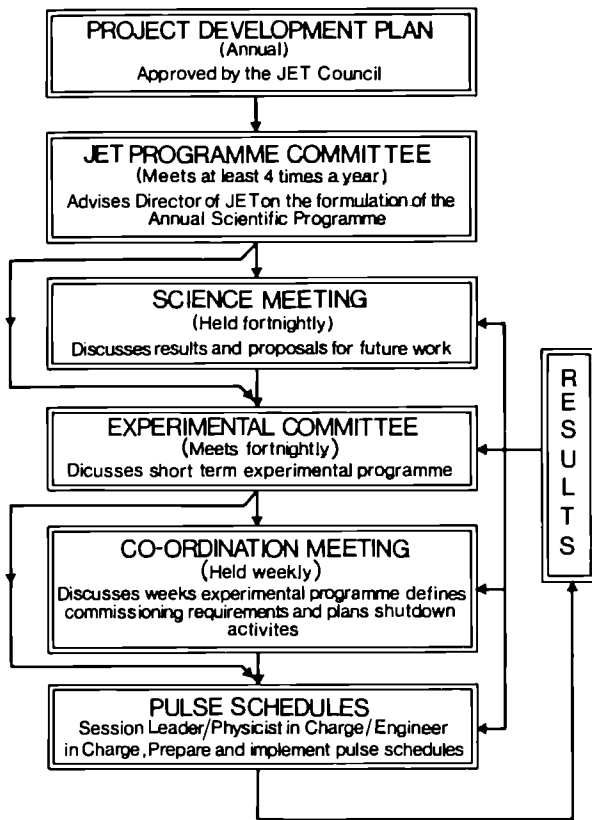


Fig. 11: Establishment of JET Operations Programme

The Engineer-in-Charge supervises the Machine Control Room which, in 1984, included Power Supplies Division Operations staff members who operated the HV pulses power supplies, and Torus Division operations staff members who monitored and controlled the other operational subsystems. CODAS staff operate the computers and maintained the CODAS/CISS part of the operation.

The Physicist-in-Charge supervises the Experimental Control Room which in 1984 included diagnostic physicists from Experimental Divisions 1 and 2, and members and the Theory Division and Physics Operations Group who assist in data acquisition and its interpretation. This operations team in the Control Building J2 was supplemented in 1983 and 1984 by Power Supplies Division staff in certain power supply areas. In addition, some on-site staff were 'on-call' to solve problems with systems, and some staff who were required only at certain times for specific 'other tasks' (such as, inspection and locking up tours of the Torus Hall, and the preparation of the gas introduction system). With the introduction of the shift technicians, it is planned to reduce the number of system Responsible Officers on-call. These specialist staff members will then be called out only in emergencies.

The shift-technicians man the JET control room 24 hours per day, monitor JET subsystem equipment and JET buildings for proper operation and take corrective

Fig. 12: Numbers of Staff directly involved in Operations

	On Duty			
	In J2	In P.S. Areas	On Call	Other Tasks
SENIOR DUTIES				
Engineer-in-Charge	1	—	—	—
Physicist-in-Charge	1	—	—	—
Session Leader	1	—	—	—
ROSTERED DUTIES				
Torus Operation Group	3	—	1	1
First Wall Group	—	—	2	—
Vacuum System Group	—	—	3	—
Magnet and Instrumentation Group	—	—	1	—
Power Distribution Group	—	—	1	1
Poloidal and Toroidal Group	—	2	—	1
Advanced Power Supplies and Systems Operation Group	—	—	—	—
Computer Operation Group	3	—	—	—
Computer and Control Group	2	—	—	—
Diagnostic Data Acquisition Group	1	—	—	—
Electrical and Instrumentation Group	—	—	2	—
Experimental Division 1 (average)	8*	—	*	—
Experimental Division 2	4	—	5	—
Theory Division	1	—	—	—
Physics Operation Group	1	—	—	—
Technical Services	—	—	1	—
Machine Services	—	—	1	—
TOTALS	28	3	17	6

*The number of staff rostered for duty or call depends on the experimental programme.

action when necessary. They undertake specific control Room duties during tokamak operation. During 1984, 11 out of a total complement of 12 shift technicians were recruited, the first one arriving in April, and the last two early in December. This permitted the progressive phasing out of JET staff from the Vacuum Group who were doing most of this work as extra duties, during shift technician recruitment and training. Training was essentially carried out on-the-job backed up by specialist courses run by JET Responsible Officers. On-the-job training allowed a quick handover of essential machine and silent-hours duties associated mostly with the vacuum system, but in 1984, this was backed up by strong on-call support. The shift is based on a six week cycle with two weeks set aside for standby duties (or daywork). This provides for coverage during holidays or sickness. Normally, two shift technicians would be on a shift, although this was not always possible during 1984, and so some staff, mainly from the Vacuum Group were called for shift duties. In early 1985, and particularly when the twelfth shift technician has started, it is anticipated that the shift technicians rosters will be fully independent, requiring no further coverage from other JET staff.

Description and Operation Manuals/Emergency Procedures

(P. Chuilon, B.J. Green, R. Rigley)

The description and operation manuals for the large electrical and mechanical integrated JET systems have been required for reliable and trouble-free operation of JET. These manuals form the basic documentation for training of the team who take responsibility for machine systems and building services.

Each document contains three parts: the description complete with the important schematic diagrams; operating procedures in local remote conditions; and procedures in the event of non-normal occurrences. JET has placed Contracts with two firms experienced in the preparation of such technical documents. Sixteen different manuals are initially foreseen. The documents available or nearing completion are: the JET cooling systems; the compressed air system; the electrical baking system; the Personnel Safety and Access Control System; the poloidal and toroidal field system instrumentation; and the gas introduction and glow discharge cleaning system.

Considerable progress has taken place in compiling a file for emergency procedures. The file so far contains six sections sub-divided to cover individual systems (i.e. (i) Building Services; (ii) Machine and General Services; (iii) Vacuum System; (iv) Diagnostics; (v) Testbed (vi) Area Standing Orders). In all, 24 procedures have been issued and more sections are in preparation. Those documents already issued must be updated regularly as systems are expanded or modified to suit operational requirements.

Operation Planning

(B.J. Green, R. Saunders, D. Webberley)

In 1984, planning work included the weekly preparation of a three-week rolling plan for operation and commissioning, assistance in the preparation and presentation of the longer term, outline operation and commissioning plan, and maintaining a detailed list of outstanding commissioning activities. Related tasks were the preparation of rosters, definition of duties and assistance with manuals and machine statistics.

The three-week rolling plan shows more detail than the outline plan, and takes account of actual progress. It is discussed at the weekly Coordination Meeting for Commissioning and Operations, modified, approved and distributed to appropriate Project team members for information. Outstanding commissioning activities are regularly discussed at this Coordination Meeting, their priorities assigned or modified, and the short-term plan during commissioning weeks appropriately modified.

A task which took considerable effort was the establishment of staff rosters. This involved preparation for Torus Division staff, and collection for all other Divisions and Groups involved in operation, to form a unified document for distribution to the Project team. Rosters were necessary for control room and other operation duties, including those of the shift technicians and of on-call staff. A list of Responsible Officers to be contacted in emergency-only situations was also prepared.

The definition of monitoring and surveillance duties for the shift technicians was another task undertaken. This involved drawing up check lists of items for regular inspection for correct operation, particularly during overnight and weekend hours. It required close liaison with system Responsible Officers and for most of the year, relied on on-call support. Associated with this definition of duties was the organisation of training courses for shift technicians, and preparation of emergency procedures and description and operation manuals.

Some time was also devoted to the preparation of machine operation statistics. This involved the collection of relevant information for all JET pulses and the extraction of statistics illustrating performance.

In the second half of the year, a small computer system was acquired, and has been used in most of the above activities. It has enabled daily rosters and commissioning lists to be prepared more efficiently as these are frequently changed, and it was used to store and calculate operation statistics. It has also been used to establish certain data bases, e.g. the schedule of cables and connections to the JET limb junction boxes.

Personnel Safety and Access Control System (PSACS)

(F. Erhorn, B.J. Green)

The details of this system were described in the 1983 Progress Report (EUR 9472EN). During 1984:

- the master key switch panel of the door status and

access control system was modified to improve its reliability;

- connections to CODAS and to CISS were made and tested so that the basic hardware interlock and CISS/CODAS back-up was brought into operation which prevents high voltages appearing on the coils and their busbars when access to the Torus Hall and Basement is possible;
- the warning system was installed and made operational;
- the emergency push button system was made operational;
- certain modifications were proposed following operational experience, (e.g. the warning light operation will be modified);
- door entry systems to the Torus Hall and Basement consisting of barriers and entry and exit identity card/dosimeter readers were installed but have not yet been made fully operational;
- a further element (a laser beam block) was added to the basic hardware interlock of PSACS, when a large (20J) pulsed ruby laser is positioned to fire from the Roof Laboratory into the Torus Hall.

Further door entry systems are being designed for the Roof Laboratory and Access Cell, and these should be installed in 1985. All PSACS equipment has been appropriately signed and a maintenance programme is being established. The first draft of a description and operation manual was prepared. Provision of several CODAS and CISS signals are needed before completion of the door status and access control system for Phase IV of the JET programme and the warning and emergency system will be extended to complete certain areas (e.g. the RF and neutral beam heating power supply areas in the J1 North Wing).

The System Reliability Service of UKAEA's Safety and Reliability Directorate (SRD) initiated a study on the reliability of PSACS. Discussions with SRD are continuing.

Fire Detection, Alarm and Suppression System (FDASS) (F. Erhorn, B.J. Green)

Detailed reviews of the existing fire alarm and detection system in the JET Buildings J1 (non-shielded areas only), J2, J3, J4 and J5, were carried out. The fire alarm and detection system for the J1 Torus Hall and Basement was designed, and as a result the existing J1 fire alarm control panel will be replaced to cope with the increased number of zones. Several important new features, (e.g. individual zone isolation and remote switching of alarm bell ringing type) have been included in the design of the new control panel.

A grid of point (optical) smoke detectors has been installed in the basement, and alarm call buttons (break glasses) and alarm bells have been installed in the J1 shielded area. Point smoke and heat detectors have been installed in the J1 service tunnel adjacent to the valve pit and in the valve pit itself.

The fire detection system for the Torus Hall and part of that for the Basement consists of units of the Very Early Smoke Detection Apparatus (VESDA) type. These units sample air and can detect with extreme sensitivity the particulate products of combustion. In both the Torus Hall and Basement, VESDAs will sample air in the ventilation extract ducts, and others will sample air outside the ducts.

Smoke tests were carried out in the J1P Power Supply Control Room to assist Power Supply Division in their choice of a fire detection system. This became necessary since it was decided to leave this room unmanned during operation in 1985. Further tests in other areas were carried out to determine whether existing fire detection was adequate and discussions concerning new requirements were also held.

The type and arrangement of fire extinguishers in the Torus Hall and Basement were reviewed and all will now be of the halon 1211 (BCF) type, which have now been delivered. The problems of fighting fires in the Torus Hall and, in particular, on the machine were reviewed and it was decided to install a hose reel at the top of the Octant No.6 tower which provides access to the top of the machine. This will be permanently connected to a halon 1211 supply cylinder at the bottom of the tower.

The problem of fighting fires in the basement was reviewed and a call-for-tender action was initiated to select a contractor to design, provide and install a gas (halon 1301(BTM)) flood system in 1985.

Magnet Systems Group

(D. Cacaut, G. Celentano, J.R. Last, S.J. Turley, J. van Veen, M.E. Young, J.W. Zwart)

The Magnet Systems Group is responsible for: maintenance and operation of the coil systems and structural components: maintenance and operation of the machine instrumentation and keeping instrumentation records: electromechanical safety of the machine-safety of personnel when machine assembly work is underway and checking and supervising all mechanical assembly work.

The toroidal field systems

Operation

In 1984, the toroidal field system was commissioned and routinely operated at the full design field value of 3.45T, for which the current delivered from the power supply is 67kA. A flat top time of 10s was used giving an energy delivered per pulse of 5000MJ - very close to the maximum design value of 5500MJ.

Instrumentation

The parameters which have been measured on the toroidal system are:

- inlet and outlet coil cooling water temperature. One measurement of inlet temperature is made and one measurement per coil (i.e. 32) of outlet temperature. The outlet temperature gives an

indication that the coil is functioning normally. It does not indicate the maximum copper temperature as after reaching maximum temperature the water is cooled by the outer part of a coil turn. The maximum water temperature rise was 30C;

- surface temperature of coil insulation. This is used during vacuum vessel baking to check that temperature rises are not excessive. These are limited by thermal insulation of the vacuum vessel and by the toroidal coil cooling system;
- radial expansion and vertical movement of coils. These measurements show electro-mechanical and thermal expansion effects and are in accordance with calculations. The maximum radial expansion measured was 2.7mm;
- rotation of upper and lower rings of mechanical structure. This is measured by the displacement of laser beams which strike mirrors mounted on the structure. This measurement has not been very satisfactory due to conical deformations of upper ring and difficulties in setting up the laser. The laser setting equipment has been improved and this system should be recommissioned in 1985. It is suspected that the conical deformations of the upper ring may be due to sliding joints between ring and collar sticking instead of sliding;
- vertical expansion of poloidal coil No.1. This is affected by the toroidal coils and causes vertical movement of the upper collar of the mechanical structure and hence the conical deformations mentioned above. The expansion of poloidal coil No.1 due to the maximum toroidal field is 2.6mm;
- relative displacements between mechanical shell octants. Some typical measurements have been made. As expected these movements are negligible i.e. a few microns.

Instrumentation which is installed but not commissioned includes strain gauges and crack detectors on the mechanical structure. This has not been completed due to shortage of staff to commission the instrumentation, and to collect and analyse the data. The instrumentation will be commissioned in 1985, before the machine reaches full performance.

Safety System

The short circuit detection system (part of the Direct Magnet Safety System (DMSS)) compares the voltages across adjacent coils and these should be identical. If a fault is detected the voltage from the power supply is removed, which is achieved by de-exciting the generator and switching off the static units. A crowbar switch, which would operate after a delay to allow partial generator de-excitation, has been commissioned but is not now connected because too many spurious trips have been generated.

These spurious trips have been generated during plasma disruptions or vertical instabilities when fast variations of poloidal radial flux take place. This is

believed to have a non-axisymmetric distribution due to the insulation gaps in the mechanical structure. The problem should be eliminated by rewiring the system in order to compare coils in similar positions relative to the mechanical structure. The frequency response of the detection system will also be reduced.

Maintenance

A complete survey of busbar joint resistances has been made during the year. Some high resistance joints have been detected and rectified. Joint resistances will be monitored during the non active phase of the machine to reduce the risk of problems in the active phase. Experience to date indicates that joint conditions are stable.

The Poloidal Field System

Operation and Improvements

The poloidal field coil system includes the primary circuit (Coil No.1) and the position and shape control circuits (Coil Nos.2,3 and 4). The primary circuit has been commissioned and used for plasma operation in the slow rise phase up to the full design current of 80kA. This value has in fact been exceeded and on one occasion was taken to 100kA (representing a 50% force overload). All displacements measured during this pulse indicated a sound behaviour of the coil, and the inspection after the event revealed no damage. This demonstrated that the design and construction are robust and have adequate safety margins. However, steps have been taken to ensure that such an event could not be repeated, as it could lead to fatigue problems.

Although the primary circuit has operated at full current in the slow rise phase, it has not been possible to use the full pre-magnetisation current, as it has been found that the initial rate of rise of plasma current must be kept low to obtain good quality discharges. This limits the acceptable voltage when the circuit breakers open at plasma start up. With the commutating resistor set to its minimum value (0.15 Ω , the pre-magnetisation current has been limited to 40kA. This gives a total applied voltage of 6kV (20V/turn) compared to the design value of 40kV.

To enable the full pre-magnetisation current (and thus full flux swing capabilities of the magnetic circuit) to be used, new busbars have been made to enable poloidal coil No.1 to be connected in series instead of parallel. These bars will be installed in early 1985. The full pre-magnetisation current will then be 40kA which will give 13kV total and 23V/turn with a 0.33 Ω commissioning resistor.

The outer coils have operated at currents up to 15kA in the case of the vertical field circuits. This current is dictated by the requirements of operation. Full design current will be reached when the machine operates with a fully heated maximum current plasma.

The shape of the plasma (i.e. ellipticity) was controlled by adjusting the number of turns on coils Nos.2 and 3 which are connected in series with coil No.4. This system

has worked as foreseen but, of course, the machine must be shutdown and the Torus Hall entered to change the turns.

The problem of vertical plasma instabilities due to uncontrolled plasma elongation has prompted a modification of the outer coil circuit so that the shape can be actively controlled. In the new circuit, coil No.4 is connected to one amplifier and provides vertical field and horizontal position control. Coils Nos.2 and 3 are connected to another amplifier and control the plasma elongation. Busbars for this new circuit have been manufactured and were installed in the October shutdown. The machine will start with the new configuration in 1985.

Instrumentation

The parameters which have been measured on the poloidal systems include:

- inlet and outlet coil cooling water temperature. The inlet temperature is common to all coils and the outlet temperature of each sub-coil of coil No.1 and of each pancake of the outer coils is measured. The temperature rises measured have been very small (not exceeding 15C) because even for coil No.1 the effective pulse length has been short;
- vertical expansion of poloidal coil No.1. The poloidal coil stack expands vertically (due to the Poisson's ratio effect) when the toroidal field is applied and contracts vertically (due to magnetic attraction forces) when the poloidal field is applied. It also expands due to its own temperature rise. The contraction at 80kA was 2.4mm and the expansion due to a 15C temperature rise was 1.6mm;
- radial expansion and vertical displacement of outer coils Nos.3 and 4. Measurements of radial expansion at four equi-spaced points on each coil show that the coils expand symmetrically about the vertical axis. The vertical displacements indicate deflection of supports and deflection of the coil due to bending between supports. Displacements measured have been small and in accordance with design calculations;
- currents and ampere-turns. The currents in the coil busbars and ampere-turns of the outer coils are measured using Rogowski coils (helically wound delay cable wrapped round the busbar or coils) and integrators. These measurements show that the coil system is behaving as expected;
- voltages across coils. These voltages are measured using resistor-capacitive potential dividers with a frequency response up to 20kHz. These measurements show that the coil system behaves as expected. The frequency response of the dividers on the outer coils will have to be lowered as the ripple frequency is higher than the sampling frequency and so give a random component in the measurement. A good frequency response is required for the inner coils so that switching transients can be measured;
- flux crossing the coils. The flux loops are mounted on the coils and measure the radial and vertical flux crossing the coil. It is intended to combine these measurements with coil current to calculate forces on coils but the software for this is not yet available;
- strains in coil No.1 support rings. Strain gauges are stuck on the coil No.1 support rings to measure vertical and hoop strain. These measurements show variations of strain due to both toroidal and poloidal fields. The strain due to toroidal field is less than expected and the strain due to poloidal field is greater. The extra strain measured for poloidal field may be due to magnetostriction.

Safety System

The short circuit detection system (DMSS) compares the ampere-turns (measured by Rogowski coils) of each pair of upper and lower coils. In the absence of a fault, these are equal and are balanced out in the detector amplifiers.

In the case of the inner coils, it was not possible to encircle these with Rogowski coils so only the radial fields between coils were measured, upper and lower coil pairs being balanced against each other. Unfortunately this system detected the unpredictable radial fields due to plasma disruptions and so generated spurious trip signals. It may be possible to prevent these spurious trips by reducing the frequency response to DMSS.

Due to problems of spurious trips and also because a lower operating voltage has been used, the crowbar switch (which was intended to short circuit the power supplies in the event of a fault) has not been used.

Maintenance

A survey of all the outer coil joint resistances was made during the year. These were compared with previous measurements and show that joint resistances are stable. Some progress was made in covering coil and busbar connections. Covers for other parts of the coil and busbar system have been designed.

Assembly work in the Torus Hall

The Group carries out overall supervision of all work in the Torus Hall during shutdowns. This includes issue of work permits, control of work and inspection of the machine at the end of a shutdown.

Access to the machine has been improved by installation of:

- (i) a bridge from an access tower to the upper poloidal coil No.4;
- (ii) a handrail for the upper coil No.4 walkway;
- (iii) a new stairway to the machine pit;
- (iv) access ladders for coil No.4 connection regions;

A new walkway for the upper coil No.4 is being made.

Vacuum Systems Group

(S. Baumel, B. Bignaux, D. Baker, C. Cacaut, W. Daser, D. Froger, K. Grabenstätter, J. Hemmerich, D. Holland, J. Orchard, R. Thomas, E. Usselmann.)

The main responsibility of the Vacuum Systems Group is to produce and maintain a high vacuum within the vessel, which includes the torus proper and the vacuum pumping system, the vacuum interface of components connected to the vessel, and also the gas heating/cooling plant and the electrical baking system. In addition, the Group provides a service to all Divisions for such activities as leak detection, operation and maintenance of vacuum equipment and instrumentation, and the supply of standard vacuum components.

Vacuum Performance

During shutdown, the Vacuum Group participates in all vacuum related activities inside the JET vacuum vessel and on attached systems, such as:

- establishment of clean working conditions including clean access control, supply of special clean conditions garments, supervision of all in-torus work;
- leak testing during installation of all equipment (e.g. major systems installed in 1984 were two R.F. heating antennae including vacuum systems, relocation of limiters, and carbon tiles for inner wall protection);
- clean up torus after completion of mechanical work by high-pressure hot water scouring. As previous experience during torus operation had shown chlorine contamination, and analyses of commercial detergents used had revealed substantial chlorine content, subsequent water scouring was performed with demineralised water only. The effectiveness of this procedure is expected to be revealed during restart in early 1985.

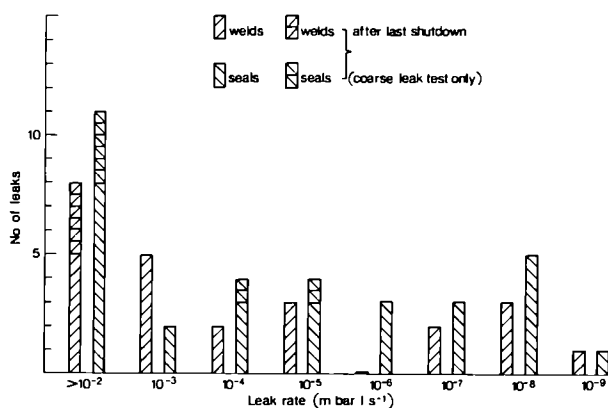


Fig.13: The number of leaks in the JET machine during the period March 1983 to December 1984. (20% of these leaks were found in the main Torus Vacuum System during or after a Tokamak operation period)

SKETCH SHOWING ADDITIONAL SUPPORTS OF ONE VACUUM VESSEL OCTANT (System repeated 8 times for complete Torus)

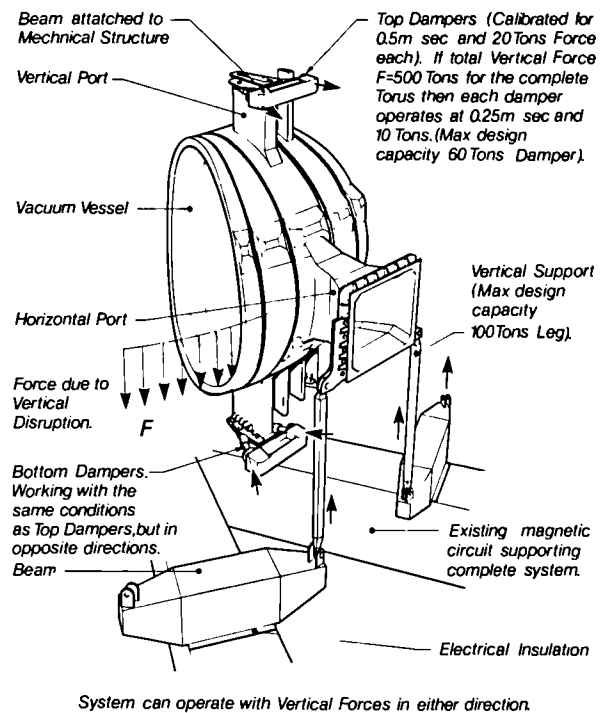


Fig.14: Additional Supports on one Vacuum Vessel Octant

Leak and Leak Detection

(T. Winkel, J. Orchard, D. Holland)

The JET vacuum vessel has more than 600 vacuum connections in the form of vacuum seals or welds with seals of diameters 32-1200mm, and welds from a few cm to 12m in length. Information on all the positions of these connections is stored in a computer data base with a location code and priority status. To aid leak detection, a list of vacuum connections can be produced at different levels of leak probability depending on proven reliability and number of previous successful tests.

Test gas is applied in different ways, namely:

- via spray tubes for inaccessible locations;
- via spray nozzles in the remote handling flanges;
- via a spray gun directly on to the weld or flange.

The detection of the test gas is facilitated by a Helium mass spectrometer leak detector in the backing line of one of the torus turbo-molecular pumps.

If the torus is in the UHV range, one turbomolecular pump backed by the leak detector is sufficient to maintain the vacuum so that all the gas is passing through the leak detector for maximum sensitivity. Leaks of the order of 10^{-9} mbar $1s^{-1}$ can be detected, with responses of a few seconds for large leaks and up to approximately 1 min for the smallest.

Since the assembly of the machine, about 60 leaks have been located in the torus connections or directly related equipment. Of this number, 60% were found in seals and

40% in welds uniformly distributed over the leak range from 10^{-2} – 10^{-9} mbar $1s^{-1}$. Leak rates larger than 10^{-2} mbar $1s^{-1}$ could not be determined with reasonable accuracy (see Fig. 13 for statistics).

Additional Supports of the Vacuum Vessel

(W. Baker, D. Cacaut, C. Froger)

Pulse No. 1947 (May 1984: elongated plasma, $b/a = 1.68$ and $I_p = 2.7$ MA) underwent a fast vertical instability, so that the feedback control system did not have sufficient time to respond. As a consequence the plasma shifted suddenly downwards producing a total force of approximately 260t on the vacuum vessel. Since the vacuum vessel is supported solely around its outer periphery, each octant turned around its fixing points, producing high stress resulting in small permanent deformations. As a consequence, it was decided to install additional supports capable of resisting a vertical instability of twice the value described above without causing further damage.

The principle of the system (shown in Fig. 14) is to limit and cushion the rotational movement of each octant. Each octant is mechanically attached to the magnetic circuit by means of vertical legs fixed to the main horizontal port (defining the rotational axis). Absorption of rotational motion is achieved by means of hydraulic dampers attached to both top and bottom vertical ports and fixed to the mechanical structure.

Contracts were placed during August 1984 for the manufacture of the various components. At the same time, a test programme to define the characteristics of the hydraulic dampers was in progress. The hydraulic seals used in the construction of the damper were required to withstand pressures of 0 to 700bars and to operate at maximum radiation levels. Assembly of the system onto the torus was started in mid-October and completed during the shutdown period.

Rotary High Vacuum Valve (RHVV)

(B. Bignaux, C. Froger)

The RHVV is a valve which has been specifically designed by JET for the purpose of isolating the Neutral Injection System from the torus. It operates on the principle of a vertically suspended rotor able to turn through 90° giving open and closed positions. Tightness in the closed position is provided by 2 Helicoflex seals, one on the torus side the other on the Neutral Injection side and pumping between. The first valve was installed on Octant No. 8, at the beginning of 1984, commissioning took place. At the manufacturer's workshop, the valve was rotated to check it opened or closed in the correct position; and it was Helium leak tested with 1bar helium pressure on one side and a detector on the other side (for which a leak rate of <10 mbar $1s^{-1}$ in both directions was observed. At JET, the valve was baked in the oven to 350C, and leak rate remained unchanged. It was then installed on Octant No. 8, and in the open position, the valve was electrically baked to 500C. After retesting, the leak rate was unchanged.

Opening the valve is permitted only if the rotor of the valve is deflated, and closing the valve only if the rotor is in the closed position (pressure 4.7bars). Rotor position, vacuum and pressure are checked for proper sequence by means of a microprocessor from which the RHVV can be operated step by step or automatically.

Spare Octant

(M. Walravens)

In the event that one of the machine octants must be removed, months of work will be saved by using a spare octant as a replacement. Therefore, it was decided to modify the existing prototype octant to bring it up to the standard of the vacuum vessel octants. The main alterations being carried out are: fitting four new bellows assemblies and two U-joints; modification and reinforcement of the bellows protection plates and the rails used for their fixture to the rigid sectors; electropolishing of the rigid sectors and port inner walls; and fitting diagnostic ports.

The old bellows units have been removed from the prototype octant. Dimensional surveys of the sectors have shown that their D-shaped profiles were acceptable. The major part of the work on the rails and bellows protection plates has been completed. The sectors are now in the process of being electropolished. The method employed on this octant is different to that of the previous series octants. In those cases, the procedure was to electropolish the various plates and sections before they were formed into the octant sectors. As this octant has already been fabricated and is formed of five sectors, it is necessary to electropolish each sector as a complete unit. The major technique being used is the 'mobile cathode method'. The sector is positioned on a suitably angled plate to form an electrolyte container and the inner wall surface is electropolished. A mobile cathode mounted on rails travels around the inner perimeter electropolishing the surface as it passes. Two of the five sectors have now been completed.

The octant re-assembly and leak testing at the manufacturer's should be completed in mid-1985. It will then be baked at 525C and leak tested in the JET furnace.

Baking Plant

(S. Bäümel, W. Daser, K. Grabenstätter, J.L. Hemmerich, R. Thomas)

During 1984, the gas baking plant was operated for 3824 hours. The operating temperature was at 250C for 60% of the operating time. Most of the JET discharges were performed at this temperature. A smaller amount (10%) were carried out at 150C. The remainder were equally distributed drying runs at 100C (after shutdowns) and baking to 300C (after drying runs). Throughout 1984, the gas baking plant was operated with a small provisional blower (volume flow rate ~ 100 m³ s⁻¹) with air as the heat transport medium. After detection of a small interspace to main volume leak of 10^{-7} mbar $1s^{-1}$ in June 1984, the plant was operated with pure N₂, maintained by a continuous purge gas flow, with an oxygen content below the detection limit ($<0.1\%$).

Starting with the shutdown in October 1984, the final blower, a single stage radial turbocompressor (rotor diameter 1m, speed 5300rpm, helium volume flow rate $25\text{m}^3\text{s}^{-1}$) was installed and commissioned. The gas baking plant was operational in December with nitrogen as the process gas. After completion of leak testing, the plant will be operated with helium as process gas offering the following advantages:

- low Z, i.e. relatively large interspace to main volume leaks would not affect plasma parameters;
- no activation and ease of decontamination are of particular interest for the JET Active Phase.

Pumping for A₀ Antennae

(E. Usselmann)

The two RF A₀ antennae which have been installed at Octant Nos.2 and 6 each have a small high vacuum pumping unit to provide sufficient pumping capacity to run the RF antennae in a workable vacuum. The Group was involved in the design, manufacture, tests and installation of the controls of these units. The design requirements followed closely the principles of the main torus vacuum pumping system. Each unit consists of JET standardised components, which are a 500s^{-1} turbomolecular pump, an all metal high vacuum pendulum valve, an all metal forevacuum valve, a vent valve and pressure gauge units consisting of Penning and Pirani gauge heads.

The unit control logic which establishes internal operation sequences and safety interlocks, if required, is executed by the JET standard microprocessor operated controller. The pumping unit can be operated by local commands from the control cubicle or by remote commands through CODAS. The forevacuum required for roughing and backing of the turbo-pumps is provided by the backing crown of the Torus pumping system.

Tritium compatible pumping system

(J.L. Hemmerich, T. Winkel)

Oil tests

During the first year of operation, it became evident that the performance of the existing high vacuum pumping system was fully adequate for the operation of the JET device. Provided that the installed turbomolecular pumps are compatible with tritium operation, the existing high vacuum system requires no further modifications for the JET Active Phase.

Testing of a complete turbopump set would have been rather bulky, requiring a high tritium inventory (each pump contains about 1l of oil) and would possibly have been inconclusive (as post mortem analysis of mechanical failures on highly tritium contaminated parts would have been extremely difficult). Therefore, a simpler approach was chosen: a micro-viscosimeter was developed and built to permit viscosimetry on a 1cm^3 oil sample in contact with ICi of tritium. Measurements will start in early 1985 (in collaboration with a Tritium Group in Jülich, Institut für Festkörperforschung).

Forevacuum System

During operation of JET, the forevacuum system will consist exclusively of cryopumps: a cryocondensation panel for the hydrogen isotopes, deuterium and tritium, followed by a cryosorption trap for ^4He (produced by the thermonuclear reaction) and ^3He (added for RF minority heating). For roughing operations, mechanical forevacuum pumps will still be required; a system consisting of tritium compatible mechanical pumps (Roots Blowers and Normetex Pumps) is presently being studied.

Vacuum Laboratory Activities and Services to other Divisions

(T. Winkel, J. Orchard, D. Holland)

The tasks of the vacuum section can be divided into several main activities and responsibilities:

- supervising the installation of vacuum systems onto the torus;
- vacuum integrity of the torus vacuum and its peripherals;
- services for other Divisions;
- development of new torus vacuum related equipment;
- development of vacuum systems for active phase.

The Vacuum Section is responsible for maintaining and monitoring the condition of the torus vacuum and supervises all installation work on the vacuum vessel.

Whenever possible systems are vacuum baked and leaktested prior to installation onto the torus and retested after final installation. Man-hours spent on services for Divisions are approximately: Torus Division 40%, Experimental Divisions 25%, Neutral Beam Heating and Radio Frequency Heating Divisions each 15%, and 5% for Fusion Technology Division.

Further activities have seen the development of:

- viscosity meter for turbomolecular pump bearing oil contaminated with tritium;
- piezoelectric dosing valve;
- Saes Getters pellet appendage vacuum pumps;
- noble gas leak detector in case helium cannot be used as tracer gas (usage of He-3, D-2, T-2).

The section contributed a large extent in the setting up and manning of a continuous shift system to monitor the behaviour of the vacuum related systems since the first day of operation. Since all vacuum systems have proven to run without major difficulties, the task has not been taken over by shift technicians and the section is now only involved for on-call duties.

First Wall Group

(K.J. Dietz, A. Boschi, J. Booth, G. Celentano, L. Grobusch, B. Glossop, K. Sonnenberg, H. Jensen, P. McCarthy, G. Israel, U. Schargitz, R.L. Shaw).

The First Wall Group is responsible for the definition, design and procurement of the components of the first wall. This includes basic studies related to the use of new

low-Z materials, the development of manufacturing technologies and the testing of materials and designs in an environment as close as possible to the environment existing in the JET machine. The Group also defines and implements wall conditioning techniques such as glow discharge cleaning combined with bake-out. In addition, the Group takes responsibility for the gas introduction system which comprises the gas handling system in the West Wing of J1 and the introduction modules in the Torus Hall.

Gas Introduction System

(A. Boschi, H. Jensen, P. McCarthy, U. Schargitz)

With two introduction modules at Octants Nos.2 and 6, the gas introduction system worked reliably. The fast valves performed throughout well. By April the dosing valves were fully tested with CODAS and some problems were found due to the interfacing with the computer. A third module, at Octant No.4, was put into operation in February 1984 and was used for discharge cleaning.

During the October 1984 shutdown, all four gas introduction modules were assembled on the Torus at new locations, on top of the pumping chambers, Octants Nos.1 and 5. The entire system had been fully re-commissioned with CODAS by the year's end.

The performance of the dosing valves was improved in two ways: mechanical vibration was reduced by a slight modification of the needle and the linearity of the response was improved by adjusting the thyristor driving electronics, as shown in Fig. 15 where the movement of the valve needle is plotted versus the analogue driving signal. The plasma response (H_α light intensity and plasma density) to a rectangular waveform driving signal is shown in Fig. 16.

Discharge Cleaning

(K.J. Dietz, L. Grobusch, F.C. Schüller*, A. Tanga*)

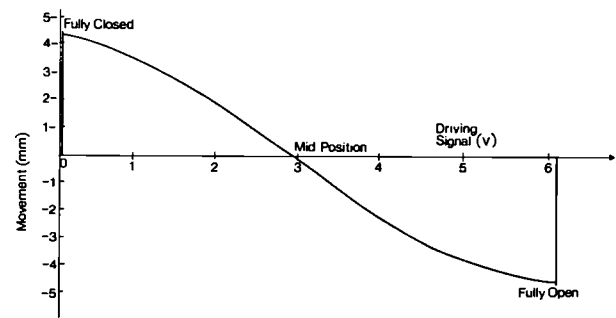
* Scientific Department

Two methods were employed for conditioning the vacuum vessel: Pulse Discharge Cleaning (PDC) and Glow Discharge Cleaning (GDC). The mechanism of impurity removal for both methods are identical (chemical reaction of low-Z impurities with atomic hydrogen to form volatile components). PDC has the advantage of higher removal rates compared to GDC (about a factor ten under JET conditions), whereas the latter can be operated continuously without the need of activating magnetic fields.

(i) Glow discharge cleaning

Two electrodes situated inside ports of the vacuum vessel were used. Each was coupled to a RF transmitter (100W, 9.7MHz) and to a DC power supply (600V, 10A), the vessel being the cathode of the discharge which was operated in hydrogen at pressures of about 5×10^{-3} mbar and a DC-current of 8A. The temperature of the vessel was typically 250C-300C. A cleaning run of 72 hours allowed plasma operation even after opening the vessel. Eventually base pressures (vessel temperature 250C) of

Fig. 15: Movement of the dosing valve needle versus the analogue driving signal;



2.5×10^{-7} mbar for hydrogen and $< 2 \times 10^{-10}$ mbar for impurities could be achieved. During the period of plasma operation, the cleaning was mainly carried out during week-ends.

The plasma behaviour at higher densities was mainly dominated by radiation from carbon and oxygen. Z_{eff} values were around six and 80-100% of the input power was radiated.

(ii) Pulse discharge cleaning

Conditions similar to a 'Taylor Discharge Cleaning' were used after optimising the impurity removal. Pulses of 0.5s duration with a repetition rate of three per minute and currents of 40kA were used, at a toroidal field of 0.15T. The discharges were carried out in hydrogen with a pressure of about 2×10^{-4} mbar and a vessel temperature 250C.

Twelve thousand discharges over a period of two weeks were performed. During this time the water partial pressure, as measured between discharges, decreased one order of magnitude to about 10^{-8} mbar. The changes in plasma behaviour after the period were modest, the Z_{eff} values dropped to 4.5, the density limit increased by 20-30%. The radiated power was still 80-100% of the input power.

(iii) Carbonisation

Following the results of a test carbonisation in JET during August 1983 and work in TEXTOR, GDC in JET

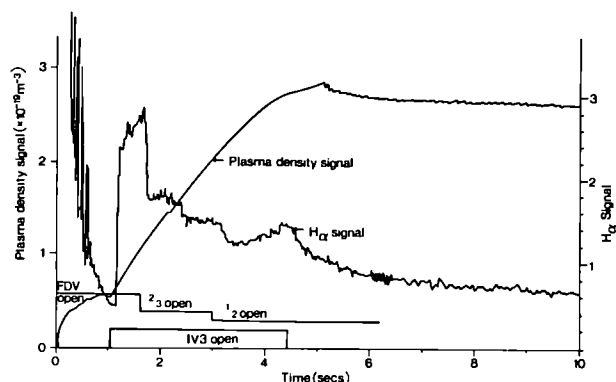


Fig. 16: Plasma response (H_α light intensity and plasma density) to a rectangular waveform driving signal on the valve.

was carried out in a mixture of 3% methane in hydrogen. This process was applied for six hours, providing a coverage of the wall by 10-50 monolayers of carbon. This resulted in a well defined change in plasma behaviour: Z_{eff} values decreased to 3 and at lower densities, only 50% of the input power was radiated. At high densities the power losses again approached 100%, the main contribution being the radiation from carbon and oxygen. Under these conditions the radiation from metallic impurities became negligible.

It is not clear whether the carbonisation process resulted in a coverage of the surface of 10-50 monolayers of carbon or whether diffusion of carbon into the wall limited the amount available. More systematic studies are needed. To that purpose, following the experience in TEXTOR, it may be necessary to carbonise at lower wall temperatures (200C) and higher methane concentrations (10%). Up to now only two electrodes out of four available have been used. The other two, due to their different geometry, only operate down to pressures of 2×10^{-2} mbar. Further work will be required to improve this behaviour.

Graphite Limiters

(K.J. Dietz, G. Israel)

Four graphite limiters have been used in JET operation. Each limiter is straight in poloidal direction and has a length of 80cm. It is curved in the toroidal direction with a projected width of 40cm. The limiters were evenly distributed at the midplane of the vessel at its outer circumference. During operation the limiters were viewed by infra-red cameras.

The limiter withstood power loads of up to 1.9MW for 5s duration, at which the surface temperature reached values above 1500C. Fig. 17 shows an infrared picture of the limiter during a discharge together with a photograph. Post-mortem analysis revealed that there was virtually no damage on the limiter tiles, but that metallic impurities could be found on the surface. This relates especially to constituents of the vacuum vessel (nickel, iron, chromium) resulting from operation, and molybdenum as a consequence of the manufacturing process. For 1985 operation, the limiter tiles were exchanged for new ones without this contamination.

The load on the limiters is now approaching the design load (350 W cm^{-2}), especially as it is not distributed evenly. During 1985, four additional graphite limiters will be installed, and the tiles taken out of the machine will be cleaned and used on the additional limiters. This arrangement permits retention of a set of tiles for one complete limiter, and in addition, six limiter tiles can be used for further surface analysis.

Nickel Limiters

(K.J. Dietz, G. Israel)

During the 1983/84 operational period, four out of the eight nickel limiters fitted in the vacuum vessel developed leaks in their water cooling circuits. The leaks were directly connected to the torus vacuum. The leak rates ranged from 10^{-6} – 10^{-3} mbar s^{-1} , increasing

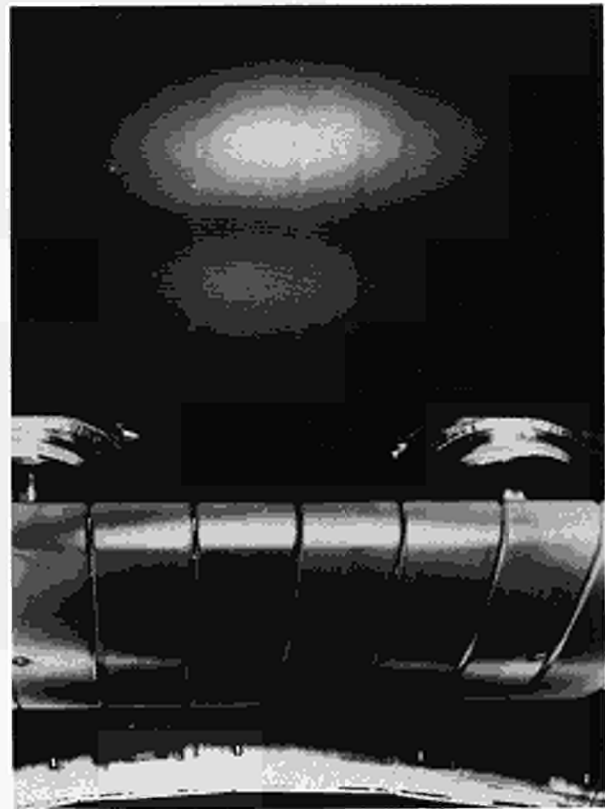


Fig. 17: Infra-red picture of a graphite limiter during a discharge and a photograph of the limiter after operation;

with time. In order to continue operation, the faulty limiter cooling circuits were pumped out and subsequently sealed. The leaking limiters were removed as soon as a shutdown allowed access to the vacuum vessel.

Investigations on the faulty limiters revealed that cracks occurred in the transition welds (electrobeam welds) on the limiter faces. The transition is made between copper chromium (CuCrZr cooling elements) and Inconel600 (cooling water tubes). Eight such cooling elements and one cooling water manifold form one limiter face. Stress calculations showed that the transition welds should withstand temperatures up to 300C (maximum vacuum vessel temperature), but it could not be excluded that thermal fatigue was the reason for failure. To check this, one thousand heat cycles between 50C and 350C were carried out on test pieces with the result that no indication of thermal fatigue was detected.

The critical transition area was redesigned, and the main changes are:

- transition (friction) welds in the tubes instead of plate-to-tube welds, which permit testing between manufacturing steps;
- reduction of water tubes material thickness to allow more flexibility;
- mechanical decoupling of water inlet and outlet on cooling elements by introducing long slits between connections.



Fig. 18: Prototype belt limiter segment under fabrication

These changes are being implemented for the four spare limiters.

Stress calculations showed a thermal stress reduction by a factor of two. The cooling elements will be heat cycled 10 times between 50C and 350C followed by as leak test before assembly proceeds. The modified limiters will be available from July 1985. Until then, four nickel limiters of the old design are still in the vacuum vessel.

Belt Limiters

(J. Booth, G. Celentano, K.J. Dietz)

At the beginning of the year, the design of the radiation cooled belt limiter was completed, so that it was able to withstand long and powerful discharges. Most of the technical parameters and features were settled in order to proceed with tender action in February 1984.

The belt limiter consists of two rings arranged in the toroidal direction of the vacuum vessel above and below the equatorial plane. Each belt limiter is made up of sixteen equal segments shaped to the toroidal radius and the segments of each ring are electrically and mechanically connected to each other. The mechanical connection allow for tangential displacements, in order to compensate the thermal expansion of the vacuum vessel during bake-out operations. For the cooling system, each limiter segment is connected with the corresponding segment of the other ring through the RF antennae. Thus, there are 16 inlet and outlet water pipes providing the cooling water for the whole limiter and RF antennae.

Each limiter segment contains 109 fins welded directly to the water pipes, between which will be placed limiter plates of suitable materials, which are likely to be either graphite or beryllium. The radiant fin surface for each segment is about 4.5m² with a heat load of 1.3MW during a pulse. The water flow is 7ls⁻¹ at a pressure of 6bars. Each limiter segment is intended to be replaced by remote handling. Design and manufacturing methods are being developed to ensure excellent interchangeability of each segment.

A remote handling assembly procedure has been drafted, in collaboration with the Remote Handling Group of Fusion Technology Division, who will procure all special tools needed for the various operations. For the interface RF antennae/limiter, a special welded pipe joint and relevant welding procedure has been developed by the Remote Handling Group. Several constraints were imposed on the limiter design by pre-existing torus fixtures or by diagnostic requirements. Thus, four special limiter segments have been designed to retain adequate viewing angles for the X-ray detector diagnostic.

A comprehensive dimensional survey of the inner geometry of the vacuum vessel and relevant parts has been undertaken in order to facilitate the design of suitable attachment points for the limiter rings and ensure concentricity with the toroidal field system, which is necessary to maintain a uniform azimuthal thermal load on the limiters. Tender action was started in February, and completed in the middle of June. The contract was placed and signed in August-September.

Stringent quality requirements were imposed for this component, as it directly faces the plasma inside the vessel. Therefore, the first stage of the contract was to design and develop jigs, fixtures and gauges to enable achievement of the dimensional accuracy required, and then to set up a production and quality control organisation that ensures the necessary high quality and reliability of the components. Fig. 18 shows the prototype limiter segment under fabrication.

Blackening of Be-tiles and Ni-fins for belt limiter

(K. Sonnenberg)

The side surfaces of the beryllium limiter tiles would be blackened by an anodising process in chromic acid. This process provides coatings with an emissivity of about 0.8, sufficient for radiative cooling of the tiles. Simulation experiments performed for thermal fatigue of beryllium showed that the coatings survived 6500 heat cycles without damage.

A contract has been placed for blackening the nickel fins of the belt limiter by plasma spraying. A low pressure spraying technique would be employed for better adhesion and lower porosity of the coating.

Tests have been performed to optimise the plasma parameters and surface preparations for the special application:

- distortion due to grit blasting has been minimised;

- He/H₂ mixture instead of argon (high Z impurity) has been employed. The ratio for He and H₂ has been varied to optimise the degree of melting of the particles;
- different coatings of Al₂O₃ and TiO₂, with and without bonding layers, have been studied. They all show a bonding strength of about 50N mm⁻², as specified by JET;
- thermal fatigue tests will be performed on coated nickel fins.

Test of Beryllium Limiters in Tokamaks

Only two low-Z materials can be envisaged with thermomechanical properties suitable for use in connection with the belt limiter: these are carbon and beryllium. Carbon has been used extensively as a limiter material in a variety of tokamaks, whereas no experience existed for beryllium. To study its performance as a limiter material and to investigate the plasma characteristics, experiments were set-up in the tokamaks UNITOR (University of Düsseldorf, F.R.G.) and ISX-B (ORNL, U.S.A.).

Sputtering and Hydrogen Retention of Be

(K. Sonnenberg)

A contract has been placed for a systematic study of the sputtering properties and the hydrogen retention of beryllium S65-B, which is envisaged as most suitable for JET applications, as follows:

- (a) Sputtering of Be by hydrogen, deuterium and helium has been studied as a function of energy, temperature, dose and angle of incidence: Sputtering yield for hydrogen is about 2×10^{-3} ; for deuterium 3×10^{-2} and 10 for helium. No dose dependence and only a small temperature dependence has been found. Also the yield does not change with energy by more than a factor 2-3;
- (b) Hydrogen retention has been measured after implantation at different temperatures, with different doses, energies and angles of incidence. Also thermal release measurements after low temperature implantations have been studied up to 650C;
 - (i) the amount of hydrogen retained (trapped) in Be increases with energy because the range of the particles increases: following room temperature implantation, (e.g. with 500eV deuterium) a maximum of about 10^{17} d/cm² can be trapped;
 - (ii) angular dependence can be understood in terms of the reduced projected range of the hydrogen for non normal incidence;
 - (iii) after low temperature implantation the hydrogen is released in two stages at around 200 and 480C. The amount released in the first stage increases with decreasing energy from 50% to roughly 80%;
 - (iv) the hydrogen retention as a function of implantation temperature is similar (somewhat

higher) to the amount retained after room temperature implantation plus annealing at the higher temperature: for an implantation temperature of 300C a maximum of about 10^{16} d/cm² was trapped for an energy of 300eV.

Beryllium experiment in UNITOR

(K.J. Dietz, K. Sonnenberg)

UNITOR is a small tokamak with the following characteristics: major radius 0.3m, plasma radius 0.1m, toroidal field 1.7T, plasma current 50kA, pulse duration 50ms, and central electron density $2 \times 10^{19} \text{m}^{-3}$. Two beryllium rail limiters with an area of $3 \times 6 \text{cm}^2$ facing the plasma were introduced. The power load on the limiter was 2kW/cm^2 , and 1500 discharges were made under these conditions.

Although only rough diagnostic methods were used, it can be stated that the discharges were improved. The loop voltage dropped and the discharge duration increased. The iron, chromium and nickel content of the plasma was reduced by more than one order of magnitude compared with the results obtained by using other limiter materials (graphite, Al₂O₃, Ni etc.). Also the number of disruptions were considerably reduced, as was the plasma resistivity.

After opening the vessel, the beryllium deposition on the wall and on the various components was studied. No volatile beryllium dust was sampled. The beryllium was washed out by diluted nitric acid until smear and scratch samples showed no further contamination of the wall. Surface studies on the Be limiter revealed a strong contamination by oxygen and chromium, nickel and iron indicating that high Z impurities may still have effected the plasma and that the wall was not completely covered with beryllium. For this reason beryllium evaporators will be employed in a further experiment to obtain a complete low Z coverage of the wall in UNITOR. The evaporator will be used also for in situ coating of graphite limiters with beryllium, as such limiters may be a possible alternative for JET.

Beryllium experiment in ISX-B

(K.J. Dietz, K. Sonnenberg)

The experiment was specified for a deuterium fluence of 10^{22}cm^2 and a rise in limiter temperature of 600C during a discharge. This corresponded to about 3000 beam heated discharges. The limiter was designed for a power flux of 2.5kW/cm^2 for a duration of 0.2s. A set of standard parameters was established with major radius 0.94m, minor radius 0.22m, elongation 1.2, toroidal field 1.4T, plasma current 120kA, line average density $4.5 \times 10^{19} \text{m}^{-3}$, and injected power 0.8MW. The operational envelope was surveyed by scans of plasma density and current, and spectroscopic measurements were carried out to assess the impurity behaviour of the plasma.

The characteristics of ohmically and beam heated plasmas were as good as those obtained earlier with titanium-carbide coated graphite limiters. The radiation

was dominated by impurities released from the wall, and mainly low-Z impurities (oxygen, carbon, nitrogen) contributed to the observed $Z_{\text{eff}} \approx 3$. The beryllium content in the plasma (centre) was 0.07%. Under these conditions the load to the limiter was 2.2kW/cm² (beam heated IMW total power). Under these conditions, no limiter damage was observed.

Since the plasmas were wall dominated, attempts were made to cover the walls with beryllium. High power discharges with limiter loads exceeding 4kW/cm² (melting limit) were performed, and the limiter surface was heavily melted. During this operation the radiation from impurities in the plasma centre (oxygen, nitrogen, carbon, nickel, titanium) dropped by a factor of four and low-Z impurity radiation in the plasma edge by about ten. The radiated power from the plasma decreased by a factor of two. The beryllium content in the discharge was about 2% and a strong getter effect was observed.

With the damaged surface, about 2500 discharges at reduced power loads (2.5kW/cm²) were performed. Local evaporation of beryllium took place at hot spots on the rough limiter surface and the getter effect continued. Melting was not observed and the limiter surface did not change considerably during these tests. The plasma performance with respect to density limits, confinement times and Z_{eff} values was comparable to those obtained earlier with titanium or chromium gettered discharges.

These tests have shown that beryllium is a prime candidate as a limiter material. A potential disadvantage is its toxicity and low melting point (compared to graphite). However, the load test has shown that, even with a heavily melted surface, thousands of reproducible discharges can be performed. Beryllium has proved to be a good getter material, it is the only low-Z material which can be used (under JET conditions) simultaneously as both a limiter and a getter.

The method used for evaporating beryllium in ISX-B (i.e. melting of the limiter during discharges) was crude. This resulted in a most uneven distribution of beryllium on the vessel. For the tests over five months, about 100 monolayers were deposited near the limiter and about 10 at other locations. For the strong effect observed, even the deposition of 100 monolayers seems to be small. To study the behaviour of a beryllium gettered plasma it is planned to introduce in UNITOR evaporators which allow the deposition of 3-5 monolayers at the walls before discharges with the beryllium limiter are attempted.

It is still an open question whether it would be possible to use beryllium coated protection tiles (graphite) or even a beryllium coated graphite limiter in JET. This would combine the better thermomechanical properties of graphite (about a factor of three for thermal shock) with the advantages of beryllium with lower hydrogen retention (about a factor of three at 300C), negligible porosity, absence of chemical reactions with hydrogen, simple conditioning methods, and its prospects as a getter material. Very little is known about a graphite-beryllium system and studies need to be undertaken.

Thermal fatigue tests on beryllium and studies for a actively cooled limiter

(K. Sonnenberg)

A major part of the ISX-B experiment was the thermal fatigue test of the beryllium limiter. In contrast to the heat load condition in JET (250W/cm², 15s), only short pulses with much higher power could be applied in ISX-B. Since the thermal stresses and their distribution will be quite different for both cases, a contract was placed with Sandia National Laboratory, U.S.A., to perform simulation tests under JET relevant conditions using beryllium limiter tiles similar to those envisaged for JET. The test is not yet completed but the first set of samples survived 6500 cycles without any structural damage, and in which only small hair cracks (1mm deep) were developing after 3000 cycles.

Some small study contracts have been placed for the development of actively cooled limiters, which will be required in case radiation cooled limiters are not sufficient. The main problem is the development of bonding techniques for Be to the heat sink material (Cu, CuCr). The following results have been obtained:

- (i) by optimising filler material, brazing time, temperature and pressure the main problem of high temperature vacuum brazing, namely brittle intermetallic phase formation was minimised. A bonding strength of 200N/mm² has been achieved;
- (ii) hot isostatic pressing (HIP) has been studied as it allows lower temperatures (500C), avoiding the problems of intermetallic phases and conserving the good mechanical properties of the heatsink material CuCr. For the combination Cu-Be the HIP-technique only works with an intermediate layer of silver. The bonding of this layer to Be has been found strongest employing ion-sputtering. Bonding strength of about 190N/mm² was achieved but the reproducibility is not yet sufficient and requires some further tests;
- (iii) another technique, which has the advantage of low process temperatures and in contrast to i) and ii) could be employed for rather complex geometries of limiters, is by forming the watercooling structure by electroplating copper on the back of the beryllium plate. The best results (200N/mm²) were achieved for Be coated with a thin silver layer by ion-sputtering. Two test modules (50mmx100mm) with electroformed water channels on the back have been prepared for testing for thermal fatigue in an electron beam facility;
- (iv) Plasma spraying of thick beryllium layers onto a copper substrate has also been studied. The usual problem of high porosity and low heat conductivity of such coatings was overcome by a subsequent HIP treatment of the beryllium resulting in a very interesting new type of

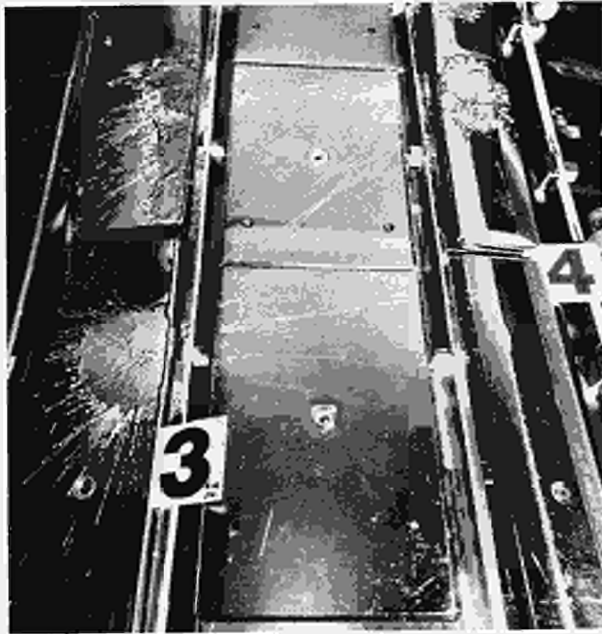


Fig. 19: Inconel protection tile showing effect of runaway electron bombardment.

beryllium (extremely fine grained). The method still suffers from intermetallic phase formation during the HIP treatment (700C) which needs further investigation (e.g. using intermediate silver layers).

Wall Protection

Damage on inner wall Inconel tiles

(K. Sonnenberg, B. Glossop)

There are two kinds of damage: (i) is due to runaway electrons (as the damaged areas are radioactive) and (ii) must probably be attributed to disruptive plasma touching the tiles.

- (i) counting the number of photo-neutron spikes (associated with the impact of runaway electrons on the wall) as well as the number of melted zones on the tiles a total of about 50 runaway electron events must have occurred. As shown in Fig. 19, the melted zones can be described as semicircular shallow craters on average 1mm deep and area about 20cm². Most of the damage is observed on inner wall midplane tiles and those which have a leading edge sticking out from the rest appear to be particularly vulnerable. Many tiles received several runaway electron impacts. In some cases, the tiles became distorted due to the first impact and as a result the bent ends were heavily damaged by subsequent electron impacts.

The conclusions drawn from the damage dimensions and appearance are:

- a total amount of melted Inconel was about 800g;
- assuming a temperature of the melt between the melting and boiling point of Inconel a

deposited energy density of roughly 100J/cm² was estimated;

- part of the melted Inconel was driven off the tiles probably due to an internal pressure as indicated by the appearance of the remaining melt after resolidification;

- a small angle of incidence must be assumed for the runaway electrons. As the high energy of runaway electrons and the energy deposition should be rather homogeneous within the range (1-2cm) of the electrons, deeper craters would be expected otherwise.

Since the energy density deposited by high energy electrons decreases proportionally to the material density, a much lower temperature would be expected for graphite (100C) or beryllium (500C) tiles. Experience from Doublet III shows that, even for graphite, severe damage can occur due to fracture by thermal stresses. This problem could be solved by using tiles specially designed for low thermal stresses or by employing fibre based graphite. Such an approach would also prevent distortion of the tiles.

- (ii) The other kind of damage is characterised by a thin (0.1mm) melted layer visible on almost all tiles. Tiles from the upper (lower) half of the vessel are mainly damaged on the left (right) side of the tiles. The damaged zone is always covered with a carbon layer of about 50-100nm thickness. This last result indicates particularly that the damage is due to plasma touching the inner wall during disruptions.

Graphite Tiles

(R. Shaw)

Post-mortem surface analysis of the limiter tiles has revealed the presence of wall material. One contributor to this contamination is the inboard wall of the vessel, where the most severe plasma-wall interactions occur causing evaporation of metal. To inhibit this source of metallic contamination, it was decided to cover the inboard wall of the vessel with graphite.

Design of this protection began in early December 1983 and contracts for both the graphite tiles and mechanical supports were placed in April 1984. The large number of graphite components involved (968 individual tiles) and the need to ensure a very high surface purity necessitated the provision of new outgassing facilities which led to a small delay in delivery. Preassembly of the graphite tiles and supports began on site in mid-September and installation in mid-October. The latter being completed within 6 weeks.

The design of both the protection for the outboard wall at Octant No.5, where the neutral beam from Octant No.8 impinges, and the extension of the inboard wall protection along the octant joints, effectively providing protection to the entire vessel, was completed in December 1984. It is planned to install both these protections in the Summer shutdown 1985.

Power Supply Division

(Division Head: E. Bertolini)

Power Supply Division is responsible for the design, installation, operation, maintenance and modification of all power supply equipment needed by the Project. The main JET Power Supplies System, its schematics, principal characteristics and design performance have been described in some detail in previous Annual Reports (EUR-JET-AR1-5) and Progress Report (EUR-JET-PR1).

The initiation and magnetic confinement of plasma in the JET device is achieved by routing and phasing of output from high-power electric supplies to the poloidal switching circuit and to the magnetic field coils on the machine. Power is taken from the CEGB 400kV system and from rotating machinery. During 1984, new supplies for the static thyristor rectifiers and invertors have been installed and commissioned and the rotating generators have achieved improved performance at full design speed. New busbars from the power modulators in the North Wing will facilitate operation with active plasma shape control in 1985. Amplifiers PVFA 1-2 will be used

for this purpose, proving their versatility in usage and control.

Power Supply Division is also responsible for: distribution of medium voltage power to the experiment; electrical building services, scheduling and contractor interphase for cabling on the JET device; high voltage distribution at 3.3kV, 11kV, and 33kV and for receiving power at 400kV from CEGB and at 132kV from SEB. The Division provides an around-the-clock on-call engineer to restore electrical supplies, when faults occur.

Due to unpredicted plasma performance, demands on power supplies during 1984 have in some cases not conformed to the modes of operation and to the specifications expected, when equipment was ordered. At times, the pulsing rate of the machine has been reduced by power supplies fault alarms caused either by malfunction, fault alarm signal transmission or by over stressing of equipment (e.g. by excessive demands on speed of reaction). It is hoped that 1985 will show further improvement in overall reliability. However, as some components start to wear, maintenance will require increased attention.

T A B L E V Status of Power Supply Subsystems at end of 1984

STATUS		SUBSYSTEM
Brought into operation	1	Toroidal Field Static Unit TF2
	2	Poloidal Vertical Field Amplifier PVFA 3-4
	3	Poloidal Radial Field Amplifier PRFA 3-4
	4	RF Auxiliary Power Supply (Temporary)
	5	RF Preionisation Unit Power Supply
	6	PINI Testbed HV and Auxiliary Power Supply and Protection Unit.
Ready for operation	7	PINI HV Power Supply 2-9
	8	PINI HV Protection System 2-5
	9	PINI Auxiliary Power Supply 2-3
	10	PINI Snubbers 2-5
	11	RF AC/DC Power Supply Unit 1
	12	Busbars for Shaping Field Power Supply
Being installed, commissioned	13	PINI HV Protection 6-7
	14	PINI Auxiliary Power Supply 4-5
	15	PINI Transmission Lines 2-5
	16	PINI Snubbers 6-9
	17	PINI SF6 Tower (First)
	19	3rd 400/33kV Transformer
	20	33kV and 11kV and 415V Distribution (Extensions)
	21	Cabling of Diagnostics on JET device
	22	TF Busbar Filter
	Being Manufactured	23
24		PINI Auxiliary Power Supply 6-9
25		PINI Transmission Lines 6-9
26		PINI SF6 Tower (Second)
27		RF Auxiliary Power Supply
Being designed, specified	28	PVFA Busbar Filters
	29	Safety Key Interlock System for HV Areas

The successful completion of Phase I of JET (Ohmic Heating Phase) was achieved to a great extent by dependable operation of the power supplies. Considerable effort was expended in streamlining the control of amplifiers and generators to accomplish the required reference profiles. Divisional personnel have contributed substantially to improved control and performance of experimental pulses.

During 1985, the need for further power supplies and passive components (e.g. filters and reactive power compensators) will be studied for installation in 1986 and thereafter. Table V presents the status of contracts for the procurement of major power supply components at the end of 1984.

During 1985, reconnection of the transformer coils from a parallel to a series arrangement will be more in line with the voltage-current characteristics of the poloidal generator and switching circuit. This is expected to allow longer plasma pulses without exceeding the critical generator current limit of 100kA. As experiments have progressed, new power supply enhancements and modifications have been initiated, such as the filtering of the power supply voltage, rearrangement of the static unit amplifiers for plasma elongation control and a re-assessment of the poloidal switching circuit.

The increasing number of power supplies of differing characteristics introduces a progressively greater responsibility role for the Division. This will be further emphasised during 1985, when major additional heating power will be introduced. This increased work within the Division has been shared across the groups according to expertise and experience.

Safety and Access Control

(K. Selin, D. Smart (Consultant))

Procedures have been specified to ensure safe access for work or inspection to the many high voltage power supply areas. The 33kV circuit breakers in J5 Substation, the disconnect-switches at the loads and equipment related to the flywheel generators in Building J3 are equipped with key interlock systems. These systems will be integrated and extended to include the load areas of static units, switching and damping circuits, protective inductor enclosures and switch platforms whereby conditions of safe working will be ascertained.

In cooperation with Torus Division, conditions have been defined for safe access to the Torus Hall and Basement. For any type of access, the busbars feeding JET coils must first be earthed and the 33kV circuit breakers and the 11kV generator excitation breakers either temporarily opened, permanently tripped or withdrawn. A system has been developed whereby the Power Supply Engineer and the Operator in the Machine Control Room are in control of and certify the required safe conditions for the pulsed power supplies. Neutral Injector and RF power supplies are being successively transferred from the commissioning stage to be under the command of the J2 Power Supply Engineer with respect to the high power 33kV supply control.

In cooperation with Joint Safety Services, work has been undertaken to meet the Electricity Safety Regulations for power distribution and for experimental areas and to tie these to the JET Safety at Work system. Safety tours are regularly carried out and improvements made to conform to relevant safety rules. As installation of new equipment, commissioning and operation of the JET device has progressed, strict ruling of personnel access and crane usage has been enforced.

Power Distribution Group

(J. Paillere, D. Halliwell, G. Marcon, G. Murphy, A. Terrington, G. Wilson, N. Walker, L. Zanelli).

The activities of the Group can be split into four main areas:

- Extension work and lay-out modifications;
- Maintenance and improvements;
- Services to other Divisions;
- Liaison with EURATOM-UKAEA Association, Culham Laboratory, U.K.

Extension Work

The bulk of the extension work has been for the 400kV and for the 33kV substation.

The third 400kV/33kV transformer

The third transformer, installed to provide enhanced security for the pulsed supplies in the event of a transformer failure, is similar to the two existing ones. This transformer arrived on site in mid-May, erection was completed in July, when the tank was filled with oil. Installation of auxiliary equipment and connection of control cables were completed by October.

In December, the capacitive voltage divider installed on SGT1A was partially tested. This divider, which is connected to the 400kV capacitive bushing of the supergrid transformer, provides a 100V signal to the Harmonic Analyser (which is installed in the CEGB 400kV substation relay room). The harmonic analyser measures the harmonics which might appear in the CEGB transmission system.

400kV substation

This work, funded by JET, is carried out by CEGB and progress is monitored in Joint Coordination Meetings. It consists of extending the 400kV busbars and installing a 400kV disconnector and links to control the third transformer. The civil works started on site in May and were completed in September. The electrical works started in August and should be completed in January 1985. Testing and commissioning of the connection to the third transformer will take place during Summer 1985.

The 33kV Distribution System

Installation and partial testing of the third busbar system took place during the year and was completed in October. This system can be connected in triangle to the two

existing ones when only one transformer is used. It is made up of one incomer, 2 bus-couplers, 6 outgoing feeders and a spare cubicle. Two feeders supply two NI modules, and four feeders supply eight AC/DC convertor systems for RF heating. The NI modules are connected through a single disconnecter, and RF units are connected through a double load disconnecter.

Modification of connections to the exciting distribution were carried out on TF2 unit, PVFA and PRFA system and NI auxiliary power transformer.

The 11kV/3.3kV/415V distribution

A new 11kV/415V transformer (3.15MVA, 8% short circuit voltage) was ordered. Following manufacture, factory tests took place in December. It is designed to provide the intermittent supply necessary for the RF auxiliaries.

Further modifications were undertaken on the 415V distribution. These included supply and installation of primary boards, section boards and cabling related to the extension of auxiliary power to the 33kV substation and to the RF system; and various detailed modifications to existing supplies.

Maintenance and improvements

400/33kV Substation

Certain spurious signals have tripped the 400kV breaker and this led to an investigation of the optical fibre control system. Modifications of several control cards and to the systematic installation of protective diodes across the 48V control relays were undertaken as a consequence.

During the same period, the inverter units supplying the AC control voltage to the transformers failed in succession, and their output voltage regulators were modified. The overall control system is still under observation and left passive, but to make sure the installation was properly protected, the existing hard-wired back-up protection of the transformers was extended and tested. In addition, the transformer CODAS interface was simplified.

33kV Distribution System

During maintenance of the breakers, it was noted that one of the spouts suffered oxidation in a systematic way. The manufacturer's opinion was sought but no immediate solution was available. However, further degradation of conditions followed, in which ozone production was evident and corona noise was heard on racked-out breakers.

An urgent investigation showed extensive tracking between phases, which was cured by replacement of the isolating plates, modifications to the spout attachment and installation of additional internal heaters. In addition, the hard-wired logic was modified to suit requirements.

Maintenance Contract

The Group also supervised 8-9 contract electricians carrying out day-to-day repairs, modifications and maintenance.

Services to other Divisions

The Group undertakes general electrical installation work for other Divisions consisting essentially of installation of cables, cable trays and supports. This also includes the installation of terminals and connection of instrumentation and power cables, and the installation in ducts of fibre optic links etc.

During 1984, about 1000 cables, totalling about 100km in length, have been pulled, tested and connected. A major part of this work was carried out for the Scientific Department to fulfil their diagnostic requirements.

Liaison with EURATOM-UKAEA Association, Culham Laboratory

The Agreement involving electricity supply from JET 33kV distribution system to EURATOM-UKAEA Association Culham Laboratory was revised and agreed between the respective managements in August. The amendment specifies that up to 10MW of power may be drawn by UKAEA, Culham Laboratory, at any time (subject to certain restrictive conditions). Pulses drawn from this system (less than 50MW instantaneous power but power greater than 10MW for 1s) require notification to and agreement from JET.

Poloidal and Toroidal Power Supply Group

(M. Huart, O. Buc, D. Corbyn (Consultant), T. Eriksson, J. Goff, L. Mears, A. Moissonnier, C. Raymond, A. Skinstad, C. Wilson).

The Group has responsibility for the power supplies to the poloidal and toroidal field systems which includes: the poloidal field generator-convertor (PFGC); the toroidal field generator convertor (TFGC); the two toroidal field static units (TFSU1, TFSU2); the two vertical field amplifiers (PVFA 1-2, PVFA 3-4); the two radial field amplifiers (PRFA 1-2, PRFA 3-4); and the Ohmic Heating Circuit.

The Group's activities with the above equipment includes: procurement, installation and commissioning of power supply equipment; assistance in the operation and commissioning of the JET coils; modification and improvements as required (to achieve higher reliability, etc); and maintenance and trouble shooting.

Progress achieved during 1984 is summarized below.

Procurement, Installation and Commissioning of Additional Power Supply Equipment

Toroidal Field Static Units (TFSU)

The second stage of the TFSU was installed on Site in 1983. The equipment was commissioned under local control on dummy load with currents up to 67kA for several seconds. Short circuit tests were performed to prove the protection circuits. The interface signals to and from the Central Control System were commissioned ready for operation on the JET coils. This sequence of tests was necessary as implementation of the central interlock system (CISS) had made it difficult to locally operate the equipment on the JET coils. Indeed, this

interlock defines windows, related to a general timing system, during which pulsing is allowed. TFSU2 was commissioned on the JET coils in May 1984.

Poloidal Vertical Field Amplifiers (PVFA)

The second stage of the vertical field amplifiers (PVFA 3-4), required as part of the extension to full performance, were installed on site in early 1984 and commissioned in local control on an inductive dummy load (prototype P1 Coil). The configuration chosen for load operation was a series connection of the two modules (PVFA 1-2) with the second module (PVFA 3-4) giving a capability of +4.6kV/-3.6kV at 25kA (for 25s). The series operation of the two modules was commissioned in local control on the inductive dummy load in May and was commissioned on the JET coils in June.

Poloidal Radial Field Amplifiers (PRFA)

The second stage of the radial amplifiers (PRFA 3-4), required as part of the extension to full performance, was installed on site during the first half of 1984 and commissioned in local control on an inductive dummy load. The configuration chosen for load operation was a series connection of the two modules (PRFA1-2 and PRFA3-4) giving a capability of +4.6kV to -4.6kV at 2kA. The series operation of the two modules was commissioned in local control on dummy load in November and on the JET coils in December.

Power Supply Smoothing Circuits

The operation of AC/DC rectifiers on the JET coils causes voltage ripples which, in turn, creates induced currents in the vacuum vessel. An RC filter was chosen to smooth the TF Circuit in view of the variable frequency of the FGC voltage ripple. The contract for the procurement of the filter and associated control was released in August. The installation of the support structure and part of the RC filter was carried out during the Autumn shutdown. Installation of this equipment will proceed during 1985.

A combination of an RC damper arm and RLC tuned arm was selected for the filter of the vertical field amplifiers. Procurement of long delivery items, such as capacitors, will proceed at the beginning of 1985.

Improvement and modification of existing equipment.

Flywheel-Generator-Converter Systems (FGC)

FGC commissioning identified two major problems that were still affecting the performance of the equipment at the end of 1983. These were overheating of the thrust bearing (limiting maximum speed) and the unbalanced magnetic pull in the pony motor (limiting motor braking power).

The thrust bearing of the generator supports the 800t generator and motor rotors. It consists of twelve white metal pads supported on a spring mattress and flooded in an oil bath. An oil film is formed hydrodynamically by the rotation of the shaft and the inclination of each pad on

the spring bed. Lubrication is assisted during start-up only, by high pressure oil injection in a central groove in each of the twelve thrust pads. This injection is switched off when the shaft rotational speed exceeds 56rpm.

Computer simulations have shown that the thermal performance of the thrust bearing depends greatly on mixing between the 'hot' oil ejected from the trailing edge and the main oil bath. Cumulative overheating can occur if the mixing is poor. A solution was proposed which relied on the injection of cold oil, drawn from the oil bath, at the leading edge of each thrust pad using a low pressure oil pump and was tested on one of the generators. The spare set of thrust pads were modified for installation during the January 1983 shutdown, together with four L.P. oil pumps with variable speed drive and associated pipework. The test of this improved lubrication was performed during February and revealed a marked improvement in the thrust pad temperature. Typically, a reduction of approximately 17C was achieved at a constant generator speed of 150rpm with an injected oil flow equal to 50% of the calculated oil film flow at maximum speed. This improved lubrication enabled the TFGC to run at full speed with acceptable thrust pad temperature. The other set of thrust bearing pads were modified and an identical lubrication system was installed on the PFGC during the Autumn shutdown.

The early commissioning stage had revealed a large deflection in the pony motor shaft resulting from the unbalanced magnetic pull (UMP). This was remedied during 1983 by the introduction of equalised connections in the pony motor stator winding to counteract the unbalance in air gap magnetic flux. This solution enabled the nominal acceleration torque to be achieved, which was vital for JET operation as it dictated the pulse repetition rate. However, this method of compensating the UMP was ineffective during deceleration as the braking system relied on injection of DC current in the stator winding. The DC braking torque was therefore derated leading to a very long braking time (in excess of one hour). Improved braking torque was achieved by changing to a reverse AC current braking, consisting of permutating two phases of the pony stator winding.

However, a step down transformer was necessary between the supply (11kV) and the pony motor to limit the maximum voltage applied to the rotor winding (limited by flash-over at the collector) at maximum speed. The AC switchgear, transformer and control gears were installed and commissioned on both FGC's during the Autumn shutdown. Tests performed in November gave a new braking time of 20 mins for 112rpm and 35 mins for full speed, i.e. a gain in excess of 40 mins.

Vertical Field Amplifiers

The JET machine design relied on the selection of the number of turns in the external coils for control of the plasma elongation (plasma shape). Operation in the first half of 1983 revealed that vertical instabilities' in the plasma position grow for strongly elongated plasma which can lead to very rapid disruptions. Active control

of the plasma elongation was necessary for safe operation at large plasma currents. Consequently, it was decided that one module of the vertical field amplifier would be dedicated to plasma shape control. A new configuration of DC busbars was defined and an order for additional busbars was placed in July, for installation during the Autumn shutdown. The new configuration of the vertical field amplifier was tested on the JET coils in December (PVFA 1-2 is the plasma shaping power supply, PVFA 3-4 is the vertical field power supply). In the meantime, a definition of requirements for a dedicated plasma shaping power supply is underway to allow a return to the original reconfiguration of PVFA 1-2 and PVFA 3-4.

Ohmic Heating Circuit

The generator remanent current was larger than expected. The switches required to interrupt the current, such as earthing switches and reverse make switches, needed modification which consisted of connecting DC breakers in parallel with the existing switches. Suitable DC current breakers were identified and an order was placed in August. The first two remanence current circuit breakers (RCB) were fitted to the reverse make switch S4 and commissioned during the Autumn shutdown, and the rest will be installed during 1985.

Operation and Commissioning of Power Supplies on JET Coils

Group staff assisted the Operation Group in the operation and commissioning of the PF and TF Power Supplies in the JET coils. Achievement obtained in this field is reviewed under activities of the Operation Group in the Torus Division section.

Notable achievements of extended performance programme are the following:

- operation of the toroidal field generator in series with the two static units at 67kA DC for 10s (energy 5200MJ) in August;
- operation of the two vertical field amplifier modules connected in series on JET coils, in June, with a capability of +4.6kV to -3.6kV at 25kA;
- operation of the two radial field amplifier modules connected in series on JET coils, in December 1983, with a capability of +4.6kV to -4.6kV at 2kA.
- Ohmic Heating Circuit: premagnetisation currents of 60kA were successfully interrupted and a generator current of 96kA was obtained at the end of the plasma flat top phase.
- The TFGC output control was successfully commissioned in August which enabled the two Static Units to be operated at full rectification. This in turn reduced the reactive power consumption and the energy delivered by the TFGC, allowing longer flat-top time to be achieved.

Maintenance and Trouble Shooting

As progress in remote control of the PF and TF power supplies and installation of new equipment demanded

progressively less manpower, effort was gradually diverted to improve reliability and availability of equipment. A professional engineer was recruited with responsibility for organising a maintenance and repair scheme, for preparing suitable procedures and documentation, for compiling a stock of spare parts and for supervising external maintenance contracts.

Maintenance contracts have been placed for the overhaul of the first stage of the toroidal field static unit and amplifiers, and a separate one for the routine maintenance and annual overhaul of the two large FGC systems. Similar contracts are being considered for the overhaul of the other power supply equipment.

A system of fault reports has been introduced to monitor faults and progress their repair. The list reveals that many of these faults were minor 'design' faults which can be eliminated quite easily.

Additional Heating Power Supply Group

(R. Claesen, U. Baur, C. Christodoulopoulos, T. Dobbins, H. Fielding, A. Eyrard, R. Perez-Taussac, G. Baldo and D. Ciscato, (consultants))

Neutral Injection Power Supplies

The first neutral beam was produced in the Testbed in January. Subsequently the full output power of 80kV and 60A has been reached. No major problems were encountered during that time, although minor alterations and modifications, mainly to the control circuits, were introduced as more experience was gained on the behaviour of the neutral injectors and their power supplies.

The main problem encountered during early commissioning and operation of the Testbed was the oscillation of the regulating tetrode in the protection system. This oscillation occurred at certain combinations of tube voltages and currents, particularly around the maximum current of 60A and anode voltages of 12kV and 8kV. In close co-operation with the tube manufacturer, a solution was found by moving the limits at which oscillations started to 75A at a tube voltage of 12kV, and at an even higher value of the current for a tube voltage of 8kV. These values were acceptable as they were more than 20% away from the maximum operating current of the power supply.

Stage 1 of the power supplies for neutral injection operation on the vessel is almost completed and has been tested on dummy loads. The outdoor thyristor rectifiers, the protection system and the auxiliary power supplies are identical to the power supplies on the Testbed. The Testbed does not have transmission lines, active snubbers or an SF6 tower. Therefore, these parts of the neutral injection power supplies have not yet been tested in conjunction with a neutral injector. During partial testing and commissioning of these parts of the power supplies, some problems were encountered.

In the design phase of the transmission lines, a test length was subjected to voltages up to 300kV. DC, without any problems. After manufacture of the first transmission lines, testing revealed breakdown at around

+180kV DC. Following investigation, the cause was located as the presence of residual moisture in the lines, remaining even after vacuum pumping for a long period. After appropriate cleaning, the transmission lines withstood the required test voltage of 260kV DC for 1 min, without difficulty.

All interior components for the SF6 tower were tested separately prior to installation. Testing of the snubbers showed no problems and these were impusle tested with the equivalent capacitance of the transmission lines, and met their design requirements. However, some minor mechanical problems were encountered during assembly of the SF6 tower. In particular, leaking of some of the high pressure cooling water hoses was found. These hoses had been factory tested to over 50bar, but tests on-site revealed leaks developing at a pressure of 10bar. A hard rubber compound was used for these hoses and during vulcanisation, airtraps remained between the compound and the reinforcement linen bands, At these spots no binding of linen and compounds existed, giving rise to weak points. Careful examination of the inside of the hoses showed these weak points. The manufacturing process was changed, to avoid these air-pockets. Newly manufactured hoses showed no further defects,

The assembled tower has been installed in the Torus Hall. After filling with SF6 gas, an electrical test was carried out during which breakdowns occurred along the surface of the main output bushing at voltages of +140kV DC. A test bushing had been investigated before manufacture, but during manufacture the length of a fibre glass nut was changed to allow for easier assembly of the bushing. This was thought to be a minor modification, but testing revealed that the breakdowns occurred at the edge of this nut. Further remedial work will be undertaken at a later date, as the present configuration does not prevent operation of the neutral injectors up to the required voltage of 80kV for hydrogen operation.

Fully integrated tests on four of the neutral injection power supplies were carried out under CODAS control, during which the power supplies were connected to their different dummy loads. In this way, all the necessary timing, interlock and control signals were tested.

Radio Frequency Power Supplies

Preionisation generator power supply.

This power supply came into service in February. The total output DC power is 400kW maximum, with two output voltage levels which can be selected depending on the requirements of the Radio Frequency (RF) generator (eg. 8.5kV or 11kV). The main components are a thyristor rectifier, controlled on the primary side of the rectifier transformer, and diode bridge on the secondary followed by an output filter. This output filter consists of an RC circuit in parallel with another capacitor. This type of filter was chosen because of its favourable properties for switching the load on and off.

Main RF power supplies

The main power supplies are those which feed the driver circuit and the output amplifiers of the RF Generators. One RF generator consists of two modules, each of which has a high frequency output power of 1.5MW, and requires 3MW DC power at its input. Two of these RF generators are fed from the same power supply through one 33kV circuit breaker. A schematic of the connection to the 33kV and to the load is shown in Fig.20.

In order to have the option of disconnecting either of the RF modules from the power supply, independently of the other, DC isolators and earth switches are planned in the DC output. On the 33kV side, isolators are installed to be able to isolate one generator unit completely for maintenance or for any other purpose, while the second generator stays in service for operation. More severe ripple requirements are imposed on the 22kV DC output than on the 11kV DC output. In addition, the power drain on the 11kV output is only approx 10% of the required output power on the 22kV. Two identical six-pulse bridges were chosen, displaced over a 50° angle and put in series. The first bridge feeds the driver circuit (11kV output), while the two bridges in series feed the output amplifier circuit (22kV output). The two power supplies which are fed from the same 33kV circuit breaker are displaced over 7.5°, in order to present a 24-pulse system to the 33kV busbar, if both circuits are loaded in the same way.

The circuit selected during the design phase for the power supply was a special kind of primary regulated

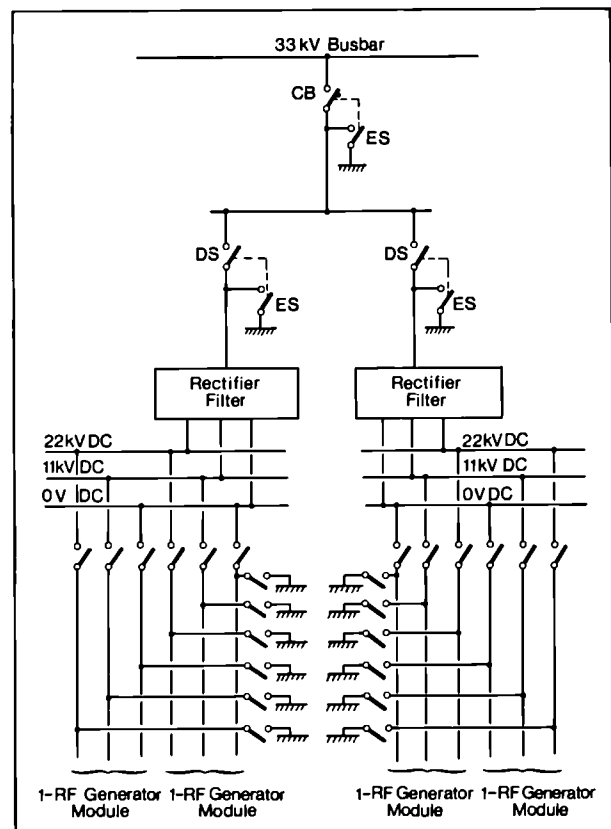


Fig.20: RF power supply connections diagram

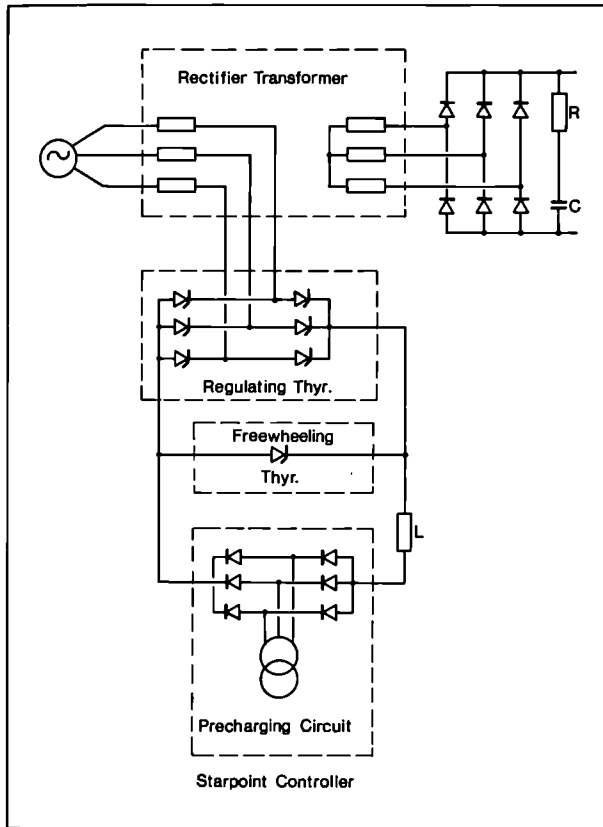


Fig.21: Schematic diagram of the starpoint controller and rectifier circuit

supply. The primary regulation necessitates a special transformer to step the 33kV AC voltage down to a suitable level of about 1kV. Although not obvious for a DC level of 30kV output, this circuit proved to be more economical than a rectifier with a DC thyristor bridge output.

By using a starpoint controller, in which the regulation thyristors are connected near the open starpoint of the rectifier transformer in the same way as a conventional six-pulse bridge, the inductive part of the filter was transferred to the primary side of the rectifier transformer and placed on the DC side of the bridge. The actual value of the inductance was then reduced by the square of the transformer ratio. This arrangement has the great advantage of requiring only low isolation levels and low inductance values. The output filter was completed with an RC filter combination. Fig.21 shows the schematic circuit of the starpoint controller and rectifier circuit.

Optical link interfacing of all the control, interlocking and alarm signals with the RF generator was preferred over a direct wired link. This eliminates all common mode voltages between the power supply and the RF generator, and avoids any RF interference on the power supply. Where possible multiplexing of the signals prior to transmission was performed.

As the RF power supply is not connected directly to any circuit on the machine, and all control loops and interlocks are dictated by the RF generator, it was decided to incorporate no direct link between the power

supply and the CODAS system. All signals to and from CODAS are routed through the RF generator. These signals are processed and used internally before they are passed on either to CODAS or to the power supply.

Four distinct modes of operation are envisaged for the power supply:

- JET Pulse: 20s long, repeated every 10min;
- Short pulse: pulses of 5 to 150ms with a duty cycle of 20%. The maximum current at the 22kV output is limited during this mode of operation. This mode is mainly used for conditioning of the antennas and the main transmission lines;
- Set pulse mode: this mode is used during the commissioning of the RF generators. The pulse length is between 2 and 5ms, with a minimum waiting period of 30ms between pulses. The output power of the power supply is limited during this mode of operation;
- Continuous mode: this mode is used during cleaning or when very low power is required from the power supply. Output power is limited to about 20% of the power required during JET pulse operation.

Each of these modes of operation imposes different demands on the power supply. On the one hand, the voltage must react within a few ms to any voltage variation asked for by the RF generator, and on the other hand, it should not react to fast load variations during different short pulse modes.

These different requirements cannot be met with a single control circuit. Adaptive control was therefore necessary in which the control circuit was changed automatically with the mode of operation of the power supply. Different constants are used for the proportional, differential and integral components in the feedback loop of the control circuits.

One of the main control loops between the RF generator and the power supply is the voltage control loop. In order to minimise the integral dissipation of the output tetrode under varying load conditions, the DC voltage must be varied.

This is achieved in the RF generator by maintaining a constant screen grid current. Any change of this screen grid current is detected and the anode voltage is changed in the correct way. Because of the nature of the antenna load (i.e. the plasma), rather fast variations in voltage can be expected. In JET pulse mode operation, the time constant of the power supply must be less than 5ms.

During operation, arcs may develop in the antenna or in the transmission line. The RF output power is then stopped within microseconds. When the power supply detects a sudden drop in load, the freewheeling thyristor in the starpoint controller is fired. In this way, a path is formed to divert the current in the self-inductance from the main thyristor bridge to this freewheeling thyristor. The time constant of this freewheeling path is about 10ms. If the load is reapplied within 5ms, the current is commutated back to the main thyristor bridge. This arrangement, which is one of the advantages of using a starpoint controller, limits the voltage overshoot at

sudden load drops and also limits the voltage drop when the load is reapplied.

The same procedure is adopted when the load is applied for the first time at the beginning of each pulse. By precharging the inductance prior to connecting to the load, the voltage drops is minimised. This precharging is achieved with a special low power rectifier which is fed from the same point as the rectifier transformer. The command signal to start the precharging is given by the RF generator about 1s before the pulse starts.

In the HV area between Buildings J4 and J5 there are two complete AC/DC power supplies installed, of which one is CODAS commissioned. The installation of the remaining first stage Unit 3-4 will be completed in April 1985.

Advanced Power Supply Systems and Operation Group

(P.L. Mondino, T. Bonicelli, P. Doidge, A. Keymer, V. Marchese, A. Santagiustina, S. Shaw)

The main tasks of the Group lie in its involvement with power supplies performance during JET operation and with developments required to meet extended

performance parameters. These activities include:

Commissioning; Operation; Improvement of Operation; and Design Activity.

JET Commissioning and Operation

The scope for testing the power supplies before connecting them to the JET coils (Toroidal and Poloidal Field Coils) was limited: it was possible only to use a prototype inner poloidal field coil (called P1) as a dummy load. So it was necessary to test the power supplies and the coils simultaneously, as part of an integrated test programme.

An effective approach was followed during the final stage of installation and early commissioning of all subsystems necessary for JET operation during the Ohmic Heating Phase. Since time allocated for the integrated tests was limited, commissioning was initially performed only up to the level necessary to permit the next stage of operation, as determined by the experimental programme. Commissioning and operation were alternated: 2-3 weeks of commissioning was followed by 3-4 weeks of operation. Adequate rosters for both commissioning and operation were prepared to meet this procedure.

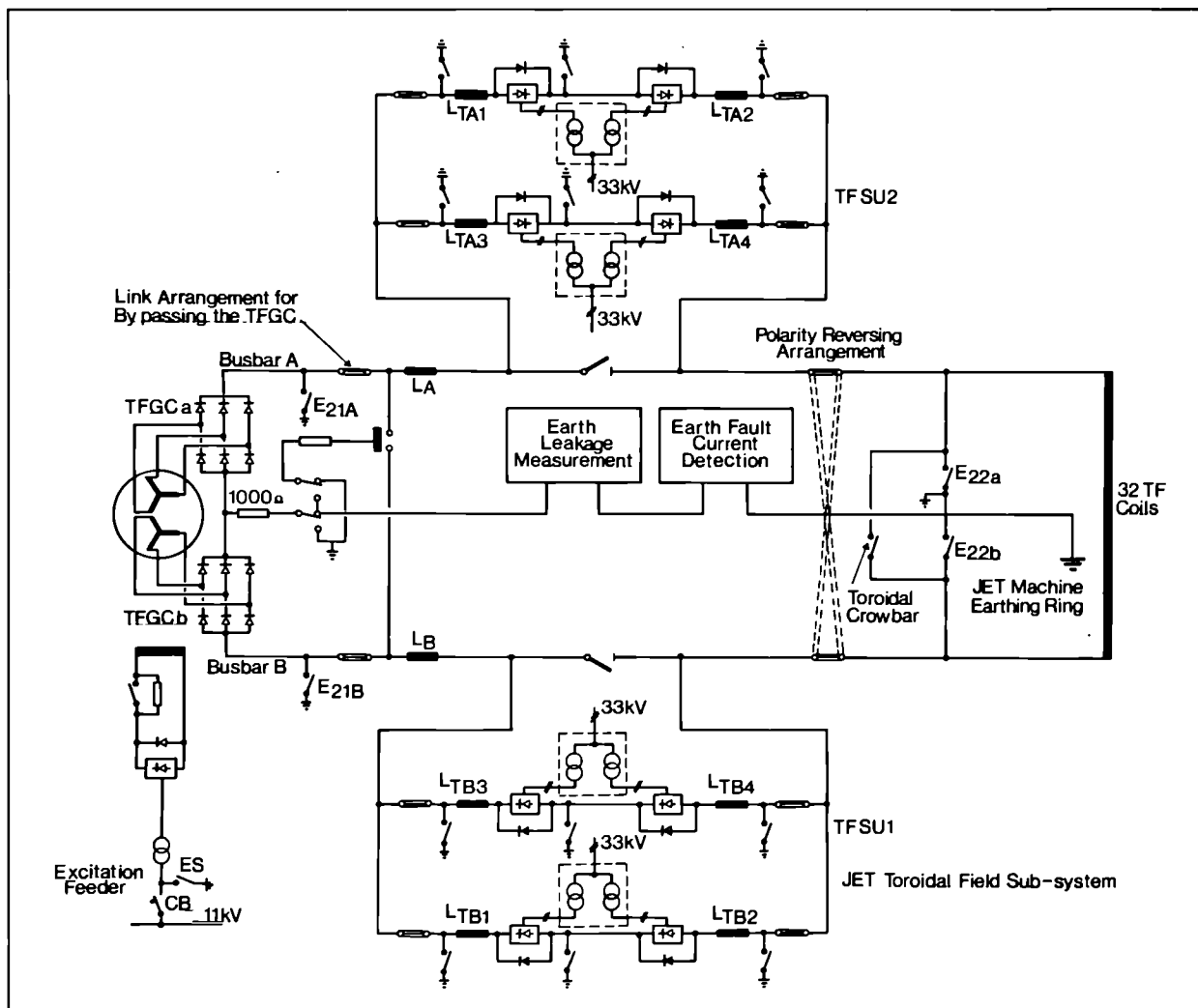


Fig.22: Toroidal field subsystems

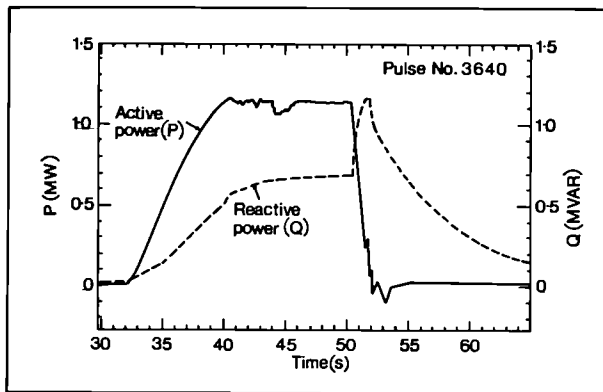


Fig.23: Waveforms of the active and reactive power flow during a typical $I_{TF} = 67\text{kA}$ pulse at the output of one of the 400kV/33kV transformers.

Commissioning

T.F. Subsystem

During March, the Toroidal Field (TF) Subsystem supplied by the Generator and the Static Unit 1 was tested up to 50kA with 12s flat top starting from the operational speed of 210rpm and subsequently up to 60kA, 6s starting from 225rpm. A nominal energy of 2.6GJ was extracted from the flywheel during these two pulses. During the April-June phase, tokamak pulses were performed at the 60kA level.

Installation of the second Static Unit had started in August 1983 and was ready for commissioning in February. The integrated test of the second Static Unit, with the Generator supplying the TF Coils, was performed in June up to 50kA with a 12s flat-top; both power supplies were voltage controlled.

In August, the current control system of the Generator was successfully tested, followed by integrated tests of the complete TF subsystem as shown in Fig.22 in which 67kA with a 10s flat-top was reached. The Generator was current controlled, and both Static Units were voltage controlled. This choice of control strategy allowed selection of maximum output voltage for full pulse length from both Static Units. This provided two advantages: maximum energy absorption directly from the mains and minimum reactive power absorption during the T.F. flat-top.

The 67kA current level corresponded to the full design performance of JET. The length of the equivalent square wave pulse was 17s compared to the 20s full design performance, which has not yet been reached as it has not yet been required within the experimental programme.

Fig.23 shows the waveforms of the Active and Reactive Power flow during a typical $I_{TF} = 67\text{kA}$ pulse at the output of one of the 400kV/33kV transformers. The Reactive Power waveform shows a peak of 115MVAR at the end of the pulse when the voltage of both Static Units is reduced to zero, whereas the current decays very slowly. Operation of the Static Units with sequential control of the thyristor firing angle should

reduce the Reactive Power. Commissioning of sequential control will be performed during Spring 1985. An Active Power of 230MW is presently taken from the mains compared to its 575MW capability.

Poloidal Field (PF) Subsystem

During Autumn 1983, one interference problem had been encountered caused by the commutating capacitor C2 when charged above 20kV. In February, modifications in the trigger signal wiring of the commutating Start Switch, performed in close collaboration with the Supplier, solved the problem. The commutating capacitors then operated normally up to the nominal charging voltage of 25kV.

During March/April, the operation was undertaken with premagnetisation currents up to 40kA. During a commissioning period in April, interruption was achieved at 50kA and at 60kA. The commutating capacitor charging voltages were 22.5kV and 25kV, respectively. Operation with 50kA premagnetisation was tried in May and again in September in a few shots, but the plasma current rise was too fast. However, operation with 40kA premagnetisation was normal.

During operation in March, the PF subsystem was prepared for 40kA premagnetisation, followed by fast rise, slow rise and flat-top. Due to an operational error, an incorrect reference waveform was sent to the generator: full excitation was applied and, the current during premagnetisation reached 100kA in 1s and then remained constant for the next 2s, as the current limit at the generator convertor (FGCP) output was set at 100kA. Then, the commutating capacitors were discharged and the circuit breakers were tripped. During the post-inspection, no damage was found to the coils onto the OH circuit. The Circuit Breakers and the Switches were disassembled and inspected without finding any appreciable effects. The incident established the following:

- the Circuit Breakers are rugged and can interrupt high current even without an artificial zero, provided the applied voltage across the contacts is kept low;
- the fast protective actions were effective.

Operation

During 1984, JET Power Supplies were operated by five staff under the coordination of the Power Supply Operation Engineer. The mode of operation of both the TF and PF subsystems evolved from experience.

The operation of the Magnet Power Supply is coordinated via CODAS. Basically, different categories of centralised control can be identified.

- Level 1: coordinates the subsystem computer (Countdown program);
- Level 2: the subsystem computer commands and supervises the local unit (e.g. the setting up of the Ohmic Heating Circuit configuration).

Back-up action is executed in each subsystem by a Programmable Logic Controller (PLC) coordinated by a

Supervisor (PLC) (Central Interlock and Safety System - CISS).

The pre-pulse operation is guided by the countdown program in combination with operator control intervention. The pulse triggering is made by the operator and the phases of circuit operation, after the start of the pulse, is controlled through the CTS. The normal operation can be divided into the following phases:

- Countdown;
- Start Pre-pulse actions (PR);
- Start Toroidal Field (STF);
- Start Poloidal Field Magnetisation (SPM);
- Fast Rise, Start Main Circuit Breakers Opening Sequence (SCB);
- Slow Rise and Flat Top, Start Poloidal Field Reverse Make Switch (PFR);
- Post Pulse;

Improvement of Operation

Definition of Written Procedures of Operation

The definition of written procedures (check lists of all necessary actions to be performed for Start up, Start of Pulse, End of Pulse, Shutdown) was important for two reasons: firstly, to reduce the probability of operational errors; secondly, only well established Procedures can be translated in Software for automatic operation.

Availability of essential machine signals at the end of Pulse

At the beginning of 1984, only a few machine signals were available at the end of the pulse to judge quality, and in case of fault, to permit identification of the causes. This limited capability often necessitated the use of oscilloscopes and chart recorders during commissioning.

Only at the end of 1984 was limited manpower available to tackle this problem. A substantial improvement is expected in 1985.

Definition of the logic of the Central Interlock and Safety System (CISS)

At the beginning of 1984, the first rudimentary version of CISS GS (General Service Subsystem, of which the 33kV Distribution is a major part) and of CISS TF (Toroidal Field Subsystem) were available. During January/February, the logic of CISS PF (Poloidal Field Subsystem) and of CISS OH (Ohmic Heating Circuit) were defined and commissioned, and became operational during March/April operation. During May, the second version of CISS (including the Supervisor) for the various subsystems was defined and commissioned.

The presence of the Interlock made operation much more resilient against operational errors, but it proved to be too hard on the consequences of a fault. Moreover, commissioning became much more difficult. During Autumn shutdown, the CISS concept was reviewed: a new transition was defined 'Immediate Inhibit Pulse' that worked successfully during December commissioning.

Development of Level 2 Software

During January/February, the Level 2 software of the OH Circuit and of both Generators was defined and commissioned. Subsequently, some sequences of events (performed before and after the pulse to make the plant ready for operation) have been carried out by Level 2 software, including important checks on the plant state. Moreover, the Start-up and the Shutdown (open and close earthing switches, etc) have also been performed by Level 2 software.

Improvements were progressively introduced into the software, so that, by the end of the year, real time programs were established inserting into CODAS the Start-of-Pulse (Countdown) and End-of-Pulse sequences. Equivalent Level 2 software was defined in the Autumn for the Static Units and for Vertical and Radial Field Amplifiers and will be commissioned during Spring 1985.

Definition of class and message for the Alarm Handling Package

During January/February, the Alarm Handling Package became available so that all alarms from the local units were centrally monitored. Four levels of alarm were devised where the two most urgent levels are used for alarms which create a CISS action. An image of mimics of the CISS interlock logic was not then available and, in addition, not all alarms to CISS were duplicated to the CODAS system. Some problems were therefore encountered during fault finding.

A second version of the Alarm Handling Package was released in May, and a third version was available in Autumn. Meanwhile, in order to give the operator the essential information concerning a fault, a conditioning of the alarm signals has been defined and will be commissioned during Spring 1985.

Development of efficient Mimics and Touch Panels

During January/February, the first series of improvements were made on the rudimentary mimics and touch panels available in 1983. Difficulties encountered in operation made it necessary to continue the series of improvements, implemented in May, when the three essential mimics (TF Configuration, PF Configuration, PF Earthing Switches Status) became operational. A few more were defined and commissioned from June to August.

Lack of manpower limited effort available for this activity during the Autumn. As a consequence, only two new mimics are likely to be available in early 1985.

Re-organisation of the touch panel tree has been fully defined and will be commissioned early in 1985, since this is considered an essential step to simplify operation.

Training of Personnel for two shift operation

During November, a decision was taken to operate JET in two-shifts from the beginning of 1985. A high priority training programme for divisional staff was introduced to cope with this requirement. Eight seminars of three hours each were organised on the various topics and were held

between mid-November and mid-December. Each seminar was followed by practical demonstrations on equipment on-Site.

Design Activity (New Projects)

Due to pressure of the work described in the previous sections and due to lack of staff, new design work was not a priority activity. The only design produced was a filter for connection in parallel with the Vertical Field Amplifier to reduce interference on certain diagnostics. All other new projections had to be delayed to 1985.

Conclusion

The work performed during 1984 has been mainly devoted to commissioning, operation, and improvement of operation. 1984 has seen a long period of hard work in difficult conditions. The pressure of operation has delayed certain improvements, produced more equipment down-time and increased stress on limited staff. With the recent addition of new staff, it is hoped that the situation will improve during 1985.

Future Work and New Tasks

During 1985, the Division's activities will be devoted to the following main tasks:

- Operation of JET power supplies during JET commissioning and plasma sessions;
- Through fault statistics, improve performance and decrease power supply down-time;
- Make new items (see Table V) ready for operation;
- Study the feasibility of switching PVFA 3-4 from a series to a parallel connection of units 3 and 4 during pulse operation;
- Study the possibility of a thyristor circuit breaker for fast decay of the PVRA 3-4 amplifier current;
- Study possible poloidal switching circuit enhancement for plasma currents of 5MA and above;
- Study ways of reactive power load reduction and methods of reactive power compensation;
- Consider what economic savings might be made through an optimised JET pulsing schedule taking into account electric power tariffs and through further tariff negotiations with the power supply companies.

Control & Data Acquisition System (CODAS) Division

(Division Head: F. Bombi until 31st October 1984
H. van der Beken from 1st November 1984)

The Control and Data Acquisition System (CODAS) Division is responsible for the implementation, upgrading and operation of the computer-based control and data acquisition system for JET. The purpose of the control and data acquisition system is to allow the

centralised control and monitoring of all actions performed and information obtained during normal operation. It is based on a network of minicomputers interfaced with the experiment through CAMAC instrumentation and signal conditioning modules. For each pulse, all reference values specified by the operation team are set and all relevant information is acquired and gathered into a single 'JET Pulse File' (JPF). Some information is analysed immediately and displayed in the control rooms. Each JPF is also sent through a data link to Harwell, where more elaborate data analysis is performed on the IBM-CRAY computers.

The Division is structured in four Groups as follows:

- The Computer Group, which is responsible for the procurement and operation of the computer network;
- The Control Group, which is responsible for the control subsystems and for overall software development co-ordination;
- The Data Acquisition Group which is responsible for diagnostic subsystems and for the acquisition software;
- The Electronics and Instrumentation Group, which is responsible for the Division's electronics and for a number of auxiliary systems.

During 1984, activities were concentrated on two main targets:

- expansion and consolidation of facilities required to provide more efficient operation;
- addition and commissioning of subsystems included within the extension to full performance plan, mainly the subsystems for neutral beam and radio frequency addition heating.

The Division's workload was again at a very high level due to the conflicting demands of operation and of development. The number of computers installed on site reached 34 at the end of 1984 and the number of installed CODAS interface cubicles reached 102.

During 1984 the Division experienced a high turnover of staff. The Division Head, Dr. F. Bombi, left the Project to take a Chair at the University of Padua. During his ten years with the Project, his contribution to the successful design and implementation of CODAS was invaluable. The Computer Operation Group Leader, RKF Emery, also left in September.

At the end of 1984, there were 65 CODAS staff on-site; of which 33 were employed as permanent staff, or contractors blocking a staff post (10 in the electronics maintenance pool; 11 computer and system operators; 3 in the cable management team, and 9 in the software development teams).

Computer Group

(H.E.O. Brelen, P.J. Card, G.P. Davies)

The Computer Group is responsible for:

- procurement of computers;
- procurement of peripherals and associated services, such as terminal multiplexer, line



*Fig.24: Overview of control area in J2 building.
 Foreground: Machine control room;
 Background (Left): Experiment control room;
 Background (right): Computer room.*

concentrator for central error device, printer multiplexer, etc;

- maintenance of the CODAS computer network and peripherals;
- implementation of back-up and software update procedures;
- software quality assurance;
- daily operation and troubleshooting.

The CODAS computer system (Fig.24) has been extended to 34 machines (see Table.VI) which have been commissioned and are now split in 3 different clusters. The first cluster constitutes the on-line network (see Fig.25) used for the daily operation. The second cluster constitutes the off-line network (see Fig.26) used for program and system development and for commissioning additional subsystems or diagnostics. These computers can be used as standby machines in case of a fault on one element of the on-line network. The third cluster (see Fig.27) consists of the three computers used for database applications. Some re-allocation will be made during 1985.

The operation of the computers is supported by a team of 9 computer operators working on a 3 shift system from Monday to Saturday, and a librarian.

Their main activities are:

- providing general support during experimental hours;
- backing up experimental results and newly developed software during non-experimental hours (night shift);
- installing new software and maintain software libraries;
- exchanging computers in case of faulty on-line machine;
- primary fault investigation and call for service;
- configuring the terminal network;
- handling consumables.

It is necessary to keep the computer system at highest possible availability level. For that purpose, preventative maintenance contracts have been made with all hardware suppliers. In case of hardware failure, rapid on-call service is contained within the contracts. Many spare parts and even complete disk drives are kept on-site and, as engineers from the computer supplier are often present, repair time can be kept to a minimum.

To further improve availability for the most vital part of the system (the on-line computers) the off-line

computers are regarded as reserve machines. In that way, availability of the on-line network has been held at about 99%.

TABLE VI
CODAS Computer Configuration at the end of 1984

Sub-system	Model	Memory (Mb)	Disk (Mb)	Use
AH	100	1.0	1x75	NI Additional Heating
CA	100	0.375	1x10	Off-line Hub
CB	100	0.375	1x10	On-line Hub
DA	520	2.25	2x75	On-line Diagnostic KC1, KG2, KA1
DB	520	2.25	1x75	On-line Diagnostic KR1, KB1
DC	520	2.25	2x75	On-line Diagnostic KK1, KE1
DD	520	2.25	2x75	On-line Diagnostic KS3, KH1, KN1, KP1
DE	520	2.25	2x75	On-line Diagnostic
DF	520	2.25	2x75	On-line Diagnostic KT2
DG	520	2.25	2x75	Diagnostic Commissioning
EC	570	3.0	2x75	Experimental Console
CXA		1x288		
EL	100	0.5	1x75	Electronics
GS	100	1.0	1x75	General Services
HL	100	0.5	2x10	Harwell Link
MC	100	1.0	1x75	Machine Console
PF	100	1.0	1x75	Poloidal Field
RB	100	0.75	1x75	Radio Frequency Testbed
			1x288	
RF	100	1.0	1x75	Radio Frequency
RH	100	1.0	1x75	Remote Handling
SA	560	2.25	1x75	Storage & Analysis
			1x288	
SB	100	1.0	2x75	Standby
			2x10	System tests
			1x288	Back-up
			2x625	
SS	100	1.0	1x75	Safety & Access
TB	100	1.0	1x75	NI Testbed
TF	100	1.0	1x75	Toroidal Field
TR	520	2.25	2x75	Tritium
TS	100	1.0	1x75	Test
VC	100	1.5	1x75	Vacuum Computer
YE	100	1.0	1x75	CODAS Development
YB	530	2.25	2x75	Development
			1x288	
YD	570	2.5	2x75	Scientific development
CX				
YC	530	2.25	2x75	Development (NIB-C)
			1x288	
AS	Comp	0.75	1x45	Database
MD	530	1.25	2x75	Database
SD	Comp	0.75	1x45	Database

Control Group:

(M.L. Browne, T. Budd, C.R. Grace, O.N. Hemming, R.F. Herzog, S.R. James, P.A. McCullen, G.D. Rhoden, C.A. Steed, C. Torelli (to 12.10.84), B.A. Wallander, F. Youhanaie, I.D. Young.)

During 1984, work was concentrated in the following main areas:

- Consolidation of existing software to further improve reliability;
- Provision of new software providing integrated control (Level 2) in many areas;
- Improvement of the operator interface, following experience gained during ON-LINE operations;
- Commissioning of new installed hardware before its ON-LINE introduction.

Five additional subsystem computers have been brought into operation during the year:

- Three additional diagnostic subsystems (DB, DE, DF), covering the rapidly growing number of diagnostics;
- The Radio Frequency subsystem (RF) which controls the RF generators providing additional heating for the JET plasmas;
- The additional heating subsystem (AH) to enable commissioning of Neutral Injector Power Supplies.

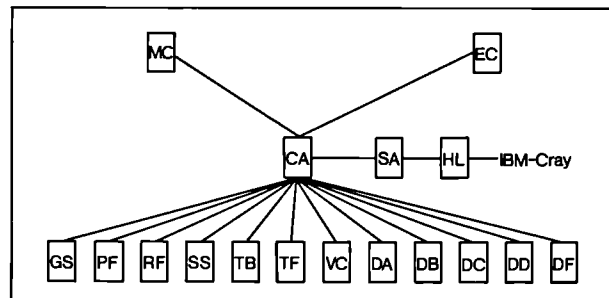


Fig.25: On-line Computer Cluster

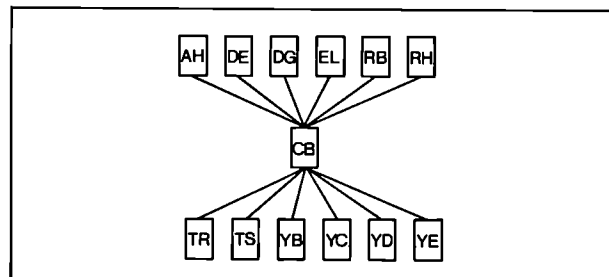


Fig.26: Off-line Computer Cluster

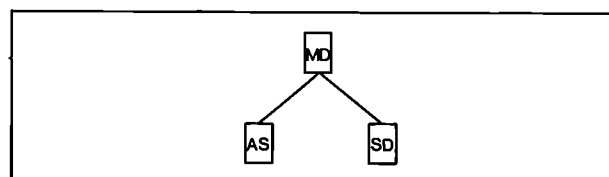


Fig.27: Date Base Computer Cluster



Fig.28: Overview of the main console for machine control. Pictures of overhead displays are available on the CCTV network.

These five additional subsystems bring the total number of computers connected to the device to 20. Sixteen are used in daily operation.

Major developments have been introduced in the software at all levels:

- Following installation of the improved version of the communications software, it has become possible to concentrate operations on the Machine Console (see Fig.28). All operations of Power Supplies and coordination of operations is now effected through touch panels and MIMICs installed on the Machine Console computer;
- Greatly improved safety checks are now routinely performed by software, enhancing safe operation;
- The Safety & Access subsystem (SS) has been enhanced to include software covering the access control systems, badge readers, and personnel dosimetry systems;
- The electrical baking control software has been fully commissioned in its various modes, and additional enhancements provided for auto-calibration of the feedback control loop parameters. In addition, a number of additional areas requiring control have been introduced throughout the year, as requirements arise for

baking extra components on diagnostics (interface valves). This area is likely to continue to expand;

- The Alarm Handling software has been installed and fully commissioned, and during 1984, four versions have been released each one providing more features. The final version provides sophisticated facilities for implementing complex logical filtering of alarms. This enables a substantial reduction in the number of alarms generated by eliminating those which are consequential on an earlier alarm or some combination of alarms;
- Pre- and post-pulse operation of the PF and TF Flywheel Generators;
- Pre- and post-pulse control of the Ohmic Heating power supplies including interlock and safety checking;
- Control of the interface with the CEGB supplies, providing pulse warning and end of pulse sequences and handling the CEGB Pulse Inhibit;
- Electrical baking software has now been installed on a diagnostic computer to allow baking of diagnostics;
- Various applications for the CAMAC auxiliary crate controller (CAC) covering the following:

- Control of the fast alignment of mirrors on the laser scattering diagnostic (KE1)
- Control of the video tape recorders and time code generators during tokamak operations for the limiter viewing diagnostic (KL1);
- Waveform generators implementing plasma density feedback control of the gas introduction system, and feedback control of plasma current;
- Control of the Neutral Beam Scanner used as diagnostic on the Neutral Injectors;
- Software enabling centralised waveform selection and checking.

Data Acquisition Group:

(H.E. Clarke, E.M. Jones, E. Mathi, J.J. Saffert)

This year, major effort has been concentrated on commissioning diagnostic hardware and software. Four ND-500 computers are now used to support the on-line diagnostics and a fifth to support commissioning. During the year, four diagnostics have reached full on-line status (KK1, KB1, KJ1 and KR1) and six are in their commissioning phase (KT2, KG1, KL1, KE1, KY3 and KK2), to go on-line early in 1985.

The link to the Harwell IBM and Cray computers has proved extremely reliable, and work has continued to enhance the data transfer rate. Improvements include the change to asynchronous transfer of data to Harwell, so that the JPF is completed on the Storage & Analysis (SA) computer before the transfer to Harwell starts. This allows JPF data to be available earlier to local users without undue delay in the transfer to Harwell and permits a higher pulse rate. The automatic transfer of all JPFs not archived at Harwell has also been implemented, providing automatic recovery from temporary interruption of the data link. In order to further analyse the computer performance during a JET pulse, statistics and resource utilisation programs have been implemented.

Considerable effort has been expended in the production of integrated CAMAC drivers for the hardware modules, specially purchased for the diagnostics. This led automatically to changes in the General Acquisition Program (GAP), to allow use of the new modules and new templates also had to be produced. Other improvements to GAP included the addition of timing nodes to facilitate access to the module trigger time from the start of pulse. Routines to reconstruct the timing information relative to the start of pulse are provided.

Among a large number of enhancements to GAP, two major changes were:

- GAP now uses an enlarged logical space (APT segment), which allows the collection of data from more channels;
- The facility to build shortlists only when there has been a change in the tree, which speeds up the pre-pulse section of GAP.

In the general area of user support, several improvements have been made or are planned. The

graphics package has three-dimensional and contour plotting added, and a completely independent package has been written to access the Westward Graphics Manager. A new version of the program to display data held in the JET Pulse Files (JPFDISP), a general data display facility, has been started and should be available early in 1985.

With the increase in the number of diagnostics, both on-line and in the commissioning phase, the need for tape transfer/translation facilities has increased, and a set of procedures is being produced.

Electronics & Instrumentation Group:

(W.J. Brewerton, A.N. Cleaves, S.E. Dorling, K. Fullard, J.P. Nijman, D.S. Nassi, C.G. Pollard, V. Schmidt, J.E. van Montfoort, J.R. Watkins)

At the beginning of 1984, most of the CODAS interface cubicles of the control subsystems included in the basic performance had been installed (see Fig.29). However, there has been no respite in the rate of preparing new cubicles. There are now 102 cubicles in place, compared with the 65 at the beginning of the year. The additions were mainly involved with new diagnostic devices and with the two Additional Heating schemes.

Each cubicle is individually designed and contains the electronic equipment needed to connect the signals associate with a single piece of plant to the CODAS computers. All the signals to and from the computers travel at high speed (5MHz, bit serial) in digital form along fibre optic CAMAC serial highway cables. The high efficiency and isolating properties of these cables allows the cubicle to be placed close to the plant itself, so shortening the myriad of wires which emerge from the plant. This approach has proved especially valuable in the case of the R.F. Heating cubicles, now being commissioned, each of which is grounded to its associated R.F. generator. Thus, the generators themselves can follow the potential of the individual torus octant which they feed, without prejudicing communication with their central control computer.

Within the cubicles, the most common signal type is the slow digital input or output where a computer response time of greater than 100ms is acceptable. In CODAS there is already the capacity for some 32,000 such signals, so their efficient handling is crucial. The Line Surveyor/Driver modules which achieve this in the cubicles provide isolation and filtering for every signal each of which can produce an individually controllable computer interrupt if required. To reduce the load on the computers, and to use the Serial Highways more effectively, most of the signals are not allowed to produce interrupts, but are polled by the computer using an efficient block transfer of up to 512 signals per block. These LSD modules are conservatively designed with normal industrial components and have proved reliable, with a failure rate of less than 2% for a year of continuous operation. Failures have occurred, but mainly in the components directly connected to the plant.

During the year several new module type have been introduced. Some, such as the CAD8 250kHz transient



*FIG.29: Overview of the Computer Room.
Cubicles in background house services like terminal multiplexer, CAMAC serial highway patching, CCTV.*

recorder waveforms during the pulse, take advantage of newly available technology. Others, such as the UST6 gating module, have been required to optimise control of JET systems in the light of operational experience. The Eurocard standard (DIN 41494, DIN 41612) has proved a convenient and low cost medium for this second class of module, which are usually required at short notice. Quality assurance testing of these new, and of the older, types of modules has needed continuing major efforts to ensure the trouble-free commissioning of new systems. The numbers of modules of each class are shown in Table VII.

The Central Interlock & Safety System has played an increasingly important role in JET operations. Further refinements have been added to the interlock logic so that full safety of personnel and equipment can be maintained, whilst causing the minimum hindrance to normal operations and commissioning. The TF, PF, GS and SS systems are now fully commissioned.

The Central Timing System has further expanded, especially in support of new diagnostics. Some users now take advantage of the full one microsecond resolution of which the system is capable. The time settings are pre-programmed in CAMAC modules and the time signals are distributed as pulses of light in fibre optic cables. Six basic time marks well related to the machine cycle are

widely distributed and individual timer modules are used locally to provide for special needs.

The Electronic Maintenance Team has remained at constant strength, with nine people directly engaged in commissioning and maintenance work. Commissioning work was the major task throughout the year, but although the failure rate among modules has fallen because of increasing experience in their use, the number of modules in use has approximately doubled, resulting in a constant maintenance workload. The majority of immediate repairs are affected by module interchange. Even though the circumstances are now always clear, it is usual to exchange suspected modules with a minimum of field investigation, because this maximises the availability of the affected CODAS subsystems.

Further console bays have been commissioned to meet the needs of diagnostics and additional heating. There are now 50 full console bays and 30 terminal bays in use, included in 9 mobile consoles which are used primarily in commissioning work. The closed circuit TV system has been brought into use during the year. Currently, it is used only for monochrome pictures. Two switching matrices, one 20x20 and the other 30x30, form the core of the system. TV camera and computer-generated pictures can be switched to control room monitors and to a network of 12 points around the site, where the viewer

TABLE VII
Summary of Interface Electronic Components

Component	Delivered at	
	End 1984	End 1983
CAMAC crates	187	146
CAMAC system modules (controllers, LAM graders, etc)	629	511
CAMAC auxiliary crate controllers	75	51
U-port adaptors	119	116
CAMAC digital input and output modules	581	502
CAMAC analogue input and output modules	629	461
CAMAC display modules	255	237
Timing system modules	698	283
Digital signal conditioning (Eurocard)	3257	1273
Analogue signal conditioning (Eurocard)	1684	1014
Cubicle frames	123	105
Eurocard subracks	705	489
Console devices (TV screens, touch panels, etc)	313	218

can select one of 30 pictures. These are used to keep staff up to date when working in locations remote from the Control Room, such as alongside diagnostic equipment. The TV cameras allow continuous observation of the JET machine and will later be used in remote handling work. Critical personnel access points are also monitored from the control room safety console.

In the effort to produce high availability of CODAS, an important background aspect is the proper accounting of the module inventory. This is achieved using a SIBAS database on a Norsk Data computer, providing 20 different screen presentations of the stocks, condition, orders and locations of 15,000 items. The data occupy 20 Mbyte of disk storage overall.

Future Work

In 1985, the main objectives of CODAS Division will be:

- Installation and commissioning of the extension required by:
- additional neutral beam heating (Neutral Injectors at Octants Nos. 8 and 4 and corresponding PINIs);
- extension of the R.F. system;
- extension of diagnostics.

- Improvement of operational facilities in providing more convenient user interface and more resilient software;
- Study and partial implementation of required changes to improve performance of system response and data throughput;
- Study and design of the computer support for Remote Handling facilities;
- Study and analysis of computer support for the Tritium plant;
- Implementation of the new release of the operating system (version J of SINTRAN III).

The new installation will require design and manufacture of 36 further CODAS interface cubicles and expansion and reconfiguration of parts of the CODAS service network.

These activities will impose a heavy staff workload as most are also involved in shift duty which, in some cases, represents 50% of their activities. Vacant positions within the Division will have to be filled urgently by contractors, as it becomes more difficult to identify suitable candidates.

Neutral Beam Heating Division

(Division Head: G. Duesing)

Neutral Beam Heating Division is responsible for the construction, installation, commissioning and operation of the neutral injection system including its development towards full power operation. The system consists of two injectors on JET with 8 beam sources each, and of a Testbed on site. The Division also participates in the investigation of the physics of neutral beam heating. These topics are undertaken by three Groups: the Neutral Beam Testbed Group, the Beam Line Construction Group, and the Neutral Beam Operation Group.

The main achievements in 1984 are summarised below:

- The Testbed has been taken into operation with power supplies for single beam source operation, and the diagnostics and data acquisition systems have been commissioned. The Testbed is to a large extent modelled on the injector systems on the Tokamak.
- Ion beam sources have been operated in the testbed at the full 80kV and 60A parameters with beam pulse durations of more than 15s.
- Ten beam sources have been manufactured, and have been tested at EURATOM-UKAEA Association, Culham Laboratory including 100 pulses of 5s duration from each source at 75kV and 56A.

- The plasma source species mix has been improved at Culham Laboratory in close co-operation with JET. By superimposing a long range filter field on the original multipole magnetic field, the $H^+ : H_2^+ : H_3^+$ ratio in the extracted beams has been increased from 64%:28%:8% to 84%:12%:4%;
- The 262 beamlets from a beam source are steered towards a focus to minimise overall beam divergence. This steering is produced by an offset of the apertures in the deceleration grid of the extraction system. The required offset values were experimentally determined at Culham Laboratory in co-operation with JET, and the design values were corrected. The apertures of the existing deceleration grids were all re-drilled to about 50% of the original offset;
- At EURATOM-CEA Association, Fontenay-aux-Roses Laboratory, a modified JET beam source with a three-electrode extraction system has been operated with deuterium beams of 5s pulse duration at 160kV extraction voltage and 37A extracted current;
- Major problems in the manufacture of the dumps for the fractional-energy ion beams and of the deflection magnet liners were overcome. By the end of 1984, the assembly on-site of the Central Column of the first neutral injector was near to completion. This Central Column comprises the deflection magnets; all beam dumps and a retractable calorimeter for the beams from 8 sources; and the supply lines of 1800m³/h cooling water. It is attached to the lid of the injector vacuum box;
- The first cryopump with a nominal hydrogen pumping speed of $8 \times 10^6 \text{ l s}^{-1}$ was successfully tested on-site;
- The installation and commissioning of the helium refrigerator has made good progress. Liquid helium was produced in the cold box with a power of 560W at 4.6K;
- Installation for the first injector at the Tokamak have included the Torus duct beam scrapers, the vacuum valve between Torus and injector, the injector vacuum box with a fast shutter, further beam scrapers, the cryopump, the turbomolecular pump system and external magnetic shielding. Six pre-tested beam sources were also installed and connected to the high voltage transmission tower (see SF6 Tower).

Neutral Beam Tested Group

Testbed

(R.S. Hemsworth, H.D. Falter, P. Massmann, G.H. Deschamps, M.J. Mead)

During 1984 the JET Neutral Injection Testbed has been operated at the full performance specification with a single ion beam source (PINI), and the majority of the diagnostics have been commissioned. This has been

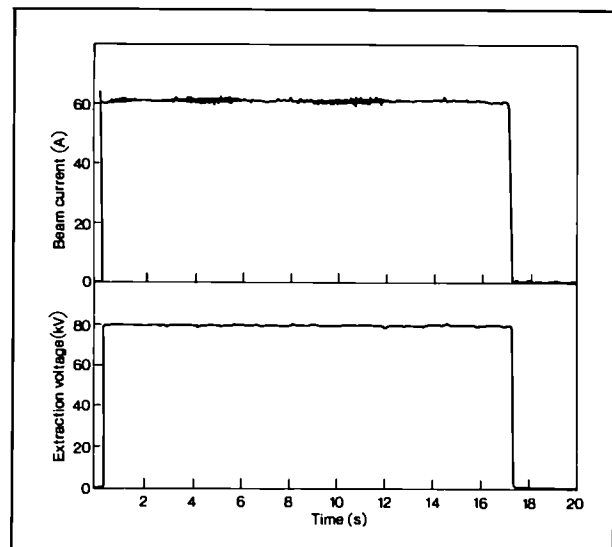


Fig.30 Waveforms of the 17s, 5MW beam from the JET PINI operating on the NI Testbed

achieved without major modifications to either the Testbed itself or its associated power supplies. The power supplies and the services for a second PINI are presently being commissioned in order that simultaneous operation of two PINIs may begin in the immediate future.

PINI and System Operation

(R.S. Hemsworth, H.D. Falter, P. Massmann, G.H. Deschamps, F. Long, D. Martin, A. Browne, H. Hupfloher, D. Raisbeck, D. Kausch)

The first PINI installed on the Testbed had been fully tested at Culham Laboratory, with a 'checkerboard' bucket plasma source [1] and had the original aperture offset for beamlet steering on the third (negative) grid. (The design basis for this was taken from Ref.[2].) The power and energy extracted from this PINI was gradually increased until operation at 80kV was achieved in August 1984. Throughout late August and September, this PINI was operated at 80kV, including the first pulse each day. The system proved extremely reliable, with typically less than two breakdowns occurring during a 5s pulse. After it was established that the actively cooled components of the Testbed (the PINI, the Ion Dump and the scraper system) reached or approached thermal equilibrium during the first four seconds of beam operation, and that only modest temperature excursions were recorded on inertially cooled elements, the pulse length was gradually increased until pulses of 17.5s duration at 80kV, 60A were extracted (Fig.30) with no detectable deterioration in system performance. The measured beam transmission through a simulation of the Torus entrance duct was 70%, whilst the power loadings on the grids and on the back-streaming electrons were measured as similar to those reported by Culham Laboratory during the PINI testing (see below). Only one modification to the system was necessary to enable the PINI to work with the

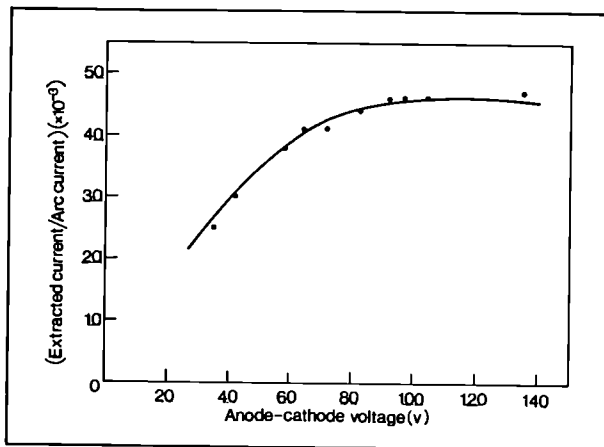


Fig.31 Ionization efficiency versus arc voltage for the JET high proton yield plasma source

JET power supplies. The plasma source started in the well known inefficient mode before 'flipping' into the efficient mode [3,4]. This was prevented by placing a $100\mu\text{F}$ capacitor between the source anode and the extraction grid. This made the source anode area appear much larger for a very short initial period ($\ll 1\text{ms}$). With this modification, the source consistently switches into the efficient mode.

A different PINI was installed at the end of September 1984 incorporating a 'filter' bucket plasma source [5,6] (giving an enhanced proton yield), and a negative grid with the final offset aperture steering pattern. The only significant differences found with this 'final' type of PINI were in the operation of the plasma source. The arc current was found to be a much more sensitive function of the filament heating current and (via ion back bombardment heating of the filaments) of the anode-cathode voltage. This is not a significant effect as the JET supplies control the arc current through a feedback loop operating on the filament heating current. One other important effect observed with this plasma source was a large beam current overshoot ($<70\%$) as the beam started. This overshoot, which lasted for a few milliseconds (decay time $\sim 2\text{ms}$), was found to stem

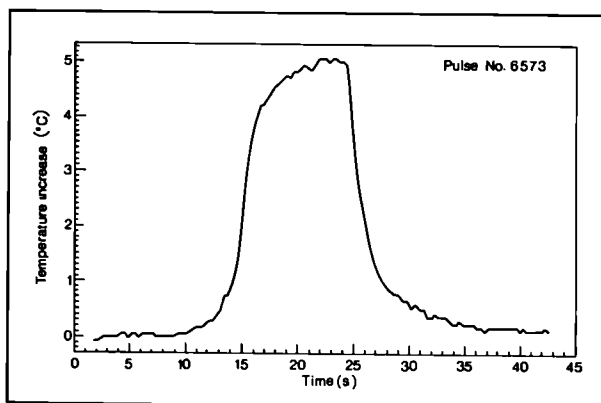


Fig.32 Temperature increase for the plasma source body cooling water for a 60kV, 38A, 10s pulse

from a real beam enhancement. This was established by monitoring the beam profile using optical beam scanners. No arc current or voltage overshoot accompanied the beam current overshoot, which has also found to be essentially independent of the gas flow. The present hypothesis is that the arc efficiency changes on beam extraction. This large overshoot drives the source well over perveance match, when the flat-top condition is set for match, and this leads to breakdowns. Two techniques have been used to suppress this. Firstly, the filament heating current was decreased prior to beam initiation and then increased again as the high voltage was switched on. This worked well, but provided a coarse control with a long time constant. The second technique now used on the Testbed consists of increasing the arc voltage from an initially low level (50V anode-filament) to the operating level (100V anode-filament).

As can be seen from the arc ionisation efficiency versus arc voltage curve shown in Fig.31, this has the effect of increasing the ion flux to the extraction plane at a rate controlled by the arc supply at the same time as the efficiency is decreasing due to beam extraction.

Testbed Diagnostics and Data Acquisition

(M.J. Mead, G.H. Deschamps, T.T.C. Jones, H.D. Falter, A. Browne, D. Raisbeck, D. Kausch)

The Testbed data is recorded by both digital storage oscilloscopes and chart recorders as well as by Nord 100 computer. This combination enables the oscilloscope and chart recorders to be used for immediate data analysis, (which minimises the turn-around time between pulses), whilst the computer is used for permanent data recording and in-depth analysis of the data. Computer data analysis is available between shots, as required, and may also be run overnight for any set of selected shots.

The most important diagnostics on the Testbed are the thermal diagnostics, which rely on the measurement of temperatures using thermocouples with a typical sensitivity of $40\mu\text{V}/^\circ\text{C}$. Two principal forms of thermal diagnostics are used: water flow calorimetry (WFC) and transient inertial calorimetry (TIC). About 300 thermocouples are remotely monitored through a multiplexing, amplifying system which feeds the analogue-to-digital converters that interface through memory modules to the computer. The multiplexing and amplification of the signals is done remotely (about 50m from the equipment) to simulate closely the system to be used on the main injector where electronics cannot be placed local to the injector in the radiation environment of the Torus Hall. In general WFC involves monitoring temperature increases (ΔT) of 1-10°C whilst TIC involves $\Delta T \sim 100^\circ\text{C}$. Thus, voltages must be measured accurately to $<40\mu\text{V}$. This level is now routinely achieved by the Testbed system; a typical output from the WFC system is shown in Fig.32.

Water flow calorimetry involves measurements of the cooling water temperature increase and the water flow rate. This monitors the power to the main components on

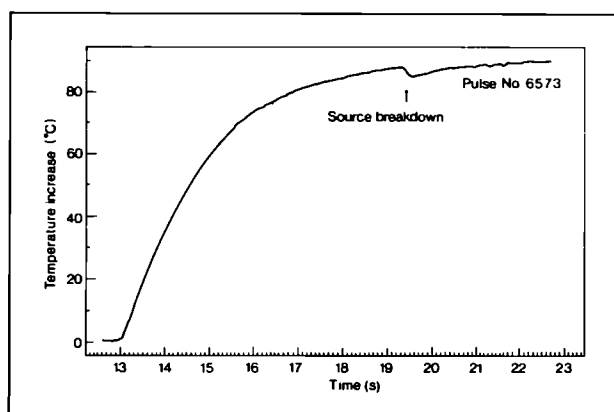


Fig.33 Temperature increase for a 'fast' thermocouple in the Testbed ion dump for a 60kV, 38A, 10s pulse with one breakdown

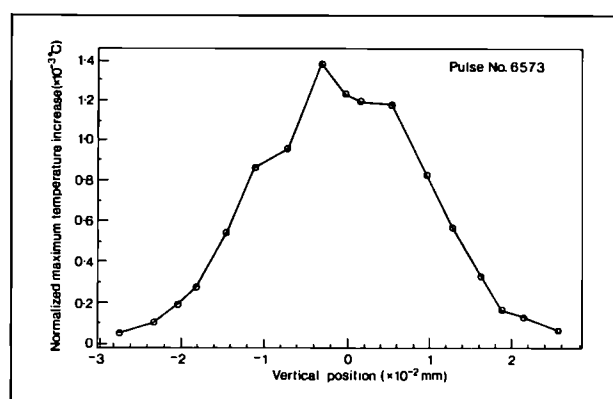


Fig.34 Beam profile derived from the normalised maximum temperature increase measured by the 'fast' thermocouples in the Testbed ion dump. The normalisation takes account of the variation in the angle of incidence of the beam with respect to the different heat transfer elements that make up the ion dump

TABLE VIII

Power Accountability on the JET Testbed from Water Flow Calorimetry – Shot No.6573

Extracted energy = 22MJ (at 60kV, 38A)

Total energy dissipated in plasma source = 1.02MJ

Component	Fraction of Beam Energy(%)
Plasma Source Body	2.4
Grid 1	1.2
Grid 2	0.3
Grid 3	0.6
Grid 4 + 1st Stage Neutraliser	1.2
2nd Stage Neutraliser	3.9
Testbed Box Scrapers	9.0
Testbed Left Duct Scraper	0.3
Testbed Right Duct Scraper	0.1
Testbed Ion Dump	68.5
TOTAL	87.5

the Testbed, and Table VIII gives a typical power accountability for a shot. The uncertainties in this type of data arise from the difficulties of measuring accurately the large water flow (~100m³/h) to such high power components.

As so many water cooled-components are connected in series and/or parallel, it is not practical to have sufficiently straight lengths of pipes required for accurate flow measurements. Therefore, the data obtained from potentially very accurate ultrasonic flow meters are of limited accuracy. Methods of improving this overall accuracy are still being investigated.

Inertial calorimetry is used to obtain beam profiles from 'fast' thermocouples in the Testbed Ion Dump. These consist of bare chromel-alumel wire junctions brazed into the beam stopping elements 3mm behind the exposed surface. A typical output from such a thermocouple is shown in Fig.33. A beam profile may be derived from the maximum temperature recorded as shown in Fig.34. Although such a profile is distorted (as the relationship between the maximum temperature and incident power density is non-linear), it is representative of the beam for a fixed pulse length.

A quantitative beam profile can be obtained by TIC, which involves measuring the temperature rise rate during the period when the element can be regarded as thermally inertial, (ie before the incoming power has reached the cooling water [7]). This requires good time resolution. Initial tests indicated good agreement with other methods of measuring local power densities. However, the results obtained are not yet completely satisfactory. Over- or under-shoots of extracted current result in beam perveance variations, and give variations in the power density during the measurement period. Optical diagnostics used on the Testbed are described in the section on optical beam scanners.

Tests of Cryopump Loading

(A.P.H. Goede, R.S. Hemsworth, W. Obert, E. Kuessel, F. Long, C. Mayaux, D. Martin, D. Kausch)

Two modules of the open-structure cryopump had been installed in the Testbed and tested in 1983 (20 such modules are installed in the actual injector). The pump performance in the presence of the beam has now been tested. Preliminary data show no significant effect on LHe and LN₂ consumption rates from a beam of >2.5MW of 10s duration passing the pump.

It is expected [8] that power from the beam, through energetic particle reflection and particles charge-exchanging in the deflection magnet, will reach the cryo-modules during injector operation. An array of small inertial calorimeters installed in front of the modules has been used to measure the power flux in the absence of either the deflection magnets or the calorimeter. Power fluxes of up to 2Wcm⁻² per MW of beam power have been measured when the system is operated at perveance match. The power flux was not a function of the source of neutraliser gas flows and was thought to arise from aberrations in the extraction optics. According to these

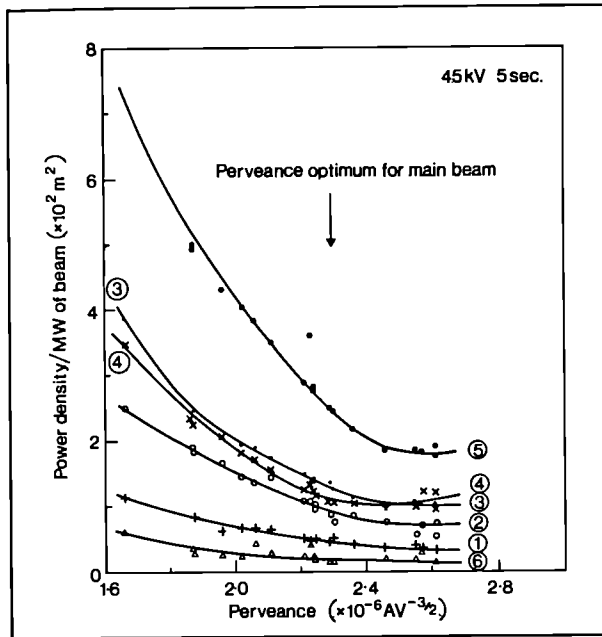


Fig.35 Variation of the power density to various calorimeters located at the entrance to the cryopump as a function of the beam perveance

measurements, the power to the cryo-modules was found to be a strong function of the beam perveance (Fig.35), but did not go through a minimum at optimum perveance.

Gas Flow Tests

(R.S. Hemsworth, H.D. Falter, H. Hupfloher, D. Martin)

The gas density distribution and, hence, the gas target for beam neutralisation have been measured in the absence of the beam. The pressure distribution had the expected profile along the neutraliser, but the conductance was significantly lower than calculated. These results are still being assessed.

The gas streaming profile was measured at about 50cm from the neutraliser exit, to determine the pressure profile inside the deflection magnet.

Carbon Tile Test

(A. Stabler, P. Massman, F. Long, D. Martin, D. Kausch)

The power handling capability of the carbon protection tiles covering the vacuum vessel inner walls have been tested in the Testbed. (The high power densities on the Testbed make this an ideal facility for such tests: Power densities of $1\text{--}10\text{kWcm}^{-2}$ are readily achieved over many tens of cm^2 and many seconds). For this test, a Torus wall protection tile was exposed to power densities of up to 4.1kWcm^{-2} . The tile eventually cracked when exposed to 2.6kWcm^{-2} for 1.0s. The conclusions are that the inner wall protection tiles should easily withstand the expected power loading due to beam shine-through $<250\text{Wcm}^{-2}$ for the full beam pulse length (10s) and should tolerate the unattenuated beam power $\sim 2\text{kWcm}^{-2}$ for $\sim 1\text{s}$.

Beam Source Development and Testing

Testing of 80kV Sources

Testing of the production ion sources (PINIs) has continued throughout 1984 at the EURATOM-UKAEA Association. Culham Laboratory [6]. Each source was tested for vacuum integrity and high voltage hold-off on a small dedicated test rig before undergoing conditioning and testing up to full power on the Culham Megawatt Beam Line (MWBL). Concurrent with this testing, work on the two problems previously identified with the PINIs - beam steering and species mix - have also continued at Culham, on both the MWBL and a special plasma source test rig.

During 1984, 12 PINIs completed the full testing (or re-testing) schedule; of these 6 have had the high proton yield plasma source (see below) and 8 had the improved (final) aperture offset in the negative grid (G3) (see below). All the results confirmed the robustness and reliability of the basic PINI structure. The main results from the commissioning were:

- A typical PINI 'conditions' to operate at $>75\text{kV}$, 56A, 5s pulses in 600 pulses;
- When operating at 75kV, the power loading to the plasma source body, the extraction grid (G1), the gradient grid (G2), the negative grid (G3) and the earth grid plus the first stage neutraliser (which have a common water cooling circuit) are 2.3%, 1.0%, 0.4%, 0.3%, and 1.2% of the extracted power, respectively.
- Transmission through an aperture representing the Torus entrance duct is $\sim 70\%$ at 75kV.
- The beamlet divergence at 75kV is 0.58.
- Operation at a plasma source filling pressure of $4 \times 10^{-3}\text{mbar}$ (measured in the absence of extraction) with a neutraliser gas flow (introduced between the first and second neutraliser stages) that results in an increase of the source filling pressure (without extraction) by $2.2 \times 10^{-3}\text{mbar}$ is routinely achieved.
- The final test of each PINI is a reliability run consisting of 100 consecutive 75kV, 5s pulses at perveance match ($\sim 56\text{A}$). The performance of each PINI during this test is very similar to that already reported. Typically all the pulses give an $\int IV dt > 95\%$ of the expected value and the most probable number of HV breakdowns in between 1 and 3.

Beam Steering

Continued investigation has confirmed the initial conclusion that the aperture offsets on the negative grid used to focus the beam have resulted in over focussing. In addition to diagnostics previously used for this work - optical beam profiles measured in Doppler shifted H_α light and calorimetrically measured profiles - a new diagnostic has been introduced. This is essentially a pin-hole camera located at the end of the MWBL, about 10m

from the ion beam source. This pin-hole camera allows an accurate measurement of the angle with which each horizontal row of beamlets is moving in the vertical plane, and of the origin on the extraction system of each row of beamlets. The camera measurements confirm that the original aperture offset results in almost twice the desired angular deflection of a given beamlet. A typical result from the original extraction system is shown in Fig.36. As this strong focussing is unacceptable for the JET injector, the aperture offsets on G3 have all been changed to 50% of the original design value. All the PINIs are now equipped with re-drilled G3s and are being tested (or re-tested) in this final configuration.

Computational work was initiated in order to understand the reason for the unexpectedly strong focussing. Results from two dimensional (2D) codes confirmed the original design calculations. However, three dimensional (3D) code work, [9], and then, in more detail, [10] predicts a much stronger angular displacement for a given G3 aperture offset (Fig.37). The examination of the 3D code output revealed the reason: with the 2D-code, the strength of the electrostatic lens at the entrance to the G3 aperture is accurately predicted and agrees with that derived from the 3D code; the 2D simulation assumes that the beamlet deflection arises only from the displacement of this lens. However, moving the G3 aperture creates an electric field shear which gives an additional beamlet deflection, which cannot be predicted by the 2D- representation. The predicted lens strength for the JET G3 from the 3D-code is 36 mrad/mm, in good agreement with the experimental data (cf. the design (2D) value [11] of 20mrad/mm).

Species Enhancement

As previously mentioned the proton beam fraction extracted from the PINI equipped with the 'checkerboard' magnetic bucket source is 65%, which is unacceptably low for the JET injector. It was also established that a modification of the external permanent magnets on the bucket source could produce a 'filter' field giving a high proton content near the extraction grid. The presence of such a field produced a low floating potential (3-4V) in the region of the extraction system. Three magnetic configurations were identified giving both low floating potentials and adequate plasma uniformity. Tests on the MWBL allowed one (designated SC15/S3) to be selected for all PINIs, which gives the species mix, shown in Table IX [5].

160kV Sources

The development of the 160kV extraction system has been carried out at the EURATOM-CEA Association, Fontenay-aux-Roses Laboratory, resulting in a modification of the 80kV structure from a tetrode to a triode extraction system, in which spacers have been placed under the (original) G2-G3 post insulators to increase the G1 to G3 gap; and G1 has been replaced and G2 was omitted. During 1984, work concentrated on commissioning and characterising the system for long

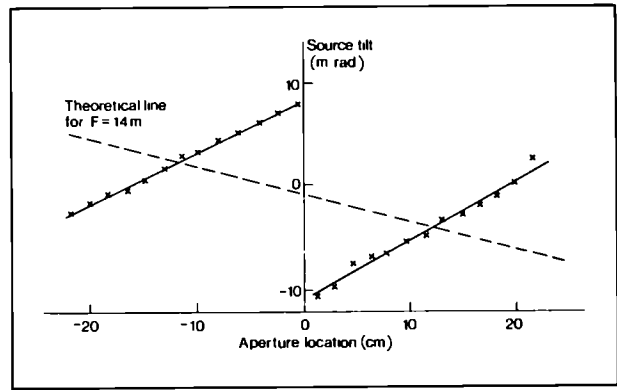


Fig.36 Source tilt for maximum intensity for a given row of apertures versus aperture location (The tilt is proportional to the beamlet steering angle)

(5s) pulses in D₂, and was carried out in a specially built neutron shielded Testbed [12].

Operation with long pulses required replacing the inertially cooled extraction grid with an actively cooled grid. Following this change, the system was rapidly conditioned to 160kV operation in D₂ and more than a hundred 5s pulses have now been successfully extracted. The beam profile was measured at 4.8m and 7.4m from the PINI (see Fig.38), and showed a beamlet divergence of 0.6 and the correct beamlet steering. However, in view of the unexpectedly strong focussing observed with the 80kV tetrode system, calorimetric profile measurements are now being made 2m from the extraction system, and the Culham pin-hole camera is being used in a collaborative experiment to determine the beam focussing.

The PINI at Fontenay-aux-Roses is operated with a Peri-plasmatron plasma source, which operates at a typical filling pressure of 13×10^{-3} mbar (no extraction). The power loadings are being measured as a function of

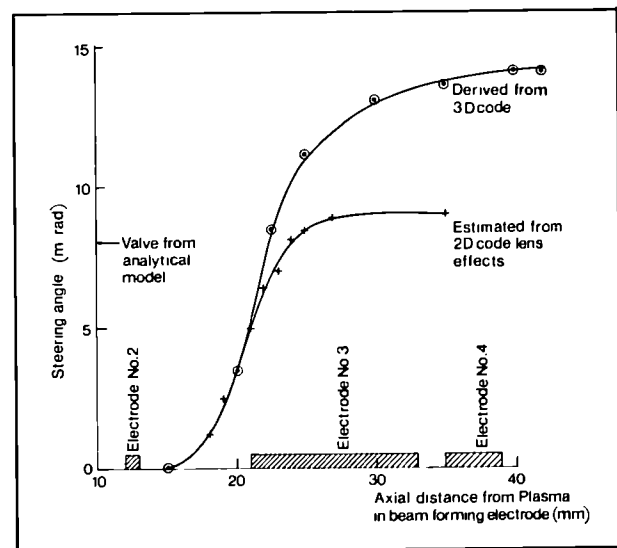


Fig.37 Comparison of beamlet steering, as the beamlet is followed through the extraction system, from 2D and 3D codes

TABLE IX

Plasma Source Development
Species mix at 55A extracted current

	Prototype source	chequerboard plus supercusp	
		optical	magnetic
H ⁺	64%	82%	87%
H ₂ ⁺	28%	14%	11%
H ₃ ⁺	8%	4%	2%

Uniformity: $\pm 8\%$ over 45cm \times 18cm

filling pressure to allow extrapolation to the JET operating conditions. Typical values with 13×10^{-3} mbar filling pressure were: power to extraction grid, negative grid, earth grid and first stage neutraliser of 0.75%, 0.42%, 1.0% and 0.75% of the extracted power, respectively. The species mix from the Periplasmatron when operated in D₂ at 100mA/cm² was D⁺:D₂:D₃=48:27:25. The measured optimum perveance at 160kV was $5.8 \times 10^{-7} \text{AV}^{-3/2}$, (ie 37A extracted). This current is too high for operation on JET, and it will be even higher with the higher proton yield of the bucket plasma source. the current may be reduced either by increasing the extraction gap or by decreasing the number of grid apertures.

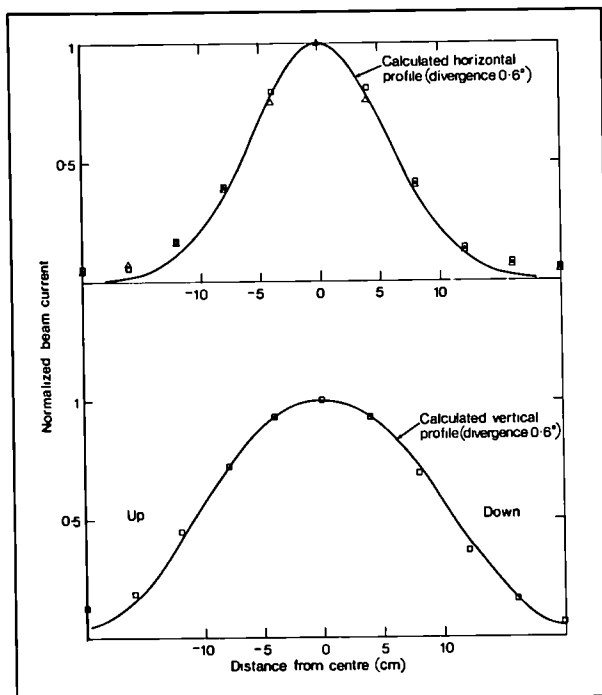


Fig.38 Beam profile from the JET 160kV triode extraction system (Data for 120kV at 7.4m from the source)

Beam Line Construction Group

Beam Line Systems

(R. Haange, H. Altmann, C.E. Brookes, A.J. Dines, J. Gallacher, F. Hurd, J. Jensen, G. Lundqvist, S. Papastergiou, R.B. Tivey, M.J. Watson)

Component Procurement

Delivery of all components for the first beam line system was completed during the year. All high heat load components were subjected to thermal cycling as part of their acceptance tests, including the calorimeter and its back panels that act as beam scrapers, the magnet liners, the dumps for full-energy and fractional-energy ion beams, the Torus duct scrapers, other beam scrapers, the fast shutter and the neutralisers. The thermal cycling took place inside a vacuum oven with the components being heated by radiation or with steam to 300C or 150C before being cooled to room temperature. Generally 10 cycles were carried out, and this proved to be a stringent test of component reliability. A full energy ion dump assembly is shown in Fig.39.

The first fast shutter system was installed in the Neutral Injection Box (NIB). It is actuated pneumatically, and tests show that the actuation time can be brought down to 0.5s. A recalculation of requirements indicate that this is acceptable. Consequently, the operating system with hydraulic actuators (as reported in the 1983 Progress Report PR-1) is no longer needed. The fast shutter for the second beam line has been assembled on the manufacturer's premises and is waiting for delivery of bellows and flexible hoses which are presently undergoing full life cycle testing.

All PINI beam sources for the first beam line system were dismantled, grids G3 removed and re-machined to the new aperture offset, and the PINIs re-assembled. Fortunately, the extraction hole diameter for G3 is not critical and the existing grids could be re-used by increasing the hole diameter slightly while obtaining the new offset.

Manufacture of the water-cooled grids for the second set of PINIs is progressing. Earlier problems with blockages inside the cooling channels and manifolds have been overcome, and delivery of grids is due to start in early 1985. The present grids are manufactured from OFHC copper bases with cooling channels and manifolds machined by spark erosion. A combination of aluminium inserts and wax is used to fill the manifolds and channels before closing the grid with a layer of electro-deposited copper. The aluminium and wax are later removed with suitable solvents. A programme of grid development is continuing with investigations into other methods of manufacture. Cooling water to the grids is supplied through flexible stainless steel hoses and some of the earlier hoses are showing signs of corrosion at welded joints. All hoses for the second set of PINIs have been pickled and passivated, followed by cleaning in demineralised water in a powerful ultrasonic bath to remove all corrosive residues. Eventually all flexible

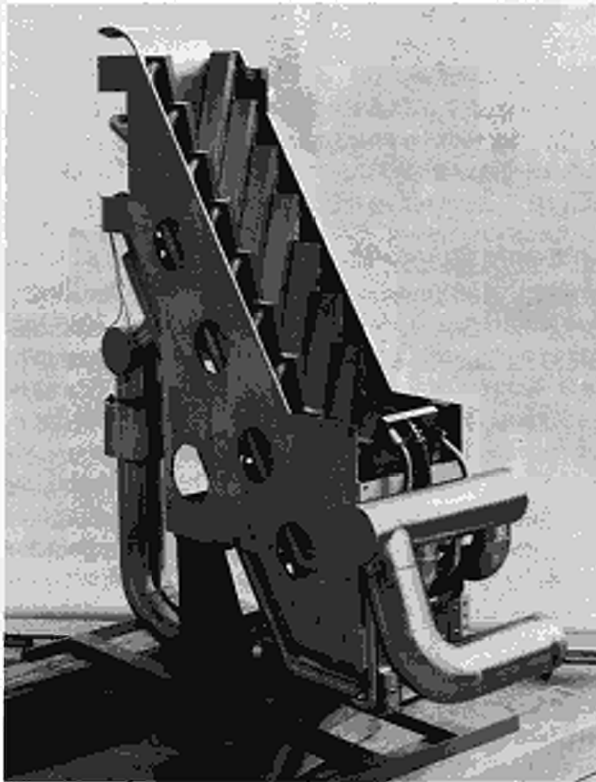


Fig.39 Full energy ion dump showing the Hypervapotron beam stopping elements and cooling water manifolds

metal hoses inside the PINIs will be replaced with ones made from Inconel.

All components for the second beam line system are under manufacture and due for delivery by October 1985. Neutraliser preparation for assembly into the Neutral Injection Box (NIB) has started and all units should be in place by mid-1985. Fig.40 shows a neutraliser before assembly into the NIB. All second system neutralisers are already being fitted with Inconel flexible hoses.

A prototype liquid nitrogen cooled neutraliser (first stage) has been designed and manufacture has started

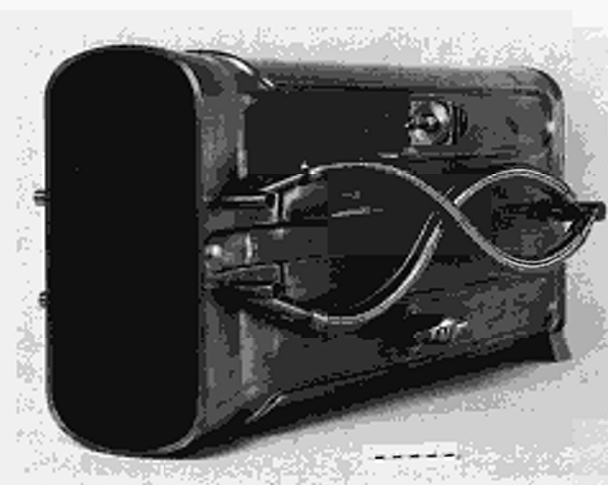


Fig.40 Second-stage Neutraliser showing the water-cooled entrance duct which acts as the first beam scraping element

with the intention of fitting it into a prototype PINI for testing on the Testbed in mid-1985. It is hoped in this way that a gas target with the same neutralization efficiency as compared to the present neutralisers can be produced at a reduced gas flow rate, thus making pumping in the NIB more efficient. If a decision is taken later to incorporate first stage LN₂ cooled neutralisers into all PINIs, the conversion will take place during re-building of the PINIs for 160kV operation.

Pre-assembly of deflection magnets (Fig.41) for the second beam line has started. Building K3 was converted to a clean-assembly room with filtered and temperature-controlled air during 1984, and magnet assembly is continuing inside this area. Eventually Building K3 will become the main area for PINI maintenance and re-building, together with any other JET assemblies requiring clean-room conditions. The building is being installed with high voltage and vacuum testing facilities.

Six additional PINIs were ordered at the end of 1984, with delivery starting at the end of 1985. These PINIs will be equipped for 160kV operation initially and, together with the two prototype PINIs due for conversion to 160kV operation, will allow a smooth transition of JET operation from 80kV to 160kV.

Assembly and Installation

The NIB for the first beam line was installed at Octant 8 in the Torus Hall and welded in place to the Rotary Vacuum Valve. All neutralisers were installed and aligned and their water supply hoses were welded in place. The PINI mounting flanges, on the NIB were aligned during October and November when the opportunity arose to fit an alignment target inside the beam line entrance to the Torus. A special alignment PINI, fitted with a telescope on the beam axis, was mounted at each PINI position in turn and used to set the adjustable supporting flanges. An external laser alignment system was used to record each flange position for future alignment checking.

The high voltage transmission tower was installed behind the NIB. Six PINIs were fitted to the NIB and all water, gas and electrical connections were made between the tower and PINIs. Fig.42 shows two PINIs in position. An inertially cooled calorimeter, suitable for short pulse operation, was installed in the NIB, which will allow the high voltage transmission tower, power supplies and PINIs to be commissioned without interrupting the normal Torus operation.

Manufacture of busbar systems and associated high current vacuum feedthrough assemblies for the current feeds to the magnets inside the NIB have been completed and the first system has been assembled and tested. These radiation cooled UHV structures were manufactured from 15mm thick OFHC copper which is glass bead blasted to enhance the emissivity to a value of 0.3 and are surrounded by a black anodised shielding structure to exclude background plasma.

A Central Support Column (CSC) was prepared with all the components assembled, including one quadrant

with extensive instrumentation, for installation into the Testbed NIB. Completion of the CSC assembly was delayed by a problem of weld cracking in the fractional energy dumps. These components were re-built and fitted to the CSC at the end of 1984. Fig.43 shows a single fractional energy dump element, and Fig.44 shows it fitted between the bending magnet liners.

Assembly and alignment of the second beam line system was started at Octant 4 in the Torus Hall. The support stand, NIB and magnetic shielding were aligned both for co- and counter-injection positions. The duct scrapers were fitted and welded in place.

Cryogenic Systems

(P. Kupschus, A. Jones, E. Küssel, C. Mayaux, M.J. Mead, W. Obert, R.L. Roberts, F. Spath*)

*Kernforschungszentrum Karlsruhe, F.R.G.

Cryopumps for Neutral Injection

The first large cryopump system (nominal pumping speed $8 \times 10^6 \text{l/s}$) to cover the side walls of the neutral injector box (NIB) was delivered in sub-units and assembled on-site by the manufacturer into an assembly stand in early 1984 (Fig.45). After leak testing it was then mounted into the NIB (Fig.46), and an acceptance test performed in the JET Assembly Hall proved that the heat loads to the system without the Central Support Column being inserted (ie 35W and 7kW for LHe at 4.2K and LN_2 respectively), lie well within the respective design limits of 80W and 12kW if extrapolated to final load conditions. The amount of LHe to cool down the 1.5t of LHe structure was found to be less than 1000l revealing efficient use of gaseous helium enthalpy. No particular control actions to the LHe and LN_2 flows during cool-down were required. The NIB has since then been transferred to the Torus Hall, the cryogenic sensors and their signal conditioning equipment have been commissioned with CODAS, and the pump system has been connected via the already installed cryolines to the LHe back-up system. This configuration is now awaiting final commissioning as an integrated system including regeneration tests after extensive hydrogen pumping.

In parallel, tests have been performed using the double-cyromodule pump installed in the Testbed and presenting one-tenth of the full-scale cryo-system. Apart from the confirmation of pumping speeds and cryogenic consumption, experience was gained in two important areas: regeneration of the pump under conditions of heavy coverage of hydrogen and thermal behaviour during multi-second neutral beam operation. In the first case, confidence was gained that despite uncertainties in the extrapolation to the large system the thermal loads and the subsequent pressure rise during regeneration, particularly in the LHe part, can be handled as expected. In the second case, it could be shown that the pump remained operational and stable despite possibly quite high heat loads; however, no change in the consumption rates were found and this discrepancy is still being assessed. The manufacture and partial testing of the

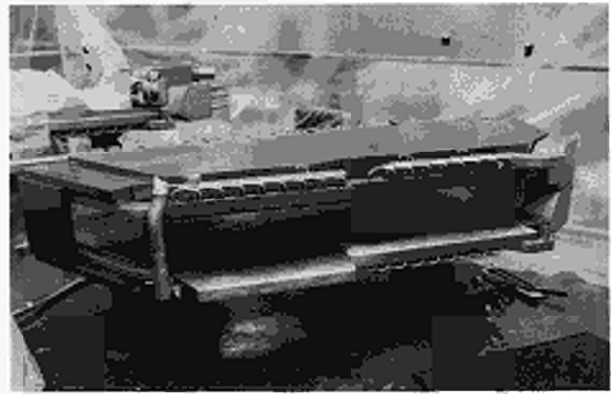


Fig.41 Bending magnet fitted with liners, showing the cooling water manifolds

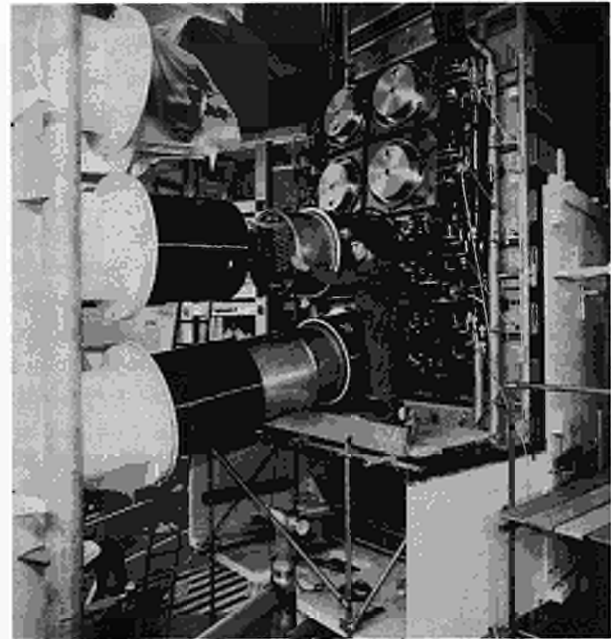


Fig.42 Neutral injector box in the Torus Hall showing two beam sources in position, the SF6 tower insulators and the Faraday cages covering the high voltage interface

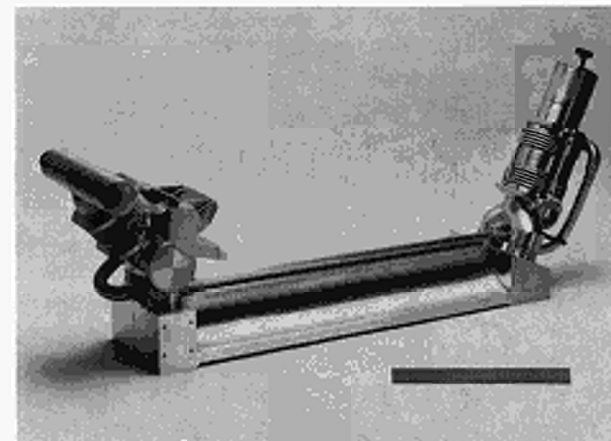


Fig.43 Fractional-energy ion dump, complete with cooling water connections, prior to fitting onto the bending magnet assembly

cryopump system has been reported recently [13, 14, 15].

The second large cryopump system which is to go into the second neutral injector at Octant No.4 has been dealt with in the same manner; delivered in September, it is now installed in its NIB and is awaiting acceptance tests in the Assembly Hall.

Cryo Supplies

During 1984, the remaining major parts for the LHe refrigerator plant have been delivered: the LHe cold box, the LHe/LN₂ valve box for distribution of cryogenics to three loads, the 5000l LHe storage tank, the control panel including the programmable controller and the He recovery system including 200m³ of NTP storage of He in balloons (equivalent to the contents of three cryopumps) and 2000m³ of NTP equivalent high pressure storage (equivalent to the total He content). These items were installed (Fig.47), integrated with all necessary services and preliminary acceptance tests were carried out. LHe was then produced inside the cold box within the contractual date; the generated power was measured to be about 560W at 4.6K, which exceeded that for the final acceptance test, (ie 300W at 3.6K at the valve box outlets). Meanwhile, further tests have been run in successive integration of further components, and the refrigerator now maintains routinely a level of about 3000l LHe in the storage tank. Final acceptance tests and the start of operation with the cryopump system are planned for the first half of 1985.

In parallel, a LHe back-up system has been procured, assembled and part-commissioned consisting of a LHe sub-cooler to be supplied from externally procured dewars or tanks, a pair of Roots blowers to permit operation under sub-atmospheric pressure at 3.6K and the respective control system to be operated from CODAS. This system will carry out the first integrated tests on the large cryopump system before it is connected to the refrigerator.

The cryogenic supply and distribution system for the NI Testbed with its controls and monitoring panel has been commissioned and (apart from a LHe line to the target tank which will be fitted later), it is in routine operation.

Cryo Components for the Tritium Plant

This activity has just started. A small test stand is being procured in which prototype components for the future Tritium Recycling Plant (a cryo transfer pump and a cryo accumulation panel have been ordered) will be tested in the first half of 1985.

Neutral Beam Operation Group

(E. Thompson, N.E.B. Cown, A.P.H. Goede, T.T.C. Jones, A. Stähler*, D. Stork)

*MPI für Plasmaphysik, Garching, F.R.G.

Efforts have been concentrated in two major areas: participation in the programme of the Testbed and preparation for operation on the Tokamak.

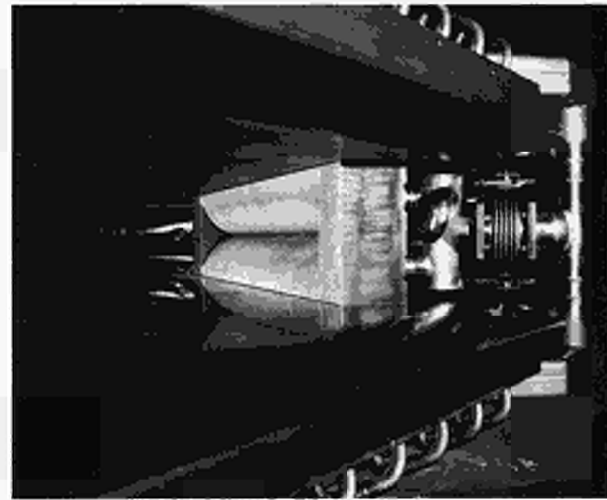


Fig.44 View in between the bending magnet liners, showing the fractional-energy ion dump

Control and Data Acquisition Software

(T.T.C. Jones, D. Stork, M.E. Rodgers, K.D. Starley)

During this period, most of the NI data acquisition system and associated software has been brought into routine operation of the Testbed. This covers 450 data channels with time resolution ranging between 4μs and 40ms depending upon the application (fast channels for beam source power supplies, slow channels for thermocouple data). Some channels incorporate event driven data recording, to economise on data storage.

Various data reduction and display programmes have also been brought into routine use, such as waveform averaging and display, contours of thermal data and subsequent calculation of beam parameters, archiving



Fig.45 Fully assembled cryopump system in assembly stand

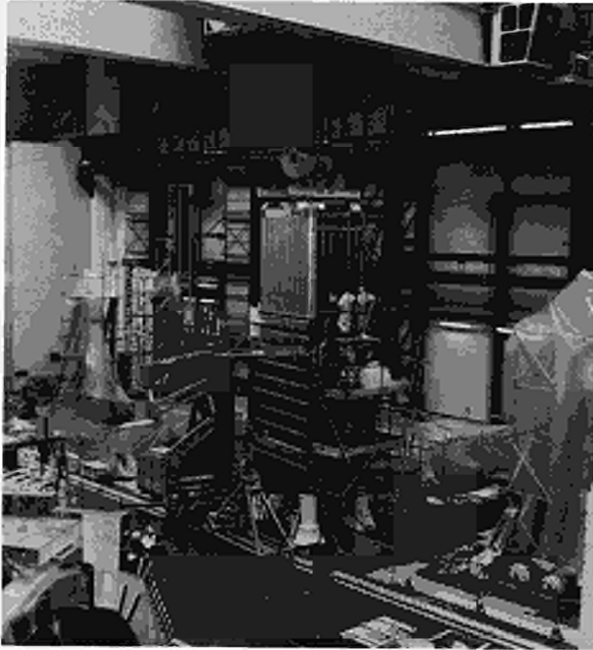


Fig.46 Cryopump system during installation on Neutral Injector Box (NIB);

and retrieval of derived parameters with graphical display of inter-parameter dependencies. All of the operational 'data driven' acquisition and display programmes which incorporate standard CODAS software products are virtually identical to the system now installed on the computer to be used for the first beam line system on the Tokamak. The same philosophy of using, where possible, identical software in the Testbed as that employed in the Torus Hall system, was also applied to the control software. This has been carried out for the single point manipulation and power supply

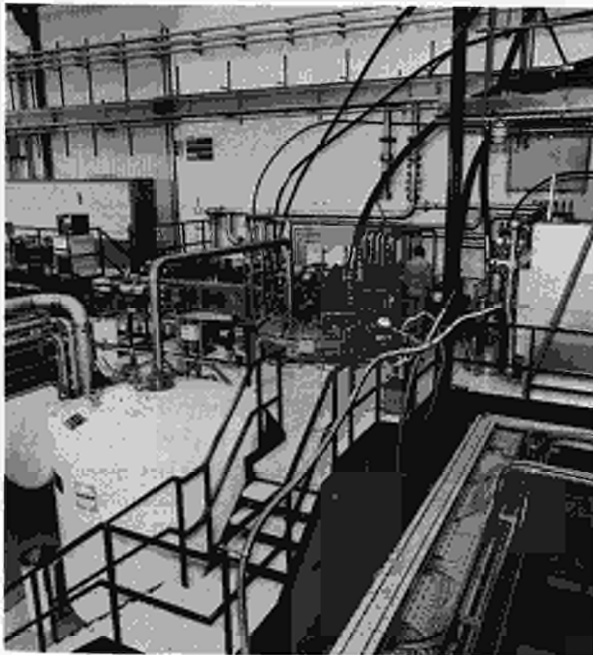


Fig.47 View of LHe refrigerator platform with cold box, valve box and LHe backup system;

set-point definition (level 3 control) and the higher level (level 2) control for the gas introduction system. A particularly valuable feature also in routine operation is the definition of the sequence of central timing system by the supervising programme SCHEDULER [16]. Additional software specific to the Torus Hall installation for the setting of multiple power supplies has been defined and is being produced by CODAS Division.

Control and Data Acquisition Hardware

(D. Stork, A. Burt, D. Cooper, D. Ewers, D. Young)

The design, installation and commissioning has continued of all the local control cubicles of the first NI system. These control cubicles and associated electronics interface the 'local units' to the CODAS system, and include the gas handling and introduction system, the thermocouple instrumentation for the total beam line system, optical beam scanner control, fast shutter control and the protection plate viewing system (PPVS) described below. The majority of these cubicles have been installed and commissioned or are in the final stages of commissioning with CODAS.

Protection Plate Viewing System and Plasma Density Interlock

(A. Stähler, D. Cooper, D. Stork)

Due to the high power density of the neutral beams, it is mandatory to prevent damage to the Torus in the event of inadequate attenuation of the injected beam by the plasma. The areas of the inner surface of the Torus which could intercept the beams are covered by graphite tiles which protect the Torus wall under two different conditions:

- (a) 'Shine-through' of the attenuated neutral beam due to insufficient plasma density for the total duration of an injection pulse;
- (b) Interception of the full unattenuated beam power of $\sim 2\text{kWcm}^{-2}$ due to either lack of synchronisation of the beam with the plasma or rapid loss of plasma due to a disruption during a NI pulse.

The performance of the graphite tiles under both conditions have been analysed in detail and resulting limits on operational parameters have been defined.

The operational density limits for 'shine-through' are found to be $\bar{n}_e > 0.75 \times 10^{19} \text{m}^{-3}$ and $\bar{n}_e > 2.6 \times 10^{19} \text{m}^{-3}$ for the 'tangential' and 'normal' beams (making two or one pass through the plasma respectively) in the case of 80kV H^o beams. These limits, which are not restrictive in terms of presently achieved plasmas, are imposed by the requirement that the inconel tile support structure temperature should not exceed 650C. The limiting duration for interception of the completely unattenuated beam has been determined from calculations of the thermal stress produced in the tiles when subject to a surface power loading of 2kWcm^{-2} , which leads to a limiting duration of 100ms to prevent cracking of the tile.

To ensure that both of the above conditions are maintained during routine operation, a Protection Plate

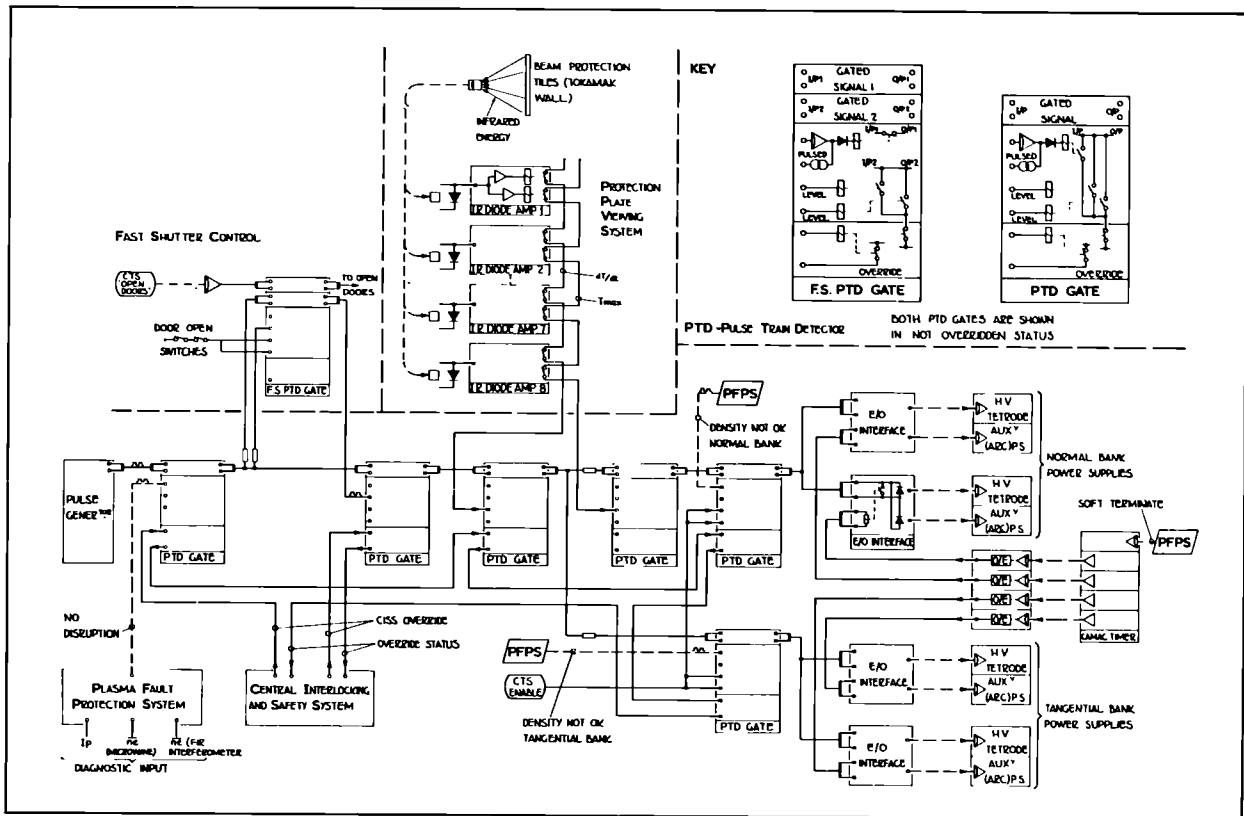


Fig. 48 Schematic of control scheme showing interfaces of protection plate viewing system (PPVS) with the JET plasma fault protection system (PFPS) and NI power supplies

Viewing System (PPVS) has been designed for incorporation into the JET Plasma Fault Protection System (PFPS) [17].

The PPVS uses IR sensitive diodes about 40m from the Torus (to prevent radiation damage) coupled to the viewing optics via low-loss radiation-resistant optical fibres. The high degree of reliability required is achieved using built-in redundancy and internal checking facilities. Signal processing electronics will produce trip levels for both the temperature of the graphite tiles and its time derivative for incorporation into the PFPS.

The total injection-related PFPS system (shown schematically in Fig.48) consists of several widely separated units, each of which perform different tasks. A considerable effort has been made to ensure fail-safe operation. The basic scheme relies upon the need to supply a 1kHz pulse train to the main high voltage power system of each accelerator in the neutral beam system to enable them to be switched on and their output to be maintained. Loss of this pulse train results in the power supply being switched off in one period of the pulse train and disabled for the remaining duration of the requested 'on' time.

The passage of this pulse train to the power supplies can be interrupted by the closure of any of several relay contacts which are all in parallel across the signal cable.

The relay contacts are normally closed and are only maintained open by the presence of signals from:

- the PFPS to indicate that both the measured plasma density and plasma current are above pre-set threshold levels;
- the fast shutter control to indicate that it is in the open position;
- the PPVS to indicate that the temperature and its time derivative are below pre-set values;
- the JET Central Interlock and Safety System (CISS) to indicate that a proper mode of beam line operation and control has been selected.

Signals (a) and (b) are pulse trains themselves and thus give constantly 'refreshed' status information. Signals (c) and (d) are maintained levels and the disappearance of any one signal channel would result in closure of the relay contacts which crowbar the signal necessary to switch on and maintain the high voltage power.

Optical Beam Scanners

(D. Stork, N.E.B. Cowern, T.T.C. Jones)

There will be six optical beam scanners installed on each of the two injectors in the Torus Hall. These are rotating mirror devices (Fig.49) which detect the Balmer- α light emitted by the beam and residual gas in the beam line.

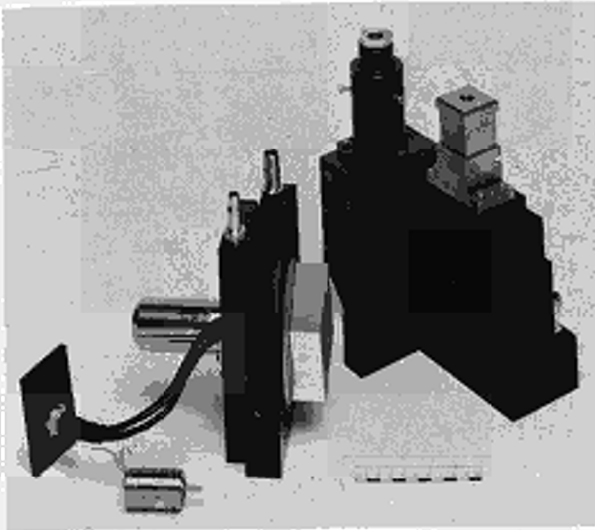


Fig.49 Optical beams scanner partially disassembled to show rotating cube mirror. The resolver angular transducer which measures the angular position of the mirror is also shown separately.

The spatial profile of this radiation can then be related to the beam intensity profile at the plane of viewing. Beam profiles can be obtained at various rates up to one every 3ms dependent upon selected speed of the feedback-stabilised mirror rotation.

The assembly containing the scanning mechanism which is close to the Torus is designed to be both radiation resistant and compatible with remote handling requirements for the active phase of JET Operation. The light signals are conducted away from the Torus by long lengths of fibre optics to the photomultiplier detectors and associated signal processing systems. Subsequent data recording is event driven by the digitised mirror position signals.

Complete systems have been brought into operation on the Testbed and scanners are currently in use to give beam profiles in different planes at varying positions along the beam line.

Further developments include the studies of adding a Fabry-Perot etalon to a scanner in order to obtain spatial profiles of the various energy components of the neutral beam by utilising the Doppler shifted light from excited beam atoms.

During operation of the scanners in the Testbed it was observed that temporary fluctuations in the light emitted by the beam could be used as indicators of the perveance matched condition of the beams which could prove useful for operation on the Tokamak.

Commissioning of the Injector System in the Torus Hall
(D. Stork, T.T.C. Jones, J.F. Davies)

To both simplify and minimise the commissioning of the total injector system in the Torus Hall, an inertial calorimeter has been installed in the injector box at

Octant No. 8. This will enable all the beam sources and associated power supplies, gas and water systems plus their control and data acquisition to be fully commissioned prior to installation of the beam line system attached to the central support column. At present, six of the eight beam sources are installed and connected to their power supplies and one plasma source has been operated from the JET control room.

Historically, commissioning of the total power systems has been the major time consuming process in bringing the injectors into operation. By starting this task early, it is expected to considerably shorten the time between the beam line system installation on the Tokamak and its full operation.

Preparation of Tests of the CSC Assembly (E. Thompson, A.P.H. Goede)

In parallel with commissioning and testing the beam sources and power systems in the Torus Hall, the Central Support Column will be installed in the Testbed and one quadrant tested using the operational beam source. To simulate as closely as possible the gas pressure profile of the final installation in the Torus Hall, temporary gas baffles will be attached to the CSC. In addition to the existing thermocouple instrumentation, provision has been made for viewing various components with an infra-red camera during these tests.

Future Work

In the first half of 1985, the Division will be involved in two main tasks on the first neutral injector:

- After completion, the Central Column system will be tested in the Testbed, where power supplies for a second beam source have been installed. Essentially the test will be limited to one quadrant of the system;
- The injection system of power supplies and beam sources with their controls will be commissioned in their final configuration. Short-pulse beams will be extracted from pre-tested beam sources and dumped in an inertially cooled dump that has been temporarily installed in the injector vacuum box in the Torus Hall. The aim is to operate eight sources simultaneously and during Tokamak plasma discharges.

The Central Column system will then be transferred from the Testbed into the Torus Hall for final system commissioning and beam heating experiments to start after the JET shutdown in Summer 1985. In parallel, component procurement and assembly of the second injector will continue.

References

- [1] Culham Neutral Injection Group, Culham Laboratory, Proc. 12th Symp. on Fusion Technology, Jülich (1982) p.1329
- [2] Holmes, A.J.T., Thompson, E., Rev. Sci. Inst. 52, 172, (1981)

- [3] Ehlers, K., Leung, K., Rev. Sci. Inst. 53 1423 (1982)
- [4] Goede, A.P.H.G., Green, T.S., Phys. Fluids 25 1814 (1981)
- [5] Green, T.S., Coupland, J.R., Hammond, D.P., Holmes, A.J.T., Martin, A.R. Hemsworth, R.S., Thompson, E., Proc. 10th Int. Conf. on Plasma Physics and Controlled Fusion Research, London (1984)
- [6] Culham Neutral Beam Development Group, Proc. 13th Symp. on Fusion Technology, Varese, 693 (1984)
- [7] Jones, T.T.C., JET Internal Report PDN 13 (1982); Falter, H.D., JET Internal Report JIDT 3/83 (1983)
- [8] Nielsen, B.R., Goede, A.P.H. Hemsworth, R.S., Thompson, E., Vacuum 34, 37 (1984)
- [9] Ohara, Y., Matsuda, S., private communication
- [10] Spaedtke, P., Conf. on Linear Accelerators, Sieheim (1984) (to be published)
- [11] Neutral Injection Group, Culham Laboratory, Internal Reports CLM.RR/J3/1 and 2 (1979)
- [12] Fumelli, M., Bayetti, P., Becherer, R., Bottiglioni, F., Desmons, M., Raimbault, P., Valckx, F.P.G., Proc. 13th Symp. on Fusion Technology, Varese, 617 (1984)
- [13] Boissin, J.C., Bacca, J.P., Obert, W., Küssel, E., Kupschus, P., Mayaux, C., Sonnerup, L., Construction of the Large Cryopump Systems for JET, Le Vide/Les Couches minces, Suppl. to No.221, (April 1984)
- [14] Obert, W., Küssel, E., Kupschus, P., Mayaux, C., Santos, H., Boissin, J.C., Bacca, J.P., Large Scale Cryopumps for JET, 10th International Cryogenics Conference, Helsinki (1984)
- [15] Obert, W., Duesing, G., Küssel, E., Kupschus, P., Mayaux, C., Rebut, P.H., Santos, H., The JET Cryopump System and its Cryolines for Neutral Injection, 13th Symp. on Fusion Technology, Varese (1984)
- [16] Jones, T.T.C., Brenan, P.R., Rodgers, M.E., Stork, D. Young I.D., Control Data Acquisition and Analysis for the JET Neutral Injection Testbed, 13th Symp. on Fusion Technology, Varese (1984)
- [17] Stork, D., Cooper, D., Gondhalekar, A., Lomas, Noll, P., Reed, K., Schüller, F.C., Stäbler, A., 26th Meeting of the Plasma Physics Division of the American Physical Society, Boston (1984)

Radio Frequency (RF) Heating Division

(Division Head: J. Jacquinet)

Radio Frequency Heating Division is responsible for the design, construction, commissioning and operation of the RF heating system during the different stages of its development to full power. The Division also participates in studies of the physics of RF heating and is responsible for performing the related experiments on JET.

It was decided only in 1981 to use waves in the ion cyclotron resonance frequency (ICRF) range as a heating method to provide a further 15MW of power to the JET plasma. Design work was started immediately, with assistance from the EURATOM-CEA Association, Fontenay-aux-Roses, France; creation of the Division followed in 1982 and most professional staff were recruited during the latter part of 1982 and 1983. Several physicists and technicians joined the Division in 1984. Recruitment will be completed in 1985, with the arrival of a second complement of technicians and of physicists coming under the Associated Staff scheme. The dates of milestones for the RF heating programme are summarised in Table.X.

1984 was a most challenging and rewarding year. All components for two RF units were first fabricated and tested separately in various locations in Europe; then, by the end of the year these were assembled together for the first time on JET. The initial tests with the first complete unit showed that all the objectives, set only two years previously, had been met, despite the originality and ambitious design of the major components. This outstanding achievement is a tribute to the quality and dedication of the staff as well as the tremendous response received from Industry and the Associated Laboratories.

T A B L E X

The main steps in the ICRF heating programme

1984	<ul style="list-style-type: none"> — 2 prototype antennae installed in JET — a 3MW unit commissioned and connected to the antennae
1985 – 1986	<ul style="list-style-type: none"> — Installation of a third antenna — Operation on JET with progressive increase of power up to 4.5MW (high grade) in the plasma (3×3MW generators, 3 antennae)
1986 – 1988	<ul style="list-style-type: none"> — Installation of 6 water cooled antennae integrated with toroidal limiters — Operation on JET of 9MW high grade power
1988 – 1990	<ul style="list-style-type: none"> — Operation with 15MW high grade power (10 antennae)

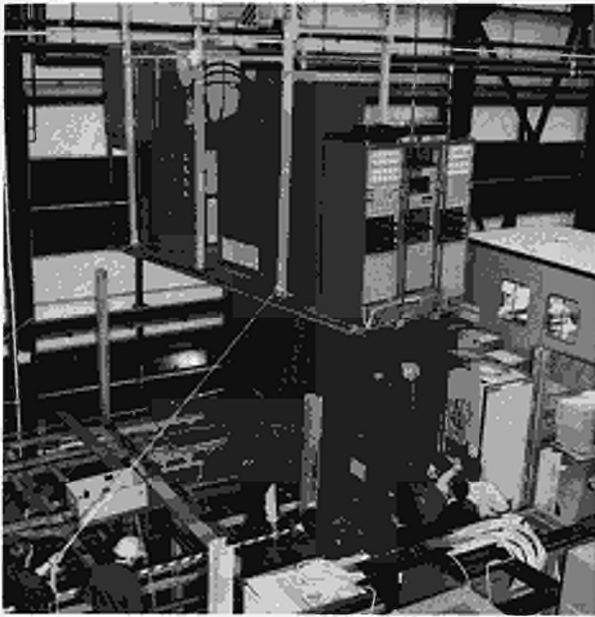


Fig.50: Installation of RF Generator

The Division's tasks can be divided into three main areas reflecting the Group organisation, as follows:

- (i) The RF Power Group is charged with the construction and operation of the generator system (33MW final output power in total), and of the matching and transmission networks (up to 1.5km of coaxial lines). The Group has also started to study possible enhancement of the present systems;
- (ii) The RF Antenna System Group is responsible for the complete design, construction and installation of the launching structures and of the equipment necessary to test a complete antenna. There is a large part of the development included in this activity, as several generations of antennae are foreseen;
- (iii) The RF Physics Group is in charge of conceptual aspects of heating scenarios and of the physics of the experimental programme.

Radio Frequency Power Group

(T. Wade, R. Anderson, G. Bosia, M. Schmid)

The work of the RF Power Group is concerned with placing contracts, installation, commissioning and operation of the complete ICRF heating plant. The plant will consist of up to ten RF generators in the North Wing of the JET buildings and 1.5km coaxial transmission lines which feed RF power through the Basement and up to the antenna vacuum transmission lines on JET. A further generator unit will be used to power the RF Testbed. During the year, the major contracts for the supply of the high-power RF generators and transmission lines progressed from design development to manufacture and installation of the first units (Fig.50).

Considerable effort was devoted to promote these contracts and as a result of pre-prototype driver and the

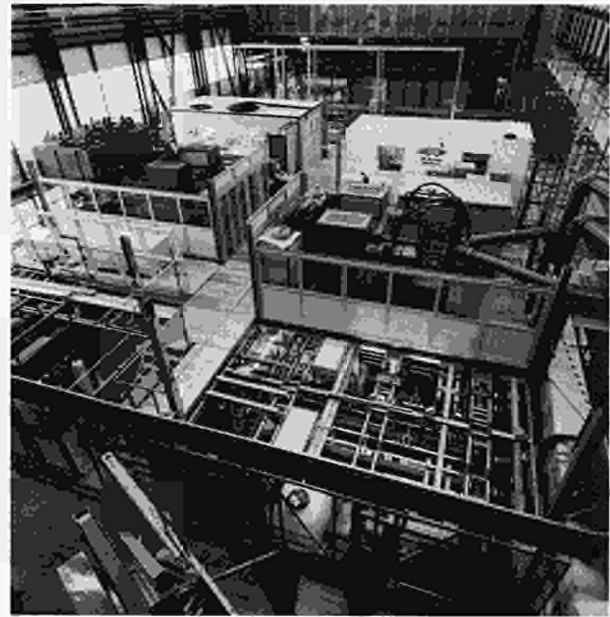


Fig.51; General view of North Wing, showing RF Generators

first 3MW unit were successfully operated on JET (Fig.51). The performance limits imposed on the RF generators by the operating parameters of commercially available RF power tetrode valves were investigated and the transmission line insulators were further developed to withstand the high RF voltages specified. Ensuring compatibility with the high-voltage DC power supplies was also a major priority, as flexibility is an important factor in maximising the RF generator's performance.

Radio Frequency Generator Plant

The design of the RF plant was based on requirements for heating plasmas with various ion species, plasma parameters and magnetic fields, which dictated an operating frequency range of 25-55MHz. Each unit (Fig.52) can deliver 1.5MW RF power into load mismatches of up to 20% reflected voltage (VSWR = 1.5) for periods of 20s.

Radio Frequency Generator Unit Design

The low power stages (including the amplitude, phase and frequency control circuits) feed wideband transistor power amplifiers providing up to 600W each to the two power amplifier vacuum tube chains. Each chain consists of three RF tetrodes producing 20kW, 100kW and 1.5MW, respectively. All tuning adjustments are motorised to provide automatic setting of the 4MHz wide generator bandwidth, within the 25-55MHz operating range. The tuned bandwidth is designed sufficiently broad to allow 'instantaneous' frequency shifts of up to ± 2 MHz to rapidly match the generator to load variations caused by changes within the plasma.

The RF power from the final stage tetrode is coupled to the transmission line (30Ω impedance) through a specially developed high-power matching network which provides bandwidth, impedance transformation and filtering for the harmonics generated in the Class B

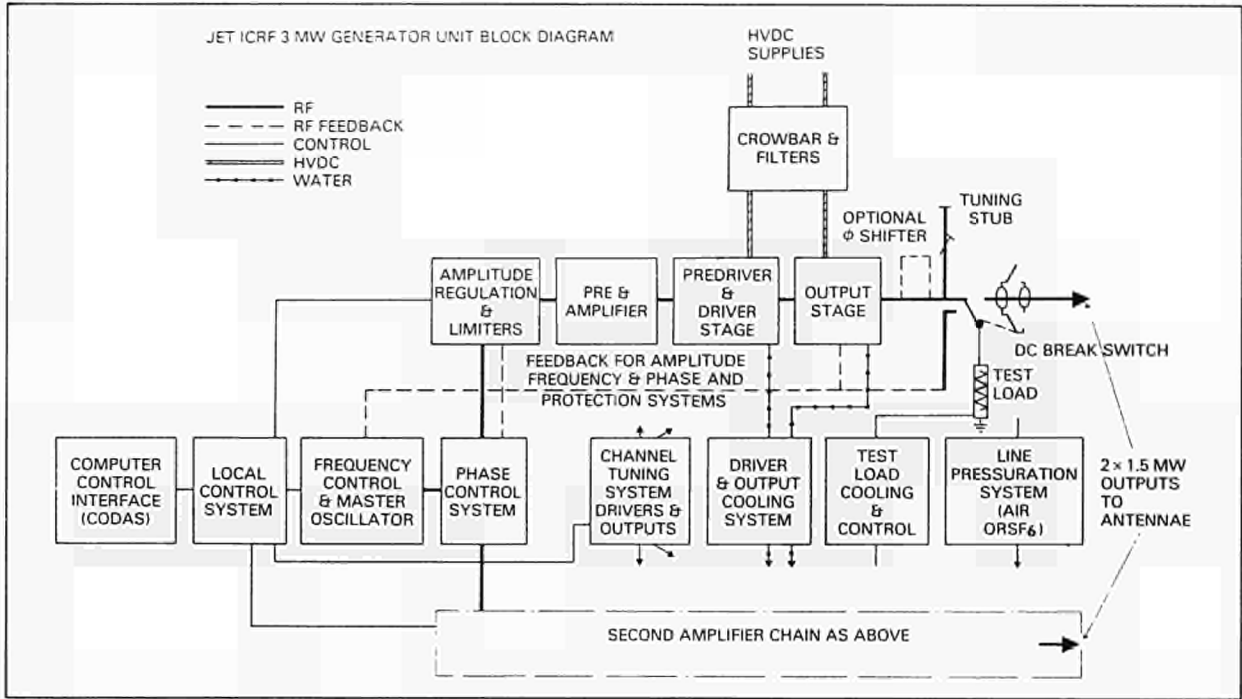


Fig.52: Block diagram of RF Generator

operating regime. Fig.53 shows the assembly of this stage during operation.

The 100kW and 1.5MW stages are water cooled and the lower power stages are air cooled. The generators are protected against flashovers by ignitrons which short circuit the DC supplies. An emphasis on unattended and fail-safe operation has been applied to the design of the control system for the generators. During normal operation, the generators will be computer controlled using CODAS.

During the initial planning of the generator contract, it was noted that development of the amplifier chains and control circuits as far as the driver stages would be completed well before the output stages. Consequently, a pre-prototype driver unit able to deliver about 200kW of driver power was made available to JET seven months before a completed 3MW RF Unit. This enabled various interface tests and antenna coupling measurements and antenna conditioning to be performed ahead of schedule (see Fig.54).

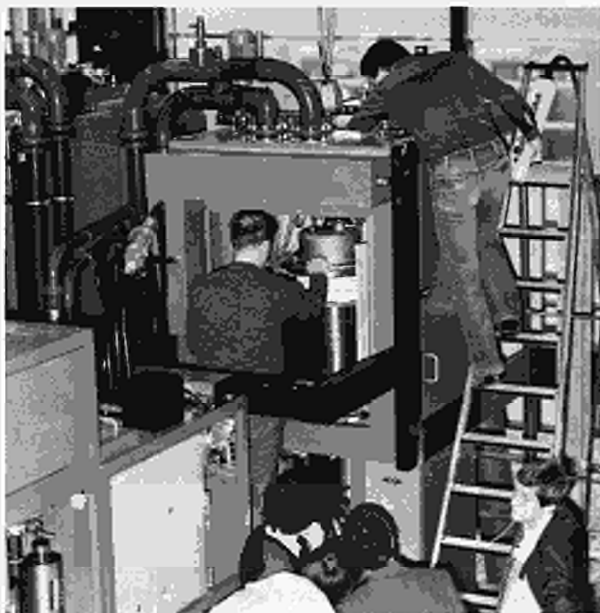


Fig.53: Installation of output tube

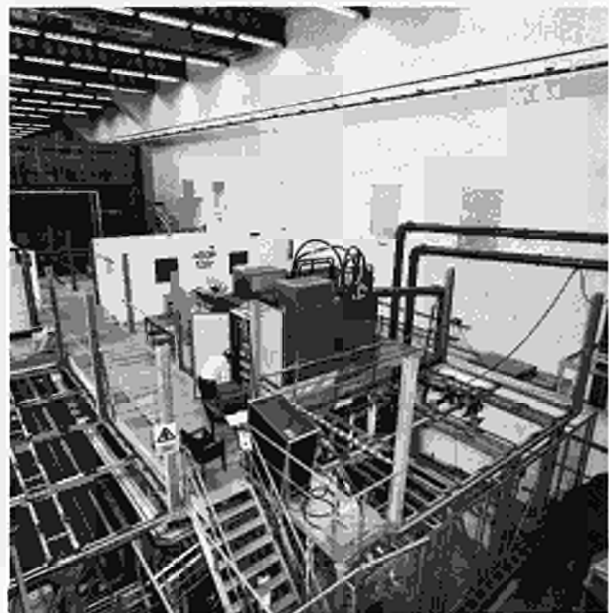


Fig.54: Prototype driver unit under test

Depending on the reflected power phase angle, a range of impedances is presented to the output tetrodes. A control circuit in the generator changes dynamically the voltage of the DC supply during the course of the 20s discharge in order to keep the tetrode within the permitted operational range. The control and monitoring circuits between each power supply and generator including the anode voltage control loop are fed through fibre optic links to eliminate induced interference over the long route. No problems have been encountered in the first period of operation of this system.

Maximum Anode Dissipation	1MW
Maximum DC Anode Current	120A
DC Anode Voltage Range	14-26kV
Maximum Anode Voltage	50kV
Screen Grid Voltage	2kV

Power contours are drawn at 100kW intervals from 100kW near the edge to 1.5MW at the centre of the diagram.

Simulation of the Final Stage Power Apability

Calculations have been performed to investigate the available power from a tetrode valve according to the phase and magnitude of RF power reflected back to the valve anode. These are represented in Fig.55 as power contours on a Smith Chart. The centre of the chart represents the matched condition of zero reflected power; in this case, the tetrode matching network presents an impedance of 120 Ω to the tetrode. Circles centred on this point of increasing radius represent an increasing proportion of reflected power and the contours on the chart indicate the limits of output power to be expected. The chart has been plotted for the following parameters:

ICRF Transmission Line System

The Transmission Line System not only transfers power from the generators to the antennae, but also forms part of a matching system between to the generators and the antenna. All the lines in the system have the same nominal electrical length to assist with phased antenna operation. The excess length of the lines feeding the nearest antenna is absorbed by running the lines round the perimeter of the Generator Hall to those generators on the far side (see Fig.51)

By using a tuning stub near the generator and rapidly varying the frequency, the best compromise for the working load during a 20s RF pulse can be obtained regarding varying antenna admittance parameters. One drawback of this system is that the major part of the transmission line can be exposed to high reactive power levels (high voltage standing wave ratios), and,

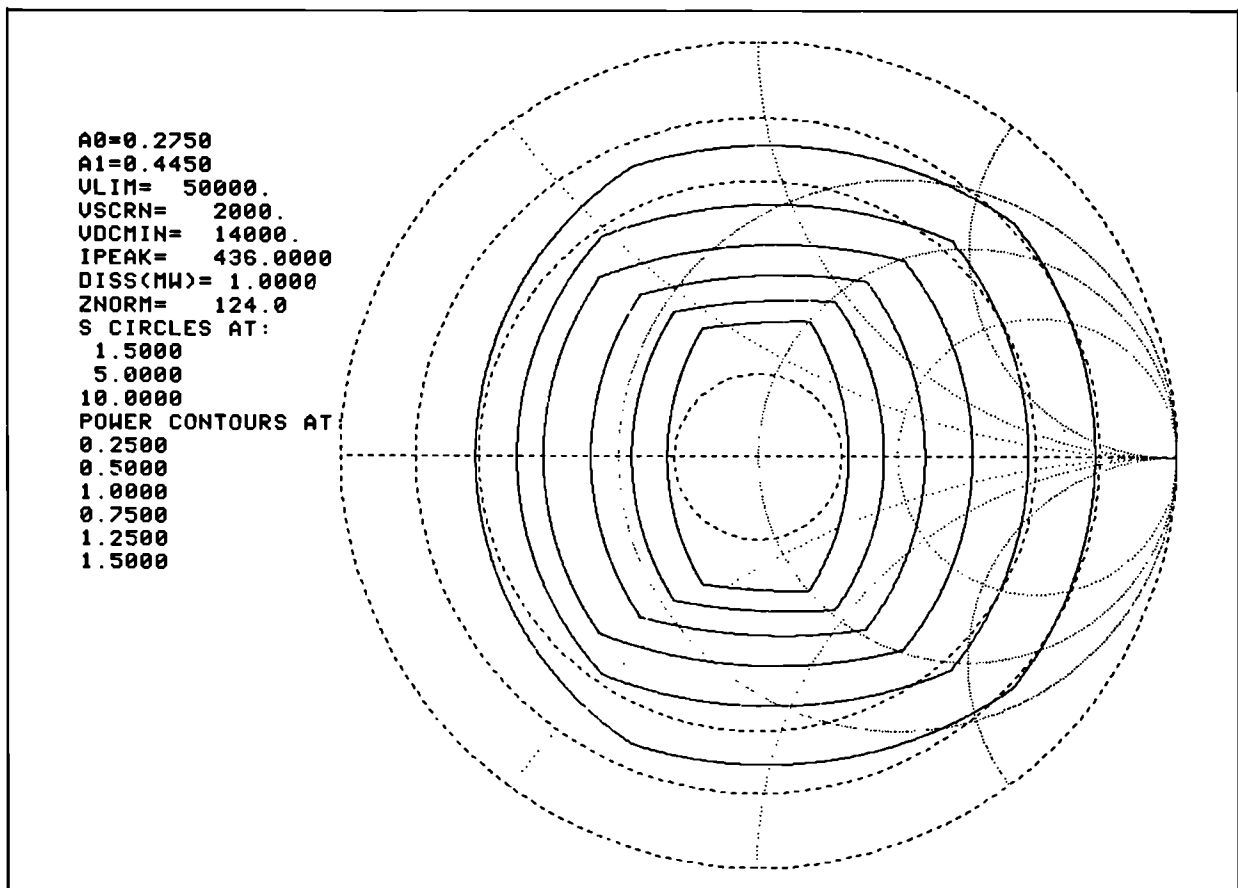


Fig.55: Power contour diagram.

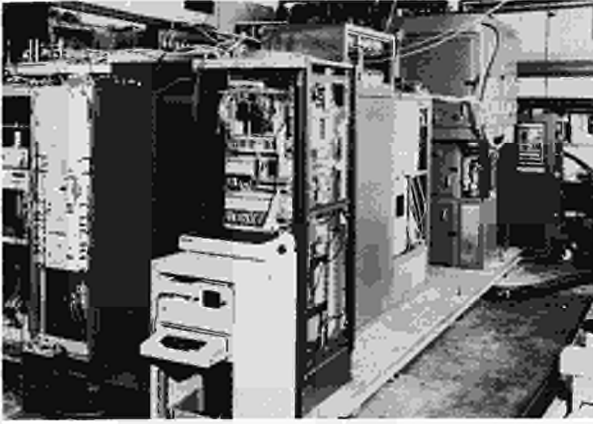


Fig.59: Prototype tests at the manufacturers



Fig.60: Tested assembly of the A_0 housing, central conductor and graphite tiles

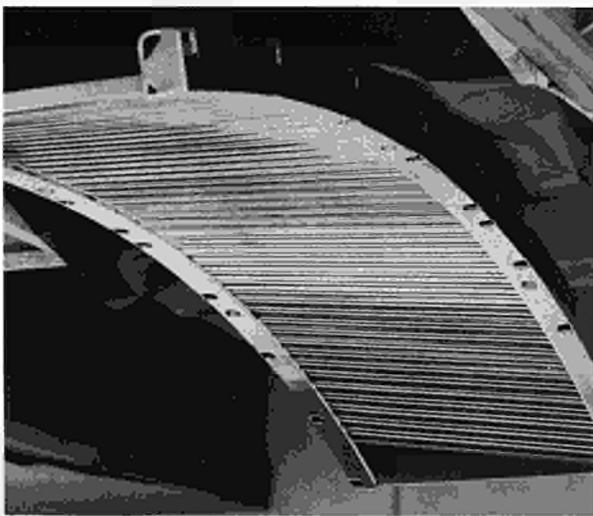


Fig.61: The A_0 electrostatic screen

RF Antennae Systems Group

(A. Kaye, J. Arbez, H. Brinkschulte, A. Franklin, E. Hanley, P. Murray, J. Plancoulaine, C. Walker)

The RF Antennae Systems Group is responsible for the design, manufacture, testing, installation and maintenance of the RF launching structures, which are mounted inside the torus to couple power to the plasma. In addition, it is in charge of the vacuum transmission lines required to transmit the power from the incoming main transmission lines, through the vacuum wall and to

the antennae. The Group is also responsible for the on-going development and testing of components to improve the performance of the system.

During the year, major progress has been made in completion of the manufacture and testing of the two prototype A_0 antennae and installation and commissioning of these in the torus. In addition, following a decision to instal a third A_0 antenna in the torus in the 1985 shutdown, the manufacture of this new antenna is well advanced. In parallel, the design of the A_1 antennae has continued and the main manufacturing contracts placed. In preparation for testing of the antennae, the RF Testbed has been transferred from Fontenay-aux-Roses to the JET site and is being up-graded.

Design and Manufacture of the Prototype Antennae

The design of the A_0 antennae was largely completed in 1983 and the manufacturing contracts placed. The A_0 antennae are designed for short pulse operation (typically 1s) at maximum power (1.5MW into the plasma) to provide detailed design information for subsequent antennae. In particular, areas such as coupling efficiency, impurity production, RF losses in the components, and voltage limitations on the antennae and transmission lines can be explored. In addition, the pulse length can be increased to several energy confinement times at modest duty cycle to give useful results on the physics of RF heating.

The A_0 design was presented in detail in the 1983 JET Progress Report. The antenna comprises an open Inconel 600 box (typically 2mx0.6m) surrounded by graphite tiles for protection from the plasma, and containing either one (monopole) current carrying central conductor or two (quadrupole) central conductors. These conductors must operate at very high current (typically 1kA r.m.s.) in order to excite waves effectively in the plasma. This requires that the system operate at high voltage (35kV r.m.s. max) and in order to withstand this voltage the conductor is protected from the plasma by a slotted nickel screen which is transparent to the vertically polarised wave.

The manufacture of two of these antennae is now complete. The housings are complex welded fabrications which required careful control of shrinkage and distortion; both were found to meet the JET requirements after final machining. All surfaces in the torus vacuum have been electropolished, and all current-carrying surfaces silver plated. Both of these processes required a high level of skill by the contractors to obtain the necessary quality over the large surface areas involved. All plated components were baked to 300C to test the adhesion of the silver with satisfactory results. A trial assembly of the monopole central conductor in a housing is shown in Fig.60.

The nickel screen was fabricated by welding pre-machined bars to the side pieces with tight tolerances on the spacing between bars and the curvature of the screen; one of the screens is shown in Fig.61. These A_0 screens are not cooled and heating of these elements is the main

limitation on pulse length. The side protection tiles were fabricated from high purity fine grain graphite for its good thermal shock resistance and low atomic numbers, and were outgassed at 1200C under vacuum after fabrication. These tiles can be seen in Fig. 60.

The demands on the design of the vacuum transmission lines were particularly heavy, due to the requirement to handle 1000A at 35kV r.m.s. within the 150mm diameter of the pre-existing limiter guide tubes. The conductors were carefully profiled to minimise the electric field, with particular attention to the ceramic supports and the bellows. Current-carrying surfaces were silver plated but heating of the inner conductor, which is cooled only by radiation, remains a further limitation on the pulse length and duty cycle. Fabrication of the mechanical components of these lines required careful control of distortion of the conductors during welding and machining.

The lines include a double vacuum window fabricated by vacuum brazing alumina discs to copper conductors. This was technically demanding on the contractor, and in addition, the RF performance was found to depend strongly on the shape and position of the corona rings, which were optimised after extensive RF testing. Following these developments, the JET requirements for windows for the A_0 antennae were successfully met. The final steps in the fabrication of the transmission lines were two electron-beam welds of dissimilar materials. The inconel/stainless steel weld to the window presented some difficulties, but was successfully completed.

The vacuum transmission line is only poorly connected to the main torus vacuum, and requires additional pumping. The last major contract for the A_0 antennae covered the manufacture of this system, which was produced and tested to a very tight schedule.

Testing of the Prototype Antennae (in conjunction with B. Beaumont, Euratom-CEA Association, Fontenay-aux-Roses, France)

The Testbed for testing of components and assemblies of the JET antennae had previously been installed at Fontenay-aux-Roses, utilising the TFR RF generators, and many tests on individual components were carried out there.

During 1984, all ceramic components for installation on JET were tested at maximum voltage and again at maximum current. These tests showed some spread in the voltage stand-off of the windows; all the windows installed were successfully tested to at least 30kV r.m.s. As the window is located near a voltage minimum, this voltage should not prove a limitation for the present antennae.

In addition, each of the four vacuum transmission line (VTL) assemblies used on the torus was assembled on the Testbed, baked to 300C and tested with an open circuit at the antennae connection. These assemblies were first conditioned to withstand multipactor arcs by repeated low power pulses. The increase in pressure during the pulse was found to decay steadily with conditioning and could be used as a monitor of the

condition of the line. After conditioning, each of these assemblies was tested to a maximum voltage of 25kV r.m.s.

Each of the two antennae was also assembled on the Testbed with associated VTLs and tested by driving one of the lines with the other open-circuited outside the vacuum window. The initial tests on the monopole assembly produced arcs between the screen and the housing. The screen was electrically isolated by two 3mm thick inconel strips plasma-sprayed with alumina, running lengthwise between the screen and the housing. The arcing occurred across these spacers at both ends, apparently as a result of excitation of standing waves in the spacer. This problem was overcome by removing the insulation. The currents that will be induced by a disruption in the torus, and thus the forces on the screen, are thereby increased. This is not anticipated to be a problem on the A_0 antennae and has been taken into account in the design of subsequent antennae. With this modification, both assemblies were tested successfully to 28kV r.m.s. In addition to these high power tests, the electrical characteristics of each antenna were measured at low power and are described in the following sections.

Two spare VTL assemblies were produced, one of which was copper plated in order to assess the effect on the multipactor arc thresholds. This assembly was also tested in the Testbed. Conditioning was carried out by applying 0.1s pulses every 3s at a voltage which was just above the threshold for multi-pactors, as defined by the onset of arcing in one pulse in four, on average. Over a period of 8 hours, the threshold fell from 15kV to around 400V, at which level the arc was so tenuous as to be barely detectable. Under these conditions, the copper line was found to perform well. However, after exposure to hydrogen at 10^{-3} mbar for a few minutes (at 300C), it was found necessary to recondition the line. It was therefore decided to retain silver as the preferred coating.

Installation and Commissioning of the Prototype Antennae

The two A_0 antennae were installed in the torus in the September shutdown. This installation was completed over a period of six weeks by a team of three engineers and three technicians with the support of several craftsmen, and proceeded largely as planned. The installation required the design of many specialised tools and handling jigs which was carried out in conjunction with Fusion Technology Division.

For each system the outer conductors of the VTLs were installed first and the flange seals vacuum tested. The antenna, complete with screens and central conductor, was entered into the torus using the counterbalanced beam, manoeuvred into position on a custom-built trolley and offered up to the limiter guide-tubes. The antenna spigots were then bolted to the outer conductor. Each corner of the antenna was bolted to the torus for additional support in the event of a disruption; the necessary fixtures were welded 'in situ'. Then the remaining VTL components were installed, followed by the vacuum system and the connection to the main

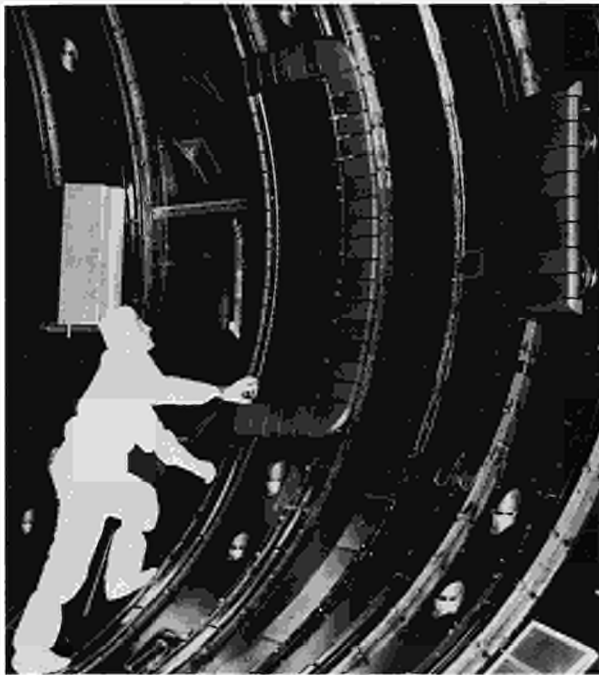


Fig.62: One of the A_0 antennae mounted in the torus

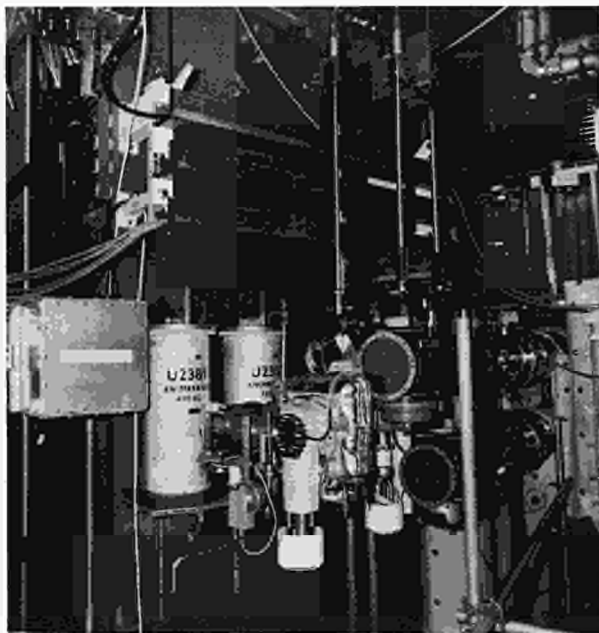


Fig.63: The transmission lines, window and vacuum system after installation on the torus

transmission lines. The graphite tiles were installed shortly before the closure of the torus.

One of the antennae is shown mounted in the torus in Fig.62. A view from outside the torus is shown in Fig.63; this shows the main transmission lines, the windows and the outer part of the vacuum transmission lines, together with the vacuum system to the left.

After installation, the antenna on Octant No.6 was conditioned to minimise the multipactor range. This was carried out using continuous low power RF supplied by the pre-ionisation generator. The multipactor onset was reduced to below 2kV after one day of conditioning. The

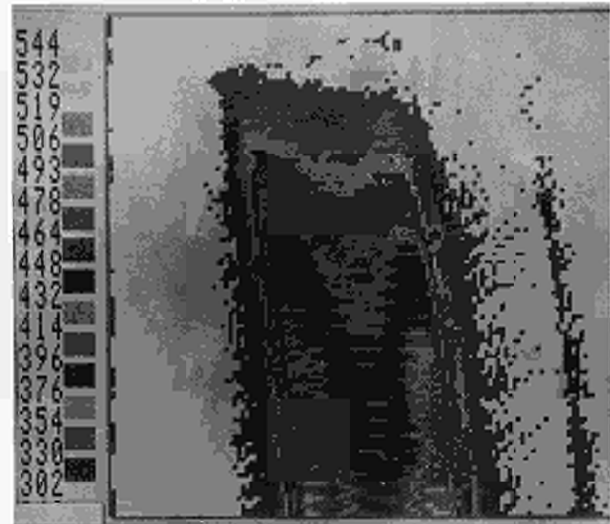


Fig.64: Infra-red photograph of the screen during RF testing under vacuum in the torus

maximum voltage which could be achieved with the pre-ionisation generator was 20kV, and this was successfully applied under vacuum conditions. The coupling resistance of the monopole antenna under vacuum was found to be 0.8Ω , including 0.6Ω due to the main transmission line. The balance of 0.2Ω arises largely from losses in the screen and is consistent with expectation.

This antenna was baked to 600C using 20kW of continuous RF power into the screen. During this baking, the screen was viewed with an infra-red camera and a typical result is shown in Fig.64. The RF losses are concentrated near the short circuit at the centre of the antenna, and at the outer edges of the screen. Quantitative analysis of this data is complicated by uncertainties regarding the emissivity of the surface; nonetheless, the observed increase in temperature is consistent with the RF losses.

After baking, carbonisation and pulsing of the toroidal field, the vacuum losses in the antennae were found to have increased from 0.2Ω to 0.9Ω ; the original value was recovered during pulsing of the toroidal field, presumably due to saturation effects in the screen. This increase in losses does not therefore impede operation of the antenna at the present time. Recent measurements indicate that the losses are not further increasing during operation on the torus. There is some indication from the infra-red thermography that the original low losses are also recovered after heating above the Curie temperature of nickel.

Third Prototype Antenna

During installation of the two A_0 antennae, a decision was taken to install a third such unit during the June 1985 shutdown. Whilst some components for such a system already existed as spares, it was necessary to place urgent orders for a new housing and screen, graphite tiles, vacuum system, and components for connection to the main transmission lines. The manufacture of these components is now well advanced.

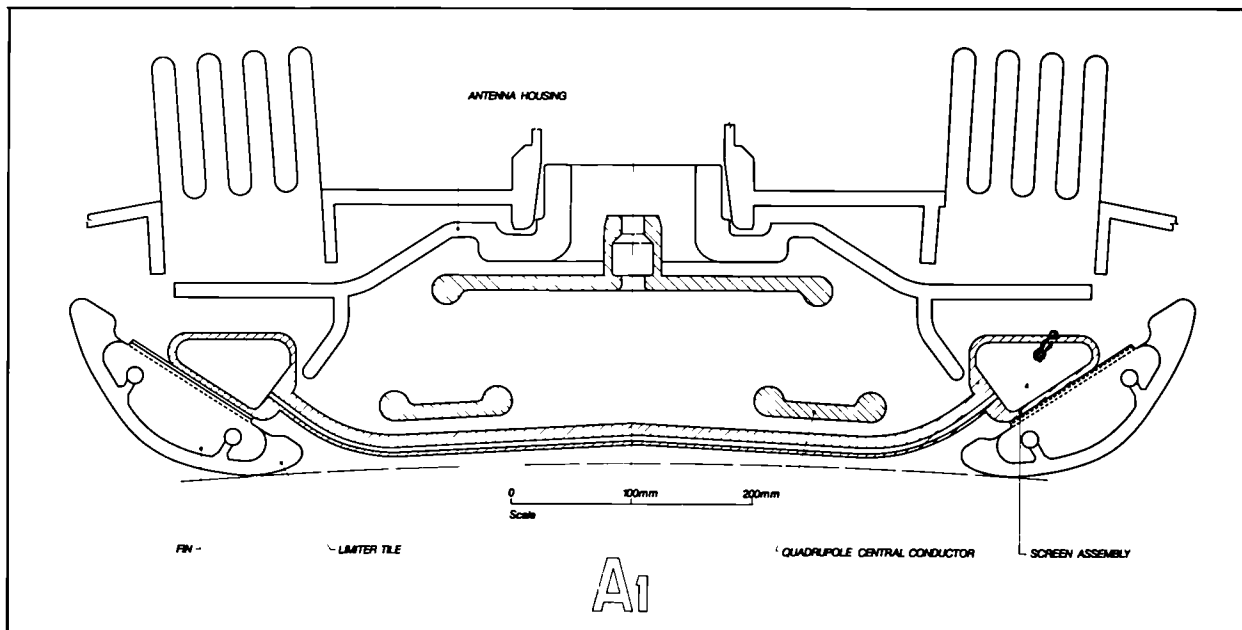


Fig. 65: A section through the A_1 antenna

RF Testbed

After completion of testing of the A_0 assemblies, the RF Testbed was moved from Fontenay-aux-Roses to the JET site. The vacuum vessel is presently being up-graded to enable baking of the antenna, as well as the VTL, before recommissioning in Building J4. A 3MW RF generator, modified transmission lines and enhanced cooling system for both the generator and the Testbed assemblies, are being installed before re-commissioning of the Testbed in the Summer 1985, in readiness for testing of the A_1 components. In the interim, component testing is being carried out on the pre-ionisation generator.

Design and Manufacture of the A_1 Antennae

Six of the so-called A_1 antennae are due to be installed in the torus in 1987. These antennae should be capable of coupling 1.5MW each to the plasma for pulse lengths up to 20s. The design of these antennae has been largely completed during 1984 and the main manufacturing contracts placed. Prototype units are scheduled for delivery in the Autumn 1985.

The main complication presented by the long pulse length is the requirement for active cooling of the screen and the inner conductor of the vacuum transmission line. In addition, the increased power into the plasma from all sources during the period of operation of the A_1 antennae requires enhanced cooling of the side protection tiles between pulses. Additional design changes have been incorporated in the light of experience from the A_0 antennae, both to improve the coupling and facilitate remote handling. A section through the A_1 antenna is shown in Fig. 65.

The side protection on the A_1 antennae is of similar design to the toroidal belt limiter, comprising 83 thin graphite tiles on each side, inclined at 30° to the magnetic field, interleaved with blackened nickel fins. These fins are welded to the screen water manifolds. The tiles are

cooled inertially during a pulse, and by radiation to the fins between pulses. The tiles are assembled in pairs onto the fins, with installation and replacement belonging to Class I remote handling operations. This design is also compatible with the use of tiles.

The screen assembly carries the graphite tiles and is in turn kinematically attached to the housing at six points, allowing differential thermal expansion. To increase the coupling to the plasma, the screen is curved to follow the magnetic field, allowing for both the ripple in the toroidal field and the effect of the nickel screen elements. The curvature at the ends allows the manifolds to be better protected, and also substantially reduces the stress in the welds due to differential expansion of adjacent elements, which have differing losses due to the alternating orientation of the T-section profile.

The screen is fabricated from Nickel 201. Each element is produced from cold-drawn, fully hard bars gun drilled with a 5mm hole from one end. The bar is then machined to the T-section outer profile, bent to the required shape, electropolished and welded to the previously machined and rolled manifold. The specification and quality control of this weld during fabrication are crucial areas and a substantial development programme has been carried out. Each of these processes has now been proven and a short assembly of five elements is being fabricated.

The electrical connection between the screen and the housing is to be established using Nimonic spring contacts with a thin silver coating (typically half a skin depth). These have the property of maintaining good RF contact, whilst reducing the current flowing in the screen, and thus the forces, in the event of a hard disruption by an order of magnitude compared to a short circuit connection.

The housings of the A_1 antennae have been increased in width to the maximum which can be installed through

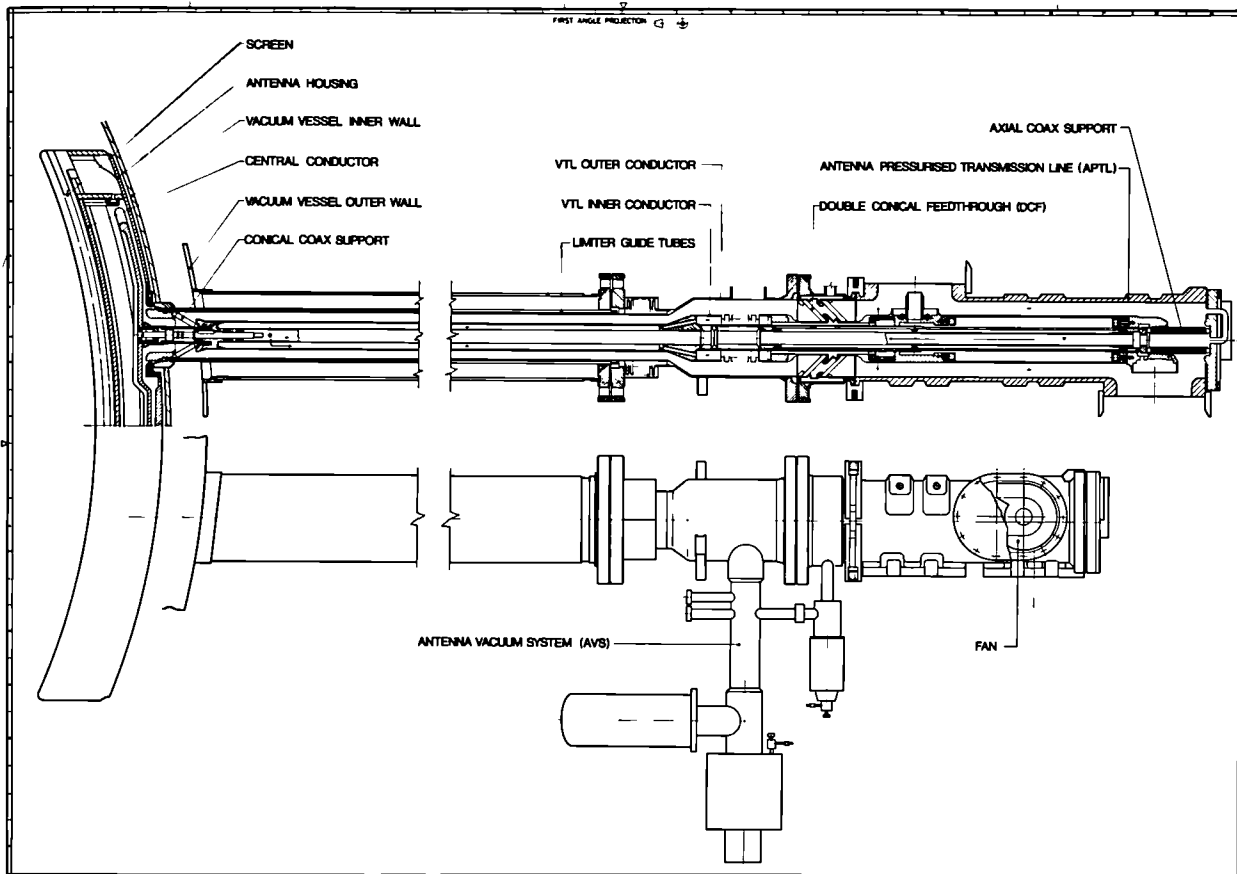


Fig. 66: A sectional view of the A_1 vacuum transmission line

the major ports. This enables the two conductors of the quadrupole to be further separated to further increase the coupling. Due to the larger numbers involved, the conductors are now cut from machined 4m diameter rings, whilst the capacitance plates are hot pressed to the required profile.

The power dissipation in each VTL inner conductor during the pulse is 30kW. At full duty cycle, this conductor must be actively cooled between pulses. In particular, the bellows are subject to a temperature rise of typically 200C per pulse. Cooling will be achieved by forced convection of gas inside the inner conductor. The flow rate required is modest and can be achieved using centrifugal fans. This cooling requires the inner conductor to be pressurised as far as the conical ceramic (c.f. Fig.66) and then to be fabricated as a single welded assembly incorporating the vacuum window. The connection of the outer conductor to the housing has also been modified to become a bayonet connection. These changes together enable the VTL to be fully assembled in the Assembly Hall with hands-on procedures, much simplifying remote installation on the torus.

A modified RF window incorporating two conical ceramics is also being developed and initial testing indicates improved voltage stand-off capabilities.

The vacuum system for the A_1 antennae must be compatible with tritium phase operation, and alternatives

to the present turbo-molecular pumps are being assessed. Design of this system is not yet complete. Prototype components for the A_1 antennae will be ready for testing in the Autumn 1985, and delivery should be completed by Spring 1986.

Radio Frequency Physics Group

(P. Lallia, W.H.M. Clark, F. Sand)

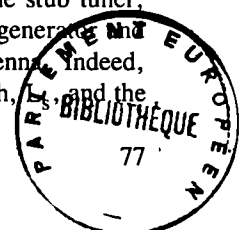
During 1984, the main activities of the RF Physics Group were concentrated on preparation for initial operations of the RF system expected to start in January 1985.

Subsequent sections report details of developments in the following areas:

- Processing and simulation of RF signals;
- Measurements on the antennae and transmission line;
- Initial wave/plasma coupling results.

RF Data Processing

As mentioned earlier, RF data after a JET pulse is processed by the same computer that controls the RF plant. The Group was responsible for that part of the software required to calculate quantities, such as the coupling resistance R_c or the length of the stub tuner, ensuring an optimum tuning between the generator and the system of transmission line and antenna. Indeed, when the system is matched the stub length, l_{st} , and the



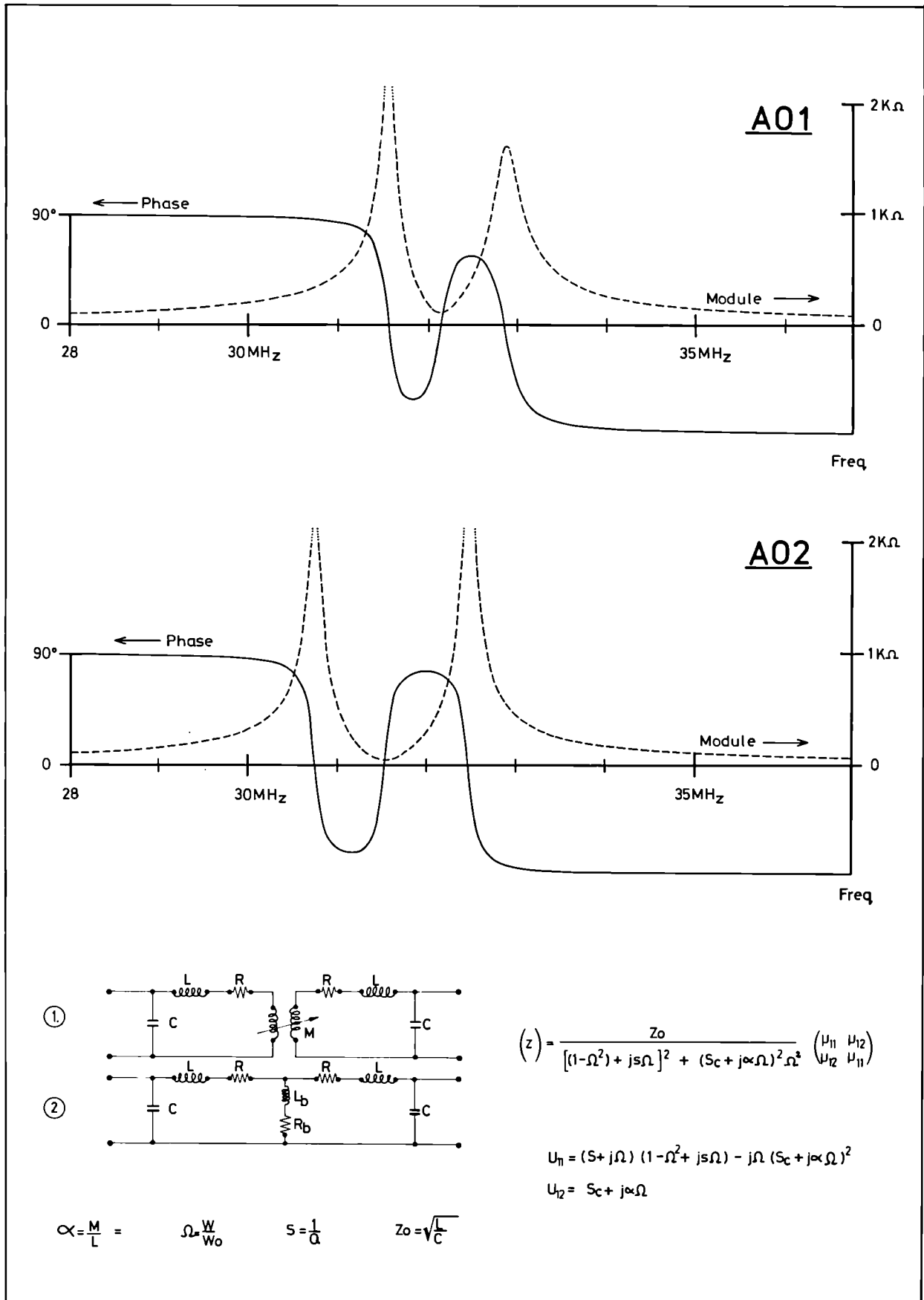


Fig. 67: Experimental input impedance of antennae A₀₁ and A₀₂ as measured before installation in JET. The antennae can be represented by lumped circuits, as shown in the inset

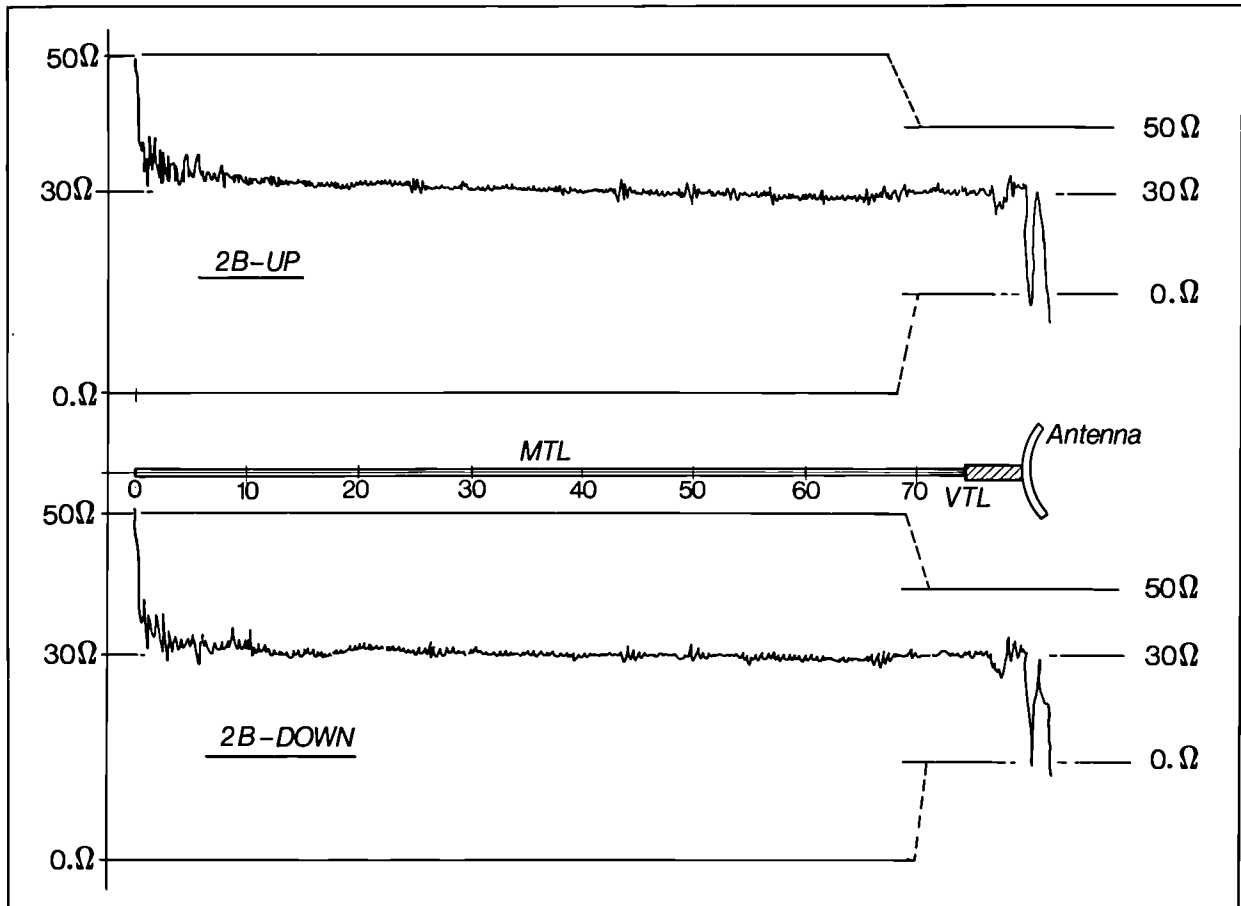


Fig. 68: Time Delay Reflectometry signals from antennae A_{01} . The corresponding positions of the components of the system are shown below

TABLE XI

	$A_{01}(\text{up})$	$A_{01}(\text{down})$	$A_{02}(\text{up})$	$A_{02}(\text{down})$
Equivalent resistance $R(\text{m}\Omega)$	145	169	113	118
Equivalent inductance $L(\mu\text{H})$	129	138	120	122
Equivalent capacitance $C(\text{pF})$	196	185	211	207
Eq. mutual inductance (μH)	5.2	5.5	6.5	6.6
Characteristic impedance $Z_c(\Omega)$	25.7	27.3	23.9	24.3
Resonant Frequency (MHz)	31.57	31.58	31.61	31.60

wavelength λ_0 are linked by the following relationship:

$$\tan \left[\frac{2\pi L_s}{\lambda_0} \right] = \frac{\sqrt{R_c Z_0}}{Z_0 - R_c}$$

where R_c is the coupling resistance of the antenna and Z_0 is the characteristic impedance of the line. The optimum wavelength is found experimentally by sweeping the generator frequency by $\pm 100\text{kHz}$. Initial operations on JET have shown that two low power frequency swept pulses are sufficient to find a good match (i.e. more than 95% of the generator power delivered to the system line-antenna).

The processing of the data from a set of RF probes between the tuner and the antenna was simulated by software to check the feasibility of measuring the impedance matrix of the antennae during JET pulses. In collaboration with CODAS Division, arrangements have been made to provide remote control of the spectrum analyser dedicated to Ion Cyclotron Emission measurements.

To provide a rough evaluation of the capability of the plasma to absorb ion cyclotron waves immediately after each JET pulse, a so-called ICRF absorption indicator has been defined, using a model developed for ray-tracing calculations. In collaboration with Theory

Division, this absorption indicator uses the actual density and temperature of the plasma as measured by interferometry, electron cyclotron emission and neutron flux. The estimated RF power absorbed by electrons and minority ions is plotted as a function of time after each JET pulse. Initial results are close to those from full ray tracing calculations.

RF Measurements on Antennae and Transmission Lines

Before installation into the JET vacuum vessel, the RF properties of the antennae were checked (i.e. resonant frequencies, characteristic impedances and resistive losses). Fig.67 shows the input impedance of antennae A₀₁ and A₀₂ as a function of frequency when the second termination on each antenna is left open, (i.e. the diagonal element of the impedance matrix describing the antenna without plasma). The components of the equivalent lumped circuit are shown in Table.XI. When installed in JET, the properties of each system comprising a vacuum transmission line and an antenna were checked by time delay reflectometry. The response of a step voltage applied to the system gives a useful ‘signature’ and allows an estimate of the impedance discontinuities. Fig.68 shows the response of such a signal applied to antenna A₀₁ and the position of the various components of the system. It can be seen that the electrical length of the antenna A₀₁ is close to twice its geometrical length.

Initial Wave/Plasma Coupling Results

The configuration of the RF system used during initial operations on JET is sketched in Fig.69. The types of excitation depending on the phase difference between the two inputs are also indicated. This is monopole or dipole for A₀₁ (in Octant No.6B) and dipole or quadrupole for A₀₂ (in Octant No.2B). The two antennae are diametrically opposed in the toroidal direction in the vessel, in order to distribute more equally the heat load on the protection tiles.

The coupling resistance R_c, mentioned above, is defined by the relationship

$$P_{gen} = \frac{R_c}{2} \left(\frac{V}{Z_0} \right)^2$$

where P_{gen} is the power delivered by the RF generator to the transmission line-antenna system and V is the peak voltage along the line (i.e. the voltage applied to the antenna when at resonance). Z₀ = 30 Ω is the characteristic impedance of the transmission line.

As a result of losses in the line and in the antenna (in the screen, in particular) R_c is not zero without plasma but actually close to 0.6 Ω (when the nickel screen is magnetically saturated). In the presence of the plasma the power coupled to the plasma P_p is:

$$\frac{P_p}{P_{gen}} = 1 - \frac{R_{cv}}{R_{cp}}$$

where the indices v and p indicate vacuum or plasma, respectively. Fig.70 shows the initial results of

(R_{cp} – R_{cv}) as a function of the distance between the antenna and the plasma, for the various possible excitation configurations of A₀₁ and A₀₂. The expected values calculated by assuming a strong absorption mechanism inside the plasma are shown in Fig.71. The agreement is good considering the sensitivity of the calculation to the experimentally poorly known quantity of the electron density profile near the plasma boundary.

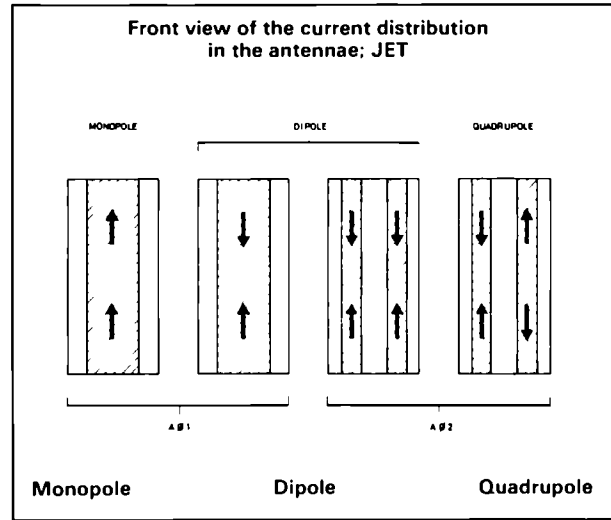


Fig. 69: Initial configuration of the RF system showing the possible types of excitation and the corresponding directions of the RF currents

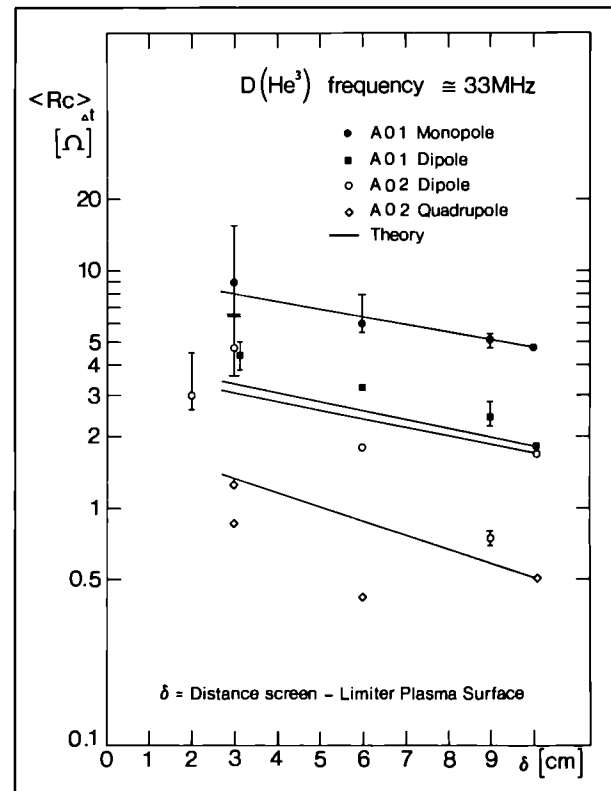


Fig. 70: Coupling resistances (R_{cp} – R_{cv}) of antennae A₀₁ and A₀₂ versus the distance between the antenna conductor and the last closed magnetic surface

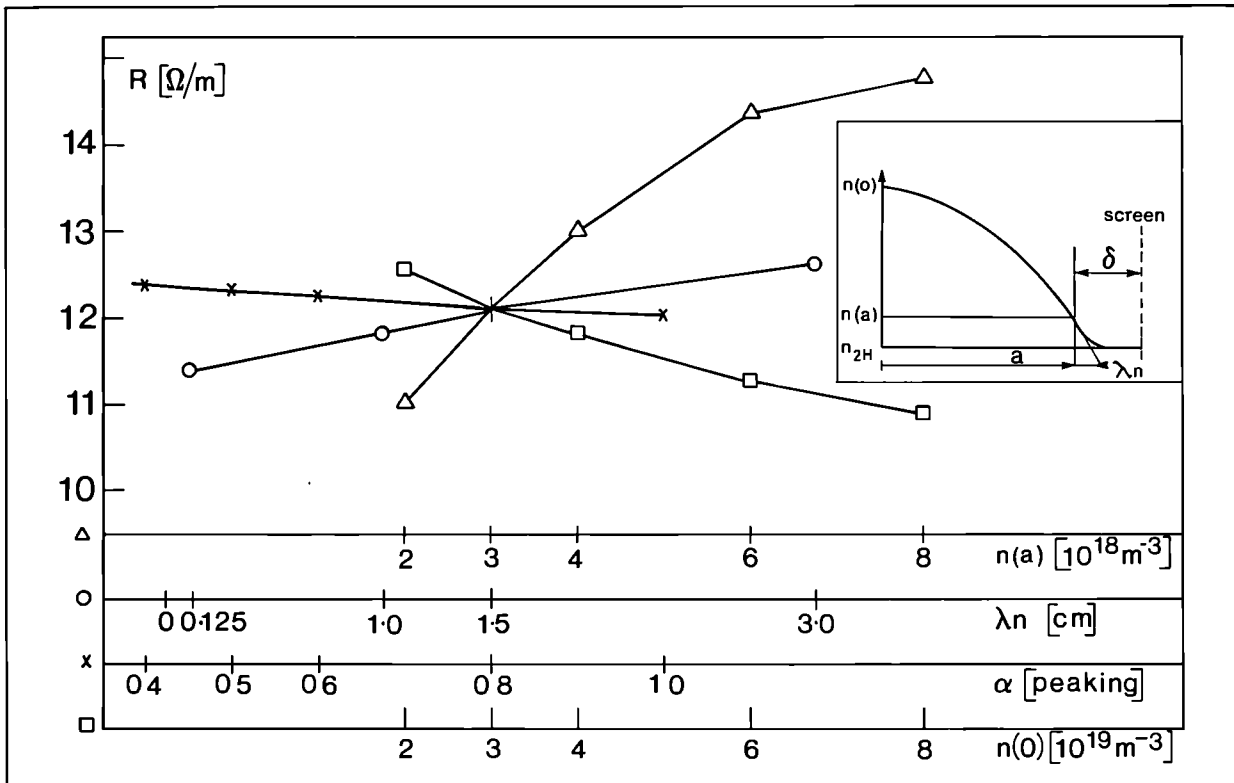


Fig.71: Calculated coupling resistance using a strong plasma absorption model

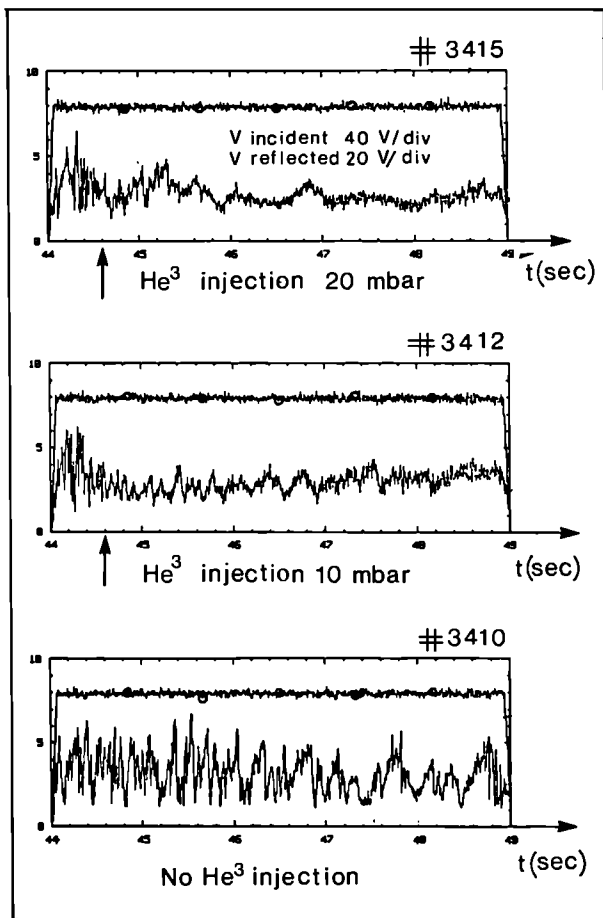


Fig.72: Experimental values of forward and reflected voltage, with and without He-3 injection.

The validity of a strong absorption mechanism inside the plasma is supported by Fig.72, showing the reflected RF voltage during injection of He-3 minority species. The oscillations of the reflected voltage (likely indications of cavity eigen-modes), are damped as soon as He-3 reaches the centre of the Tokamak (i.e.0.3s after the opening of the fast valve).

It is concluded that future performance of the quadrupole configuration will have to be far better than the dipole or the monopole, especially in plasma heating efficiency or impurity production, to counterbalance its reduced coupling resistance.

Fusion Technology Division

(Division Head: J.R. Dean)

Fusion Technology Division is responsible for the design and development of remote handling methods and tools to cope with the requirements of the JET device for maintenance, inspection and repairs. The Division also undertakes design and construction of facilities for the handling of tritium. These tasks are carried out within three groups: the Remote Handling Development Group; the Remote Handling Applications Group; and the Tritium Group.

The Remote Handling Development Group is responsible for the development, acquisition and commissioning of the general purpose remote-handling machines and viewing and sensing equipment, based

largely on robotics practices. This includes general purpose manipulators, transporters to carry and place the manipulators, JET components and special tools. Also included are special purpose, automatic, self-propelling cutting and welding machines for the standard JET lip-joints.

The Remote Handling Applications Group is responsible for applying remote handling equipment and techniques to tasks on JET, by ensuring compatibility of design and access of subsystems and components, by developing local tools to meet all needs and by preparing remote handling schedules based on procedures provided by the respective component designers. The Group will also be responsible for the safety of personnel working on the machine when lightly activated dust is present or if beryllium is introduced as a low-Z wall barrier and getter. Experiments with beryllium in a small tokamak at the University of Düsseldorf, F.R.G. and in the ISX-B tokamak (ORNL, U.S.A.) were visited and closely followed. An access cabin is now being designed which will control the movement of people and materials into and out of the vacuum vessel and prevent any spread of contamination.

The Tritium Group is responsible for the design, development and acquisition of the tritium recycling system, which will be needed when tritium is introduced with deuterium into the plasma. The Group has designed experimental forms of some of the critical items in the projected recycling system and is entering a testing phase to prove the design principles.

During 1984, eight engineers and one technician were recruited into the Division and the numbers will shortly reach a total of 16 engineers and 8 technicians. Planning the work and matching tasks to people is well advanced and the broad division of tasks between the three Groups remains unchanged. Despite the shortage of staff, a number of medium value contracts were placed at the end of 1984 for remote handling machines and a major one for two sets of master-slave manipulators.

Remote Handling Development Group

Articulated boom

(P.D.F. Jones)

The boom (see Fig.73) is designed to transport components to and from the vacuum vessel through the main horizontal ports Nos.1 and 5 using various end effectors. It will also position the general purpose servo-manipulator for maintenance work. Manufacture of the boom was completed by the Contractor and delivered to JET together with the limiter gripper in October. The boom was successfully tested with a payload of 1.25t cantilevered at 9m from the support trolley. The boom incorporates cabling for the various end effectors, the servo-manipulator, tools to be used by the manipulator and television cameras, gas piping for welding and leak detection and high pressure water piping for cutting operations and washing of the vacuum vessel.

Two support frames against the wall of the Torus Hall facing the horizontal ports at Octants Nos.1 and 5, and



Fig.73: *The Articulated Boom*

two beams spanning the limbs on either side of the ports have been installed. The support beam will be lowered onto these to place the boom in its working position by the 150t crane. Commissioning of the boom has started in the Assembly Hall. Backlash is virtually negligible which is better than expected, but the elastic constant of the rotary joints is less than half the expected value. Modifications have been designed to increase stiffness to the intended value, which was used in the computer simulation of the dynamic response of the boom.

Control of the boom

(L. Galbiati, D. Maisonnier, E. Gebler)

Control of the boom is at present effected in an open-loop manner by means of a push-button box. This activates DC motors of the boom and the limiter gripper. The speed values can be adjusted by varying the voltage to the motors. An inching mode is also provided for fine adjustments. The box also has a display showing positions of boom joints, gripper and trolley, as well as the loads on the various actuators. A closed loop controller was designed and specified, taking into account the dynamic response of the boom, and construction began in December. Input to the controller will initially be from a simple 1:5 scale model with a resolver at each joint. This 'model master' is under construction and will be tested early in 1985.

The controller includes pulse-width modulated servo-amplifiers which receive the velocity feedback from the tachometers on the joint motors and the difference between the position signals of 'master' and boom is elaborated by a CAMAC microprocessor which also provides the necessary safety interlocks.

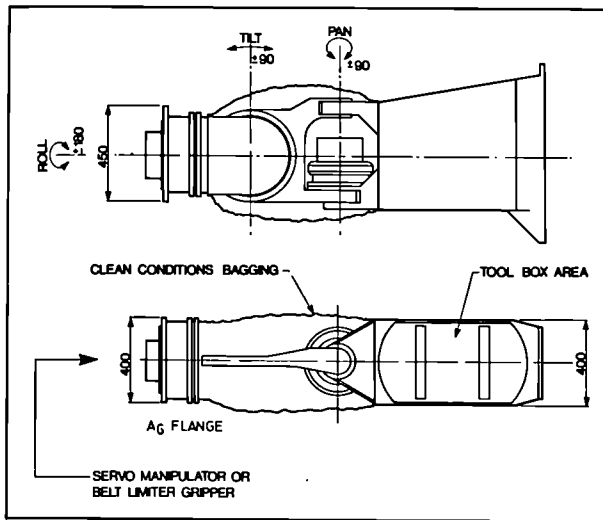


Fig. 74: The Articulated Boom extension

Boom Extension

(P.D.F. Jones)

A boom extension has been designed in detail and is out for tender (Fig. 74). The further three degrees of freedom that it provides (yaw, pitch and roll) allow the servo-manipulator, the belt limiter gripper and the antenna grabbers to be positioned in the vacuum vessel. A standard interface has been designed for remotely coupling end effectors. One section of the boom extension is an open structure to serve as a receptacle for tools to be used by the manipulator. The structure is in cast aluminium-magnesium alloy. High torque is experienced due to the load offset. The shape was optimised by a finite-element analysis and the stress concentrations checked by a brittle lacquer test on a prototype with 50% overload. At any point, stresses do not exceed 7kg/mm^2 . In order to expedite delivery (expected September 1985), long-lead items and structural sections are already being manufactured and will be given as free issue items to the manufacturer of the assembly.

Turret Truck

(R. Cusack)

An order was placed in December for a turret truck to carry components and end effectors. It will position the components so that they can be picked up and connected to the boom (or later to other transporters) by remote control, leaving the crane free for other work.

End Effectors

(P.D.F. Jones)

(i) Limiter Gripper

The limiter gripper supplied with the boom was designed to handle the type of limiters at present in use, weighing about 250kg. There are four movements for fine adjustment, and transducers provide information on the load pattern on the limiters during the 2m insertion/withdrawal from their mountings in the vacuum vessel.

(ii) Toroidal (Belt) Limiter Gripper

A design is near completion for a gripper to be used in the hands-on initial installation of the belt limiters, which will replace the present type. There will be 32 new limiters each weighing 80kg without tiles. To ease the complex insertion task, the load will be balanced by springs in the gripper. The gripper will be mounted at the end of the boom extension to reach the limiter locations 100mm above and below the equatorial plane of the vacuum vessel. The gripper is provided with adjustable yaw and pitch motions. Special bayonet engagement lugs are included on all the belt limiters for remote engagement/disengagement using the gripper. The belt limiter will be placed on a ledge to hold it captive while bolts are fitted.

(iii) Antenna Grabbers

The tools for the hands-on A_0 antennae installation, including a 9t.m counterbalanced beam, an A_0 grabber, an in-vessel trolley and special tools were designed, manufactured and shown to operate successfully during the September/October shutdown. Operational experience showed minor difficulties in alignment which called for modifications to these items. These have been carried out and will be incorporated in the equipment for installation of the third A_0 antenna in June 1985.

The A_1 RF antennae comprise of two parts, the housing (175kg) and screen (300kg) which have different attachment points and so require different pick-up devices, although using a common 'C' structure support and performing the same motions to guide the antennae parts through the narrow entrance to the vessel. The grabbers are being designed for remote handling or hands-on installation with back-driveable motions. Titanium construction of structural items is necessary to minimise weight. A special device will have to be designed to avoid overloading the pitch motion of the boom extension.

General Purpose Servo-manipulators

(T. Raimondi, L. Galbiati, R. Cusack, D. Maisonnier)

Modifications are being made to the Mascot servo-manipulator which was bought second-hand from ENEA several years ago. To reduce its dimensions so that it can pass through the vacuum vessel port a new chassis of thin aluminium plates has been designed with the aid of a finite element study. To avoid contamination of the vacuum vessel and of the manipulator itself, a closed loop air cooling system has been designed and incorporated in the device. Provision was made for adding gaiting for the arms. One arm has been re-built and work is in progress on the second.

Specifications were written and a tender called for the supply of two master-slave sets. The order was placed at

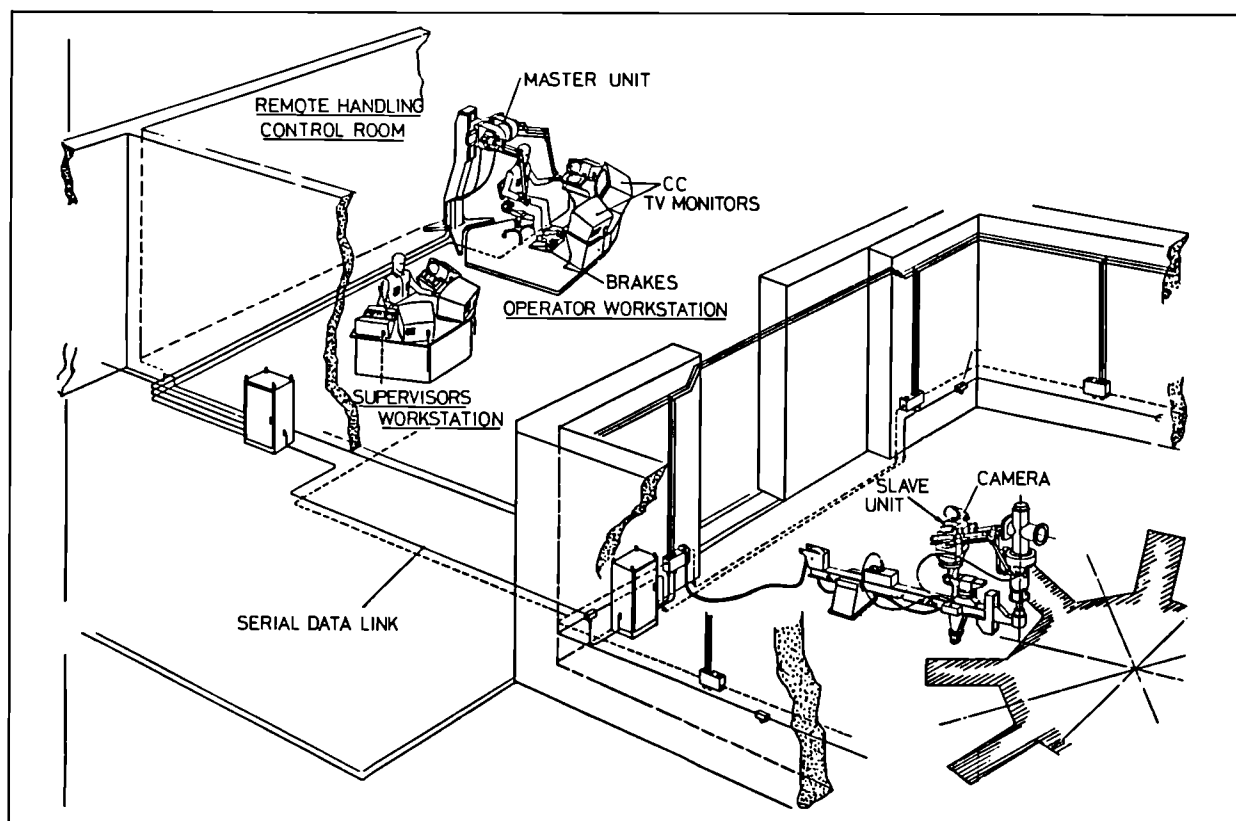


Fig.75: Remote manipulator layout - Example of operation on turbo pumps

the end of the year. The new manipulators are derived from the Mascot developed by ENEA with further reduction of size. A new control system based on microprocessors allows for multiplexing the signals without sacrificing sensitivity and time response. Fig.75 shows the operational layout.

In-vessel Inspection System (IVIS)

(R. Cusack, L. Galbiati, E. Gebler, P. Presle)

Since inserting and testing the In-Vessel Inspection System (IVIS) in the vacuum vessel during the January shutdown, the following improvements have been designed and implemented. This work was carried out in short bursts during those rare periods when access to the machine, availability of the computer system and of power coincided.

Rectilinear potentiometers to detect the angular displacements between the viewing tubes and the axes of the ports were installed. These should reduce the time taken for alignment of the system, which proved very slow when undertaken with optical instruments only. The optical alignment procedure was simplified and will be used, at least initially, to cross check the readings of the potentiometers. To facilitate the operation, a mimic display of the interior of the vessel is in preparation. It consists of plan views and elevation sections of the vessel that can be selected by the operator. He simply places a cursor on the area of the screen he wishes to observe and the camera adjustments are calculated by computer.

Software was developed in an attempt to resolve the problem of 'flickering' caused by cross-talk (transverse conductance) between adjacent cells of the video storage plate as these were scanned alternately. Reasonable acceptance results were achieved. Repair work was needed on one camera and the video circuits were returned to compensate the variation of cable parameters. The vacuum control system was installed and commissioned including a mimic diagram showing the state of the vacuum plant.

Cutting and Welding

(P. Presle, E. Gebler)

The cutter unit developed by a Contractor several years ago to JET specifications had not given good results. This year, a number of adjustments were made. The gap between punch and anvil was optimised and these were mounted with a tighter fit. Adapting the electronics, the punch was made to rotate using the feed motion of the self-propelled trolley. The result was satisfactory and joints of more than 20m long were cut without blunting the cutting edges.

The welding trolley was sent to KFK Karlsruhe, F.R.G. for a short period for feasibility tests on joints envisaged for NET, which were successful. It is now hoped to establish a co-operative effort with Karlsruhe on further cutting and welding equipment. A 'final' electronics module for this trolley was built on the basis of the experience gained in welding the vacuum vessel octants.

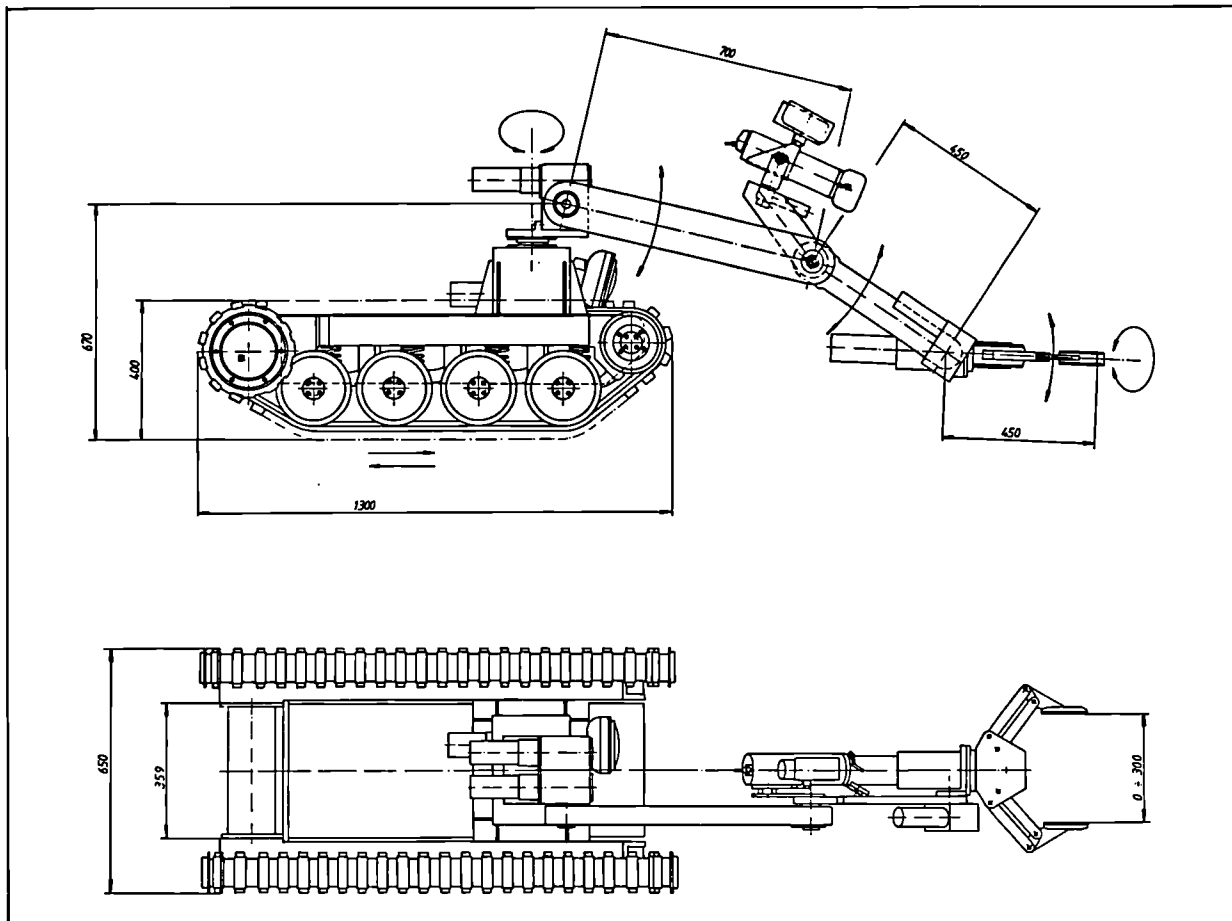


Fig.76: Overall view of support vehicle

Television System

(M. Wykes, A. Tesini, L. Galbiati)

Design is in progress on a set of motorised arms, mounted on the boom extension, for positioning a pair of cameras behind or alongside the end effectors, in particular, the manipulators. These will give a side view of the working areas. A front view will be given by a camera mounted on a short arm from the manipulator shoulders. A survey is being made to select the most suitable cameras available.

Vacuum and Water Couplings

(A. Nowak)

Further tests have confirmed the suitability of titanium nitride applied by sputter ion plating as an anti-seizure coating for nuts and bolts working in vacuum at high temperature. A report has been prepared on this subject. New heavy duty V-bands have been made and tested to replace the existing type, together with new 'O' ring seals. A new method of connecting the Rafix couplings to the hoses using a yoke was tested and standardised, as the previous method was unreliable.

Remote Handling Applications Group

Transporters

(S. Booth)

The fully remote maintenance of JET will be performed

by use of transporter mounted servo-manipulators with support from general purpose cranes and load carrying vehicles. All of the remote handling equipment will be stored external to the Torus Hall and will be re-deployed during each maintenance period.

There will be four manipulator transporters:-

- Type A: for low level work and operations beneath the machine;
- Type B: for medium and high level work around and over the machine;
- Type C: for in vessel work (Articulated Boom);
- Type D: for work inside the P1 coils, NIB boxes and SF6 towers.

In addition, there will be remotely operated general purpose transporters:-

- Support Vehicle (type E) for light (>50kg) utility work, such as connecting umbilicals and health monitoring;
- Turret truck for transportation of heavier equipment (>1500kg) between the type A, B and C transporters and flasks, racks and other storage devices;
- Cranes for general purpose lifting.

A study was commissioned to specify the configuration and performance of the A, B and D transporters. The resulting proposal for a B type transporter is shown in

and consists of a self propelled, steerable chassis with a rotatable, extending mast surmounted by an extendable and tilting jib. It is capable of carrying a two arm servo-manipulator slave, mounted on the three axis boom extension with the associated tool box and tools. The transporter is capable of positioning the servo-manipulator anywhere at the side or over the top of the machine and also of reaching the cradle of the 150t crane. The transporter is fully electric, failsafe and all actuators can be retracted by external means. The entire transporter can be locked and retrieved by the 150t crane in the event of failure. This proposal is being assessed by JET.

The A and D type transporters are currently being studied. The type E, or support vehicle, is a radio controlled device consisting of a battery powered, steerable chassis, upon which is mounted a six axis manipulator with a single tong type of gripper. Viewing is by means of TV camera mounted on the top of the chassis on a pan/tilt mechanism. A detailed specification of the vehicle was produced and a call-for-tender issued. Three tenders were received and an order for one unit was placed (see Fig.76). This will be manufactured and delivered in August 1985.

The turret truck is also radio controlled but takes the form of a conventional fork lift truck with the addition of lateral translational and rotational movement of the forks and a much greater reach. A call for tender was made and five responses were received. An order was placed for an 'off-the-shelf' vehicle which can carry up to 1500kg and raise it 8m (see Fig.77). All of the actuators are electric with the exception of the forks raise axis, which is mineral oil hydraulic in a telescoping cylinder. The shrouding of this and its possible conversion to all electric drive will be evaluated this year.

Remote Maintenance Control System

(A. Galetsas)

A concept design for the overall control system has been generated and detailed work on the major subsystems will begin in 1985. The overall control system consists of a control room with command consoles, a general purpose computer (GPC), local control units and an electrical distribution system. This control room, shown in Fig.78, contains general purpose operator control consoles, video monitors, servo-manipulator master stations, an articulated boom master station and a supervisor work station.

The general purpose operator control consoles provide for control of any transporter with video display from any camera. Each console, (see Fig.79) is based on the CODAS standard with video output and touch-panel joystick and keyboard inputs. There will be two servo-manipulator master stations (shown in Fig.80), each consisting of a two arm servo-manipulator master, boom extension camera arms master, visual displays and keyboard or pendant input facilities. The articulated boom will be controlled from a dedicated boom master control station which provides all facilities for teach/repeat boom configuration control, kinematic control and obstacle avoidance.

During each maintenance period, there will be a number of operators in the control room and these will be organised and co-ordinated by a supervisor whose work station is elevated with respect to the operators. Each transporter and associated tools/end-effects will be connected to local control units (LCU's), one for each transporter. An LCU contains the control electronics for each transporter including power supplies, servocontrollers, discrete controllers and microprocessor intelligence, where appropriate. These

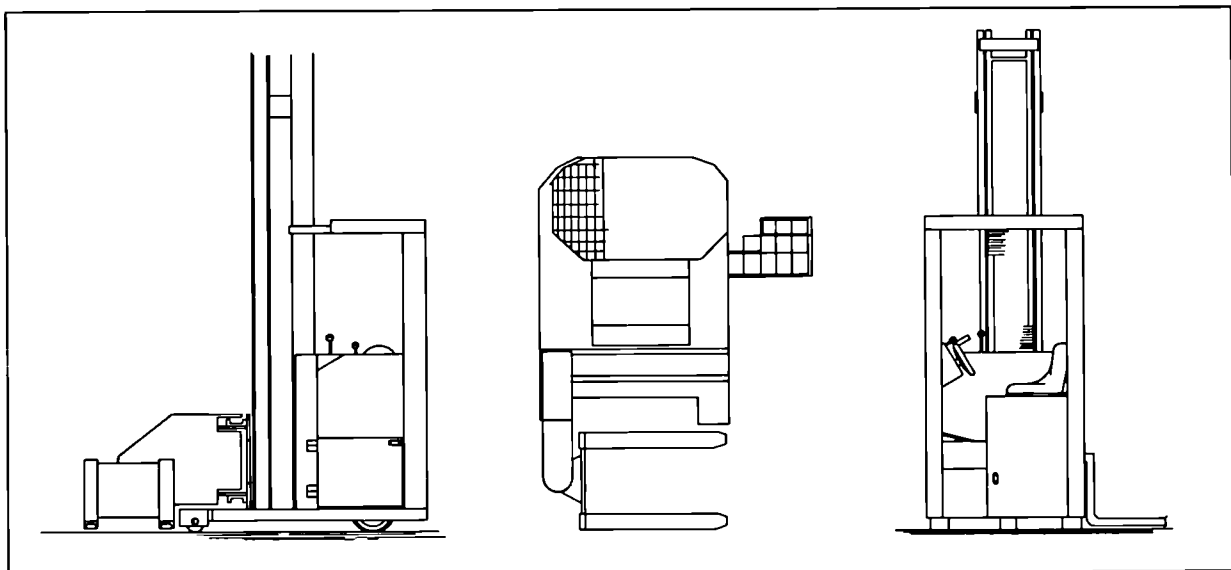


Fig. 77: Overall view of general purpose turret truck

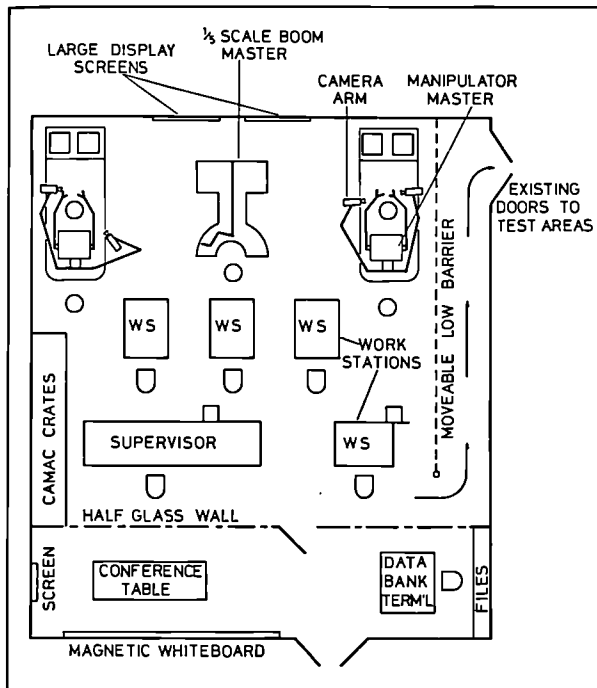


Fig. 78: Plan of Remote Maintenance control room

will be positioned within the Assembly Hall for ease of maintenance and will link to the control room consoles through the CODAS computer network. In addition, every LCU will have 'stand alone' facilities to enable each transporter to be commanded from a detachable local panel or pendant independent of the overall control system.

Each of the LCU's control room consoles and the overall viewing subsystem are connected together through the remote handling General Purpose Computer (GPC), shown in Fig. 81. The GPC provides a number of services including control console configuration, transporter command control, video matrix control and remote handling procedural management and associated database.

Intervention Module

(S. Booth)

Further work has been carried out on the problems of manual intervention in the vacuum vessel. An operational technique based on the JET intervention module has been devised which is now being detailed, with delivery planned for early 1986.

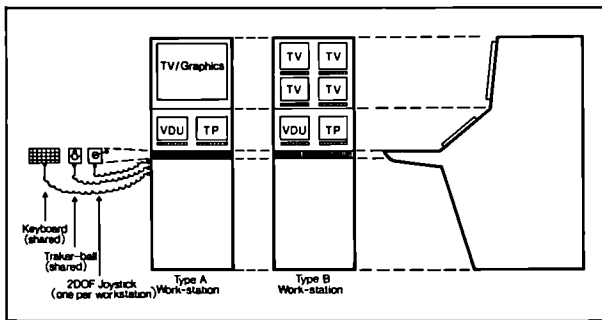


Fig. 79: Operator console

Weld head for toroidal limiters and RF antenna cooling pipes

(M. Wykes/J. Schreibmaier)

During tokamak operation, cooling water at a temperature and pressure off 100C and 10bars, respectively, flows through the cooling pipes while the external environment is 10^{-9} mbar. The waterside weld design criteria are flush surface finish with no abrupt change in section and the complete absence of crevices in which impurities could accumulate. The latter requirement is important since Inconel 600 is prone to stress corrosion cracking under certain conditions. The vacuum design criterion is the absence of defects which might grow to produce through-cracks in the weld. The joint must be remotely cut so that the joint member remaining inside the vacuum vessel can be subsequently re-welded without further preparation.

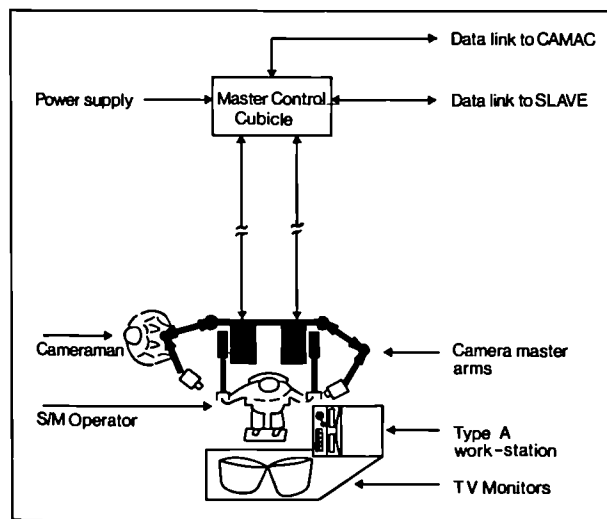


Fig. 80: Servo-manipulator master station

A number of trial welds were made using the pulsed TIG process with an orbital weld head. The autogenous method was used to ease the design requirements of a remote welding tool capable of fitting into the limited access around the joints (typically 20mm radial and 40mm axial clearance). Various joint designs were evaluated and Fig. 82 shows a sectional view through the selected joint (prior to welding), which is basically of the spigot and socket type. The spigot has a collar which fulfills the following functions: it locates the socket element with respect to the spigot prior to welding, and also acts as consumable filler metal during the welding process. The spigot nose has a chamfer to assist engagement with the socket. The radial clearance between the spigot and socket bore is designed to accommodate the maximum burr thrown up on the socket bore during joint cutting. Fig. 83 shows a typical weld section. Full penetration is achieved over the whole of the

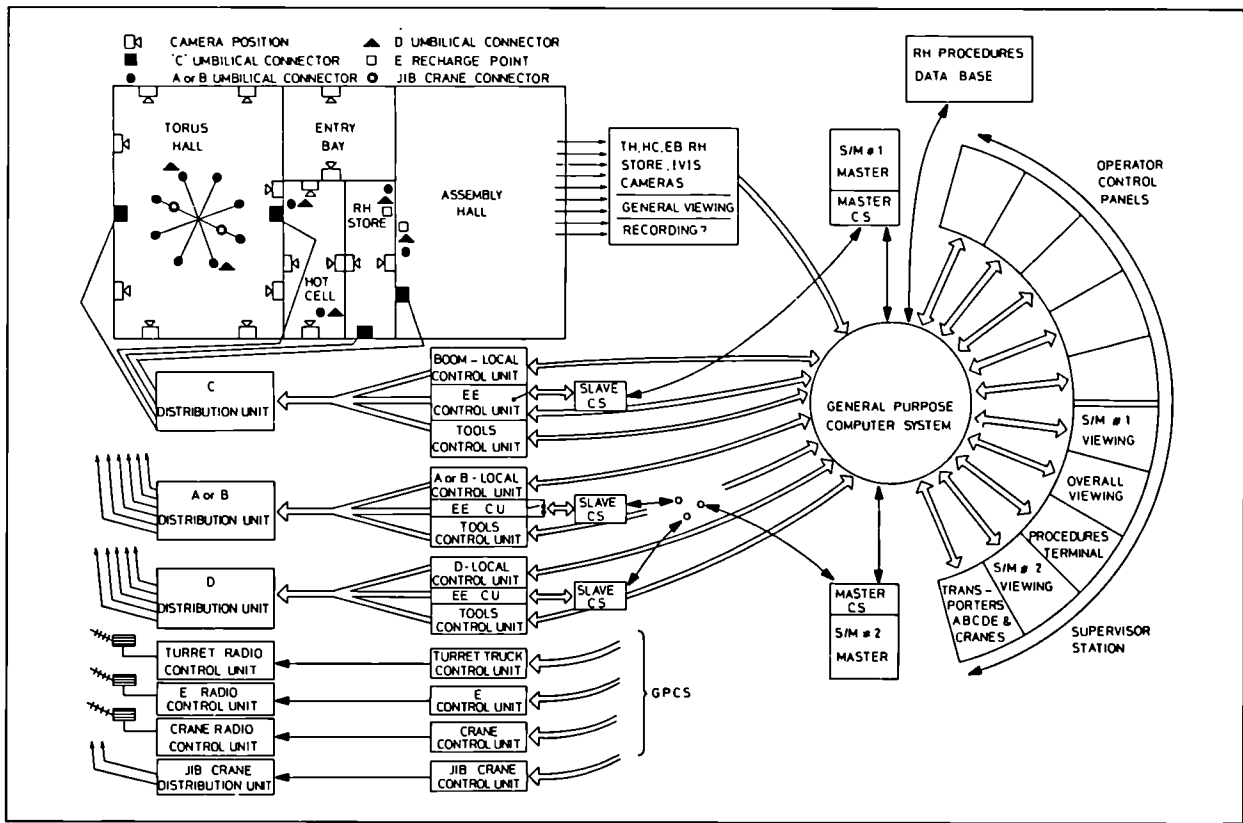


Fig.81: Overall Remote Maintenance control system

weld zone the spigot being completely melted and dispersed to form a smooth concave transition between the bores of the spigot and socket pipes. There is no crevice on the water-side. The weld thickness is at least that of the pipe wall at all sections. The welds were qualified by metallurgical examination and by helium leak testing with axial loads of $\pm 1000N$ while applying thermal cycles between 20C and 500C.

Further defects were produced in sound welds by saw cutting and by using shroud gas over-pressure to blow holes in the weld pool. Both these types of defect proved repairable by remelting without filler wire. The repaired welds were helium leak tested under mechanical loading and thermal cycling, no leaks being found. A specification for the one weld head based on the above work has been produced and a call-for-tender will be issued in early 1985.

Cutting head for the toroidal limiters and RF antenna cooling pipes
(M. Wykes/J. Schreibermaier)

Cutting tests were performed to obtain data on cutting loads, speed and feed rate, upon which to base the design of a remote cutting tool of the orbital lathe type. The tests were done at the Machine Tool Research Association Laboratory, U.K., on an instrumented lathe, using 50mm diameter by 2mm wall Inconel 600 test pieces. The goal of the tests was to determine typical values of

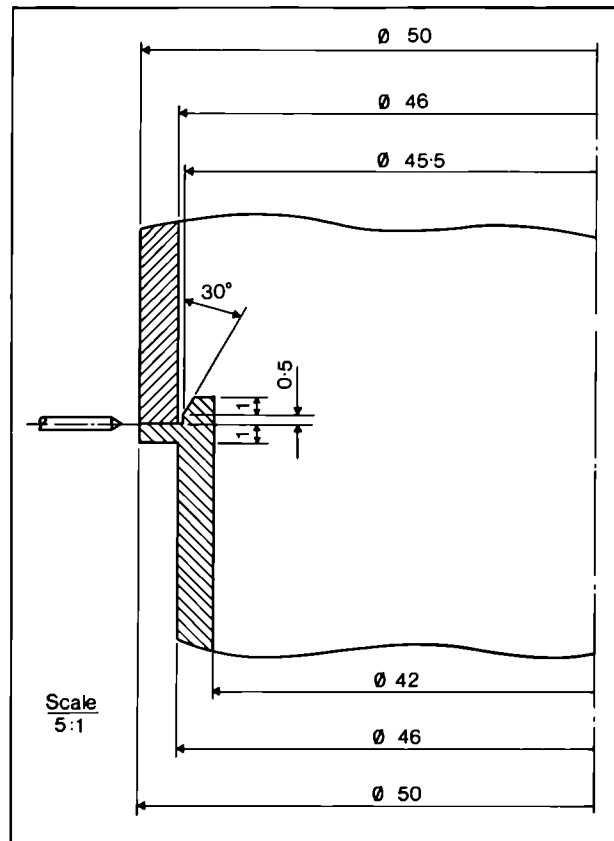


Fig.82: 50mm diameter weldment design

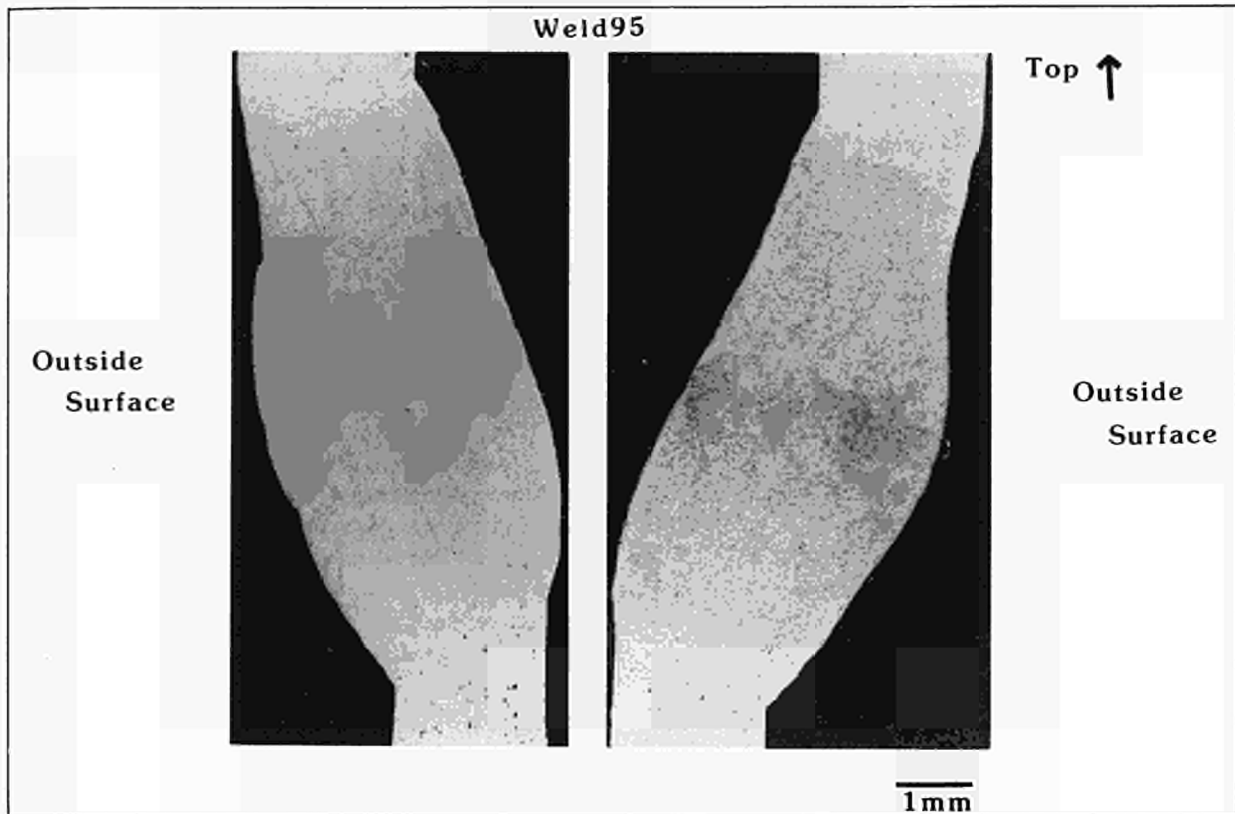


Fig.83: 50mm diameter weld section

cutting forces and minimum practical cutting speed and feed rate to minimise the power requirements of a cutting tool. Typical results are given for a 2mm wide tool bit:

- Minimum cutting speed 100mm/s;
- Radial feed rate 0.005mm/s;
- Radial and tangential cutting forces 1000N

The cut was made through the wall of the socket, 4mm from the weld line as shown in Fig.84. The bellows surmounting the socket were compressed by 4mm during first installation. During subsequent reinstallations the elasticity of the bellows was used to compensate for the socket material lost during previous cuts. This procedure caters for two remote handling operations on a limiter sector or antenna. If additional operations are required, the socket element may be replaced by cutting the internal fillet weld and installing a new socket. A detailed design study of this device will begin in early 1985.

Tritium Group (W. Riediker)

Overall Design Concept for JET Tritium Phase

During 1984, detailed requirements of the tritium handling system have been worked out and interfacing conditions to other JET systems defined. Concepts and flow diagrams have been developed for the integration of the gas supply and vacuum systems of the neutral injection and torus system into a closed gas recycling loop with the tritium handling plant. The tritium recycling system will provide for removal of impurities, compression of gases for reprocessing and separation

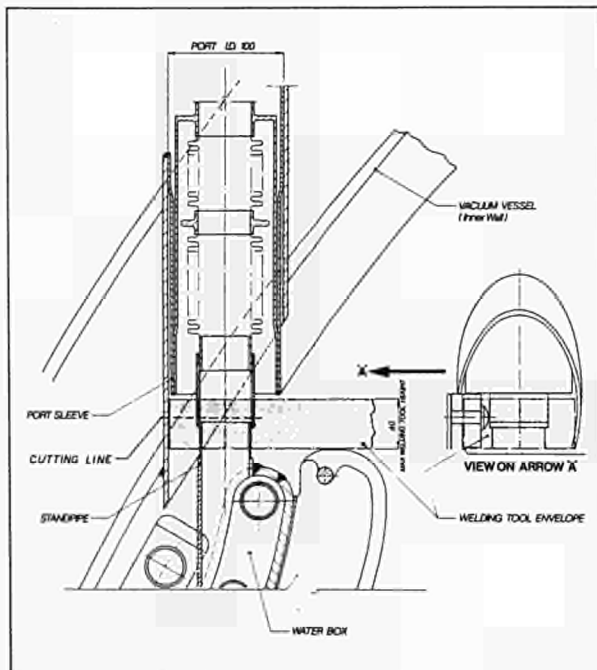


Fig.84: Position of the 50mm diameter pipe cuts

into hydrogen isotope fractions ready for re-use to feed the neutral injection and the torus system for plasma pulses or reconditioning of the torus in a closed loop glow discharge cleaning mode.

For the maintenance of systems in tritium service or to cope with gaseous waste streams from the tritium recycling plant, an air clean up system will allow processing of tritiated gases or air and also remove tritium from effluents with a high detritiation factor. The removed tritium will be fixed as tritium oxide on desiccant beds, allowing safe disposal handling. A dedicated clean-up system will also treat the helium gas of the torus baking system which will get gradually tritiated as tritium permeates through the primary torus wall. The plant duty has not yet been determined. Experimental work to measure the permeation rate of hydrogen and deuterium through the torus wall and the build-up of the respective concentrations during 1985-86 will allow the prediction of the tritium permeation rate and the definition of the necessary processing and disposal requirements.

Plant Duty

The nominal design of the Tritium Recycling System (TRS) should allow daily reprocessing of 48 pulses of 10s duration. The amount of gases introduced into the torus for a typical pulse will be approximately 1.86 normal litre (NI) of gas consisting of about 0.93NI of tritium (equivalent to 250mg or 2450Ci) and 0.93NI of deuterium, and up to 0.1NI of He³ or protium.

The gas will be transferred from the torus to the TRS after each pulse by turbomolecular pumps compressing the gas to about 0.1-1mbar at the TRS inlet. The gases are frozen out on the liquid helium (LHe) cooled cold surface of the accumulating panel, contained in one of the three parallel identical process cold boxes and accumulated for 12 pulses, while the He³ is continuously removed from the panel with a minimum of tritium carry-over. After 12 pulses, the gases will be directed to the panel in standby and the first panel warmed up to 80K. Its contents will be analysed, assessed and transferred to the LHe cooled cryotransfer pump, which when warmed up to ambient compresses the gases to 5-6bar, as required for further treatment and for separating into isotopic fractions. It is planned to separate the isotopes by two gas chromatographic units working alternately, in order to minimise the process inventory.

As there are still some scale up problems with these units, the plant duty may have to be reduced to a minimum of 20 pulses per day rather than to increase the number of gas chromatographic units, which would increase costs, plant complexity and affect related maintenance unfavourably. The gas amounts that have to be processed from the neutral injection system totals about 205NI per day (about 4.3NI per pulse) and consists mainly of deuterium with up to 2% tritium. These gases are accumulated on the cryopanel of the neutral injection boxes, released to the TRS at the end of the operating day and transferred to the accumulating panel of the third process cold box. They are then assessed and compressed

by the cryotransfer pump into an intermediate pressurised holding tank from which aliquot parts of the gas are passed into the gas processing-separation process.

The processed fractions are stored in product tanks at pressures between 0.2-0.8bar at purity levels as required for re-use in the torus or neutral injection system while interfractions containing mostly HT, HD and DT are recycled. For the closed loop glow discharge cleaning of the torus at 10⁻²-10⁻³mbar about 140NI/h of deuterium is recirculated continuously through the torus. Turbomolecular pumps compress the deuterium from the torus pressure to about 0.1-1mbar upstream of the TRS inlet. The gas stream is passed through one of the accumulating panels kept at 20K for removal of impurities before return to the torus.

The clean up system is sized to allow processing of up to 10m³/h of tritiated air or inert gases which will allow the pumping of the torus from ambient to operating pressure within 2 days. The detritiation factor of the system will exceed 1000.

Safety Aspects

The total tritium inventory of the TRS will be about 10⁴ Ci (10g) with up to an additional 5x10⁴ Ci in various locations such as make-up tanks, waste disposal tanks, and torus wall/torus pumping panels under normal operating conditions. Studies have been carried out to determine the consequences of total or partial releases of this inventory. Plant design has been developed taking account of the reliability of components of systems and consequences of potential failure modes, maloperation, maintenance and routine operation.

Typically, bulk amounts of tritium inventory are confined in primary equipment inside secondary vacuum tight and pressure designed containments. Systems, where process fluid is confined by only one containment, are being protected from building up large tritium inventories by reliable instrumentation and automatic isolating devices, which, for example, will limit the filling pressures. To minimise tritium emissions, most of the equipment will be designed to allow baking under vacuum prior to maintenance or repair.

Detailed design of plant equipment

Detailed design of long lead time equipment is well underway. Key components for cryogenic processing of the gases have been designed in detail and design options of key components such as the accumulating panel and the cryotransfer pumps are under construction with plans for performance testing in a special test rig, early in 1985. The tests will allow optimisation of the equipment for its performance, control, reliability and consumption of cryogenic liquids. Suitable engineering codes for the design of plant equipment and interconnecting piping under various thermal cycling conditions have been identified. Stress analysis on thermalloy cycled components and piping will be applied to guarantee a high degree of reliability.

JET – Scientific

Introduction

The Scientific Department is responsible for the definition and execution of the experimental programme, specification, procurement and operation of the diagnostic equipment and interpretation of experimental results. The Department, in its Operation Phase configuration, has a Departmental Directorate and one Theory and two Experimental Divisions. The structure down to Group Leader level is shown in Fig.85 and the list of Divisional Staff at December 1984 is shown in Fig.86.

Summary of Progress

During 1984, considerable activity was devoted to maintaining and operating those diagnostics already installed for the first operation of JET and to installing and making operational those further diagnostics needed for subsequent experiments. The following systems were operational by the end of 1984:

- Bolometer Scan
- Magnetic Diagnostics
- Single Point Thomson Scattering
- Multichannel Far Infrared Interferometer (partly)
- Single Channel 2mm Interferometer
- Microwave Reflectometer (prototype)
- Hard X-ray Monitors
- Limiter Surface Temperature
- Electron Cyclotron Emission (Spatial Scan) (partly)
- Time Resolved Neutron Yield Monitor
- 2.4MeV Neutron Spectrometer (prototype)
- Neutral Particle Analyser Array (partly)
- H-alpha Monitors (partly)
- Visible Spectroscopy
- VUV Broadband Spectroscopy
- Provisional Soft X-Ray Detectors
- Provisional Pulse Height Analysers
- Plasma Boundary Probe (partly)

The status of JET's Diagnostic systems at the end of 1984 is summarized in Table.XII and their general layout in the machine is shown in Fig.87. Feasibility studies on potentially new diagnostics and upgrades of existing ones have proceeded. For example, considerable progress has been made in assessing the feasibility of the LIDAR (Light Detection and Ranging) Thomson scattering system, proposed by a group at the University of Stuttgart, F.R.G. In this novel technique, an ultrashort

laser pulse is used to illuminate the plasma, and the back-scattered (about 180° scattering) radiation is collected. The spatial resolution is determined by the time delay between the transmission of the laser beam and the arrival of the scattered light back at the detector. Although the technique is new to fusion research, it is well established in other areas, such as atmospheric physics, and should be well suited to diagnosing large plasmas such as JET. The feasibility study has established that this technique could be applied to JET and could share much of the optics already installed for the existing single-point Thomson scattering system, thus reducing the cost and engineering complexity. Work is continuing on the design of this system with a view to being operational on JET early in 1987.

A new diagnostic, which was given a high priority in 1984 is the hydrogen/deuterium pellet injector system for JET. A detailed specification of performance, of the

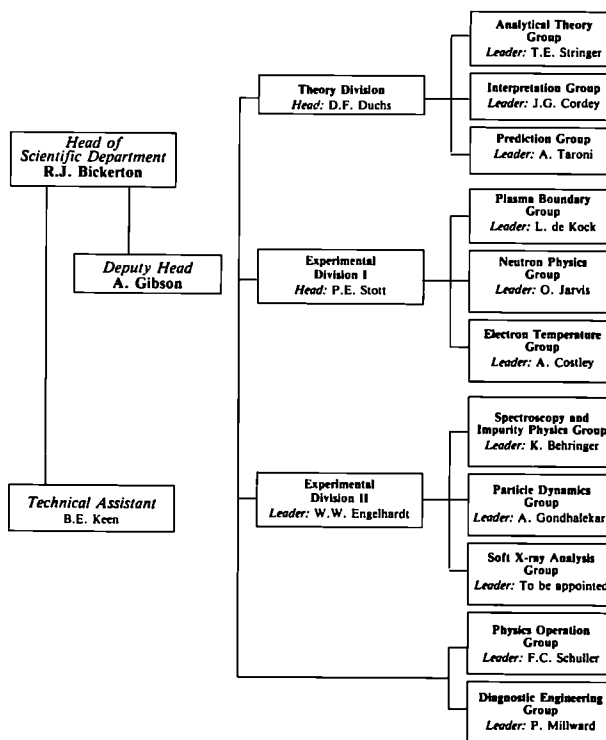


Fig.85: Scientific Department, Group Structure (December 1984)

SCIENTIFIC DEPARTMENT			
Head of Department:		R.J. Bickerton	
Deputy Head of Department:		A. Gibson	
DIRECTORATE:			
Head: A. Gibson			
A. Ainsworth	C.J. Hancock	B. Oliver	F.C. Schüller
N. Barnes	Miss T. Haynes	Mrs W. Prill	Mrs C. Simmons
C. Caldwell-Nichols	B. Keen	J. Reid	A. Tanga
S. Cooper	R.C. Lobel	P.J. Roberts	P. Thomas
Mrs S. Costar	P. Lomas	Mrs M. Rowe	Miss J.L. Thompson
N. Foden	M. Malacarne	P. Rutter	A. Tiscornia
J. Gowman	P. Millward	Miss S.J. Scard	C.H. Wilson
A. Hancock			
THEORY DIVISION:			
Head: D.F. Düchs			
M. Brusati	A. Gottardi	Mrs M-G. Pacco	T.E. Stringer
J. Christiansen	T. Hellsten	Mrs. J. Roberts	Mrs P. Stubberfield
J.G. Cordey	B. Keegan	R.T. Ross	A. Taroni
W. Core	E. Lazzaro	R. Simonini	M. Watkins
J. Davis	Miss M. Nave	E. Springmann	J. Wesson
A. Galway			
EXPERIMENTAL DIVISION I:			
Head: P.E. Stott			
D. Bartlett	J. Fessey	C. Nicholson	A. Stevens
C. Best	C. Gowers	P. Nielsen	Miss D. Strange
B.W. Brown	M. Hone	R. Prentice	D. Summers
D. Campbell	I. Hurdle	P. Roach	P. van Belle
J. Coad	O. Jarvis	G. Sadler	J. Vince
A. Costley	J. Källne	Miss K. Slavin	D. Wilson
L. de Kock			
EXPERIMENTAL DIVISION II:			
Head: W.W. Engelhardt			
K. Behringer	A. Edwards	L. Lamb	J. O'Rourke
J.L. Bonnerue	Mrs A. Flowers	G. Magyar	A. Ravestein
G. Braithwaite	R. Gill	J-L. Martin	J. Ryan
A. Bulliard	A. Gondhalekar	P. Morgan	F. Sieweke
S. Corti	J. Holm	E. Oord	M. Stamp
Miss G. Denne	Mrs E. Källne		

Fig. 86: Project Team Staff in the Scientific Department (December 1984)

interfaces to JET, and the preparation of a detailed design was completed in October 1984. Approval for manufacturing to start was given in December 1984. Piece-wise installation of the system will begin in July 1985, and full operation of the pellet injector is planned before the end of 1985. The injector will inject solid hydrogen or deuterium pellets into the JET plasma and will contain sufficient atoms to effect a 10 to 100% increase in the particle content of JET at the plasma densities and volumes expected during 1986. The pellet injector will expand the scope of studies of particle transport, confinement and recycling of the host species and also of impurities (using neon doped hydrogen/deuterium pellets), and will facilitate the tailoring of the plasma density profile to optimize

heating. It will also provide empirical data to arrive at a specification of a pellet refuelling device for JET.

In addition, during the year, staff in the Experimental Divisions, the Diagnostic Engineering Group and the Operations and Development Department, were still heavily involved in completing specifications and checking interfaces and remote handling capability for diagnostics being constructed in the Associations.

As well as assisting with machine operation and maintaining diagnostics systems, experimental planning, control room duties and interpretation of results have become an important part of the work of the Department. Considerable effort has been devoted to optimising breakdown conditions and understanding current-rise phenomena and disruptions occurring in the plasma.

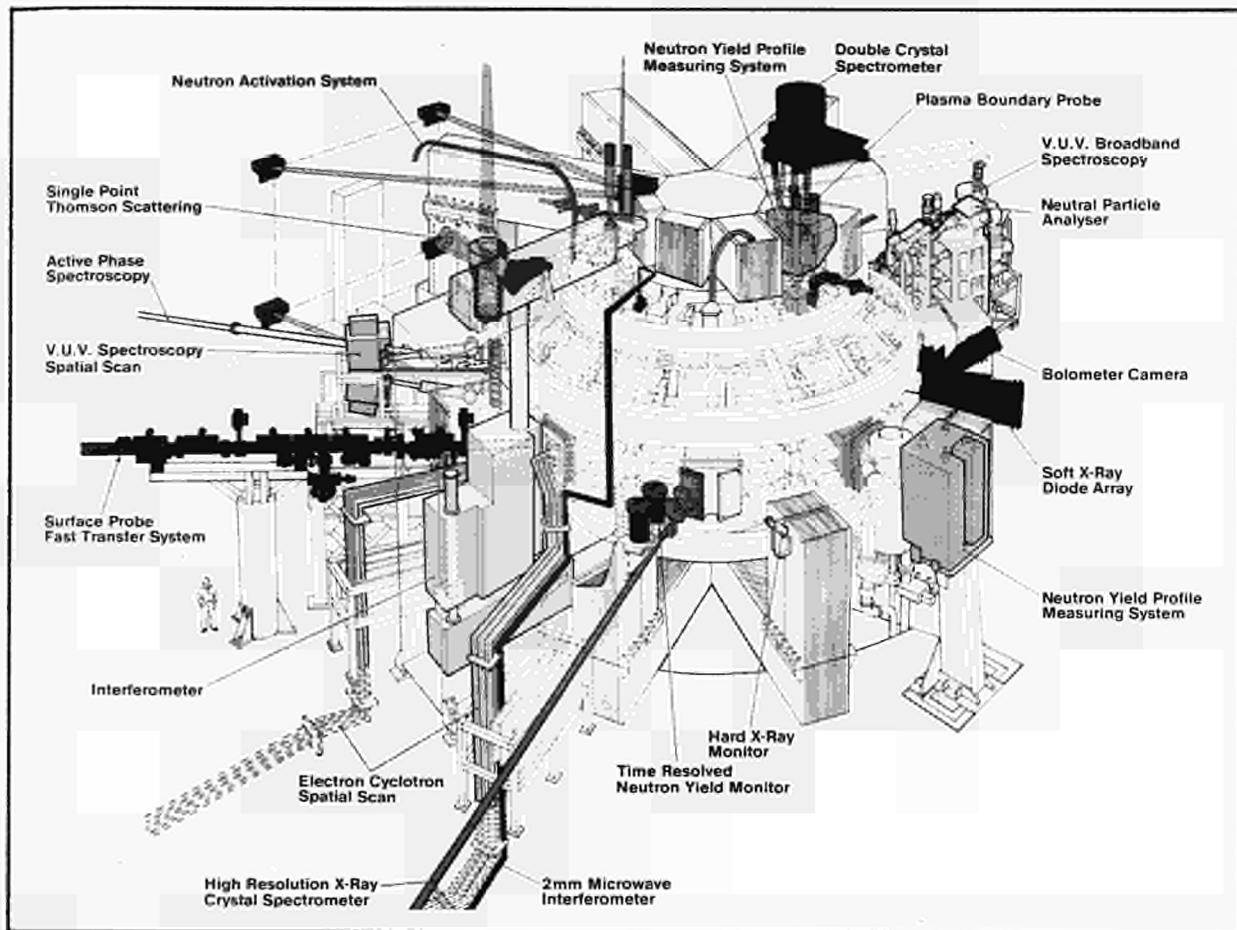


Fig. 87: Layout of Diagnostics in the Machine

Impurities still play a major role in the plasmas obtained during 1984, producing radiation losses and influencing stability. The sources, time evolution and transport phenomena were studied using spectroscopic diagnostics and methods of reducing the effects are being investigated.

Theoretical analysis, interpretation and prediction are powerful tools in providing a description of plasma behaviour and improving understanding of plasma phenomena as plasma parameters approach those necessary for a fusion reactor. Theoretical studies were active particularly in the fields of MHD stability and optimisation of RF and neutral injection heating schemes. During the year, interpretation codes have been further developed. Analysis of data, both during machine operation and subsequently, has been a priority activity. Prediction work has been important in studies of future JET plasmas, especially those involving different limiter materials, changed geometry and various heating scenarios.

The system for the attachment to the Project of staff from the Associations for periods between one month and

two years came into operation at the end of 1981. The growth of the scheme was slow and up to 1983 most assignments were for periods of three months or less. During 1984, 65 staff from nine Association Laboratories (excluding UKAEA staff) were assigned to JET, of which the majority were attached to the Scientific Department. In total, this amounted to a total of 15 man-years (plus a further estimated 8 man-years from UKAEA) of effort.

Task agreements centred around specific fields of research have permitted close collaboration with Association Laboratories, in which these laboratories have accepted responsibility to play a significant (but not exclusive) role in particular investigations. In many cases, the agreements are closely connected to diagnostic instruments built in the Associations, but they are also based on existing special expertise, and include such topics as: installation, commissioning and operation of diagnostics; physics investigations; and interpretation of results in collaboration with the JET team. Further details are included in the following sections and in Appendix I.

TABLE XII
Status of the JET Diagnostics Systems

Diagnostic System No.	Diagnostic	Purpose	Association	Status Dec. 1984	Date for operation in JET
KB1	Bolometer Scan	Time and space resolved total radiated power	IPP Garching	Operational	Mid 1983 partly Early 1984 fully
KC1	Magnetic Diagnostics	Plasma current, loop volts, plasma position, shape of flux surfaces	JET	Operational	Mid 1983
KE1	Single Point Thomson Scattering	T_e and n_e at one point several times	Risø	Operational	Mid 1984
KE3	Lidar Thomson Scattering	T_e and n_e profiles	JET and Stuttgart University	Design	Early 1987
KG1	Multichannel Far Infrared Interferometer	$n_e(r)$ ds on 7 vertical and 3 horizontal chords	CEA Fontenay-aux-Roses	Operational	Mid 1984 partly Early 1985 fully
KG2	Single Channel 2mm Interferometer	$n_e(r)$ ds on 1 vertical chord in low density plasmas ($> 10^{16} \text{ cm}^{-3}$)	JET and FOM Rijnhuizen JET	Operational Extension to 1mm	Mid 1983 Early 1985
KG3	Microwave Reflectometer	n_e profiles and fluctuations	JET	Prototype system operating	Mid 1983
KH1	Hard X-ray Monitors	Runaway electrons and disruptions	JET	Operational	Mid 1983
KH2	X-ray Pulse Height Spectrometer	Plasma purity monitor and T_e on axis	JET	Under construction Provisional systems	Mid 1985 Mid 1984
KJ1	Soft X-ray Diode Arrays	MHD instabilities and location of rational surfaces	IPP Garching	Provisional system operational. Full system under construction	Mid 1985
KK1	Electron Cyclotron Emission Spatial Scan	$T_e(r,t)$ with scan time of a few milliseconds	NPL, Culham and JET	Partly operational	Late 1983 partly Early 1985 fully
KK2	Electron Cyclotron Emission Fast System	$T_e(r,t)$ on microsecond time scale	FOM, Rijnhuizen	Commissioning	Early 1985
KL1	Limiter Surface Temperature	(i) Temperature of wall and limiter surfaces (ii) Monitor of hot spots on limiter	JET and KFA Jülich	Operational	Mid 1984
KM1	2.4MeV Neutron Spectrometer	Neutron spectra in D-D discharges, ion temperatures and energy distributions	UKAEA, Harwell	Construction proceeding	Mid 1985
KM3	2.4MeV Time-of-Flight Neutron Spectrometer		NEBESD, Studsvik	Calibration	Mid 1985
KN1	Time Resolved Neutron Yield Monitor	Time resolved neutron flux	UKAEA, Harwell	Operational	Mid 1983
KN2	Neutron Activation	Absolute fluxes of neutrons	UKAEA, Harwell	Construction proceeding	Mid 1985
KN3	Neutron Yield Profile Measuring System	Space and time resolved profile of neutron flux	UKAEA, Harwell	Construction proceeding	Mid 1985
KR1	Neutral Particle Analyser Array	Profiles of ion temperature	ENEA Frascati	Operational	Mid 1984 partly Mid 1985 fully
KS1	Active Phase Spectroscopy	Impurity behaviour in active conditions	IPP Garching	Under construction	Early 1986
KS2	Spatial Scan X-ray Crystal Spectroscopy	Space and time resolved impurity density profiles	IPP Garching	Under construction	Early 1986
KS3	H-alpha and Visible Light Monitors	Ionisation rate, Z_{eff} , Impurity fluxes	JET	Operational	Early 1983 Mid 1985 Full System
KT1	VUV Spectroscopy Spatial Scan	Time and space resolved impurity densities	CEA Fontenay-aux-Roses	Partly installed	Early 1985
KT2	VUV Broadband Spectroscopy	Impurity survey	UKAEA, Culham	Operational	Early 1984
KT3	Visible Spectroscopy	Impurity fluxes from wall and limiters	JET	Operational	Mid 1983
KT4	Grazing Incidence Spectroscopy	Impurity survey	UKAEA, Culham	Under construction	Early 1986
KX1	High Resolution X-ray Crystal Spectroscopy	Ion temperature by line broadening	ENEA Frascati	Under construction	Mid 1985
KY1	Surface Analysis Station	Plasma-wall and limiter interactions including release and hydrogen isotope recycling	IPP Garching	Construction proceeding	Mid 1985
KY2	Surface Probe Fast Transfer System		UKAEA, Culham	Construction proceeding	Mid 1985
KY3	Plasma Boundary Probe	Simplified probe system for monitoring progress of discharge cleaning and preliminary plasma-wall interaction experiments	JET UKAEA, Culham and IPP Garching	One unit operating Second unit being installed	Mid 1984 Early 1985
KZ1	Pellet injector Diagnostic	Particle transport, fueling	IPP Garching	* Under construction	Late 1985

Scientific Department Directorate

(Deputy Head of Scientific Department - A. Gibson)

The Scientific Department Directorate is composed of two main groups: the Physics Operation Group and the Diagnostic Engineering Group. In addition, it is responsible for a number of administrative functions within the Department and oversees contract work on radiological protection and shielding.

Physics Operations Group

During 1984, the focal point of the Group's activities shifted further towards Control Room duties and greater involvement in conducting experimental operations. Two Working Parties on Magnetic Limiters and on Pumping Panels overseen by the Group, concluded their work and presented final reports to the Scientific Council. In addition, two Topic Groups were coordinated by the Group: Disruptions (in conjunction with J. Wesson, Theory Division) and Plasma Optimisation.

The main activities of the Group are described in the following paragraphs.

Preparation and Execution of Experimental Operations (P. Lomas, F.C. Schüller, A. Tanga, P. Thomas)

An increasing number of experimental sessions were conducted by members of the Group in their capacity as Session Leaders. This involved preparation of the details of the daily programme, following agreement of the programme outline by the JET Experiments Committee, and of the waveforms needed for the control of the various devices one day before the actual session. In the morning before a session, a pulse schedule was produced describing all the pulse types envisaged for that day. A pulse type is described by all the set parameters and waveforms by name that control the toroidal field pulse, the ohmic network performance, the position and the shape of the plasma and the density evolution. Operations were somewhat simplified when current feedback and density feedback were introduced in September 1984.

The Plasma Fault Protection System (P. Lomas)

The Plasma Fault Protection System (PFPS) is designed to assist in safeguarding against plasma behaviour which might cause damage to the installation.

In 1983, it was demonstrated that PFPS could reliably detect faltering breakdown, excessive hard X-rays, excessive plasma light and disruptions, but the links were not in place to allow PFPS to initiate an orderly termination of the discharge.

At the beginning of 1984 a simpler set of fault detection algorithms were installed based on minimum and maximum allowed values of plasma density. For the most of 1984, the poloidal flywheel generator was controlled by preprogrammed driving waveforms, and in this mode the simplified plasma fault detection algorithms were successful in detecting fault conditions.

At the same time the links from PFPS to the rest of the plant were implemented as shown in the Fig.88. Here the response to a fault is a hard wired SOFT TERMINATION request which has the effect of aborting the waveforms for plasma current feedback in the Plasma Position and Current Control (PPCC) cubicle, but leaving unchanged the position control waveforms. When plasma current feedback is in use, this has the effect of ramping down the plasma current under full position control. For the case of plasma disruptions, a trigger signal is issued and is available for triggering data acquisition systems.

During the last few days of 1984 operation, the plasma current feedback system was brought into use, and thereby PFPS became active, with the ability to SOFT TERMINATE a discharge. In addition to the role of terminating potentially dangerous discharges, PFPS must provide the primary protection against malfunction of the plasma current feedback system to the plasma conditions. Fig.89 shows one of the commissioning tests where, for the first time PFPS terminated a plasma. This discharge was not faulty, but the minimum allowed value of current, $I(\min)$, was deliberately set to 2.0MA whereas a flat top plasma current of 1.5MA was

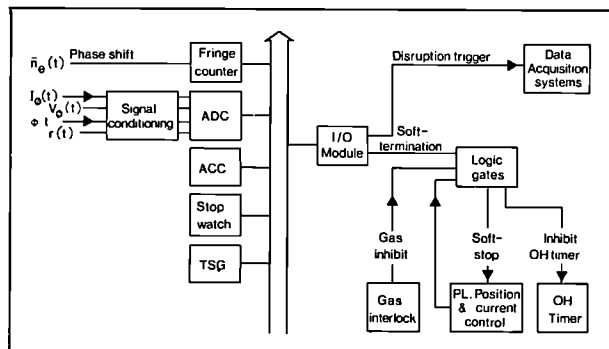


Fig. 88: PFPS hardware configuration used for real time plasma termination in cases of low or high plasma current, low density, or large hard X-ray flux

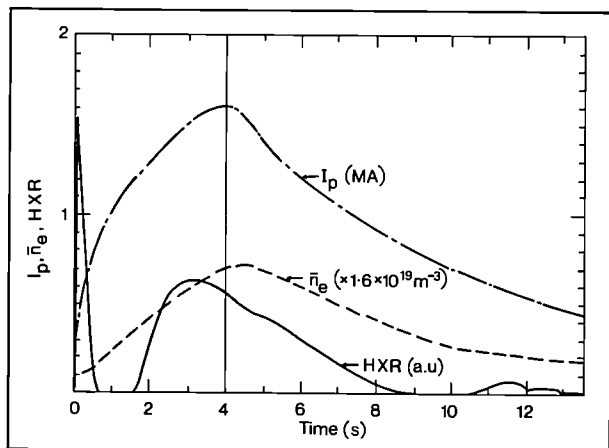


Fig. 89: An example of one of the first plasmas terminated correctly by PFPS due to a plasma current lower than required

expected. Consequently, a soft termination was issued 4s after the discharge was initiated, i.e. as soon as PFPS started to check for the presence of plasma current. The current feedback waveforms were correctly aborted and the plasma current decayed as shown (Fig.89).

Pulse Discharge Cleaning (PDC)

(F.C. Schüller, A. Tanga)

In July 1984, two weeks of operation were used for a thorough test of PDC. In this period, 12000 pulses were produced each 0.3s long with repetition rates of 3 pulses per minute. More than 90% of the pulses were made with a plasma current between 20 and 40kA at an ionisation degree of 10% and electron temperature of about 2eV. At a magnetic field of 0.25T, a driving voltage of 8V was sufficient. These parameters gave maximum water pump-out.

As a consequence, water pressure reduced by two orders of magnitude. Z_{eff} of a reference tokamak pulse reduced from 6.0 to 4.5 (from bremsstrahlung measurements). The high density limit increased by 20-30%. However, radiation loss remained close to 100% and metal radiation was still important.

Further use of PDC was abandoned on the following grounds:

- Improvement was bought at too high a cost in operational time, due mainly to a low power capability of available power supplies;
- A heavy strain was placed on the radial field amplifier, which is crucial for normal tokamak operation. If PDC should be resumed dedicated power supplies would be necessary.
- The success of wall carbonisation and the decision to clad the wall with carbon protection plates made PDC unnecessary.

Pumping Panels

(Working Group co-ordinated by A. Tanga and F.C. Schüller; Members: K.J. Dietz, H. Hemmerich, E.S. Holston*, M. Pick, R. Simonini, K. Sonnenberg)
* EURATOM-UKAEA Association, Culham Laboratory, U.K.

The group completed its work and presented a final report to the JET Scientific Council. Its main recommendation for the manufacture and installation of two test panels during the 1985 shutdown, was accepted. It was agreed that the permeation sheaths should be tested made of iron, palladium and nickel.

Magnetic Limiters

(Working Group co-ordinated by P.R. Thomas. Members: E. Deksnis, K.J. Dietz, J. Last, E. Lazzaro, P. Mondino, H. Niedermeyer*, F.C. Schüller, L. Sonnerup, E. Springmann)

*EURATOM-IPP Association, Garching, F.R.G.

The possibility of using the 'outer' poloidal field coils to generate a 'magnetic limiter' or open diverter configuration was investigated and, the results reported to the JET Scientific Council. It was shown that it was

feasible to produce such configurations and that in principle these could have favourable properties. However, it was found that the large currents required in the P2 and P3 coils generated a significant mechanical stress in one of the toroidal field coil supports. Unfortunately this is in a rather secluded part of the machine and there is no possibility of strengthening it. This stress limits the maximum plasma current to approximately 2.5MA. Plasma currents at this level would severely limit the ultimate plasma performance of JET so it was agreed that this approach would not be pursued vigorously. However, machine development is tending in a direction such that experiments can be performed which will demonstrate the properties of the open diverter configuration. Subsequently, A. Tanga and E. Lazzaro have shown that at large primary currents the stresses on the toroidal coils are related and that magnetic limiter operation should be possible at higher current levels.

Further Studies of Equilibria with Separatrices

(A. Tanga, E. Lazzaro)

Further investigations of the possibility of creating separatrices in JET, after the submission of the Working Party's report on Magnetic Limiters, showed that it should be possible to find equilibria with separatrices at a current level of 4MA provided that the primary current is very high and the poloidal beta is larger than one. In Fig.90, the poloidal flux distribution of such an equilibrium is presented. It shows the poloidal flux contours for a case in which the plasma current is 4.1MA, the plasma internal inductance is 1.0mH and poloidal beta is 0.85. The current in the coils PF1, PF2,

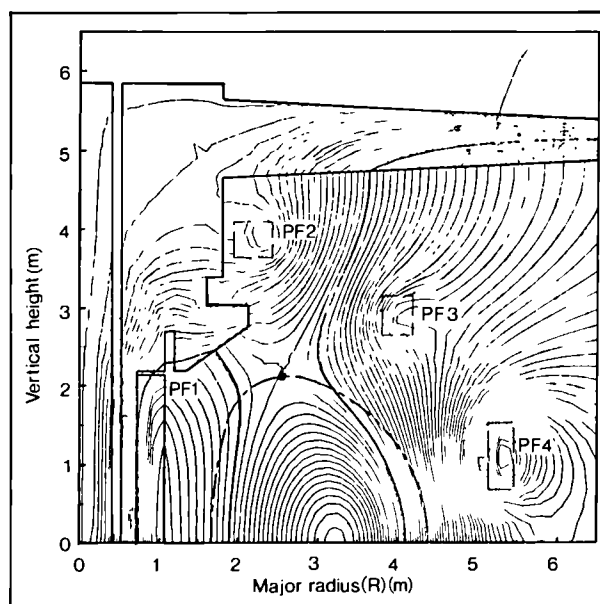


Fig.90: A numerically obtained example of a separatrix equilibrium in JET with a plasma current of 4.1MA; $\beta_p=0.85$ and $l_i=1.0$. The coil currents are $PF_1=23.5\text{MA}$; $PF_2=+1.8\text{MA}$; $PF_3=-1.33\text{MA}$ and $PF_4=-2.61\text{MA}$

PF3, and PF4 were respectively 23.48MA, 1.89MA, 1.33MA and 2.61MA. The current in the primary is large and negative and corresponds to the value routinely achieved in the final part of the plasma current flat-top for a high plasma current shot. The position of the X point is marked and is just on the vessel cross section line. The current in the coil PF2 is well within its present capabilities. The present current capability of the coil

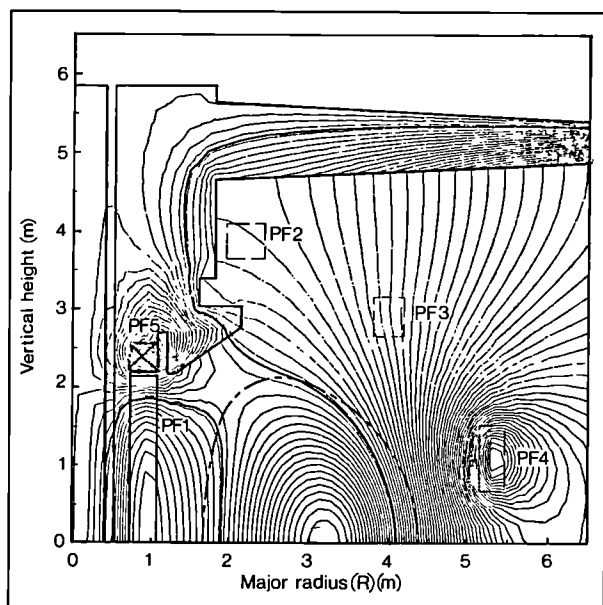


Fig.91: Same as previous figure, but with an extra (non-existing but possible coil) $PF_5 = +6.0\text{MA}$; $PF_2 = 0$ and $PF_3 = -0.08\text{MA}$

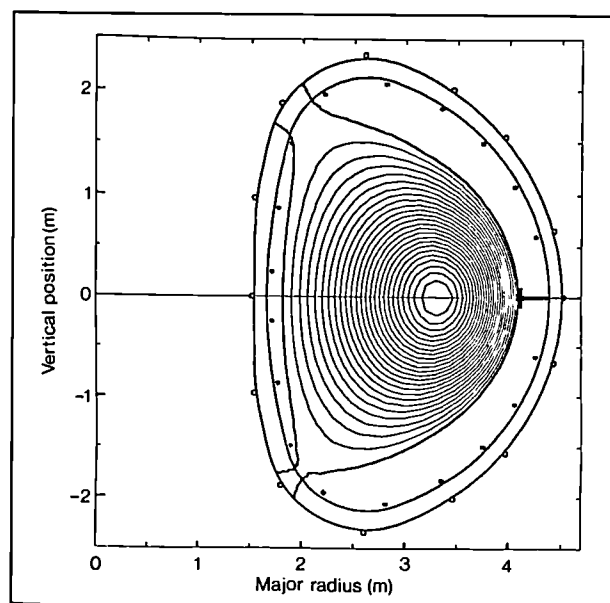


Fig.92: Experimental observation of separatrix formation during the current decay of Pulse No. 1967 with $I_p = 87\text{kA}$ and $(\beta_p + I_i/2) = 3.2$

PF2 would be sufficient for magnetic limiter operations for plasma currents in the region of 4MA, depending on the relative values of plasma poloidal beta, internal inductance and plasma dimensions.

An alternative PF coil configuration, suitable for the formation of a separatrix within the vessel, can be obtained by inserting two extra coils on the top and bottom of coil PF1, in an existing recess. The resulting configuration is shown in Fig.91.

The magnetic configuration with separatrices has already been observed experimentally in JET during the plasma current decay (with I_p up to 0.3MA) during which the poloidal beta was artificially high (up to 2.5) and the primary current was large. Fig.92 shows such an example.

Poloidal Flux Consumption

(P. Thomas)

The poloidal magnetic flux consumption is of interest for two reasons. Since the flux swing of the ohmic heating primary is limited by its current rating, the flux consumption determines the maximum plasma current and discharge duration. In addition, JET is similar in size to the next generation of reactor-like tokamaks such as NET, and therefore, the results from JET can be used to assist in the predicting the performance of these machines.

The flux consumed consists of three main terms. The most important of these in JET is the inductive flux which is proportional to the plasma current. However, it should be noted that inductance is not well defined for a distributed current such as that in a plasma column. In this case, the inductance is defined as the flux on axis divided by the plasma current. It includes a dissipative contribution which arises from the penetration of the current into the plasma column. The second term is the resistive flux loss on axis. This cannot be determined directly because there is no measurement of the voltage in the centre of the plasma. However, it can be evaluated from the magnetic measurements, particularly when the plasma is vertically elongated. The third term is due to the start-up losses. This is typically small and depends entirely on the conditions at breakdown.

It has been found that the inductive flux losses are consistent with the predictions of equilibrium codes. The resistive loss on axis can be adequately described by a constant voltage. This voltage ranges from 0.6-1.2V and depends mainly on the value of the toroidal magnetic field and the cross-sectional area of the plasma. The start-up loss is at most 3V.s. These results show that JET can be confidently expected to operate at its design plasma current of 4.8MA and that ultimately a level of 7MA should be possible at very high values of plasma pressure. The plasma inductance increases with the major radius whilst the resistive loss on axis and the start-up loss remain constant or decrease. Therefore larger devices can be expected to behave almost as pure inductances and so flux consumption can be reliably estimated using equilibrium codes.

Operational Aspects of Disruptions

(F.C. Schüller, F. Alladio*, F. Crisanti*, M. Malacarne, M. Nave, J. Thompson, J. Wesson)
 * EURATOM-ENEA, Frascati, Italy.

The Hugill diagram for disruptions during 1984 shown in Fig.93. Most of the disruptions are of the high density type normally occurring in the decay phase. Compared with 1983 results, densities obtained were 10% higher, except for the pulses immediately after PDC which were 20-30% higher. A number of discharges disrupted in the rise or early flat-top phase. There seems to be an enhanced probability around $q_{cyl} \approx 3$ but such disruptions can occur at any q . There are suspicions that this is due to arcs at plasma surface temperatures elevated by skin-effects in the rise-phase.

Nearly all high density disruptions were preceded by a $m=2, n=1$ MHD-mode. The striking phenomenon was that the mode stopped rotating but still grew in amplitude. This mode-locking occurred always in the same toroidal location, suggesting a toroidal asymmetry in the poloidal field distribution causing a preference for the mode-lock. Another possibility is that the position feedback always acts on the signals from one specific octant and therefore may cause a preferred mode-lock position, as shown in Fig.94.

The 1983 JET Progress Report mentioned that the difference between hard and soft current quenches lies in the capability of the position control system to ramp the vertical field down quickly enough after an energy quench. In Fig.95, the difference between slow and fast disruptions is illustrated by experimental examples.

In Fig.96, the influence of the voltage capability of the position power amplifier on the $\delta I/\delta t$ value after disruption. No distinction is made between the number of turns in the position control coils which partially blurs the trend that low voltage capability leads to a larger $\delta I/\delta t$. From this figure it is also clear that current quenches in the rise-phase are slower than any in the flat top decay-phase, because of the relatively large loop voltage preprogrammed to increase the current.

Marfes

(M. Malacarne, F.C. Schüller)

Coordination of the analysis of Marfe related data has been started. Previously, the occurrence of Marfes seems to be related to the high density limit, i.e. at high values of n/I . The correlation with geometrical quantities (such as elongation or distance between in-board plasma and wall) is not clear. The influence on the particle balance is strong but can lead to a sudden increase in $\delta n/\delta t$ as well as to a decrease. A more refined classification is necessary.

Circuit Codes

(P. Rutter, P. Thomas, J. Thompson)

Two codes which model the behaviour of the poloidal field system have been developed. The first of these uses a simplified model of the plasma load but has a detailed model of the poloidal flywheel generator convertor

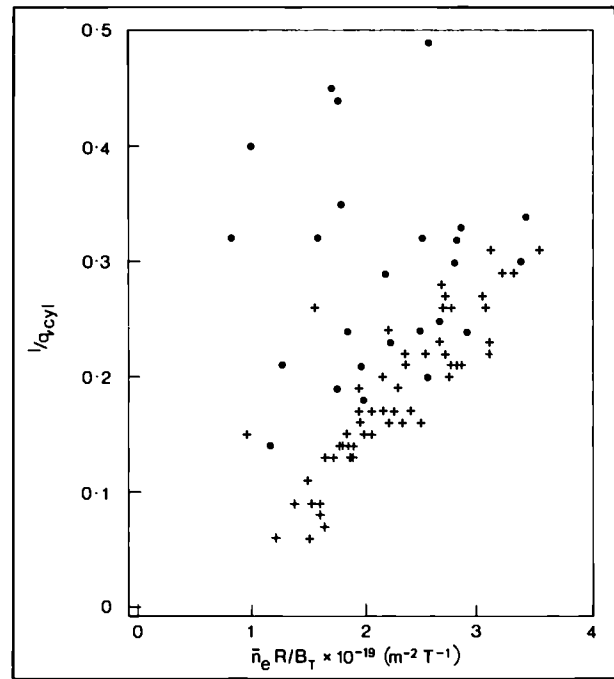


Fig. 93: Hugill-diagram for disruptions observed during 1984. The experimental points indicate the value at disruption:

- – disruptions in the rise-phase or flat-top $I_{(disr)} \geq 0.8 I_{max}$
- + – disruptions in the plasma decay-phase $I_{(disr)} < 0.8 I_{max}$

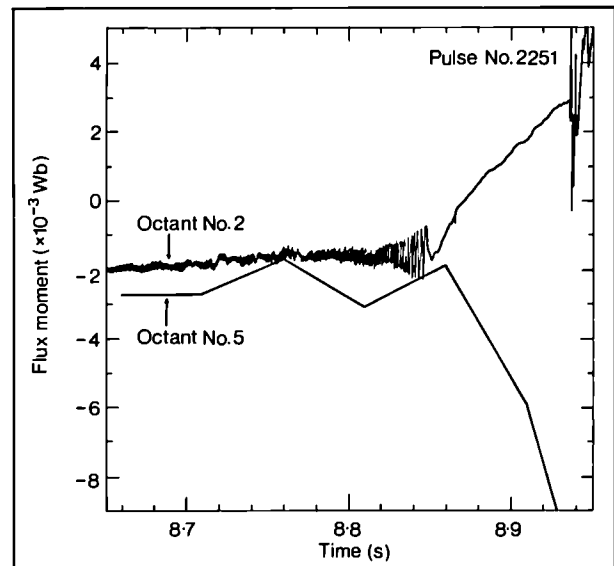


Fig. 94 The perturbation of the flux-surfaces by an $m=2: n=1$ mode before a disruption. The mode rotates until 100ms before the disruption as can be seen by the oscillatory behaviour of the flux perturbation (measured by the fast data acquisition system on Octant No.2). The mode locks, (i.e. stops rotating) but still grows in amplitude until it causes the disruption. The $n=1$ character during the mode-lock can be seen by the opposing phase between Octants Nos.2 and 5 (slow data sampling)

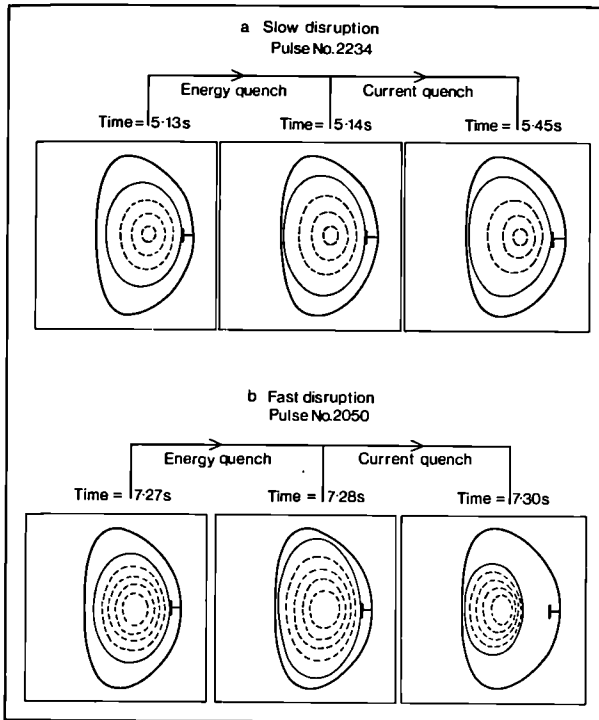


Fig. 95: The plasma cross-section during the energy and current quench of a disruption measured by the magnetic diagnostics and calculated by the ODIN-code. Note that in case of a slow current quench, contact with the limiter is maintained, whilst during a fast quench the plasma is squashed against the inner wall

(PFGC) and ohmic heating network. It is used to compute the reference waveform required for the excitation of the PFGC and the time at which the PFGC is reconnected after the fast current rise. This code has been written for the NORISK minicomputers. It is both small and rapid in execution. The accuracy of the model has been such that the plasma current is typically within 10% of that intended even without feedback control. It is intended to use this code as the basis of the Level 1 control programme for JET. The other code is considerably more complex. It creates realistically the behaviour of the position and shape control system, the plasma current feedback and the currents that flow in the structure of the tokamak. It also has simple models for the plasma power balance, current penetration and shape. This code is being used to assist in the development of the ohmic heating circuit and to benchmark simple models for use in the Level 1 control programme.

Experimental Console Software
(S. Cooper, A. Hancock)

The interpulse display software has been refined and additional features introduced over the year. The display programmes and the console pictures are controlled by touch panels on both the experimental and machine consoles. Much has been done to increase the reliability and speed of execution of the software. The retrieval of the information required to obtain the sampling rates of

the data channels used has been automated. The Group has invested considerable effort in the optimisation of the FAST analysis code (supplied by the Interpretation Group) for execution on the Nord 570 computer. As a result the analysis of the plasma shape and position is available a few minutes after the pulse.

A real-time display programme has been written and installed. This collects data from one of the diagnostic computers and sends it to the experimental console during the plasma pulse. The display is used to provide information required for the initial assessment of the success of a plasma pulse. When used in conjunction with the alarm system it can provide a speedy diagnosis of technical faults in the machine systems.

A logging programme has been written to collect a running commentary on the operating sessions. A programme has been written to enter or redisplay the comments and store them in a small database. Comments can be modified or added. Another programme stores a brief data summary which is combined with the comments and printed out as a Session Journal.

Databases

(J. Thompson)

Use is being made of the SAS package on the Harwell IBM Computer for the analysis of data. This package can

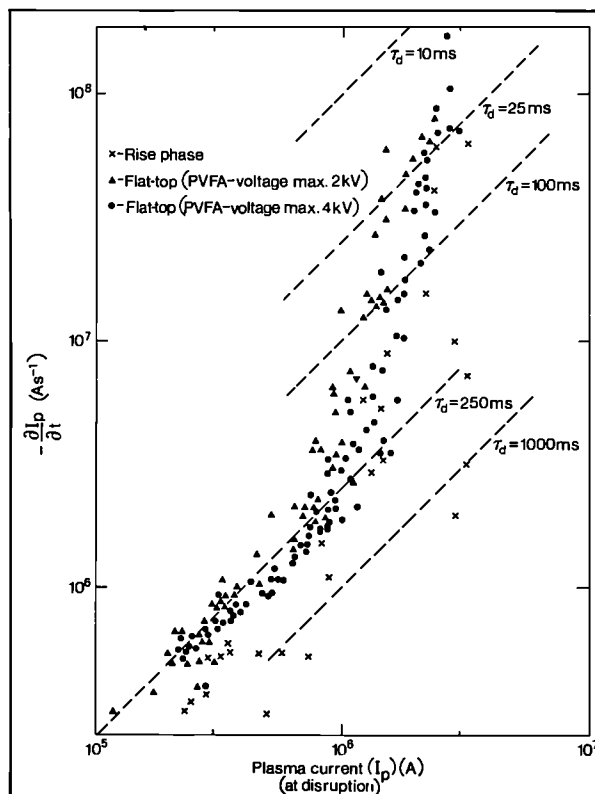


Fig. 96: The current decay rate as a function of the plasma current at disruption. Disruptions in the rise-phase (x) are slower than the others, as there is a higher driving voltage. Disruptions with a low voltage capability (Δ:2kV) of the position amplifier disrupt faster than the ones with high voltage capability (●:2kV)

be used for the maintenance and manipulation of topical databases. It has a programming language and a set of powerful built-in analyses packages. The main effort in the Group has been in the establishment of a database on disruptions, although several smaller ones have been used for other purposes. Tools have been developed to interface SAS to the main JET data files, so that it can then be used to analyse data and to display results.

Diagnostic Engineering

(A. Ainsworth, M. Barnes, C.J. Caldwell-Nichols, N. Foden, J. Gowman, C.J. Hancock, R. Lobel, P. Millward, B. Oliver, J. Reid, P. Roberts, A. Tiscornia, C. Wilson)

Throughout the year, the Diagnostic Engineering Group has remained heavily committed to the design and manufacture of interface components and to preparations for the installation of diagnostic systems during the planned shutdowns of October 1984 and June 1985. At the end of the year, all but 9 of the original diagnostic proposals were installed and in addition 5 new or provisional systems had been incorporated. This last year has included work on the larger systems which will operate in the D-T phase. These systems have required complex steel and concrete structures to provide adequate radiation shields in the Diagnostic Hall which is a free access area. This work has needed careful preparation and planning to coordinate the many different contractors and to meet the scheduled targets of the JET programme. Further details of the diagnostic systems are given in the Experimental Division contributions.

Experimental Division 1

(Division Head: P.E. Stott)

Experimental Division 1 is responsible for specification, procurement and operation of about half of the JET diagnostic systems, particularly those associated with electrical measurements, electron temperature measurements, surface and limiter physics and neutron diagnostics. In addition, the Division assists in execution of the programme, in interpretation of results and in making proposals for future experiments, in collaboration with Experimental Division 2, Theory Division, the Physics Operations Group and the Operations and Development Department.

During 1984, further diagnostic systems were installed, and by the year's end, the following systems were operational:

- Magnetic Diagnostics;
- Single Point Thomson Scattering;
- Multichannel Far Infrared Interferometer (partly);
- Single Channel 2 mm Interferometer;
- Microwave Reflectometer (prototype);
- Hard X-ray Monitors;
- Electron Cyclotron Emission (Spatial Scan) (partly);

- Time Resolved Neutron Yield Monitor;
- 2.4 MeV Neutron Spectrometer (prototype);
- Plasma Boundary Probe (partly).

In parallel, progress was maintained, in collaboration with the respective Associations, on the detailed design and construction of the diagnostics planned for installation in 1985 and 1986, which include the surface physics probes and the neutron diagnostics. A number of feasibility studies of potential new diagnostics and upgrades of existing ones, were started, including a Microwave Reflectometer, a LIDAR (Light Detection and Ranging) Thomson Scattering System and 14 MeV Neutron Spectrometers. As these diagnostics systems were progressively brought into reliable operation, greater attention was devoted to interpretation of JET measurements and to a wider range of plasma physics problems.

Long term surface samples, collector probes and samples of limiter material, after removal from JET, have been analysed by a variety of surface techniques. From this data, a picture of the plasma-wall and plasma-limiter interactions in JET is being built up. The first measurements of ion temperatures from the neutron diagnostics have been made in deuterium plasmas. Measurements of electron density and temperature provided important data for confinement and other studies, including a preliminary study of internal sawteeth modes.

Electron Temperature Measurement Group

The Electron Temperature Measurement Group is responsible for four of the main JET diagnostic systems (see Table XII): The Microwave Density Interferometer (KG2), The Spatial Scan Electron Cyclotron Emission System (KK1), The Fast Scan Electron Cyclotron Emission System (KK2), and the Single Point Thomson Scattering System (KE1). In addition, the Group is responsible for work on two diagnostics planned for the later phases of JET operation: a LIDAR based Thomson Scattering System (KE3), and a Microwave Density Reflectometer (KG3). During 1984, developments were made on all these systems.

The Microwave Density Interferometer (KG2)

(J. Fessey, C. Gowers, C. Hugenholtz*, I. Hurdle and K. Slavin)

*EURATOM-FOM Association, FOM, Netherlands

The Microwave Density Interferometer System measures the line integral of the electron density, $\int n_e dl$, along a vertical chord located on Octant No. 7 at $R = 3.14\text{m}$. During 1984, the system was the main density diagnostic of the JET plasma, and it operated reliably and virtually continuously during tokamak operation. It measured without difficulty the highest line averaged density achieved so far, $\sim 3 \times 10^{19} \text{m}^{-3}$ (see Fig.97(a)). Recently, the density values given by the system were compared with those measured by the Far-Infrared Multichord Density Interferometer (KG1), and typically, agreement to within $\sim 3\%$ was obtained.

Several improvements to the system were made during the year. Improved tapers were installed in the plasma arm, thereby reducing the attenuation in this arm by $\sim 15\text{dB}$ to $\sim 65\pm 3\text{dB}$. The data acquisition software was upgraded so that more data points could be taken during a JET Pulse and a fast sampling 'window' is now available. The fibre optic links between the electronic modules within the diagnostic itself, and between the diagnostic cubicle and the Plasma Fault Protection System (PFPS) cubicle located at the opposite end of the Diagnostic Hall, were replaced with a more rugged

design. This latter change has improved both the reliability of the diagnostic and the reliability of the link to the PFPS, and has enabled the interferometer output to be successfully incorporated into the real-time density feedback control of the JET plasma.

These changes have also improved the measurement capability. The minimum detectable density change has been extended down to $\sim 5 \times 10^{15} \text{m}^{-3}$ (20 millifringes) which represents $\sim 0.02\%$ of the typical JET line averaged density. Density sawteeth, which typically have an amplitude $\sim 1\%$ of the density signal, can be easily resolved (Fig.97(b)), and fluctuations of only $\sim 0.1\%$ amplitude can be seen on the individual sawteeth (Fig.97(c)). These results demonstrate that the diagnostic will be a powerful tool for studying density fluctuations in addition to its role as a basic density diagnostic.

Some progress has been made with the upgrade of the system for operation at a wavelength of 1mm. A 315GHz (300mW) carcinotron has been delivered and installed in the Diagnostic Hall, and prototype hardware for modulating the source at 1MHz has been developed. Since the modulation frequency of the 2mm system is also 1MHz, this development should permit the use of a duplicate of the existing detection and phase counting electronics. Final commissioning of the 1mm upgrade has been delayed by extensive civil engineering work in the Diagnostic Hall necessary for the installation of other diagnostics, and this is now planned for early 1985.

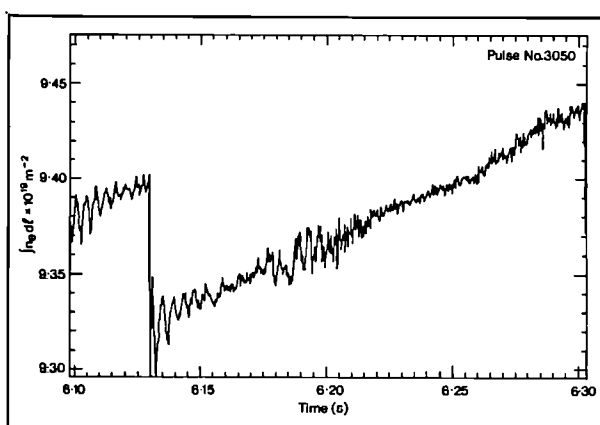
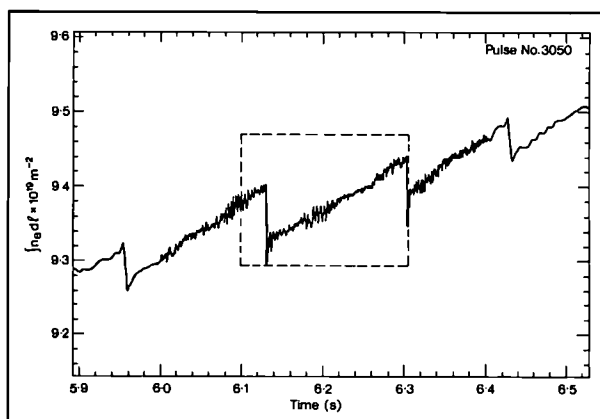
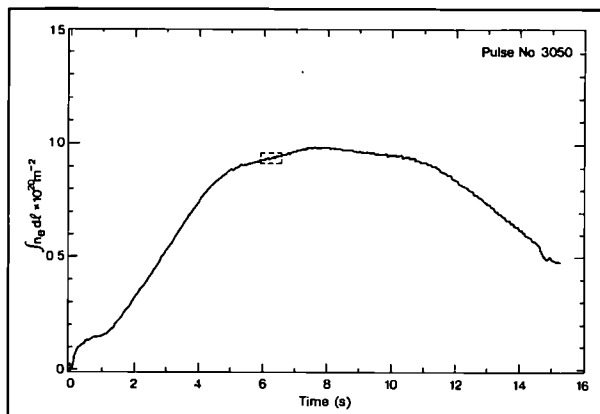


Fig.97: Line averaged density $\int n_e dl$ from the 2mm Interferometer for Pulse No.3050: (a) time period 0-16s; (b) time period 5.9-6.5s showing sawteeth oscillations; and (c) time period 6.1-6.3s, showing high frequency fluctuations on the sawteeth

The Spatial Scan Electron Cyclotron Emission System (KK1)

(D.V. Bartlett, D.J. Campbell, A.E. Costley, S. Kissel, P. Roach and E. Baker*)

*National Physical Laboratory, London, UK.

The system for transmitting ECE radiation from the plasma to the Diagnostic Hall, which is shared by both systems KK1 and KK2, was completed during 1984. The system consists essentially of ten antennae mounted inside the torus vacuum vessel to view the plasma cross section along different chords, crystal quartz vacuum windows, and oversized (S band) aluminium waveguide. During 1984, the remaining six antennae were installed in the torus along with their crystal quartz vacuum windows, and the permanent S band waveguide system was installed. An extensive series of measurements were made on the performance of the system, and the total transmission of the system (plasma to instrument location in the Diagnostic Hall) is typically $\sim 5\%$. The system is fully compatible with the active phase of JET operation.

The Spatial Scan ECE System (KK1) was developed and constructed by the National Physical Laboratory, UK. It consists of four low resolution rapid scan Michelson interferometers, one high resolution rapid scan Michelson interferometer and six rapid scan Fabry Perot interferometers all fitted with liquid helium cooled indium antimonide detectors and appropriate control and data acquisition hardware and software. The primary objective of the system is to measure the two dimensional electron temperature in the poloidal cross-section.

During 1984, one channel of the system fitted with one of the low resolution Michelson interferometers was used routinely to measure the electron cyclotron emission along a line of sight 13cm below the mid-plane. From the measurements, the time and space dependence of the electron temperature were deduced using well established procedures (Fig.98). This channel was the primary electron temperature diagnostic on JET during the year.

The remaining low resolution Michelson interferometers were installed and commissioned in the Diagnostic Hall. These will be used in the first attempts to measure two-dimensional temperature profiles in 1985. The construction of the Fabry-Perot interferometers was completed and these instruments were also installed in the Diagnostic Hall. Considerable progress was made with the construction of the high resolution Michelson interferometer. The data acquisition software was improved so that up to 150 temperature profiles can be measured during each plasma pulse with the operational channel, and the analysis software for the full two dimensional measurement system was completed, installed and commissioned on the NORD computers at JET.

There were several other important developments. A thorough comparison was made of the temperature values obtained from the ECE system with those obtained from the Thomson Scattering system (eg. Fig.99), and this showed that the two diagnostic agree within the experimental errors (ECE, $\pm 20\%$ absolute level, $\pm 10\%$ relative shapes Thomson scattering typically $\pm 10\%$). Techniques for calibrating the system using large area black body sources were improved and three separate and extensive calibrations were carried out. A contract was placed with the National Physical Laboratory, UK, for the development of improved calibration sources and techniques. Some preliminary measurements were made with one of the Fabry Perot interferometers used in its static mode and these show that the interferometers will have high sensitivity, changes in temperature $\leq 5\text{eV}$ can be observed with an electrical bandwidth of 30kHz.

The Fast Scan Electron Cyclotron Emission System (KK2)

(D.J. Campbell, C. Hugenholtz*, R. Niestadt*, T. Oyevaar*, H. Piekaar*, and B. Tubbing*)

*EURATOM-FOM Association, FOM, Netherlands.

The ECE Grating Polychromator, constructed by the EURATOM-FOM Association, FOM Institute, Netherlands, is designed to study the temporal evolution of the plasma electron temperature at up to 12 positions simultaneously with a time resolution $\ll 3\mu\text{s}$. The diagnostic system consists of a 12 channel grating polychromator, liquid helium cooled indium antimonide detectors, and associated control and data acquisition electronics and software. Radiation is transmitted to the diagnostic via one channel of the JET ECE antenna/waveguide system.

During 1984, substantial progress was made in all

areas, culminating in the commencement of installation and commissioning in September. The delivery of a number of specially designed waveguide components [1], programmable electronic amplifiers, and the indium antimonide detector systems enabled construction completion of the diagnostic hardware during the first half of the year. Low pass radiation filters for the elimination of higher grating orders were also developed

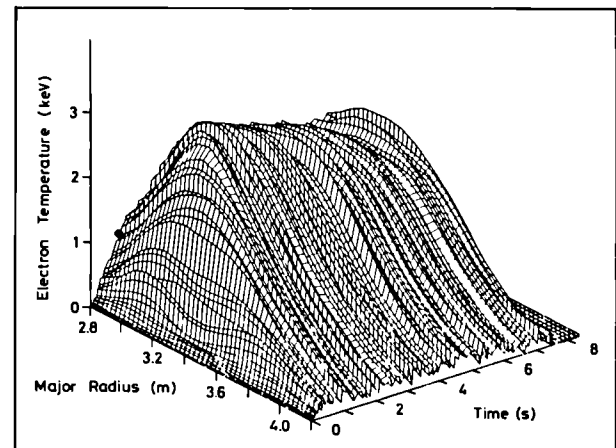


Fig.98: Electron temperature (T_e) profiles (from ECE measurements) plotted as a function of time ($t=0-8\text{s}$ for Pulse No.1697)

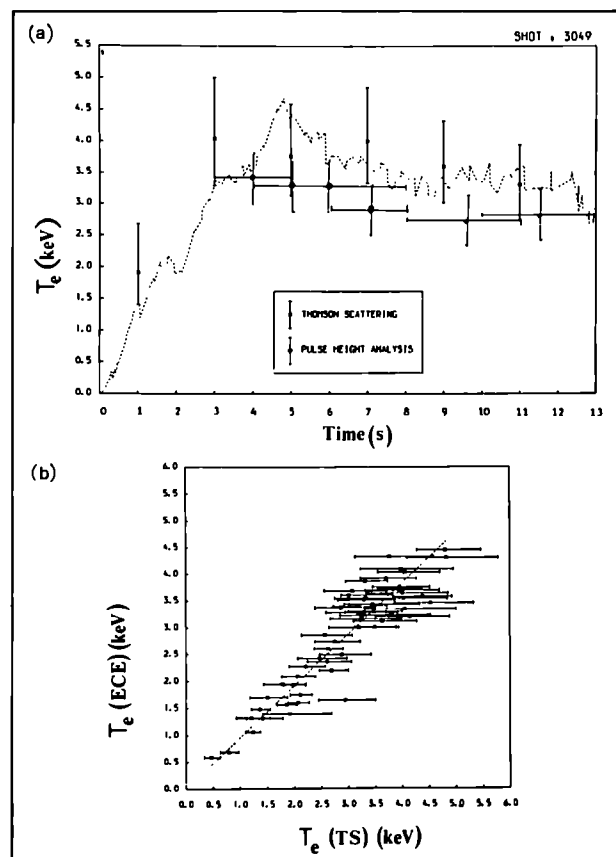


Fig.99: Comparison of electron temperature (T_e) measurement from ECE and Thomson scattering diagnostics

as the result of a collaborative effort between JET and FOM.

The construction of a new calibration apparatus, designed to exploit a novel calibration technique proposed by FOM [2], enabled extensive testing and optimisation of the polychromator. Acceptance tests carried out in August 1984 showed that performance of the system was close to expectation: dispersion and resolution curves obtained for the polychromator were in agreement with theoretical predictions, and system responsivity was close to that expected.

In the areas of diagnostic control and data acquisition, the CODAS cubicle was completed in mid-1984, and

commissioning tests commenced immediately. An extensive control-software package was completed, and significant progress made with data analysis software for the NORD computer system.

The Phase III contract for this system started in September 1984, and by the end of the year, the diagnostic hardware had been assembled at JET and interfaced to the diagnostic CODAS cubicle. Finally, connection to the ECE waveguide system has been completed in anticipation of obtaining first plasma measurements on resumption of JET operation in early 1985.

The Single Point Thomson Scattering System (KE1)

(P. Nielsen, R. Prentice, M. Gadeberg* and B. Brown)

*RISØ National Laboratory, Denmark.

The Thomson Scattering System on JET (KE1) has the conventional 90° scattering configuration. Light from a powerful ruby laser illuminates the plasma along a vertical chord, and the light scattered at 90° from a 5cm length of the beam on the midplane, is collected and spectrally resolved. The electron temperature, T_e , and electron density, n_e , are determined from the spectral width and intensity of the scattered light, respectively. The vertical chord through the plasma can be selected as any one of seven discrete major radii. Changing from one position to another takes place between plasma discharges (Fig. 100).

The laser is a low beam divergence ($\sim 0.5\text{mrad}$) ruby laser ($\lambda \approx 694.3\text{nm}$) and can be operated either in a single pulse mode giving one 20J pulse during each JET discharge, or in a multipulse mode with lower energy at repetition rates up to 1Hz. The collection system is a double Newtonian telescope arrangement; the dispersion system is a triple prism spectrometer; and the detectors are photomultipliers. Special alignment systems keep the laser beam and the collection system mutually aligned. Items sensitive to nuclear radiation, such as laser and the dispersion and detection systems, are housed behind the radiation shielding in the roof laboratory, so that the system should be compatible with the active phase of JET operation. The system has been designed and constructed by the Risø National Laboratory, Denmark.

The first observations of scattered signals were made in early 1984, and from June to October, the system was operated routinely, producing data on $\sim 80\%$ of the plasma discharges. Due to a technical problem with the auxiliary crate controller, the diagnostic was not operated on-line. Also, the two innermost scattering locations did not have windows fitted for the laser beam path. Both these items were brought into operation during the October - January shutdown, and the Thomson Scattering System has been fully commissioned for the start of 1985 operation.

Fig. 101 shows a typical example of fitted spectra when firing the laser at 2s intervals during a plasma discharge, and Fig. 102 shows the deduced time evolution of the central temperature and density on the same discharge.

Since electron temperature is studied in much more detail by the ECE system, the Thomson Scattering

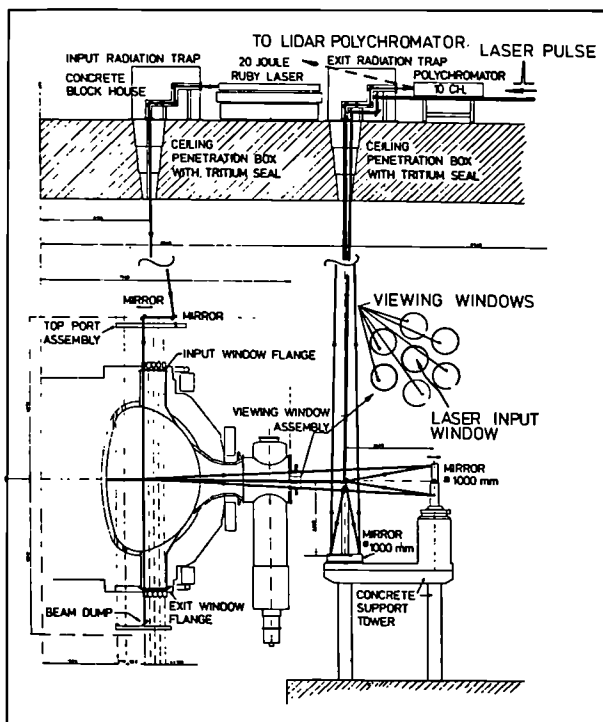


Fig. 100: Layout of Single Point Thomson scattering and LIDAR systems

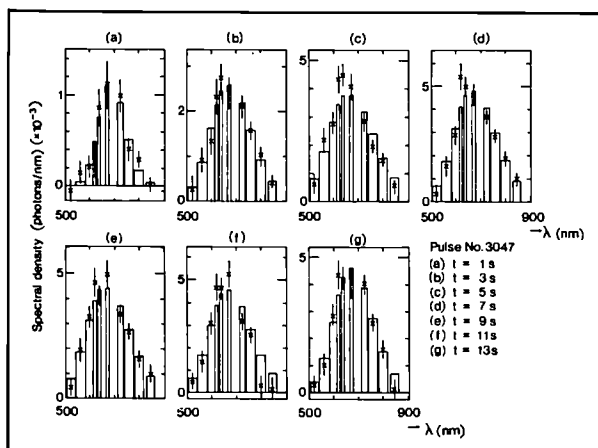


Fig. 101: Typical example of fitted spectra for Thomson scattering system (Pulse No. 3047)

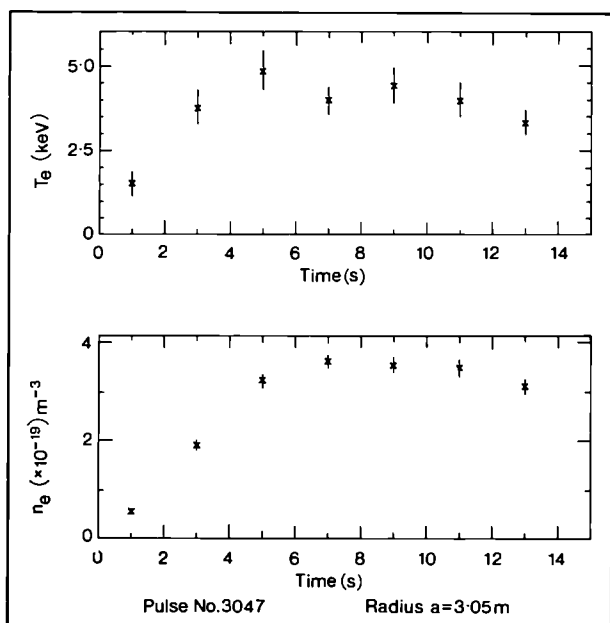


Fig. 102: Time evolution of central electron temperature (T_e) and density (n_e) (Pulse No. 3047)

system was used largely to verify the calibration of the ECE measurements. Frequency scans were made by operating a series of discharges with different values of toroidal field. A comparison of ECE and Thomson scattering temperature values on 200 discharges (1000 measurements) show excellent agreement between the two diagnostics. These comparisons are described in more detail in the section on ECE Spatial Scan (KK1) diagnostic (see Fig. 99).

The LIDAR Thomson Scattering Diagnostic (KE3)

(C. Gowers, A.E. Costley)

The possibility of using a short (300ps) laser pulse, a fast detection system and backscattering geometry to obtain the spatial distribution of the plasma electron temperature and density on JET was the subject of an experimental and theoretical feasibility study carried out for JET by EURATOM-IPP Association, Garching, FRG. The study was carried out in collaboration with MPQ Garching and the University of Stuttgart, FRG [3]. The technique considered is a novel time of flight or LIDAR (Light Detection and Ranging) Thomson scattering technique. The study was completed in May 1984 and discussed in detail in July at a JET Diagnostic Workshop. The results were most encouraging. Frequency doubled Iodine laser light was selected as the most suitable source ($\lambda_\omega = 1.315\mu\text{m}$; $\lambda_{2\omega} = 0.658\mu\text{m}$) for the diagnostic study, the available technology being capable of producing very high energies (up to 300J) in short pulses (300ps). Iodine laser pulses frequency doubled with up to 70% conversion efficiency having been secured at MPQ for some considerable time. The aim of the laser part of the study was to demonstrate 1Hz operation of an iodine laser system. 1Hz operation of an oscillator single amplifier system was achieved with a modest 90mJ/pulse input for 10-15 pulses; the energy output being constant

with the predicted performance of a single amplifier system. Good beam quality and stability were also demonstrated and 40mJ was achieved after frequency doubling, giving close to the 50% design conversion efficiency. Full life tests of the highly stressed flash tubes of such a laser showed that - 20,000 pulses could be achieved without failure. Satisfactory detector sensitivity, rise time and grating rejection were also demonstrated experimentally, both in laboratory experiments and in a stray light test with full scale optics.

Simulation code predictions of the expected performance of the system with input parabolic profiles of $n_e(r)$ and $T_e(r)$ indicated that measurement accuracies of better than 10% could be expected over the 0.5 - 15.0keV temperature range for central densities of $1 \times 10^{19} m^{-3}$, and that a spatial resolution of $\sim 13\text{cm}$ should be achievable.

Subsequently, attention has been centred on the engineering aspects of the diagnostic. Serious consideration has been given to the possibility of utilising the collection optics of the existing Single Point Thomson Scattering (KE1) for both the input and collection system for the LIDAR diagnostic (see Fig. 100). This looks feasible and furthermore, should be compatible with normal operation of the KE1 system. This scheme has now been adopted as the preferred approach for the LIDAR diagnostic.

Microwave Density Reflectometer (KG3)

(A.E. Hubbard*, A.E. Costley and C.W. Gowers)

*Imperial College of Science and Technology, University of London, UK.

Encouraged by the recent success of a microwave reflectometer on TFR, a simple prototype device was constructed to assess the feasibility of building a full system for JET.

In microwave reflectometry, electromagnetic radiation at frequency f_0 is launched at the plasma along the density gradient usually in the ordinary mode ($k//B$). The radiation is reflected at the critical density layer where f_0 equals the local value of the plasma frequency. The reflected beam is combined with a reference beam, and movements of the density layer can be determined by counting interference fringes. Different density layers can be probed by using different microwave frequencies, and under some circumstances the spatial profile of the electron density can be determined. An important point is that the density information obtained in the measurement is localised to the region of the critical density layer, rather than being distributed along the line of sight as in transmission interferometry.

In the prototype device, the source was a 100mW Gunn oscillator manually tunable in the range 29-38GHz (Fig. 103). Density layers in the range $1.0-1.8 \times 10^{19} m^{-3}$ could therefore be followed by selecting different frequencies between plasma pulses. The radiation from the source was transmitted to the scan system (KK1), and the reflected radiation was returned along the same waveguide channel. The reference beam was formed by the combination of radiation partially reflected at the

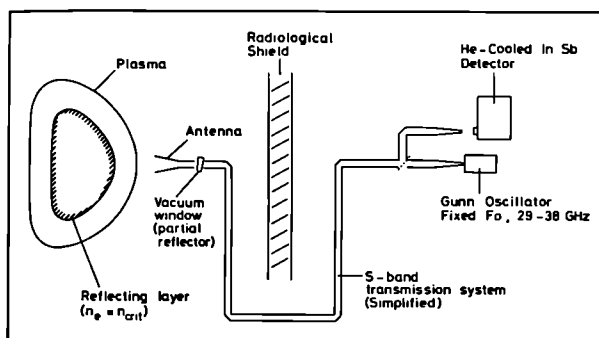


Fig.103: Schematic layout of prototype reflectometer system

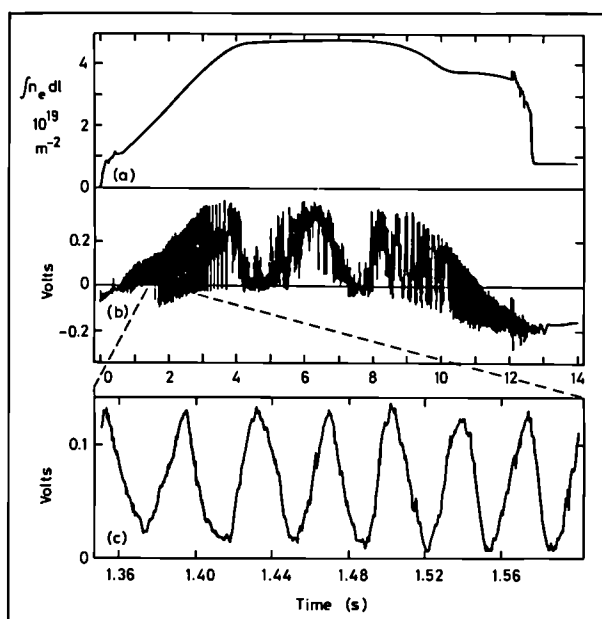


Fig.104: (a) Line density as a function of time derived from the reflectometer signals in (b). (c) shows the typical resolution obtained on an expanded time scale

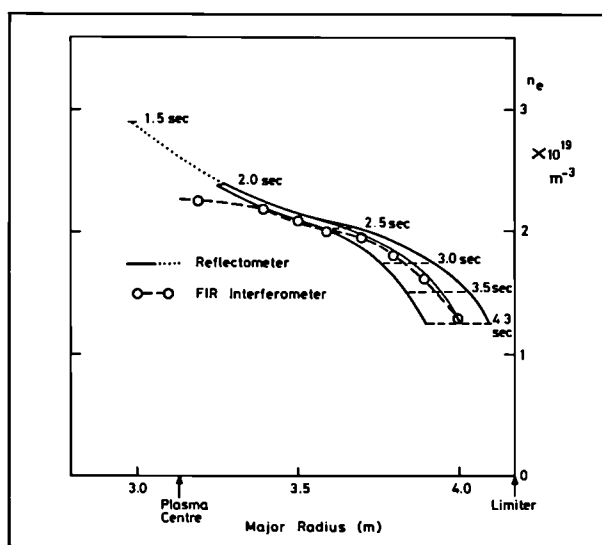


Fig.105: Derived density profile from the prototype microwave reflectometer compared with that obtained from the Far Infrared (FIR) Interferometer

vacuum window and other components in the system. The output of the reflectometer was detected with a sensitive liquid helium cooled indium antimonide detector and the signal/noise ratio was typically 50:1.

The reflectometer was used to measure the movement of the critical density layer during the density rise and decay phases of the plasma. A procedure was developed to obtain the spatial distribution of the electron density from the measurements under the assumption that the shape of electron density profile remained the same during the measurement period (typically $t=2-4s$). This latter assumption was checked by comparison with the time dependence of the on-axis density obtained from Thomson Scattering System (KE1). In the analysis procedure, it was necessary to know the position and movement of the bulk plasma and this was obtained from the Magnetics diagnostics. An example of the output from the reflectometer is shown in Fig.104 and a derived profile is shown in Fig.105.

During the equilibrium phase of the plasma, it is not possible to obtain the density profile with this simple fixed frequency device. However, it is possible to measure the movement of the critical density layer due to MHD and sawteeth activity and many such measurements have been made. At present experiments are in progress to determine a configuration of the reflectometer which will permit measurements of both the spatial density profile during the equilibrium phase, and measurements of rapid fluctuations. Attention is being focused on the edge region of the plasma which the reflectometer is well suited to study.

Plasma Boundary Physics Group

Magnetic Diagnostics

(L. de Kock, G. Tonetti, A. Stevens, D.C. Robinson*, A.W. Morris*, T. Todd*, P.S. Haynes*, M. O'Brien*, A. Pochelon+, P.A. Duperrex+, R. Keller+, Ch. Hollenstein+)

*EURATOM-UKAEA Association, Culham Laboratory, U.K.

+EURATOM-Suisse Association, CRPP, Lausanne, Switzerland.

The magnetic diagnostic system consists of a set of 18 poloidal field pick-up coils and 14 saddle or differential flux loops on each octant (see Fig.106). There are also 8 full flux (voltage) loops, special saddle loops for the feedback control, Rogowski coils and a diamagnetic loop. The system was described in detail in the 1983 JET Progress Report (EUR-JET-PR1).

This diagnostic produces 128 signals for immediate display and analysis by means of numerical interpretation codes (described in the Theory Division section of this Report). In addition, there are also a number of channels with a high sampling rate to record specific events such as disruptions or MHD activity.

The system has operated so far with 100% reliability. This performance was possible because of the redundancy of the data set. To identify quickly any faulty

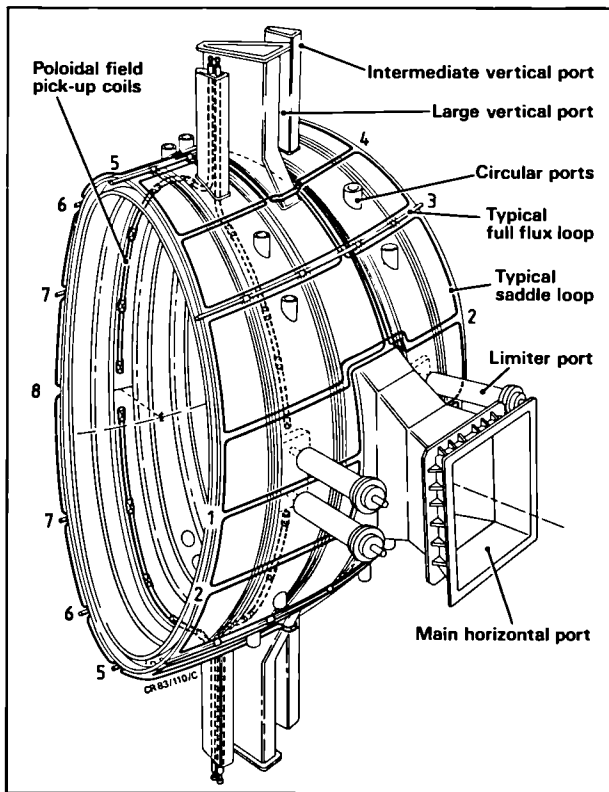


Fig.106: Typical vacuum vessel octant with the standard set of 18 poloidal field pick-up coils. 14 saddle loops and the positions of the 8 full (voltage) loops

signals, a checking programme has been developed based on the redundancy and consistency of the data set, which is run after each shot. In the near future, the validation of the magnetic data will be automatically provided by this programme.

The diamagnetic loop system based on a loop attached to the toroidal field coil has been completed. This new

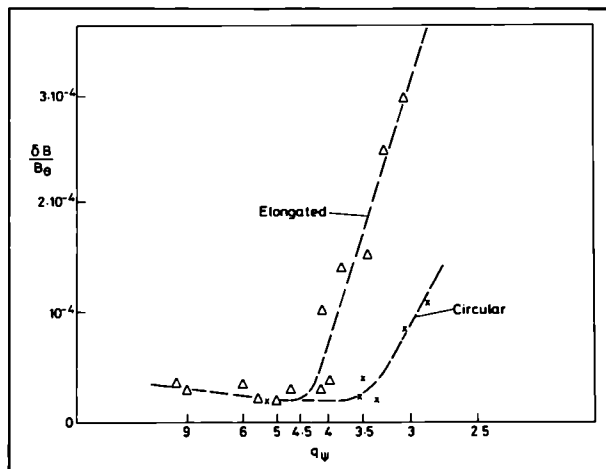


Fig.107: Relative amplitude of magnetic fluctuations $\delta B/B_0$ during the flat top of discharges on JET. The level is normalised to the equilibrium poloidal field and the variation with q and elongation is indicated

diagnostic will give the energy content and the confinement time of the plasma which are presently obtained from equilibrium codes. The preliminary results indicate that β_p values as low as 0.1 can be measured with 10% accuracy. The diamagnetic loop system will become operational in the spring of 1985.

Further studies on instabilities and disruptions on JET have been made, using the poloidal field coils and saddle loops, with data recorded on channels with high sampling rate. It is found that the fluctuation level at moderate to high values of the safety factor (q) is very low, with $\delta B/B_0$ at the wall as low as 3×10^{-5} during the flat top. This varies with q and the shape of the cross-section, as shown in Fig.107. The confinement is not degraded until the amplitude exceeds the 10^{-3} level, when the q is also low.

Under certain circumstances, sawtooth instability is accompanied by slow modulations of the magnetic oscillation level, corresponding to changes in the current profile at $q=2$. Short duration prompt signatures of the sawtooth disruption are also seen on the poloidal field coils. This takes the form of a fast magnetic pulse, lasting typically 1ms and having a toroidal mode number $n=1$ and a $2 < m < 5$ evolutive mode structure. This mode has been called the Gong-mode, due to its apparently global nature and due to the wave character which it exhibits. Effectively, there is no measurable delay between the start of the internal disruption, as measured by the ECE electron temperature on axis, and the strong magnetic pulse b_0 measured at the plasma edge, as shown in Fig.108. Exact correlation has been obtained by using channels in one single ADC.

Initially, the pulse occurs predominantly at the outside equatorial position, then progressively 'invades' the other poloidal angles. Often, this oscillation has no connection with the usual island-type Mirnov activity, which has a recognisable signature but longer periods of coherent low m activity can be promptly triggered by the

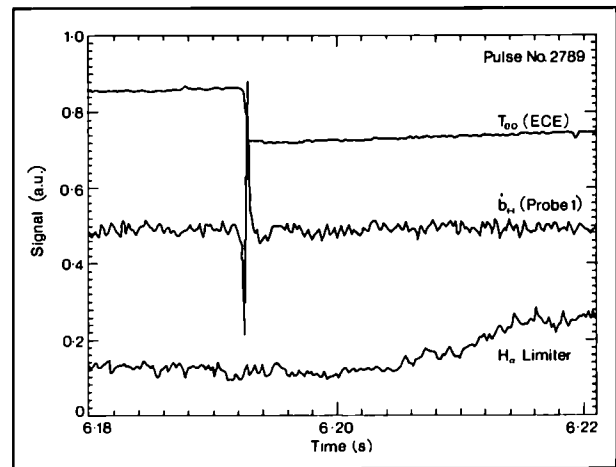


Fig.108: The 'Gong-mode' exhibited by the b_0 signal at the time of the internal disruption, shown together with the central electron temperature (ECE) and the limiter H_α -light (Pulse No.2789)

internal disruption. The helicity of the deformation is found to have the same sign as that of the field lines. The mode structure strongly ‘remembers’ the $n=1$, $m=1$ helical structure of the $q=1$ surface from where the motion originates, with the subsequent evolution to high m numbers resulting from mode coupling due to toroidal and non-circular shape effects.

Extended investigations of major disruptions show, in many cases, the presence of $n=2$ oscillations at twice the frequency of the $n=1$ component. This is consistent with toroidal motion of the instability. These have been identified as $m=3$, $n=2$. The magnetic islands associated with the $m=2$, $n=1$ and $m=3$, $n=2$ modes are estimated to cover a significant fraction of the plasma cross-section, and mutual interaction may occur, leading to enhanced transport in the period before disruption when the rotation ceases. The two signals are phase locked and there is evidence of non-linear coupling (see Fig.109). The relative phases are those expected from theoretical considerations.

There is evolution of the modes during the period when the instability is stationary, the amplitude increases and the poloidal variation changes from primarily $m=2$ to $m=3$. The disruption itself appears to be associated with

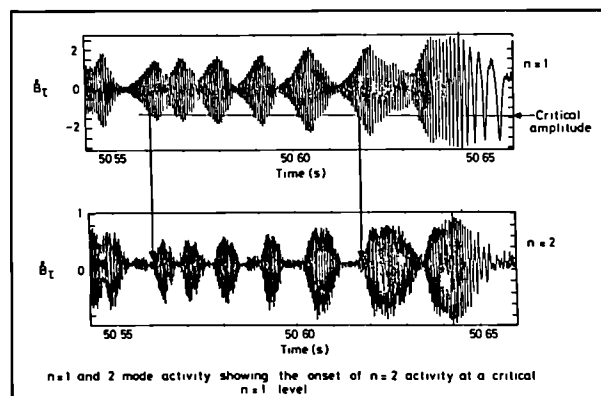


Fig.109: Coupled $n=1$, $n=2$ modes before disruption

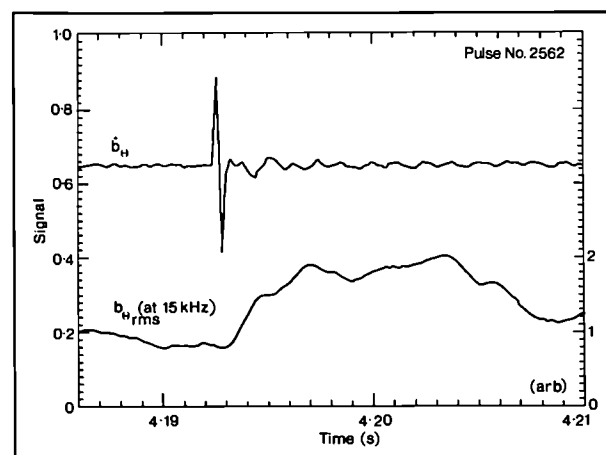


Fig.110: The pulse of magnetic broadband activity at the time of the internal disruption, the time being given by the occurrence of the ‘Gong-mode’ (Pulse No.2562)

a much faster instability with $m \sim 2$, $n \sim 1$. Bolometer measurements show a radiating layer approaching the $q=2$ surface, and the low temperature there leads to a very short local resistive diffusion time.

A continuing search for the effects of toroidicity and shaping on the structure of the tearing nodes on JET suggests that coupled perturbations at several rational q surfaces are involved, as predicted theoretically. A study of the magnetic broadband activity has been started. In other experiments, the level of magnetic broadband turbulence has been shown to be strongly related to electron confinement time both in ohmic discharges [4] and in neutral beam-injected discharges [5,6].

The magnetic broadband activity of JET has been measured, through an isolation transformer, by a quasi-equatorial poloidal field pick-up coil located behind the limiters. The b_0 spectrum, measured between 10 and 60kHz shows a f^n (where $n = -2 \pm 0.5$) frequency dependence, with typical levels of a few $10^{-8} \text{T/Hz}^{1/2}$ at 10kHz. To determine whether a relation between magnetic broadband activity and confinement also exists in JET, correlation measurements have been carried out around the internal disruption.

After each internal disruption, the magnetic broadband activity (at 15kHz) exhibits a periodic enhancement of more than a factor 3 in low q discharges, with a sharp rise less than 0.5ms after the internal disruption (see Fig.110). This increased activity is measured at the edge at a time before the heat pulse has reached the edge (as measured by the periodic H_α -light enhancements). Therefore, it is concluded that confinement and magnetic broadband activity are oppositely related, and on time scales that may indicate a wave rather than a diffusive propagation. These investigations will be continued.

Plasma Boundary Diagnostics

(L. de Kock, J.P. Coad, G. Tonetti, P. Stangeby, T. Tagle, D. Summers, A. Stevens, J. Vince, C. Nicholson, C. Lowry, G.M. McCracken*, S.K. Erements*, D. Goodall*, G. Matthew*, W. Dearing, R. Behrisch+, J. Ehrenberg+, M. Braun^o, B. Emmoth^o)

*EURATOM-UKAEA Association, Culham Laboratory U.K.

+EURATOM-IPP Association, Garching F.R.G.

^oResearch Institute of Physics, Stockholm, Sweden.

Investigations of plasma boundary phenomena have been successfully conducted during the operational period, February - October, 1984. Measurements were taken by means of multiple element Langmuir/heat flux probes yielding plasma parameters of the scrape-off layer. Surface concentrations of impurities on the carbon limiters were obtained from extensive surface analysis of the limiter tiles after removal in December 1983 and October 1984, and a good impression of the condition of the vessel wall has been obtained from the surface analysis of 100 carbon and metal samples attached to the wall. Clean carbon samples were exposed to Glow Discharge Cleaning (GDC), Pulse Discharge Cleaning

(PDC) and standard tokamak discharges, giving insight into the release of impurities from the wall and their redeposition.

Detailed measurements on the emission from the limiter, observed by means of CCD cameras, have shown that earlier temperature measurements were more due to line emission of hydrocarbons rather than to thermal emission. From these measurements, a consistent picture emerges, which, due to the scarcity of measurements, must be treated as provisional and must be confirmed by further work.

The Measurements of the Langmuir/Heat flux probes

(i) Description of the Probe Array

The Langmuir/heat flux probe array was inserted through the top vertical port of Octant No. 1D, as shown in Fig.111. The penetration can be varied from shot to shot, utilising the motorised probe bellows drive unit. The position of the last closed flux surface (shown in Fig.111 for a plasma of moderate ellipticity) is provided by the interpretation of the magnetic data (FAST) and is available immediately after the shot. Fig.112 shows the distance from the measuring element to the position of last closed flux surface (ranging from 50mm up to 300mm) as a function of time in the pulse, for a number of different pulses.

The probe consists of four carbon coated Langmuir/Heat flux elements, three facing the ion direction, separated radially 40mm, and one facing the electron drift direction. This arrangement allows radial information to be obtained at any time during a discharge, and due to movement of the plasma edge during the current flat top, parameters may be plotted as a function of plasma-probe separation. A schematic of one of the four probe elements is shown in Fig.113(a). Each consists of an electrically and thermally isolated tungsten plate (50mm²), to which is attached a single wire for current measurement, and a chromel-alumel thermocouple for deposited power measurement. The elements are operated as single Langmuir probes, the voltage being swept between -100 and +10V every 50ms throughout the discharge. Data is collected at 1s intervals. Electron temperature is measured from the slope of the exponentially rising current around the floating potential (V_f at $I=0$), and density is calculated from the ion saturation current at large negative probe potentials, together with T_e , (see Fig.113(b)).

(ii) Measurements of n_e , T_e

Results have been obtained from a variety of different types of discharge, including high current, high density plasmas ($B_T=3.4T$, $I_p=3.7MA$, $\int n_e dl=9 \times 10^{19} m^{-2}$), and reference plasmas ($B_T=2.5T$, $I_p=2.8MA$, $\int n_e dl=6 \times 10^{19} m^{-2}$). Measurements of deposited power at the same time and place as ion saturation current and T_e gives information on the ion temperature T_i . It was found that data was consistent with $T_i=T_e$. Hence, densities could be calculated from the Langmuir data by making this assumption. Fluctuations in edge density

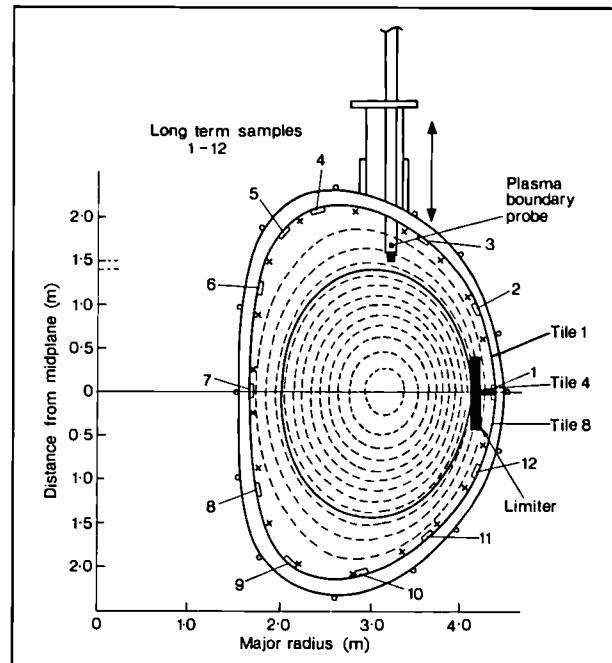


Fig.111: The Langmuir/heat flux probe array showing its insertion position through the top port

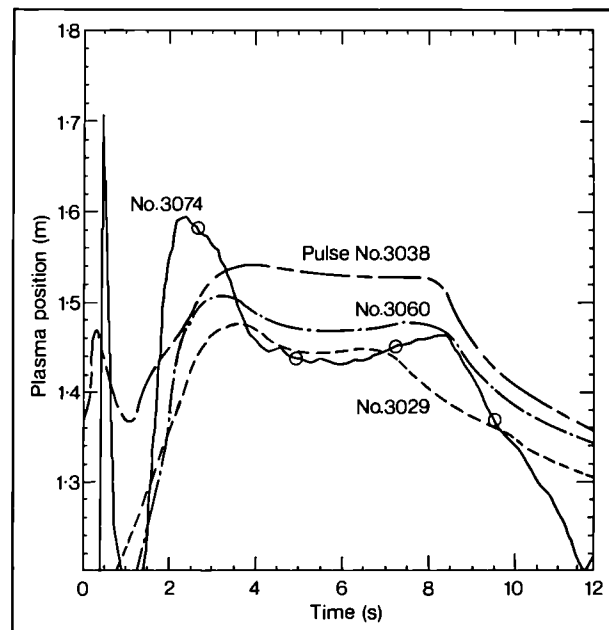


Fig.112: Distance from the measuring element to the last closed flux surface as a function of time in the pulse for Pulse Nos.3029, 3038, 3060 and 3074

between one discharge and the next in a series of constant line average density discharges, at a given plasma-probe separation, were seldom greater than a factor x2 (see Fig.114(a)). Data from one probe element to the next was also consistent, suggesting that the probe has little disturbing effect on the plasma. Densities decreased exponentially with an e-folding length of 40mm, between 50 and 300mm from the plasma edge. Local densities were higher for higher line average density discharges. 50mm from the plasma edge, densities reached

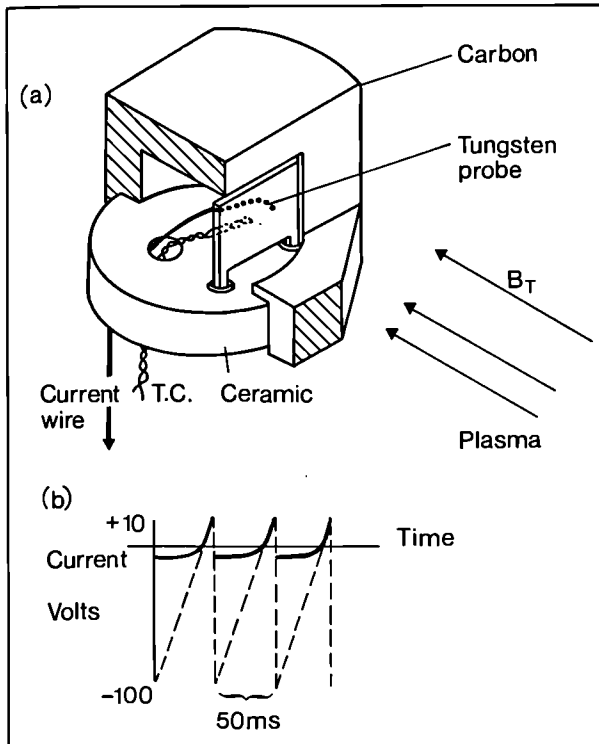


Fig. 113: (a) Schematic view of the Langmuir/heat flux probe; (b) Variation of voltage and current on the Langmuir probe with time

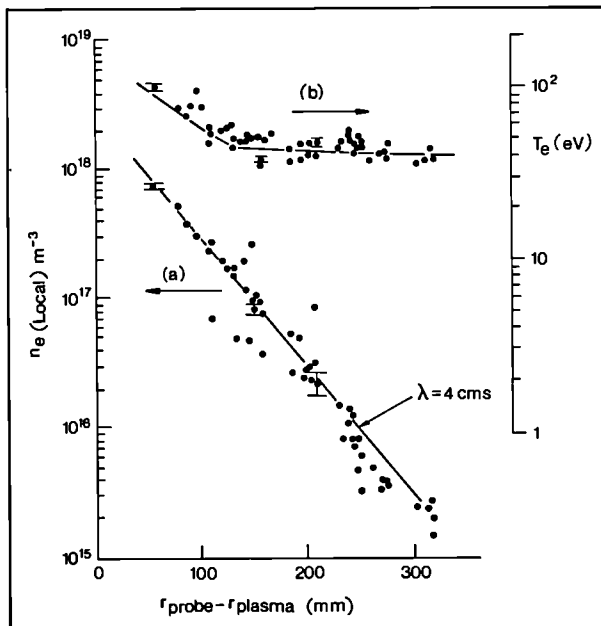


Fig. 114: (a) Local electron density as a function of plasma-probe separation; and (b) corresponding local electron temperature

$1 \times 10^{18} \text{m}^{-3}$. The electron temperature profile was found to be flat ($10-8 \text{eV} > 100 \text{mm}$ from the plasma edge) rising rapidly to 15eV between 100 and 50mm . An example of these measurements is shown in Fig. 114(b).

Deposited powers to the probe elements again decreased exponentially with an e-folding length of

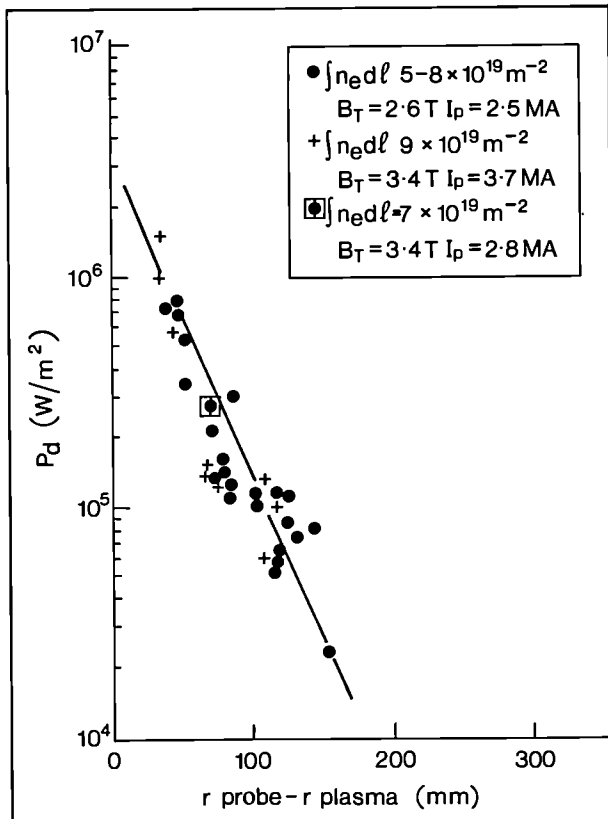


Fig. 115: Deposited power data for a variety of discharge conditions

30mm between $40-150 \text{mm}$ from the plasma edge. To within a factor $\times 2$, deposited power to the probe was independent of the discharge conditions. A maximum deposited power of 100Wcm^{-2} was recorded 40mm from the plasma edge. Deposited power data for a variety of discharge conditions is presented in Fig. 115. Due to uncertainty in the position of the plasma edge, it is difficult to extrapolate to the edge of the limiter scrape-off. Such extrapolation is discussed in the next section together with comparisons from other diagnostics. To obtain data up to and just inside the limiter scrape-off, a fifth robust Langmuir element has been mounted on the nose of the probe for future measurements.

(iii) Interpretation of the Langmuir probe data

Probe data was only obtained at a single poloidal/toroidal location and for radial positions from 50mm outward, beyond the last closed flux surface. Complete scrape-off profiles of $n_e(r)$ and $T_e(r)$ at the outer mid-plane (i.e. the limiter position) were constructed by combining data from the probe, the limiter viewing camera and the H_α limiter light. Combining data from the last two diagnostics gave the energy deposited per ion pair at the leading edge of the limiter, as shown in Fig. 116. This can be interpreted as a leading edge temperature, T_0 , and density, n_0 , provided the sheath energy transmission coefficient δ_s is known. From the ratio of heat/particle flux to the probe, δ_s was estimated to be ~ 15 at the

leading edge, indicating values of T_0 of 50-200 eV, depending on the value of n_e .

To combine this data with that of the probe, account must be taken of the radial compression of magnetic field lines between the probe and limiter (compare Fig. 113). For typical discharge parameters, this indicates that scale

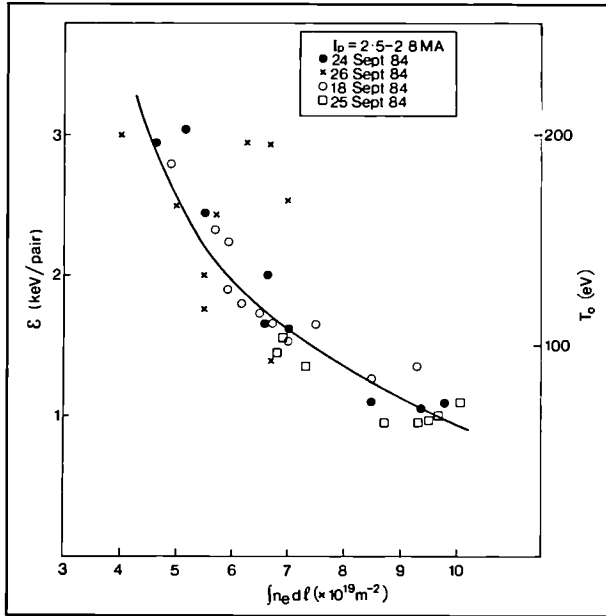


Fig. 116: Energy deposited per ion pair as a function of line averaged density ($\int n_e dl$), and its interpretation as an edge temperature (T_e)

lengths (e.g. scrape-off lengths) are ~ 2.1 times longer at the probe than at the limiter. There is no compensating increase in density since the cross-sectional area of a magnetic flux bundle is approximately unchanged from the probe to the limiter, only the shape varying. This space transformation has been used in combining the data shown in Fig. 117. The scrape-off lengths in the near-edge region, $0 < r < 3$ cm, were taken from the limiter camera power scrape-off length of 1.0 cm, and the probe particle flux scrape-off length (projected to the limiter position) of 1.4 cm.

Construction of $n_e(r)$ and $T_e(r)$ profiles by this technique is no substitute for actual probe measurements over the entire radial range, an undertaking planned for early 1985. Confidence in the validity of results such as in Fig. 117 cannot be high, due to uncertainties in δ_s ; in the location of magnetic flux surfaces (uncertain to ~ 4 cm); in the parallel field gradients between probe and limiter; and the limiter connection lengths. For the latter case, simple considerations indicate two types of flux tube: those with short direct connection, $L = \pi R q \approx 50$ cm, and those with much greater lengths. It might be anticipated that the probe would see these different lengths as q varied. However, the probe data, showed little variation with q , possibly indicating that the different flux lengths are averaged by some smoothing process, such as poloidal crossfield transport. This is the object of further study. Provided the probe diameter, d , satisfies the relationship $d < (LD_1/c_s)^{1/2}$, the probe should be 'small' (i.e. non-disturbing to the scrape-off layer

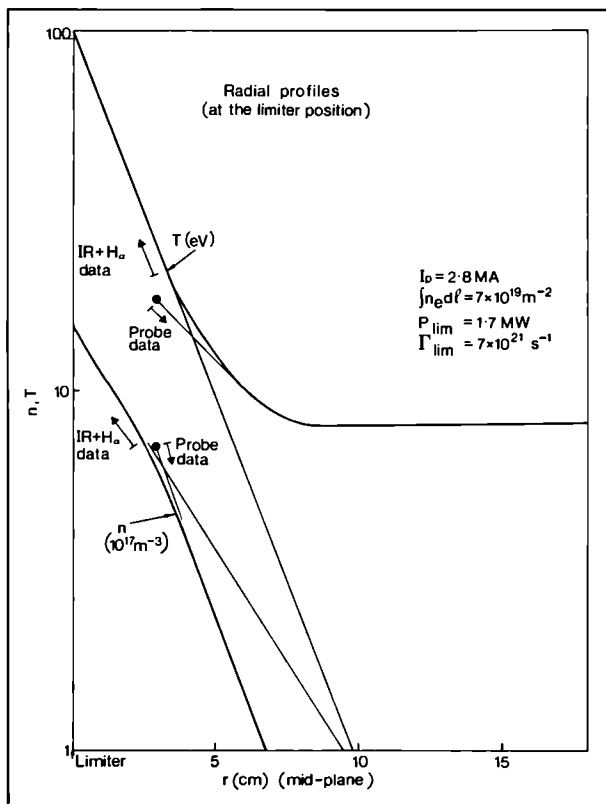


Fig. 117: Constructed density $n_e(r)$ and temperature $T_e(r)$ profiles close to the limiter

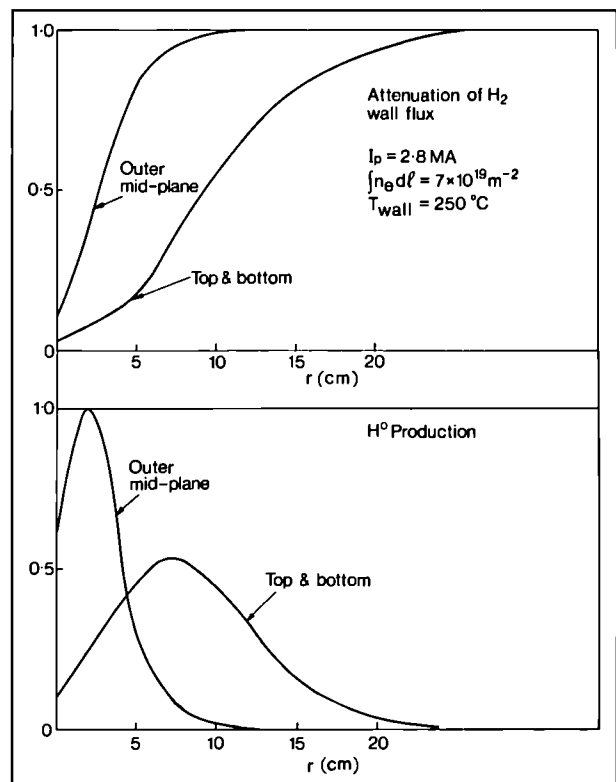


Fig. 118: Attenuation of hydrogen entering the plasma from the walls

plasma it is measuring). This relation is satisfied and the experimental results confirm that the probe is non-disturbing: (a) the measured fluxes are the same on the forward and backward facing sensors located at the same distance from the probe tip; (b) the three sensors at different distances from the probe tip measured the same fluxes when located at the same distance from the plasma edge.

The $n_e(r)$ and $T_e(r)$ profiles were used to calculate the attenuation of H_2 entering the plasma from the walls (see Fig.118). As can be seen, penetration is considerably greater at the outer mid-plane, where the edge integrated line density is smaller than at the top or bottom of the torus.

The attenuation of wall-generated impurities indicates a similar trend, shown in Fig.119. Such profiles have been used, together with a simple model relating impurity ion density in the main plasma to impurity neutral influx, to estimate the effectiveness of the scrape-off layer for impurity screening. It was found that the wall-generated impurities are effectively screened and the principal contribution to the ion impurity density in the core is from the less-effectively screened limiter impurities. Carbon densities are calculated in this way to be 2-4% of n_e , which is in accord with spectroscopic observations.

Surface Analysis of Limiter Tiles and other Collector Probes

(i) Limiter Tiles

Metal fluxes from the carbon limiter have been observed spectroscopically during tokamak discharges. To measure the source of this contamination, two tiles (4.1 and 4.4, see Fig. 120) were removed from the limiter for surface analysis during the December 1983 shutdown. Two further tiles, from the same positions, were removed during the September 1984 shutdown.

Various surface analysis techniques have been used, such as Auger Electron Spectroscopy (AES), Rutherford Backscattering Spectroscopy (RBS), Proton-Induced X-ray Emission analysis (PIXE) and Nuclear Reaction Analysis (NRA). NRA was used to detect trapped deuterium, which was used as the working gas in JET for some tokamak discharges and glow discharge cleaning runs. The distribution of the most abundant elements found on carbon tile 4.4, after exposure to the plasma during 1984 is shown in Fig.121. Besides the elements indicated, oxygen, potassium and calcium have also been found with concentrations of about 10^{20} atoms/m², 10^{18} atoms/m², and 10^{18} atoms/m², respectively. Other elements such as sulphur and chlorine were detected in trace quantities. In addition, an unidentified high mass element ($M \approx 200$) was detected (5×10^{17} atoms/m²).

The origin of most of the elements could be readily identified. Ti, Cr, Fe and Ni have been found in the correct ratios for Inconel 600 and therefore were from the vessel wall. K, Ca and S are trace elements in carbon or impurities in Inconel. Cl is a trace element of carbon but is also present in the detergent used for washing the

vessel walls. The origin of O is difficult to assess because of possible oxidation processes during the exposure of the tiles to air. Mo was found to have been deposited on the limiter during a preliminary bakeout before installation in JET. On the 1984 limiter tile, a reduction of Mo was observed, up to a factor of 10 lower than found on the 4.4 tile after the shutdown in December 1983, probably due to the large number of discharges in 1984 at

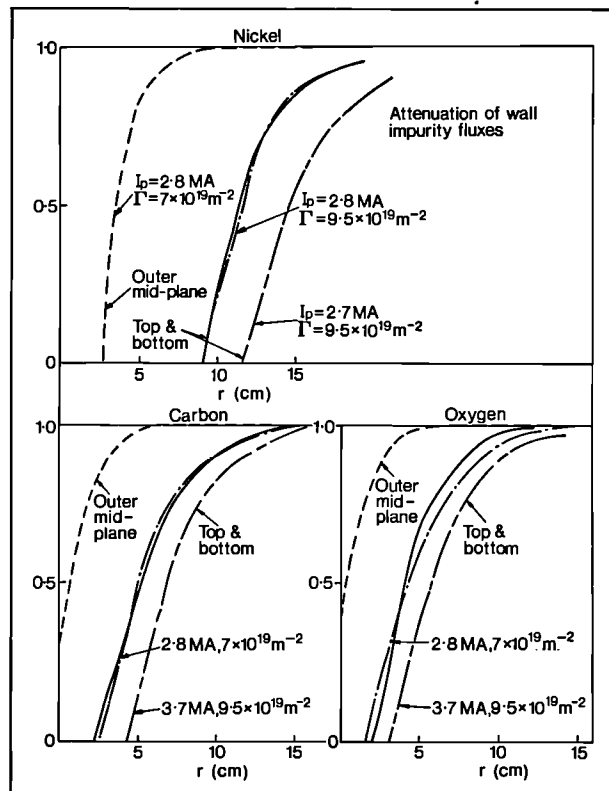


Fig.119: Attenuation of wall generated impurities: (a) Nickel; (b) Carbon; (c) Oxygen

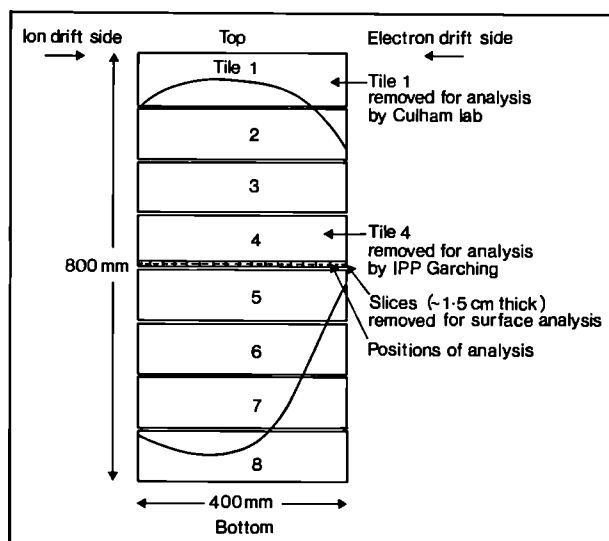


Fig.120: Carbon Limiter Octant No. 4: View from plasma

higher power. The profiles of the contaminants (Fig. 121) can be separated into two regions: the edge region below 80mm and above 400mm where lower particle fluxes are received, and a central region between 80 and 400mm where higher fluxes are incident.

The central region has low concentrations of metals compared to the edge regions. This general pattern was observed on the tiles removed in December 1983 and in October 1984. The depletion in the centre may be due partially to the glancing angle of incidence of the field lines leading both to lower incident fluxes per unit area and higher sputtering yields. The limiter tiles removed in October 1984 had lower central metal concentrations. They had been heated to high temperature ($\sim 1500\text{C}$) during tokamak operation, which would cause both evaporation of the metal from the surface and diffusion into the bulk. Both evaporation of Cr, as well as the greater depth of penetration, are observed experimentally. The edge concentration on all limiter tiles was similar. The deuterium profile (in Fig. 121) is very similar to the temperature profile measured by the limiter viewing camera: the regions which have reached higher temperatures have a lower deuterium concentration due to thermal desorption. From the separation of the minima, the thickness of the scrape-off layer was determined giving a value of 11-12mm, in good agreement with the result from the limiter viewing system ($10\text{mm} \pm 10\%$). The high deuterium content at the limiter edges can only be understood by assuming a codeposition process with carbon, building up layers of deuterium-saturated carbon.

(ii) Long Term Samples

The knowledge of erosion and redeposition processes of wall material in JET during tokamak discharges and glow discharge cleaning runs gives information about the sources for impurity fluxes into the plasma. To study this, Long Term Samples (LTS) made out of graphite, Inconel 600 and nickel have been attached to the vessel wall before the experimental period start-up in March 1984, and taken out after shutdown in September 1984. Each octant was provided with a poloidal set of samples as shown in Fig. 111. Analysis of the samples was performed by the same methods as described earlier. Fig. 122 shows the results of the deposition of the main Inconel components on the carbon samples. In general, the poloidal concentration variation within one octant is much larger than the toroidal differences. The ratios of the amounts of the elements are the same as in Inconel 600, with the exception of position 1 in Octants Nos. 2, 4, 6, and 8, where an enrichment of nickel is observed. Samples at these positions have been close to the retracted nickel limiter indicating material transport from them to the nearby wall. The inner wall of JET (position 7) where the largest deposition on the samples has been found, also showed the largest damage (melting), probably caused by plasma disruptions and runaway electrons. Arcing has been observed on the wall and is most severe at the top and bottom of the torus

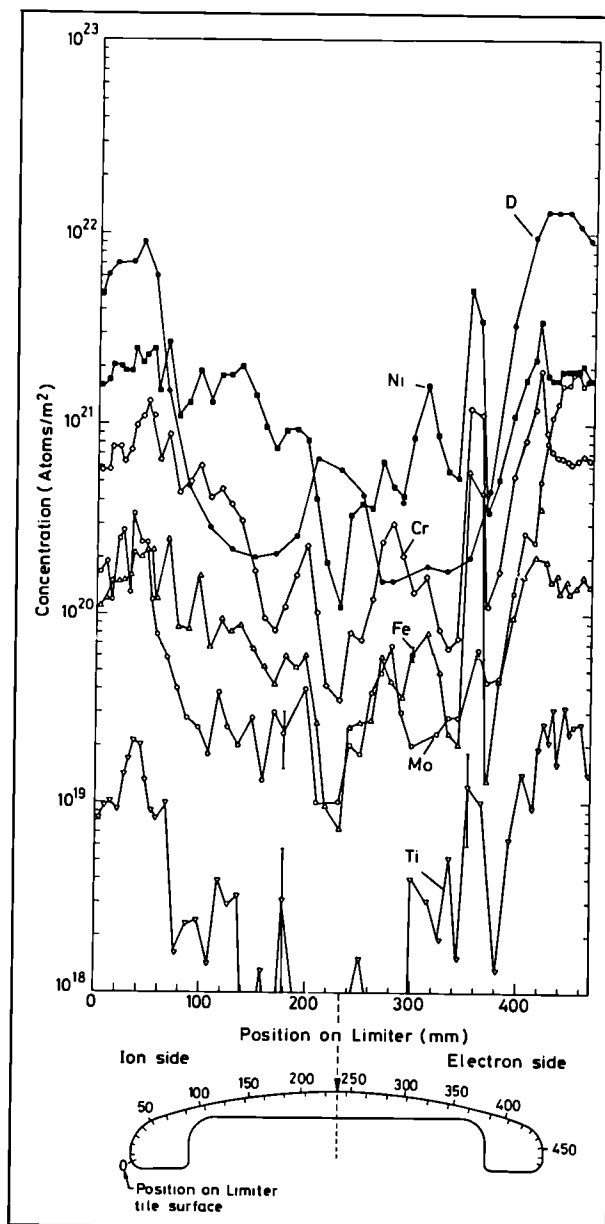


Fig. 121: Limiter tile contamination surface analysis

(positions 4 and 10). Apart from Cr, Fe and Ni, O, K, Ca, Ti and Mo have also been detected with the first five elements in amounts similar to those found on the limiter. However, molybdenum had, a considerably lower concentration (maximum $\sim 10^{19}$ atoms/m²) with the largest value at position 1, the outer vessel wall, near the limiter, and much smaller amounts everywhere else. This is qualitatively in agreement with the observation of the nickel enrichment near the nickel limiter, and the maximum Inconel deposition on the inner wall. In all cases, the location of redeposition is close to the poloidal position of the impurity sources.

(iii) Other Collector Probe Measurements

The contamination of the limiters described could be due to a number of different processes, such as:

- Glow Discharge Cleaning (GDC);
- Pulse Discharge Cleaning (PDC);

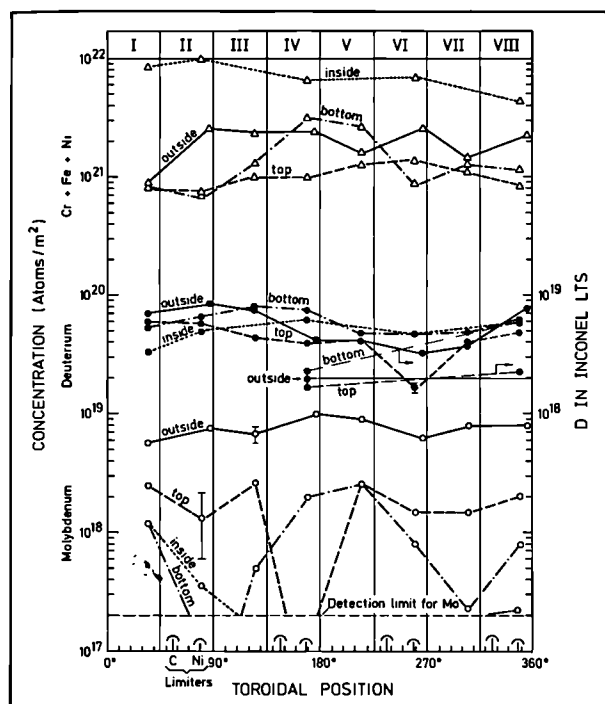


Fig. 122: Deposition of main Inconel components on the carbon samples as a function of poloidal position

- Charge exchange neutral sputtering of the wall;
- Arcing at the wall at the start or end of a discharge;
- Evaporation due to runaway electrons, damage or disruptions at the wall.

Some preliminary experiments with surface collector probes have been attempted to try to assess the effects of GDC and PDC. The probes were carbon, inserted into the torus through a vertical port on Octant No. 1D using the Langmuir probe drive system. The first sample was exposed for 70 hours under GDC at 2A and the second sample to 2800 pulses of low current PDC (50kA, 250ms) and 30 pulses of 250kA discharge cleaning for 600ms. Standard GDC conditions use up to 8-10A current for periods of 5-100 hours. PDC conditions should be compared with a total of 11,800 pulses used during June/July 1984. After exposure, the samples were analysed using Rutherford Backscattering Spectroscopy.

Further samples from the carbon housing of the Langmuir probe array were exposed to 60 standard tokamak discharges (2.5MA-3.5MA) and then subsequently analysed. The results are summarised in Table XIII:

The exposures used for the different samples are not strictly comparable except that they are typical of the time used to give a fairly extensive cleaning. It is clear that the PDC deposits nearly an order of magnitude more metal on the probe than the GDC. However, the tokamak discharges have deposited nearly an order of magnitude higher still. A possible interpretation is that the tokamak discharges themselves contaminate the limiter. However, another possibility is that during these shots metal from the limiters (which had been contaminated

TABLE XIII

COMPARISON OF IMPURITY DEPOSITION
IN DISCHARGE CLEANING
AND TOKAMAK PLASMAS
(Units: 10^{20} atoms m^{-2})

Impurity	G.D.C.	P.D.C.	Tokamak	Limiter Impurities
O	1	3	-	5
Ni	0.25	2	10	30
Cr	0.15	0.8	5	
Mo	0.02	0.0	-	30

Exposure Time	70 Hours at 2A	2800 Pulses at 50kA	60 Pulses at 2-3.5MA	July-Dec.'83
		30 Pulses at 250kA		

before the clean probe was exposed) was removed and deposited on the probe. The results are therefore still inconclusive on this point, but they do show that GDC, under the conditions used, contributes less contamination than PDC.

(iv) Preliminary Interpretation of the Impurity Deposition Measurements

Most of the impurities identified by surface analysis are also identified by spectroscopy during discharges. They include carbon, oxygen, chlorine, calcium, chromium, iron, nickel and molybdenum. In addition, traces of sodium and silicon are observed by surface analysis. The sources of these impurities are obvious in most cases.

Sputtering and arcing are expected to be the main impurity processes. Evaporation had clearly taken place in the inner protection plates, but this was caused by runaway electrons or possibly disruptions in unstable discharges. Arcing had been observed on the top and bottom of the vessel during post-operation examination. Since the plasma density is low in these regions during normal discharges, it is likely that the arcing only occurs at the beginning or end of the discharge when the discharge moves to the wall. Therefore, the evidence is that the impurities introduced in normal discharges occur by sputtering. Measurements of the flux and temperature of the plasma at the limiter (from the Langmuir probe data) allow estimates of the impurity fluxes. Physical sputtering of the limiter by hydrogen or deuterium is insufficient to explain the impurity fluxes observed spectroscopically. However, when impurity sputtering by oxygen and carbon is included a consistent picture of the impurity fluxes can be obtained. There is no evidence of chemical sputtering as the carbon flux measured spectroscopically does not change with the limiter surface temperature. Some evidence of evaporation of chromium is observed at high limiter temperatures, but it has been unimportant during the majority of discharges.

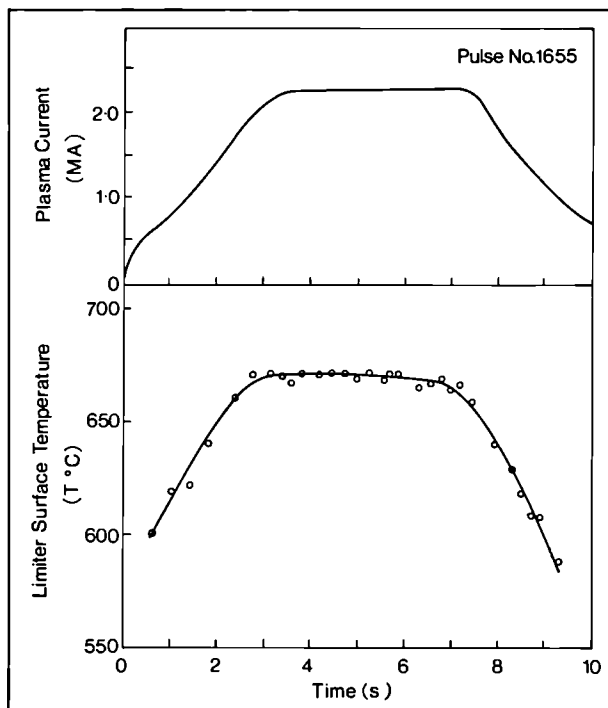


Fig. 123: Limiter surface temperature and plasma current as a function of time in the pulse (Pulse No. 1655)

The metallic impurity concentration observed in the plasma can be explained by sputtering of the metallic contamination on the limiter. Again, oxygen and carbon impurity ions play the dominant role in the total sputter yield. The results are consistent with the measured metallic concentration of $\sim 10\%$ on the surface of the carbon limiter. An attempt has been made to estimate the sputtering of the carbon and metals on the wall. However, uncertainty in the fluxes of the charge exchange neutrals at low energies have made this difficult. Calculation of the probability of ionisation of oxygen and carbon is low, and shielding is unlikely to occur in their cases.

Limiter Viewing

The surface temperature of the carbon limiter is measured using CCD television cameras fitted with infra-red filters. As these are sensitive in the visible and near infra-red wavelength regions, these devices are suitable for measurements above 600C with a dynamic range of about 300C.

Data obtained in the first half of 1984 showed the characteristic shape of the plasma/limiter interaction zones. However, the signal intensity correlated strongly with the plasma current and was independent of the thermal characteristics of the limiters (see Fig. 123). Data taken with a 700mm filter fitted showed no distinct zones of interaction and it was concluded that these images were not thermal in origin but were due to spectral emission near the limiter surface. The sensitivity threshold for thermal emission corresponds to a total power load to the limiters of 0.5MW and this value was only occasionally reached during this operating period.

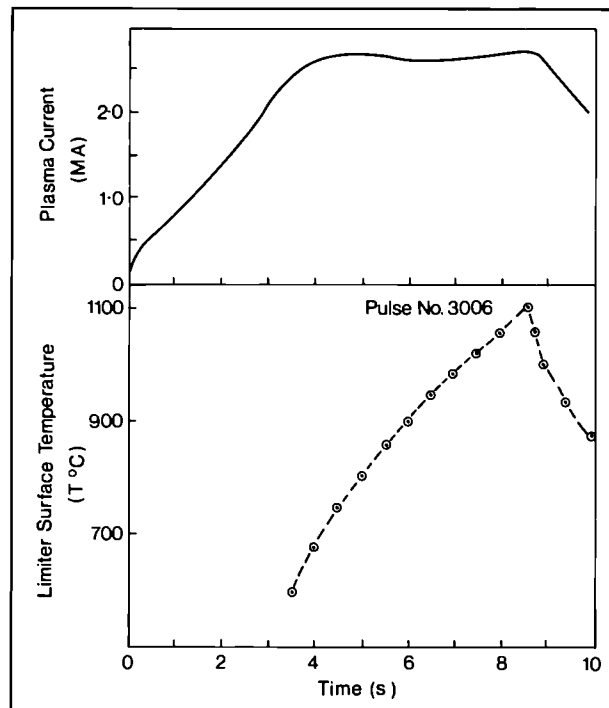


Fig. 124: Limiter surface temperature and plasma current as a function of time in the pulse (Pulse No. 3006)

Following glow discharge cleaning using a 97% H_2 +3% CH_3 mixture, considerable temperature rises were observed on the limiter surfaces, corresponding to total thermal loads of up to 2MW. The characteristic time development of these temperatures agreed closely with simple model calculations, and the limiter surfaces remained at measureable temperatures for times up to ~ 60 s after the plasma current had decayed to zero (see Fig. 124). The maximum local thermal load reached $0.7\text{kW}/\text{cm}^2$ over small areas on some occasions.

The sum of the measured values of radiated power (measured bolometrically) and the power deposited on the limiters equalled the ohmic input power for plasma pulses which did not end disruptively, e.g. Pulse No. 2882 at $t=8.0$ s.

$$P(\text{radiated}) = 1.04\text{MW} \pm 3\%;$$

$$P(\text{limiter}) = 1.4\text{MW} \pm 15\%;$$

$$\text{Ohmic Input Power} = 2.4\text{MW} \pm 10\%$$

The energy scrape-off distance, determined from the separation between heated zones on the limiter surfaces, was $10 \pm 1\text{mm}$ during the current plateau, for all conditions investigated. All four carbon limiters received similar thermal loads. Localised heating, due to runaway electron beams was observed on six occasions, none of which caused the local temperature to exceed 1200C.

Diagnostic Software Section

(C. Best, D. Wilson, K. Slavin, J.P. Jeral)

The section is responsible for interfacing diagnostics in Experimental Division 1 to the CODAS computer system. In addition, general analysis and control facilities are developed which have wider application.

The Group also serves as an advice and user service for the software developed in the Associations.

During the year, there has been considerable activity on the CODAS computers, as new diagnostics have come on-line and as solutions to their interface problems have been learned. The data acquired by diagnostics has approached 1MWord and is expected to triple next year. There has been good progress in the rapid analysis and display of this data on-line and new graphics tools have been developed. The computer control of diagnostics has developed well and more sophisticated automation is anticipated in the future.

The Section's work is described in more detail in the following three sections.

New Diagnostics and Upgrades

During the year considerable effort has been devoted to software development and design of the surface physics diagnostics. The plasma boundary probe system came into successful operation. The data acquisition and retrieval software is operational and first results were analysed on time. The control software for positioning and rotating the probes in the plasma is written and much of the control switching software is commissioned.

A review of the control requirements of the Fast Transfer System has been carried out and a system design has been made. A similar study for the Surface Analysis Station is underway. A tricky problem of bookkeeping (relating probe samples, probe history and analysed results) has been isolated. This has formed the basis of a special design of a bookkeeping system and database. The surface analysis data is particularly difficult to interface to the rest of the JET data since the sample analysis is delayed with respect to other diagnostics. A new acquisition program and data handling system is being designed. A similar system will be needed for the Neutron Activation System which also produces delayed data in the form of spectra.

The software to upgrade the 2mm interferometer to a dual 1mm/2mm system has been written and tested. The analysis and display of this system has been fully automated. The control software is being upgraded currently to complete the work on this diagnostic.

Several extensions to the Magnetic Diagnostics have been undertaken since original start-up and more are planned in the future. A new automatic data validation program has been written. This program checks the consistency of the data after correcting for the stray toroidal field components. The hardware computed signals are compared to the software computed values and checks made on flux sums, zero offsets and drift values. In this way it is hoped to detect hardware failures of the equipment on-line. An example output of the graphics display program is shown in Fig.125.

A real time control program for the Fast ECE system has been written and tested. This program starts a beam chopper at a set frequency, handles error conditions and scans amplifier settings. This is synchronized to the JET pulse and the retrieved settings and conditions are archived in the JET Pulse File (JPF).

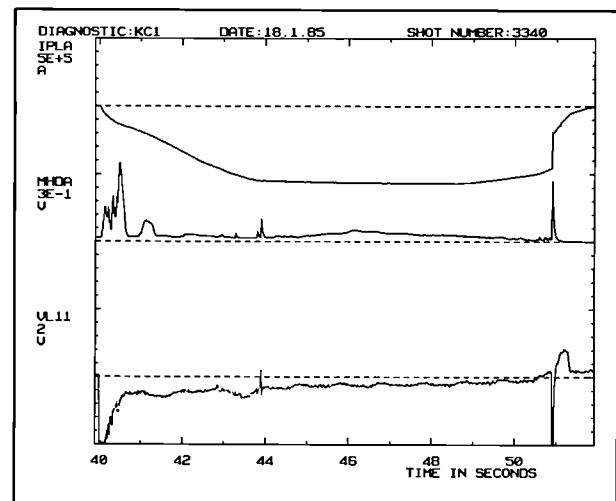


Fig.125: Example of output of Graphics display for Magnetic Diagnostics (Pulse No.3340). Upper trace: Plasma current - Scale 0.5MA per division; Middle trace: MHD Voltage loop - Scale 0.3V per division; Lower trace: Loop voltage - Scale 2V per division

General Programs

Three general purpose programs have been developed; as follows:

- GDAC provides diagnosticians with control over data acquisition parameters, allowing easy changes to data sampling rates and parameter settings. The program provides protection against faulty settings and can be used between pulses;
- HVCON provides computer control of photomultiplier high voltages. The operator can quickly change between different sets of photomultiplier gains;
- BROWSE is a general display program allowing easy graphical access to nearly all the signals from any pulse. It is designed to work on the analysis machine, providing powerful interactive graphics. It is based on GETDAT and the General Display graphics described later.

Facilities

A number of tools have been developed to simplify and streamline the programming for scientific users of the computers, and these are described below.

GETDAT is an important advance in allowing easy access to recorded signals in the database. This system provides a subroutine interface to the signals (-1000) currently stored each pulse in the JPF data base. Details are hidden from the user of decoding the data recorded in different CAMAC modules and triggered by several different timing devices. This is proving powerful in the fast development of new analysis programs.

An interactive dialogue package (TSS) has been written based on an existing CODAS package, which provides a standard user interface to programs allowing

verified numerical input. Programs using this system can be easily automated.

In collaboration with Experimental Division 2, a large effort has been devoted to the development of high level graphics tools for diagnostic data. This should ease the workload for future diagnostics and standardise graphical displays. The Group has contributed to the development of new 3-D display software unavailable in PLOTIO. This is proving popular and robust and has been incorporated in several diagnostics. An example display is shown in Fig.126. A documented library of useful routines has been produced for use by anyone writing diagnostic software. General purpose subroutines are included to help new diagnostics. The documentation forms the basis of the Diagnostic Handbook, which brings together documentation on the above facilities, program write-ups and useful tips on Diagnostic/Computer interfaces.

Neutron Diagnostics Group

(O.N. Jarvis, G. Sadler, J. Kallne, P.van Belle, M. Hone, V. Merlo, G. Gorini)

Runaway Electron Studies

The Hard X-ray Monitors are used to study the emission of Bremsstrahlung radiation from the limiters, produced by high energy runaway electrons, which can be expected in low density or disruptive discharges. The monitors are operated in current mode, and logarithmic response amplifiers have recently been installed so that both steady-state and disruptive conditions can be studied without changing the amplifier settings. In addition, the first of a group of three monitors to be operated in pulse-height mode has been installed on the North Wall of the Torus Hall to provide a means of measuring the Bremsstrahlung energy spectrum.

Some post-mortem studies of runaway electron effects have been undertaken and three interesting observations can be mentioned. The most dramatic is the significant damage to the Inconel wall protection tiles caused by runaway electrons generated in a disruption; the plasma always collapses inwards (and downwards) in a serious disruption so that the damage occurs on the lower portion of the central column. One of these disruptions struck a tile on the horizontal mid-plane, causing severe distortion to the tile. This event was correlated with the observation of a localized region of enhanced radioactivity on Octant No.7 horizontal port window, lying on a tangential line from the damaged tile. This radioactivity is interpreted as due to (γ, xn) reactions produced by the forward-peaked cone of bremsstrahlung radiation associated with high-energy electrons. Within this localized region of radioactivity, decay γ -radiation from the 6.1 day half-life nuclide $N_i \sim 56$ Ni has been observed, which is produced through a $(\gamma, 2n)$ reaction from $N_i \sim 58$ Ni having a Q-value of -22.5MeV. This provides first proof that the runaway electrons in JET are accelerated to energies of well over 20MeV.

The other two observations may be different facets of

the same phenomenon, although this cannot be demonstrated directly. During a few discharges, it was noticed that the broad illumination of a limiter due to ion bombardment [7] was briefly replaced by an intense, small area of illumination at the horizontal mid-plane; this was evidently due to runaway electron bombardment. The times at which this spot appeared were well correlated with the occurrence of mini-disruptions from which the plasma recovered, at least partially. These disruptions provided a source of runaway electrons and the persistence of the plasma current provided the confining mechanism which ensured that the electrons in the outer regions of the plasma were lost to that limiting surface which defines the size of the plasma. It has been found that this particular region of the limiter surface contains a small but detectable level of radioactivity associated with the

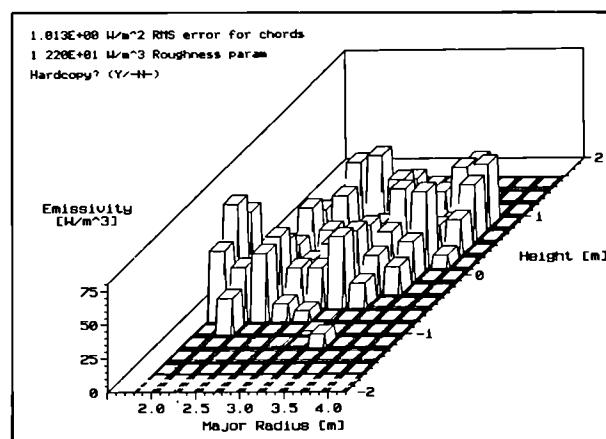


Fig.126: Example of display of emissivity (W/m^3) as a function of plasma major radius and height

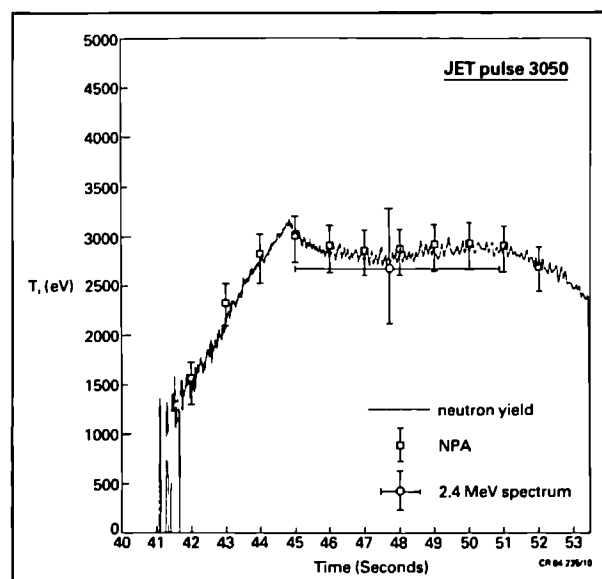


Fig.127: Ion temperature (T_i) as a function of pulse time from neutron yield, neutral particle analysis (NPA) and 2.4MeV neutron spectroscopy measurements (Pulse No.3050)

53 day half-life nuclide Be-7, produced by electron or photon-induced spallation of C-12, for which the reaction Q-value is -26.3MeV. This shows that very high energy runaway electrons also strike the limiter.

Neutron Diagnostics

The production of deuterium plasmas in JET, during August-September, provided the first opportunity to investigate the performance in the JET environment of the various neutron detectors, which will eventually be built into the neutron diagnostic system. The major installed neutron diagnostic, the Neutron Yield Monitor System, had previously been rigorously tested by intense photoneutron generation following severe plasma disruptions. The list of new detectors studies include a He-3 ionization chamber [8], a hydrogen spherical ionization chamber [9], nuclear emulsions [10] and a time-of-flight detector array [11], all destined to be used for 2.5MeV neutron spectrometry, a silicon diode [12] and a large NE213 liquid scintillator both devoted to measuring the weak 14MeV neutron flux (resulting from $d+d \rightarrow t+p$ primary reactions) in the presence of the strong 2.5MeV neutron flux.

In general, the neutron detection problems associated with the use of the neutron spectrometers in the Torus Hall and in the Roof Laboratory were investigated for orientation purposes only and none has yet been optimized nor have the results yet been fully analyzed.

Neutron Yield Monitors

The time-resolved neutron yield from low to moderate neutron yield d-d plasmas is measured with three uranium-235 fusion counters mounted on the vertical limbs of the transformer, at the level of the horizontal midplane of the torus. For high neutron yield plasmas, three uranium-238 fusion counters are also available.

The relationship between the instantaneous neutron emission from JET plasmas and the counter responses has been extensively investigated using standard radioisotope neutron sources and a 14MeV neutron tube placed at different positions within the torus. Because of the heavy vacuum chamber support shell, neutrons can escape from the torus only through the diagnostic ports and other lesser penetrations. Consequently, each fusion counter is sensitive mainly to the volume of plasma near the horizontal port closest to it. As a result of the calibration studies [13], the absolute neutron yield from a plasma can be determined to an accuracy of about $\pm 10\%$, provided the plasma is well centred spatially.

The neutron yield is used to obtain information on either the deuterium ion density n_d , or ion temperature T_i ; for d-d plasmas at 2 to 3keV ion temperature, the yield scales approximately as $n_d^2 T_i^4$. In practice, it appears that the central deuteron density is quite uncertain in JET under present operating conditions whereas the ion temperature can be inferred with some accuracy from the Neutral Particle Analyzer. Consequently, the neutron yield has been used to demonstrate that the central deuteron density is typically about 50% of the electron density. Typical neutron

emission intensities during deuterium plasma ohmic heating discharges are of $\sim 3 \times 10^{13} s^{-1}$. Sawteeth with peak-to-peak amplitudes of about 30% are usually clearly visible on the time-resolved neutron signals, but appear with reduced amplitude in the T_i traces (see Fig.127).

Neutron Spectrometry

Due to the relatively low temperatures achievable in purely ohmic heated discharges, and the corresponding low neutron yields from d-d plasmas, some initial effort was devoted to the use of the physically small neutron spectrometers, the He-3 ionization chamber [8] and the hydrogen spherical ionization chamber [9], within the Torus Hall and as close as possible to the plasma using a small (100kg) radiation shield. It was found that the electrical interference problem was such as to rule out the customary nuclear physics laboratory approach to signal transfer, that the shielding efficiency against thermal neutrons for the He-3 counter was inadequate and that the collimation channel was poorly engineered. These findings confirm that the purpose-built KM1 radiation shield (under construction) is essential for work in the Torus Hall.

As a result of these experiences, attention was transferred to the vertical line-of-sight from the Roof Laboratory (Fig.128) which became available for use at the same time as the first deuterium discharges were run. Due to the large distance (20m) between plasma and spectrometer in the Roof Laboratory, it was not expected that statistically acceptable results could be obtained from just a single discharge. However, some measurements have been obtained from the He-3

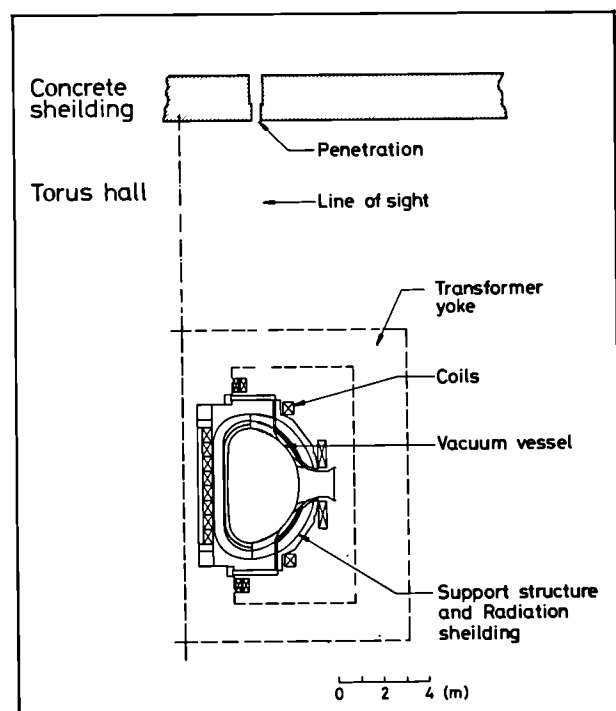


Fig.128: Schematic layout of the line-of-sight arrangement for neutron spectroscopy

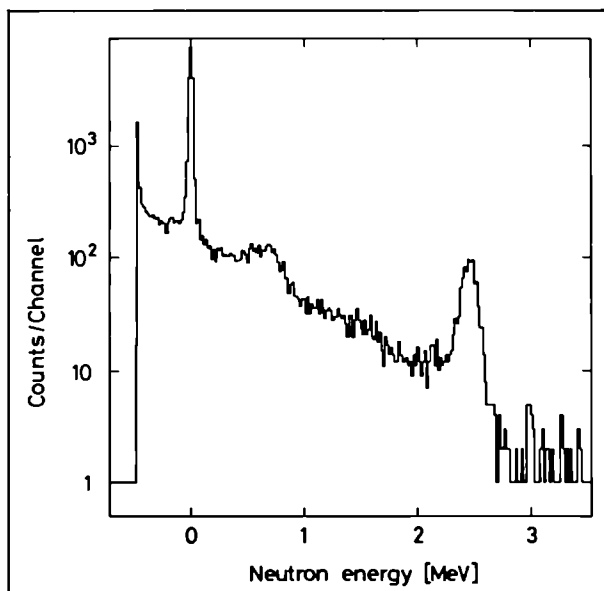


Fig. 129: Plot of neutron counts versus neutron energy (0-3MeV)

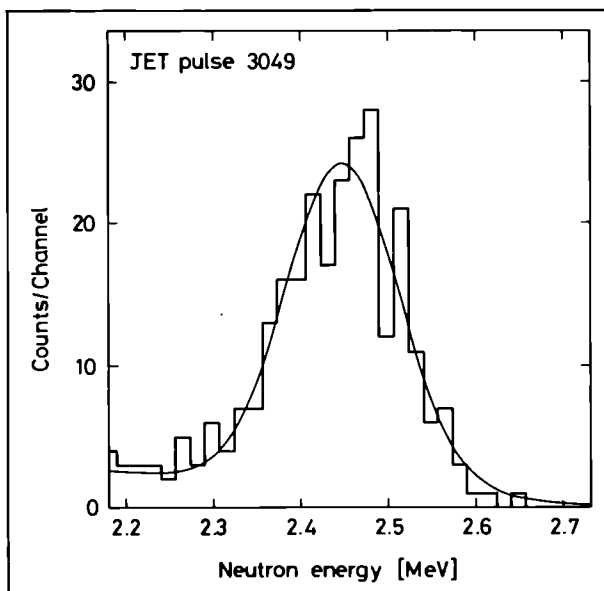


Fig. 130: Plot of neutron counts versus neutron energy (2.2-2.7MeV)

ionization chamber as shown in Figs. 129 and 130. The ratio of total count in the spectrum to useful counts within the full energy peak is $\sim 50:1$, which leaves some room for improvement but compares favourably with the best which has been achieved in the laboratory. The overall count rate was less than 3kHz, which is comfortably within the limit of 10kHz which can be handled by conventional electronics. Whilst the number of useful events acquired during the 6-8s flat-top of a discharge was rather low (<300 counts), it was sufficient to provide ion temperature estimates with uncertainties of 15% or better. It should be noted that the f.w.h.m. width of the He-3 detector resolution function is ~ 60 keV, much smaller than the measured width of the neutron spectrum

~ 120 keV. A full analysis of the measured spectrum must await the measurement, at a suitable accelerator facility, of the energy response function of the detector, which is dependent on neutron energy. Comparison with response functions reported [14] for similar devices suggests that the low-energy tail to the near-Gaussian peak is inherent to the detector as a wall effect rather than being due to a 2.5MeV neutrons, which have lost energy by scattering somewhere in the JET structure or collimation channels. Fig. 130 shows that the plasma is Maxwellian (giving a Gaussian shaped neutron energy spectrum) and that there is no high-energy tail to be attributed to a suprathermal ion component. The ion temperature deduced from the width must be corrected upwards by about 10% to obtain the temperature corresponding to the centre of the plasma, since the spectrometer provides a line integral measure (see Fig. 129). The corrected ion temperatures obtained are about 90% of the electron temperatures and agree well with results from the Neutral Particle Analyzer (as was shown in Fig. 127). The ion temperature estimate so produced can be used in conjunction with the neutron yield to obtain reasonably accurate ($\pm 10\%$) estimates of deuterium density for the higher temperature discharges ($T_i > 2.5$ keV). This result does not depend on plasma theory or results from other diagnostics.

The spherical hydrogen ionization chamber [9] is still in the development stage and has not yet been optimized for use at JET. Nevertheless the energy resolution was about 5% (120keV) or better. This is not yet competitive with the He-3 ionization chamber but better than the NE213 liquid scintillator which is in common use and which offers only 8% energy resolution. The particular advantage of the hydrogen ionization chamber over the He-3 ionization chamber is its insensitivity to thermal neutrons.

The neutron fluxes in the Roof Laboratory were too low for reportable results to be obtained with the nuclear emulsions or for the measurements of the 14MeV/2.5MeV neutron ratio.

Neutron Diagnostic Systems under Construction

The neutron spectrometer (KM1) (see Fig. 131) diagnostic comprises a massive (30t) shielding and collimation arrangement to be installed in the Torus Hall, to house a variety of 2.45MeV neutron spectrometers. The design of this structure has just received interface approval prior to start construction.

A second neutron spectrometer (KM3) (see Fig. 132) based on the well-known time-of-flight method has been constructed and is destined for installation in the Roof Laboratory in the near future. This spectrometer offers an energy resolution of 5%, not as good as that of the He-3 ionization chamber but it will have a wider dynamic range of operation than that obtainable with ionization chambers. Some preliminary measurements with part of this spectrometer have already been made in the Roof Laboratory, confirming that the level of background radiation is very low. The energy resolution function for this instrument must be determined

accurately, since its f.w.h.m. is comparable with that for the neutron spectrum to be measured for plasma temperatures of $T_i \approx 3\text{keV}$: this work is presently being undertaken in the Studsvik Energiteknik Laboratory, Sweden.

The neutron activation system (KN2) will be used to measure the total neutron yield from JET plasmas, regardless of electrical interference problems during the discharge. The diagnostic involves transport of suitable activation foils between positions close to the torus vacuum vessel and radiation counting stations in the Diagnostic Hall, using a pneumatic capsule transport system. The transport system has been constructed and is undergoing tests at the responsible Association (UKAEA, Harwell, U.K.), as is the associated gamma detection system. A delayed neutron counting system has been designed by CEN/SCK, Mol, Belgium and a contract has been placed for its construction. The layouts for installation on the machine, in the Basement and in the Diagnostic Hall are being finalised.

The determination of neutron yields through the activation method necessarily involves calculations of the transport of neutrons within the torus to the foils. These are located inside the mechanical structure so that their environment is of a relatively simple geometry, suitable for precise computational modelling. A toroidal geometry neutron transport code has been specially adapted for this purpose [19].

The neutron profile measuring system (KN3), (see Fig.133) consists of two massive concrete shielding blocks defining 9 vertical and 10 horizontal lines-of-sight to measure the neutron emission across a vertical section of JET plasma. The design has successfully passed the interface check prior to start of construction. All of the neutron detectors (NE213 scintillators) to be used in deuterium operation have been delivered to the responsible Association (UKAEA, Harwell) and new electronics for high count-rate gamma-neutron discrimination have been ordered.

14MeV Neutron Spectrometer

The 2.5MeV neutron spectrometers presently being constructed for operation with d-d plasmas are intrinsically unsuitable for use in the tritium phase. Accordingly, a total of four different types of neutron spectrometer are being studied in the Associations for possible use with the 14MeV neutrons emitted in d-t reactions. Two complementary spectrometers are being considered at Harwell, U.K., a tandem-radiator proton recoil device [15] and a set of silicon diodes exploiting the $^{28}\text{S}(n, \alpha_0)$ reaction [12]; these spectrometers would be housed inside a massive shield/collimator assembly located in the Torus Hall and providing a tangential view of the plasma.

Two, also complementary, neutron time-of-flight systems are being studied by the Swedish Association; an associated-particle time-of-flight technique [16] is being investigated at Chalmers University, Gothenburg, Sweden, whilst a deuterated-scintillator backscatter technique has been proposed [17] as a joint venture with

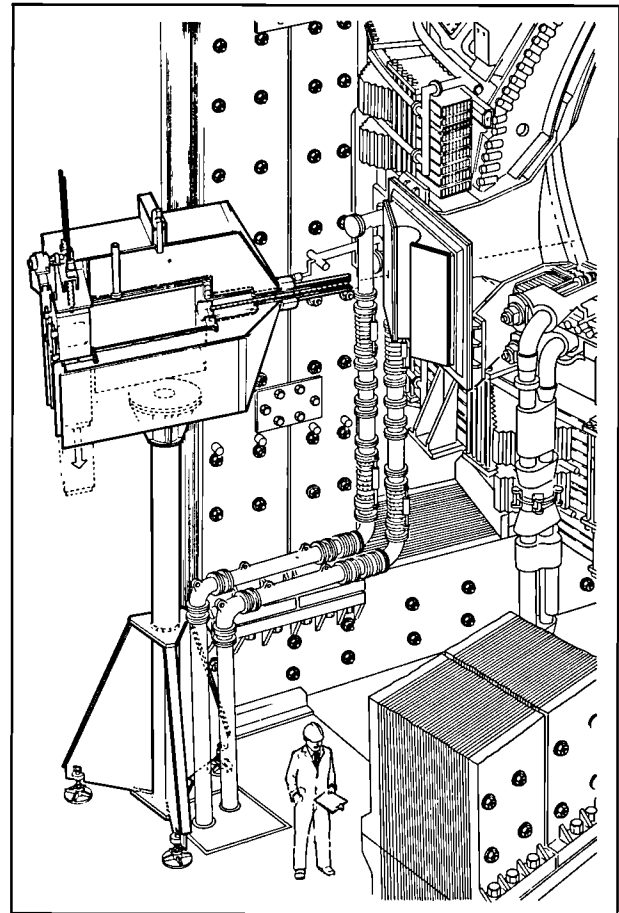


Fig.131: Layout of Neutron Spectrometer (KM1)

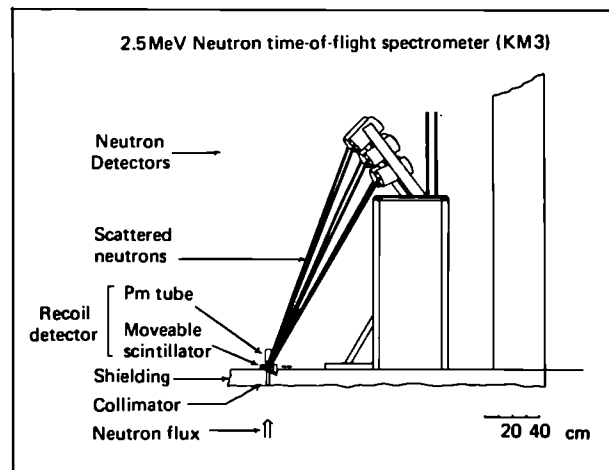


Fig.132: Layout of Neutron Spectrometer (KM3)

JET staff and is being tested experimentally by the Royal Institute of Technology, Stockholm, Sweden. The time-of-flight techniques seem most useful for use in the Roof Laboratory due to their sensitivity to background radiation but both offer excellent energy resolution. The Stockholm/JET proposal is rather similar to the 2.5MeV time-of-flight system which will be installed soon. It offers a particularly high detection sensitivity and other features which make it potentially suitable for measuring the small proportion of 14MeV neutrons from secondary

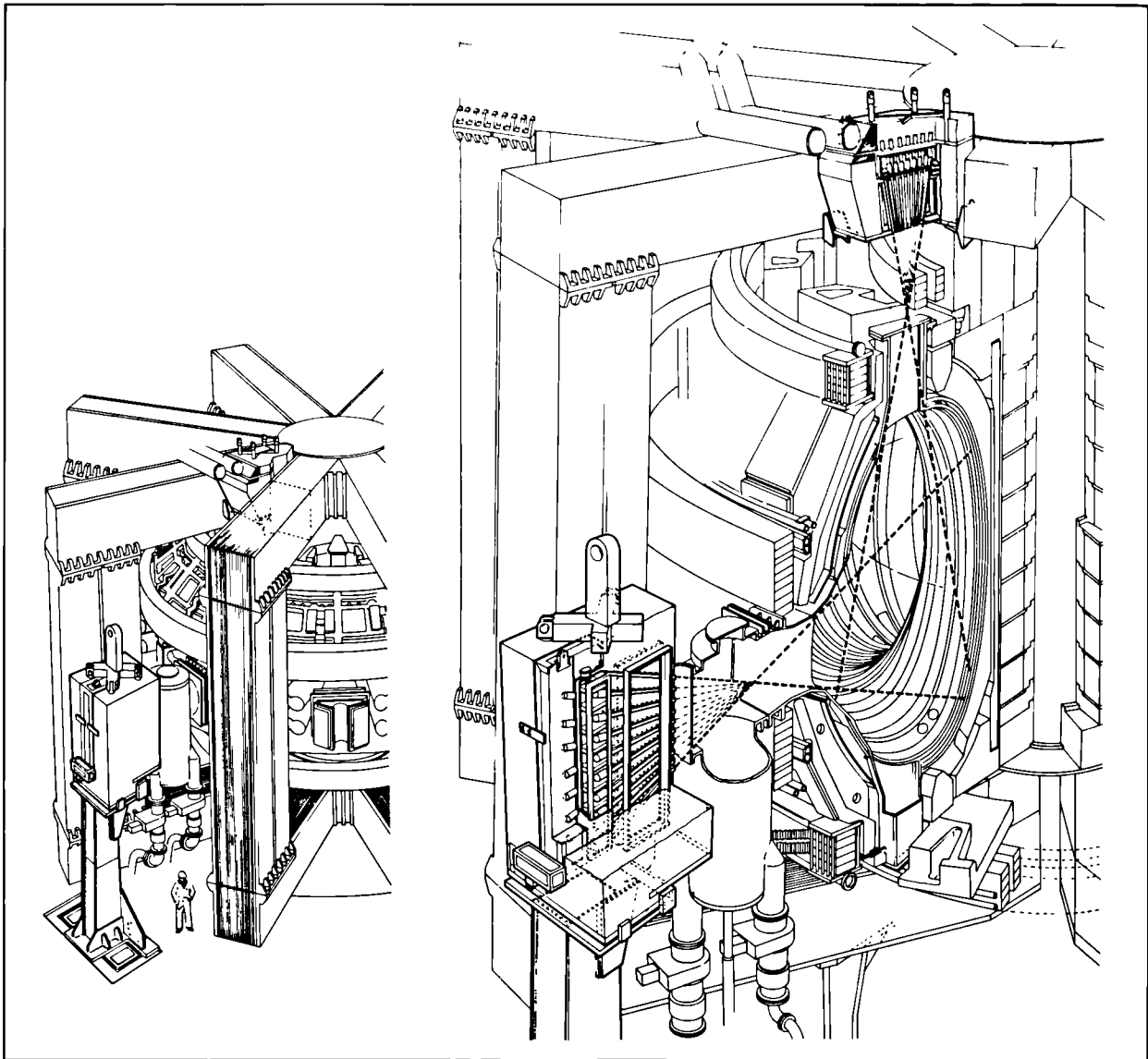


Fig.133: Neutron profile measuring system (KN3)

t-d reactions in d-d plasmas, and may constitute a valuable device for early studies of triton confinement in JET.

Charged-Particle Diagnostics

The first of the additional heating methods to be brought on-line will be the resonant heating of minority He-3 in D plasmas. Whilst the overall heating efficiency can be deduced from the yield and energy spectrum of d-d neutrons, the coupling efficiency of RF power to the He-3 species is best inferred from the He-3 ion distribution function. Fast He-3 ions undergo ${}^3\text{He} + \text{d} \rightarrow \text{p} + {}^4\text{He}$ reactions; the 15MeV protons produced are only partially confined in JET. Therefore, the proton energy spectrum can, in principle, be measured to provide the He-3 ion velocity distribution function as well as the densities of the reacting species, in direct analogy with d-t neutron measurements [18]. Therefore, a proton detector has been planned for use in JET.

Detecting fast charged particles as opposed to neutrons leads to some extra experimental problems. The detector must be placed at the plasma boundary where it intercepts the particle orbits determined by the magnetic field. A silicon surface barrier detector will be used as a proton energy spectrometer; it will be enclosed in a secondary vacuum chamber made from an inconel tube and provided with a $2\ \mu\text{m}$ stainless-steel window to permit the entry of the protons. The detector housing has already been installed on the machine and a detector/preamplifier assembly, together with cooling arrangements, are being designed with the aim of having the complete system operational in Spring 1985.

REFERENCES

- [1] 'Design and Construction of a Mode Converter from TE_{10} to TE_{11} ' B.J.D. Tubbing, Rijnhuizen Report 84-158, (1984).

- [2] 'An Absolute Calibration Method for Electron Cyclotron Emission Spectrometers' B.J.D. Tubbing, Rijnhuizen Report 83-149, (1983).
- [3] LIDAR-Thomson Scattering Final Report, G. Braderlow, J.E. Gruber, K. Hirsch, H. Röhr, H. Salzmann, K.J. Witte, Garching Report IPF-84-3 (1984).
- [4] P.A. Duperrex et al., Magnetic Broadband Turbulence Measurements and Ohmic Confinement in the TCA Tokamak, Physics Letters 106A (1984) 133.
- [5] B.A. Carreras et al., Transport Effects Induced by Resistive Ballooning Modes and Comparison with ISX-B Tokamak Confinement, Phys. Rev. Lett. 50 (1983) 503.
- [6] E.J. Strait et al., MHD Stability of High-Beta Plasmas in Doublet III, Proc. 11th EPS Conf. on Controlled Fusion and Plasma Physics, Aachen, Vol. I (1983), Paper AO9.
- [7] JET JOINT UNDERTAKING Progress Report 1983, EUR 9472 En (EUR-JET-PR1), p.91, Limiter Surface Temperature Measurements;
- [8] SEFORAD-APPLIED RADIATION LTD., model FNS-1 Spectrometer;
- [9] Hoenen, F. 'Optimierung Sphärischer Ionisations kammern für die neutronen Diagnostik an Tokamakanlagen'; (1983), ISSN 0366-0885;
- [10] Hubner, K, Univ. of Heidelberg (Private Communication);
- [11] Elevant, T 'A neutron spectrometer suitable for diagnostics of extended fusion plasmas', Nucl. Instr. and Methods, 185 (1981) 313;
- [12] Jarvis, O.N. 'Neutron detection techniques for plasma diagnostics', in Diagnostics for Fusion Reactor Conditions EUR8351-1EN, Vol.1, p.353, (1982);
- [13] Källne, J. et al 'Calibration of the Neutron Yield Detectors in the JET Tokamak', JET-IR(84)02;
- [14] Fisher, W.A. et al 'A fast neutron spectrometer for D-D fusion neutron measurements at the Alcator Tokamak', Nucl. Instr. and Methods in Physics Research, 219 (1984) 179;
- [15] Kang, H.D. and Chung M.K., J. Kor. Phys. Soc 8(1), 9(1975)
- [16] Grosshoeg, G. et al 'Combined proton recoil and neutron time-of-flight spectrometer for 14+ MeV neutrons', ISSN 99-0358 116-5 (1983);
- [17] Källne, J. and Elevant T. 'Neutron time-of-flight spectrometer for diagnostics of d-t fusion plasmas'. To be published;
- [18] Heidbrink, W.W. 'Tokamak diagnostics using fusion products', Ph. D Thesis, Princeton University (1984);
- [19] Verschuur, K.A. 'FURNACE, a toroidal geometry neutronic program system, method, description and users manual' ECN-162 (1984).

Experimental Division 2

(Division Head: W.W. Engelhardt)

Experimental Division 2 is responsible for specification, procurement and operation of about half of the JET diagnostics systems, particularly those associated with spectroscopy, bolometers, interferometry, soft X-ray array and neutral particle analysis. In addition, the Division assists in execution of the programme, in interpretation of the results and in making proposals for future experiments, in collaboration with Experimental Division 1, Theory Division, the Physics Operation Group and the Operations and Development Department. At present the Division consists of two groups: 'Spectroscopy and Impurity Physics' and 'Radiation and Particle Analysis'. It is planned to introduce a third group ('Soft X-ray Analysis') in mid-1985. These groups reflect the focal points of physics investigations being pursued in the Division.

Impurities play a major role in tokamaks as they induce radiation and influence the stability of the plasma. Their sources, concentrations, time evolution and transport behaviour are being investigated with classical spectroscopic methods in the spectral range from the X-ray regime to the visible. Integral radiation measurements are being carried out by bolometers and, with coarse spectral resolution, by soft X-ray detectors.

Particle transport is the second extensive field being investigated in the Division. Electron density distributions are measured by interferometry, the particle sources determined by spectroscopic methods, neutral particle energy distributions analysed and deliberate perturbations of particle densities will be induced by the injection of pellets. Spectroscopic Doppler measurements and neutral particle analysis provide insight into the ion energy distribution.

The analysis of ion heating and ion energy confinement is another important field which will be investigated. Active beam diagnostics, either by using the existing heating beams or by installing a devoted probing beam, in conjunction with charge exchange recombination spectroscopy, will enlarge the diagnostic capabilities. It should then be possible to measure rotations and velocity distributions of fully stripped ions in the plasma interior giving information on ion temperature, plasma rotation, power deposition during auxiliary heating and light impurity concentrations.

The Division was established at end of 1982 and has built up during 1983 and 1984. It should be near to planned size in 1985. In order to compensate for the limited JET staff available, several Task Agreements were concluded with Associated Laboratories resulting in fruitful collaboration and in efficient support of the experimental programme on JET. The main collaboration with Associated Laboratories is organised through these Agreements centred around specific fields of research activities. In many cases, these are closely connected to diagnostic instruments built in the Associations, but also based on special expertise. The tasks include installation, commissioning, operation of

diagnostics, physics investigations and interpretation of results, in collaboration with the JET team. Task Agreements in progress are summarised in Appendix 1, where further details may be found.

During the year, work continued on supervision of diagnostics constructed in Associated Laboratories. A survey is given in Table X and details are dealt with in the following sections. During the start-up phase of JET, only limited diagnostics were ready and some were installed only in a provisional way. However, further systems have come on-line and results obtained are presented in the following paragraphs. A consistent picture of the impurity situation was obtained with these methods.

Progress in Construction and Installation of Diagnostics

Bolometry (KB1)

(G. Magyar, A. Ainsworth, A. Bulliard, E. Oord, J. Ryan, F. Mast+, H. Krause+)

+ EURATOM-IPP Association, IPP Garching, F.R.G. In January/February, the installation and commissioning of the bolometer cameras in their final form was completed. This took place under a Task Agreement with IPP, Garching, F.R.G., who sent key personnel to supervise the installation of the two horizontal bolometer cameras and to assemble the necessary electronics. At the same time, the control and data acquisition software was installed. With the onset of operation in March, the three bolometer cameras, with a total of 42 channels, were commissioned and have since operated normally.

Multichannel Far Infrared interferometer (KG1)

(G. Magyar, G. Braithwaite, C.J. Hancock, J. O'Rourke, E. Oord, A. Gondhalekar, D. Veron+)

+ EURATOM-CEA Association, CEA, Fontenay-aux-Roses, France.

The C-frame was fully equipped and partially aligned in the Assembly Hall: it was then installed in the Torus Hall and aligned with the JET machine.

First priority was given to completion and operation of the vertical channels. After final alignment of the total vertical system, commissioning of the He-cooled detectors data acquisition hardware and software was undertaken. Line-integrated densities were measured in 5 channels in September. During the following shutdown, the remaining windows were fitted, two damaged internal mirrors were replaced and the assembly of the remaining optics was completed (except the compensating interferometer). Operation of the full system is expected by mid-85.

X-ray Pulse Height Spectrometer (KH2)

(R. Gill, N. Foden, J-L. Bonnerue, A. Gondhalekar, K. Hilber)

This system contains three Si(Li) X-ray detectors cooled to liquid N₂ temperatures, which view the plasma along three nearly identical chords through sets of adjustable apertures and Be foils to make detailed time resolved

measurements of the X-ray spectrum. These spectra will provide measurements of the continuum and line emission spectra, from which will be deduced the plasma temperature, the X-ray anomaly factor and plasma impurity concentrations.

Detailed design of the non-active phase system has been completed and manufacture of the beam line and aperture assemblies are underway. The detectors and their associated electronics are already available. Installation is planned for mid-1985.

Provisional Pulse Height Spectrometer (KH2)

(R. Gill, E. Källne, J. Gowman, J-L. Bonnerue, E. Oord, G. Decker)

A provisional single chord system consisting of a HgI₂ detector looking along a major radius has been installed to observe the X-ray pulse height spectrum between 4 and 100keV. The line-of-sight is defined with a dual set of apertures and the detector looks through a 300 μm beryllium window on the torus. The diagnostic was calibrated with a set of calibrated radioactive sources ranging from 4 to 30keV. X-ray spectra were automatically recorded with a time resolution of 100ms during the full plasma discharge. The installed electronics has a limited dynamic range and the aperture set was complemented with an extra aluminium foil to reduce the high fluxes from high current shots. A software package was developed and installed to facilitate on-line data inspection and analysis. The diagnostic provided electron temperature and nickel impurity concentration measurements, during the year.

Soft X-ray Diode Arrays (KG1)

(R. Gill, A. Ainsworth, A. Edwards, A. Gondhalekar)

This system, built by EURATOM-IPP Association, IPP Garching, F.R.G., consists of two X-ray cameras which view the plasma from the vertical and horizontal directions with a total of 100 detectors. The cameras will provide spatially and time resolved measurements of the plasma X-ray emission, allowing time resolved mapping in a poloidal plane of the plasma emissivity, and interpretation in terms of impurity transport, MHD activity, etc. During 1984, the vertical camera was manufactured and construction was also started on the horizontal camera after approval of the detailed design proposal. Most of the electronics system has been built and delivered to IPP for final testing, and the CODAS system has been specified and built at JET. It is planned to install both cameras on JET in mid-1985.

An outline design has been made for the vertical camera's radiation shield and further progress has been made in defining the parameters of the horizontal radiation shield. Provisionally, a system consisting of four diodes, with individual Be foil filters, viewing the plasma along four nearly identical chords in the midplane, have been installed and operated routinely during 1984.

Neutral Particle Analyzer Array (KRI)

(S. Corti, B. Oliver, J-L. Bonnerue, L. Lamb, E. Oord, A. Gondhalekar, G. Grosso+, G. Buceti+) + EURATOM-CNEN Association, Frascati, Italy.

During 1984, the first channel of the Neutral Particle Analyzer Array became operative. This is a channel viewing along a chord in the midplane of the torus at an angle of 10° to a major radius. The first results obtained with this analyzer are given separately in this report. Towards the end of the year installation of three more analyzers was started, which are expected to be operating by mid-1985. During 1985, the last channel of the array will be installed and commissioned, so that by mid-1985, the full array of 5 analyzers will be available.

Active Phase X-ray Crystal Monochromator (KS1)

(E. Källne, R. Lobel)

Detailed design for the manufacture of a double crystal monochromator has been started. The instrument will survey the X-ray emission from highly ionised impurity atoms along a line-of-sight in the midplane of the torus. With a scanning frequency of up to 5Hz, the full spectral range (0.2-2nm) can be covered in 1s. Absolute intensities of impurity line emission from metals and from light impurities will be measured with a resolution of 1000, with the possibility of increased resolution for the shorter wavelengths. Neutron shielding and collimation will be installed to reduce the background sufficiently for the instrument to operate during all JET phases. The detailed design and construction should be completed by early 1986.

Spatial Scan X-ray Crystal Monochromator (KS2)

(E. Källne, R. Lobel)

A double crystal monochromator, closely coupled to the JET torus chamber, is under detailed design and construction with the task of measuring spatially resolved X-ray emission in the region 0.2-2nm. The design of the monochromator is fixed on standard double crystal geometry in parallel mode with an additional rotation of the first crystal allowing a scan of the plasma cross-section through a vertical line-of-sight. Thus, the spatial distribution of impurity lines can be measured continuously for given wavelengths. The design of the crystal motion will allow both spatial and spectral scans during the JET pulse. The close coupling interface to the torus (via a thin window) necessitates installation of shielding and neutron collimation for operation during the D-D phase. The instrument should be completed for installation by early 1986.

 H_α and Visible Radiation Monitors, and Poloidal Scan Array (KS3)

(P. Morgan, C. Wilson)

During the early 1984 shutdown, the system was extended to provide a total of 8 vertical lines-of-sight, arranged symmetrically around the torus at a major radius of 3.11m and 4 horizontal lines of sight in the plasma equatorial plane. The latter viewed one Ni limiter

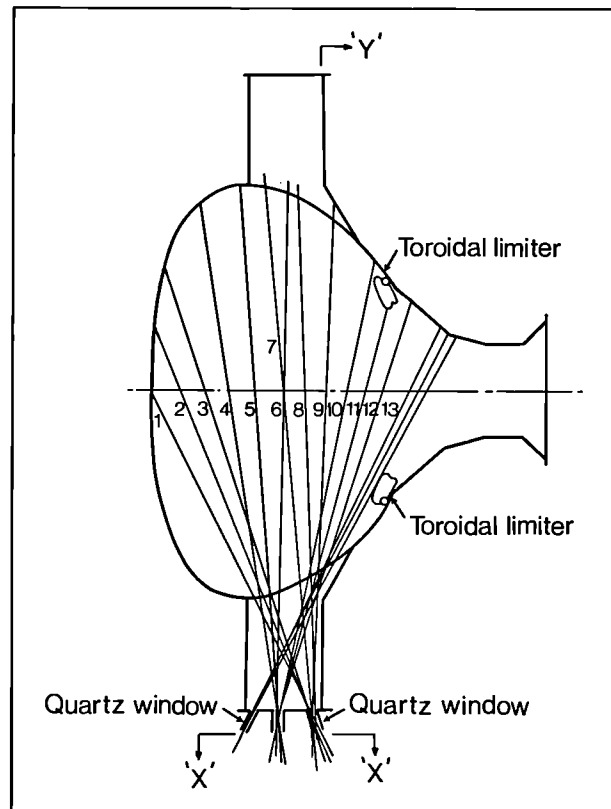


FIG.134: Poloidal Scan Array showing the lines-of-sight of the 13 telescope array

on Octant No.6, which, however, was withdrawn by 10cm from contact with the plasma, and 3 graphite limiters on Octants Nos.2,4 and 6. This permitted checks on the uniformity of recycling at the C limiters.

During the year, the outline design was completed, and much of the detailed design accomplished, for a 13-telescope array to view the plasma cross-section in nominally the same poloidal plane. Fig.134 shows the arrangements of the lines-of-sight. Each telescope will use an optical fibre to relay the light collected, through 3 quartz windows mounted on the lower main vertical port of Octant No.8. The poloidal scan array will permit the radial variation of Z_{eff} to be determined and the poloidal symmetry of H_α emission to be studied. Four of the lines-of-sight are included at 3.5° to the vertical plane, such that they will intersect the path, through the plasma, of the beam from the neutral injector to be installed on Octant No.8. This will facilitate the study of beam-plasma interactions, such as charge-exchange recombination. The installation of the array will begin during the 1985 Summer shutdown, and commissioning and operation will start in the Autumn 1985.

VUV Spectroscopy Spatial Scan (KT1)

(G. Magyar, R. Lobel)

During the year, testing and calibration of the spectrometers on the TFR tokamak were completed. The two horizontal beamlines were manufactured and successfully vacuum tested at EURATOM-CEA Association, Fontenay-aux-Roses, France. During the

shutdown at the end of 1984, the two beam lines and spectrometers were installed on Octant No.6, and commissioning started. Operation is expected in mid-1985. Detailed design of the third beamline, for the vertical line-of-sight, was also completed.

VUV Broadband Spectroscopy (KT2)

(G. Magyar, R. Lobel, B. Denne, N.C. Hawkes+, J-L. Martin, A. Ravestein)

+ EURATOM-UKAEA Association, Culham Laboratory, U.K.

The system, based on a McPherson Model 251 broadband spectrometer, came into operation in May 1984. The line-of-sight is in the midplane of the torus at Octant No.3, at an angle of 12.5° to the major radius. With its two interchangeable gratings, the spectrometer covers the wavelength range 10-170nm. Approximately 70 full spectra are routinely recorded during a plasma pulse, providing time evolution of the various impurity lines with 16ms resolution for the first 600ms of the pulse, and with 600ms resolution for the remainder.

High Resolution X-ray Crystal Spectrometer (KX1)

(E. Källne, B. Oliver, N. Foden)

A classic large Rowland circle geometry X-ray crystal spectrometer is under construction. The high resolution of the instrument (15000) will permit line profile measurements from individual impurity lines of highly ionised atoms.

The line-of-sight is in the midplane of the torus at Octant No.8 at an angle of 22° to the major radius. This geometry permits a tangential view across the plasma. The design and tests of the large Be window separating the torus vacuum from the diagnostic has been completed and installation is expected during 1985. Installation of the wall penetration tube has been concluded as planned. The instrument must be housed in a large concrete housing, which has been designed and construction has started. The full diagnostic is expected to be operational by the end of 1985.

Hydrogen Pellet Injector System (KZ1)

(A. Gondhalekar, C. Wilson, L. Lamb, P. Roberts)

During 1984, the full specification of the Pellet Injector system's performance, and of all the interfaces to JET were completed. Detailed design and approval were also completed, and manufacture started in late 1984. Partial installation of the system will begin during the 1985 Summer shutdown. Installation of the Pellet Injector is planned for the end of 1985.

Extreme Ultraviolet Spectrometer (KT4)

(G. Magyar, C.J. Hancock)

A feasibility study for the extension of the existing Broadband VUV Spectroscopy System (KT2) in the far VUV region was carried out. A system based on a commercially available Grazing Incidence Spectrometer was recommended. Procurement has been approved, and detailed design and manufacture are in progress.

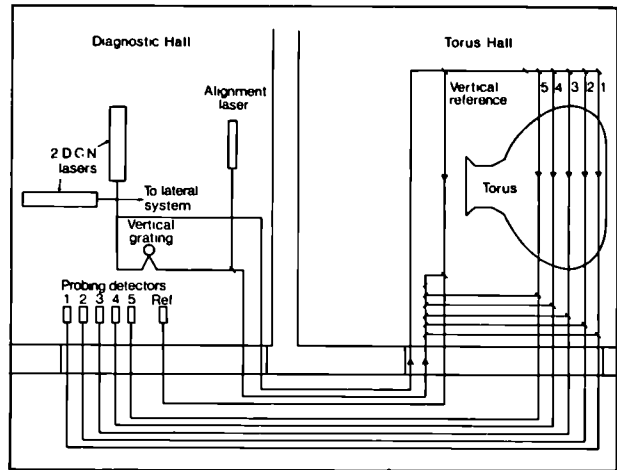


Fig.135: Schematic drawing of the JET multichannel infrared interferometer

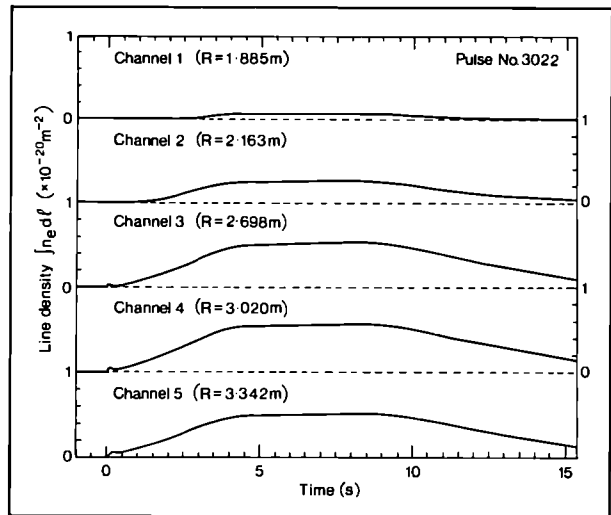


Fig.136: Evolution of the line integrated density during Pulse No.3022

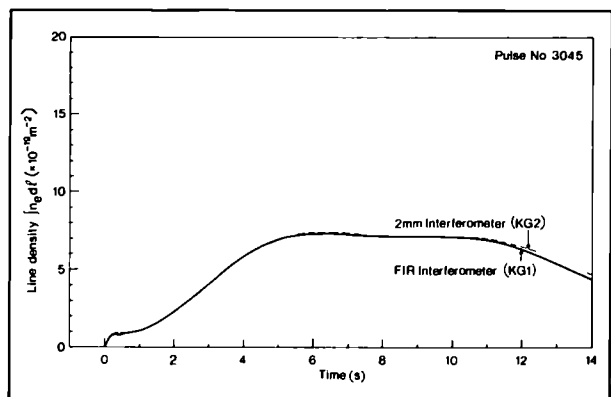


Fig.137: Comparison of central line-integrated densities from the FIR and 2mm microwave interferometers

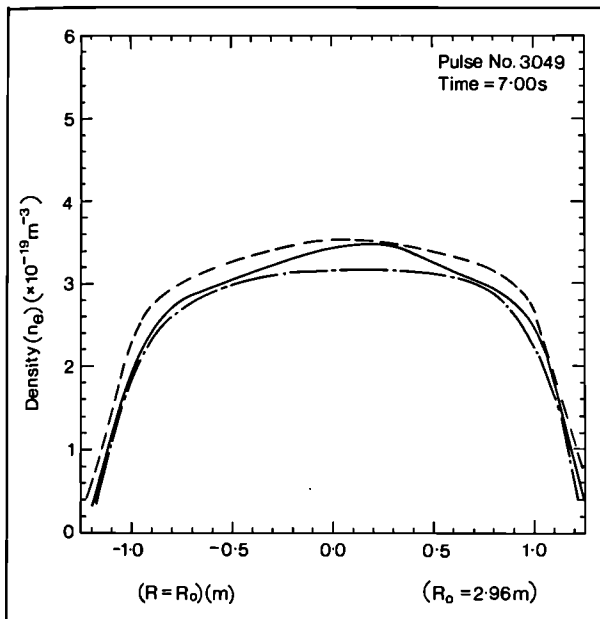


Fig.138: Abel inverted profile for Pulse No.3049, at 7s

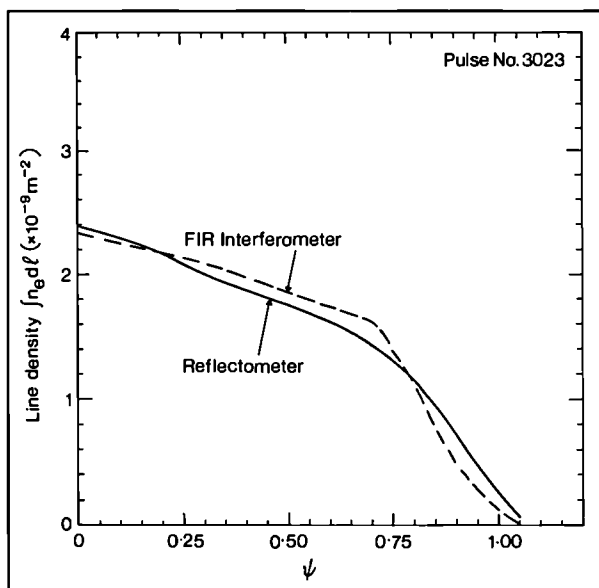


Fig.139: Comparison of FIR Interferometer and Reflectometer profiles

Installation and commissioning are expected in mid-1986.

First Results from Newly Installed Diagnostics

Far-Infrared Interferometer (KG1)

(J. O'Rourke, G. Magyar, G. Braithwaite)

In the last period of operation, the far-infrared (FIR) interferometer (Fig.135) furnished some preliminary results. Five of the planned ten channels were commissioned. The provisional nature of the installation did not permit operation of the system since the laser radiation ($\lambda \sim 195\mu\text{m}$) is strongly absorbed by water vapour this led to some losses in detected power.

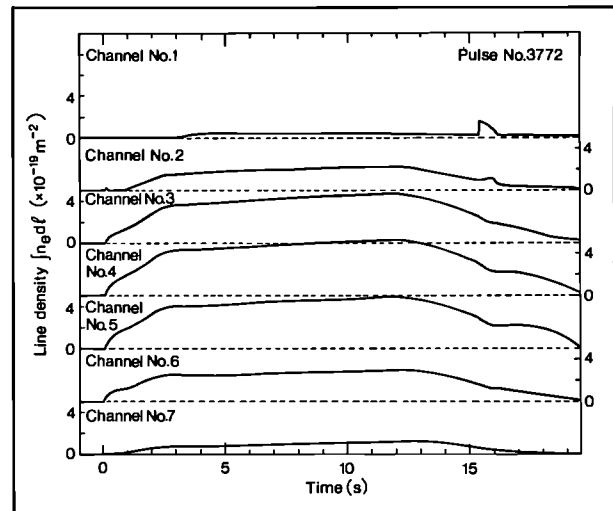


Fig.140: Evolution of the line-integrated density during Pulse No.3772, with a 'marfe' at 15.52s.

Furthermore, the DCN laser source was not operated at full capacity and the path of the FIR beam was aligned only crudely (neglecting its gaussian character) by using a HeNe laser. Even so, the signal to noise ratio was about 50:1. Data were acquired in local mode for many shots beginning with Pulse No.3005.

Fig.136 shows typical traces of phase versus time for the five working channels. Neither loss of fringes nor mechanical vibrations are important sources of error, and the trace returned to zero after the end of the discharge. Sawteeth are not normally resolved at these densities.

Fig.137 compares the central FIR interferometer (KG1) channel with the 2mm microwave interferometer (KG2) for Pulse No.3045. The agreement is generally very good (better than 5%). The discrepancy at the beginning and end of the discharge can be accounted for by profile/position effects (the KG2 paths is displaced by 12cm outward along the major radius).

Fig.138 shows an inverted density profile, obtained using pixels based on magnetic measurements of the plasma boundary. The dashed lines indicate the band within which profiles can be obtained using the same data but varying the assumed pixel structure in two respects:

- changes of $\pm 4\%$ in the position of the plasma boundary;
- changes in the position of the magnetic axis.

A fit of a density distribution of the form $n \approx n_0(1 - \psi^2)^\alpha$ (where ψ is the flux label), typically yields $\alpha \approx 0.6 \pm 0.1$. Most of the pulses for which data were obtained have central densities (during the flat-top) in the range $2.0 \sim 3.5 \times 10^{19} \text{m}^{-3}$.

Fig.139 shows a comparison of the density profiles obtained from the FIR interferometer and the reflectometer data. The reflectometer data has been arbitrarily 'truncated' at the geometric centre of the torus. The more peaked nature of the reflectometer could be the result of profile changes during the density rise, since the peaking varies from $\alpha \sim 1.1$ at 1s into the pulse to $\alpha \sim 0.8$ at 4s. Also, the reflectometer measured

the outer profile, which for the FIR interferometer four of the five operating channels were on the inner side.

Fig.140 shows the line integrated density along the seven vertical chords of the interferometer, for Pulse No.3772. During the current decay (at ~15.5s), a marked asymmetry in the density profile develops. This is evidenced by a steep rise in the density along the innermost chord (R=1.885m), while along the outer chords the density continues falling. Such asymmetries have been observed on other tokamaks [1], and have been termed ‘marfes’.

The density in a ‘marfe’ often shows periodic fluctuations (see Fig.141). Although it lasts only ~1s, the subsequent evolution of the density is different from that prior to the ‘marfe’. It is seen that the profile becomes increasingly peaked, as the density along the peripheral chords decreases much more rapidly than along the central area. The rate of density decay, dn_e/dt , decreases by a factor of ~3 (see Fig.142).

The edge bolometer signals show a drop after the ‘marfe’. The particle flux (deduced from the D_a signals)

from the limiter drops from $\sim 10^{21}s^{-1}$ to $\sim 9 \times 10^{19}s^{-1}$, while the wall flux rises from $\sim 4 \times 10^{19}s^{-1}$ to $\sim 8.5 \times 10^{19}s^{-1}$, becoming comparable with the limiter flux. It is concluded that the plasma becomes ‘detached’ from the limiter during ‘marfe’ behaviour.

Using the relationship:

$$\frac{dN}{dt} \approx -\frac{N}{\tau_p} + \phi_w + \phi_e + \phi_g \approx -\frac{N}{\tau_p} (1-R) \phi_g$$

where N is the total number of electrons, and ϕ_w , ϕ_e and ϕ_g are the wall, limiter and gas valve fluxes, respectively, as τ_p is the global particle confinement time, and R, is the recycling coefficient. τ_p rises from 0.65s before the ‘marfe’ to 1.5s, after. R falls from 0.8 to 0.67 in this interval.

Clearly, this has serious implications for JET operation. Such a decrease in the density decay rate during the current ramp-down means that the plasma is being pushed toward the density limit and has a higher probability of disrupting. Since the ‘marfe’ seems to be a precursor to the process of plasma detachment from the limiter, it may be possible to use it as a trigger for changes in plasma position or current ramp-down rate which would inhibit detachment.

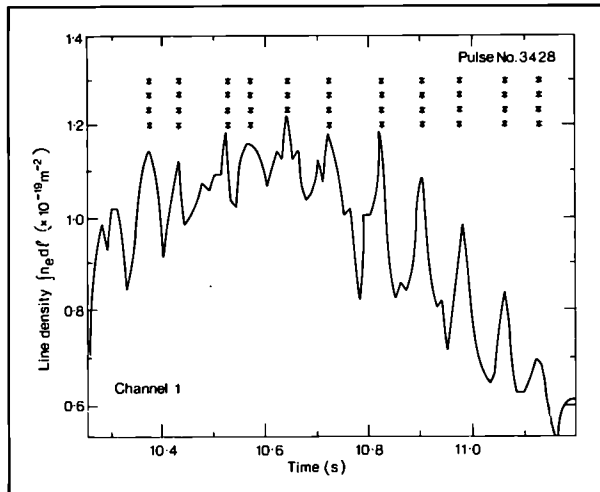


Fig.141: Periodic density fluctuations during a ‘marfe’

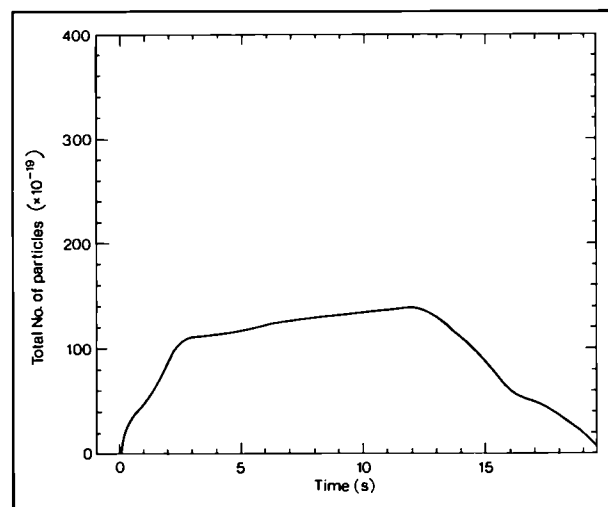


Fig.142: Evolution of the total number of electron during Pulse No.3772

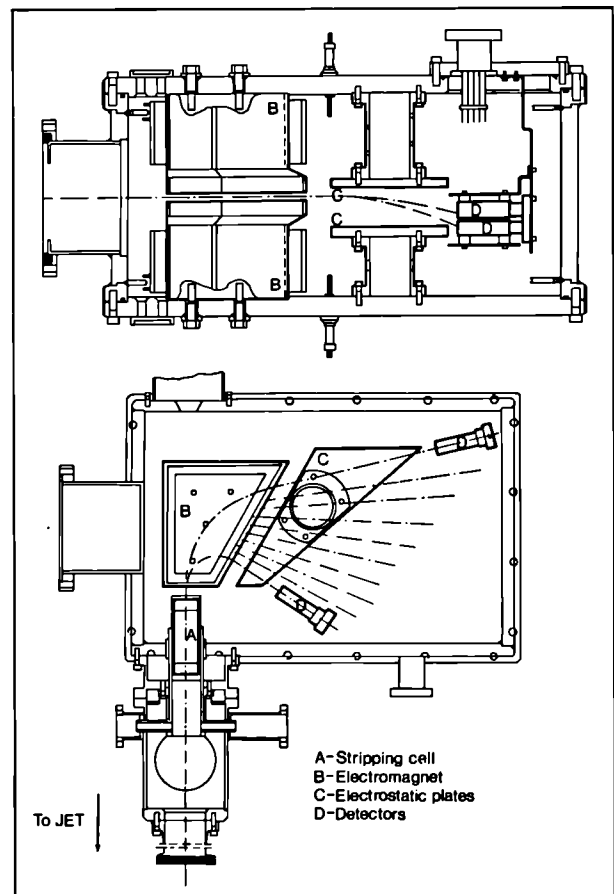


Fig.143: (a) Side and (b) top view of the analyser

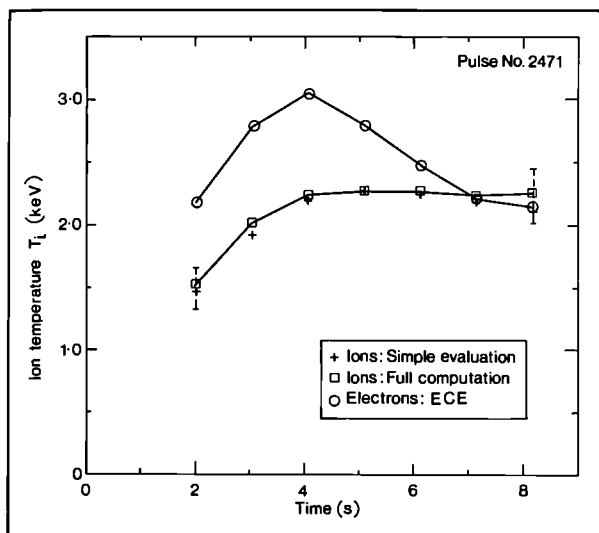


Fig.144: Peak values of T_e and T_i versus time for Pulse No.2471 in Hydrogen

Particle Analysers (KRI)

(G. Bracco*, G. Buceti*, S. Corti, G. Grosso^o, S. Mantovani*, L. Panaccione*, B. Tilia*, V. Zanza*, G. Bitti*, J.L. Bonnerue, L. Lamb, B. Oliver, G. Ventura*)

* EURATOM-ENEA Association, Frascati, Italy;

^o EURATOM-CNR Association, Milan, Italy.

By 1984, the installation of the first of five neutral particle analysers (NRA) on JET was completed. The analyser, shown in Fig.143, views a horizontal chord in the equatorial plane of the torus. The angle between the line of sight and a major radius is presently fixed at 10, in order to avoid direct observation of the ripple trapped ions which would make the data analysis very complex. The neutrals emanating from the plasma are ionized in a gas stripping cell and energy and mass analyzed using a magnet and two electrostatic plates in a geometry in which B is parallel to E. At the exit of the analysing fields are two horizontal rows, each of ten channeltrons, used for detection. The geometry of the system is such that:

- ions of a given mass are detected by channeltrons placed in the same row;
- the lower row detects particles with a mass twice the mass detected by the upper row.

In this way, the energy spectrum of both hydrogen and deuterium can be obtained simultaneously.

For each detected particle, the detectors give a 10mV pulse which is then transmitted into the Diagnostic Hall through 100m long coaxial cables. After conditioning, to remove low level noise and to shape the pulses, these are transmitted to a latching scaler for counting at a pre-programmed acquisition rate.

The analyser has been calibrated absolutely both for H and D. The detectable energy is in the range 0.3 to 320keV for H and 0.3 to 160keV for D. The typical energy resolution of a channel is $\sim \pm 10\%$. The temporal resolution is limited only by the background noise: so far, acquisition times as short as 10ms have been used. At the

end of a plasma shot the counting rate of each channel is stored in the JET Pulse File (JPF) as a function of time, together with the energy detected and the efficiency of each channel. Thus makes all quantities needed to transform the raw data into physical quantities available at any time.

A display program, working both on the NORD 500 and on the IBM computers, allows display of all the accumulated information (i.e. the time behaviour of the neutral flux measured by each channel; the neutral spectra at selected times; and the ion temperature obtained with a linear fitting of the neutral fluxes Γ versus the energy E). This method gives the value of the central ion temperature for a homogeneous transparent plasma. The presence of plasma layers with lower temperatures along the line of sight causes an increase of the neutral fluxes at lower energies with a consequent under-estimation of the temperature. The situation is quite different when the plasma opacity is taken into account. Neutrals with high energy escape from the plasma more easily than those with low energy: this causes an over estimation of the temperature. If the opacity is too high, the signal comes mainly from the outer plasma regions having lower temperature, again causing an under-estimation of the central ion temperature. In order to evaluate the importance of these effects and to obtain the correct peak ion temperature along the line of sight, a complete elaboration code is available on the IBM for off-line analysis.

The code calculates the neutral flux, given by

$$\Gamma(E) \approx G \int_a^a n_o n_i \langle \sigma_{cx} v \rangle g(T_i, E) \eta(E) dx$$

where

- n_o , n_i are the neutral and ion densities respectively;
 - $g(T_i, E)$ is the ion distribution function assumed Maxwellian;
 - G is a geometrical factor taking into account the features of the analyser;
- $\eta \approx \exp(-\int_x^a d\xi / \lambda_{mfp})$ is the plasma transparency.

The neutral density $n_o(r)$ is computed by solving the continuity equation for neutrals with the value of the neutral density at the plasma edge $n_o(r)$ as an adjustable parameter.

In this calculation, cylindrical geometry and Maxwellian distributions both for ions and electrons are assumed. Neutral particles are considered to be isotropically distributed in velocity space. Contributions from 'cold' neutrals at the plasma edge and from 'hot' neutrals created inside the plasma are taken into account separately. Cold neutrals are assumed to be monoenergetic with temperature T_o , while hot neutrals are generated at energy $E \approx 3T_i/2$ where T_i is the 'local' ion temperature.

The values of the peak T_e electron temperature (from ECE measurements) and of the line average density measured by the 2mm interferometer are read from the JPF. Fixed profiles of the form:

$$F(x) \approx F(1-x^\alpha)^\beta + F_o$$

are used for the density and temperatures. At present, a parabolic profile is used for density (ie $\alpha \approx 2$, $\beta \approx 1$) and a

parabolic square profile for T_i and T_e (ie $\alpha = 2, \beta = 2$). The ion temperature value and the neutral density at the plasma edge are adjusted in order to make the calculated fluxes fit the experimental ones.

The following two JET discharges are used as examples to illustrate typical results obtained:

- i) Pulse No.2471 : a high density hydrogen discharge;
- ii) Pulse No.2519 : a deuterium discharge with density up to $2.5 \times 10^{19} \text{m}^{-3}$.

For discharge (i), Fig. 144 shows the time behaviour of the peak value of both T_e and T_i . As can be seen, the ion temperature obtained from the complete analysis is almost equal to that given by the simple on-line calculation; even at high density the two values are within the error bars. Fig. 145 shows the profiles used for the complete computation and the neutral density profiles obtained. Fig. 146 presents the comparison between the energy spectra obtained with the code and the experimental one.

Figs. 147, 148 and 149 show similar computations for the deuterium discharge. In this case, it should be noted that the simple calculation under-estimates the peak temperature by about 20% at the higher density, while agreement with the computed value is good in the initial phase of the discharge. This effect is partly due to that, at an early stage of the discharge, the portion of the spectrum used for the simple T_i calculation (i.e. 4-12keV) comes mainly from the central region of the plasma, while later, at higher density, it comes from a region outside a radius of 50cm. In Fig. 150, the plot of the T_i/T_e ratio versus density is shown, in which the trend of the curve is as expected, (i.e. T_i/T_e increases with density). To improve the calculation, the following corrections are being investigated:

- introduction of the real experimental geometry;
- use of actual profiles for n_e and T_e ;
- effects of impurities.

Bolometry (KB1)

(H. Krause+, F. Mast+, N. Gottardi, A. Bulliard, J. Ryan)

+ EURATOM-IPP Association, IPP Garching, F.R.G. During the current flat-top, the majority of discharges radiated (P_{rad}) away 70% to 100% of the ohmic input power (P_{Ω}). No obvious relationship could be found between this power ratio ($P_{\text{rad}}/P_{\Omega}$) and Z_{eff} , the plasma shape, or the density. Fig. 151 shows, for a series of discharges, the radiated power as a function of the ohmic input power. There is some indication that higher toroidal fields correlate with lower power ratios.

During the last weeks of 1984 operation, the Inconel walls of the vacuum vessel were ‘carbonised’ by running a glow discharge in a gas filling of H_2 with a few % CH_4 added. This significantly reduced the metals content of the plasma and reduced the radiated power to only ~40% P_{Ω} . Under these conditions, there is a weak dependence of the power ratio on density over most of the

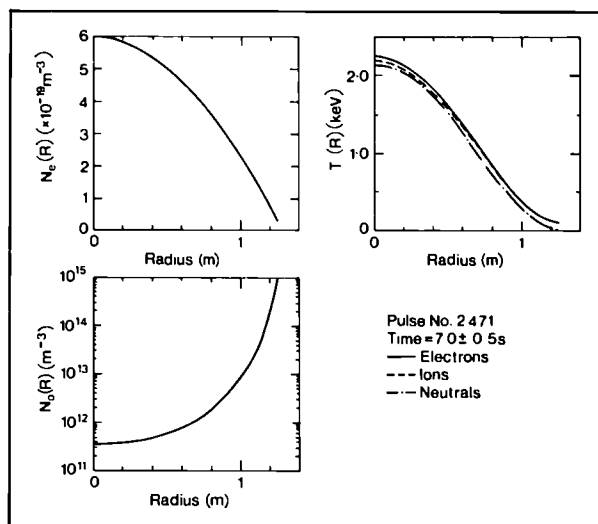


Fig. 145: T_e , T_i , and n_e profiles used in the computations (Pulse No.2471) and computed neutral density profile $n_o(r)$ at $t=7s$

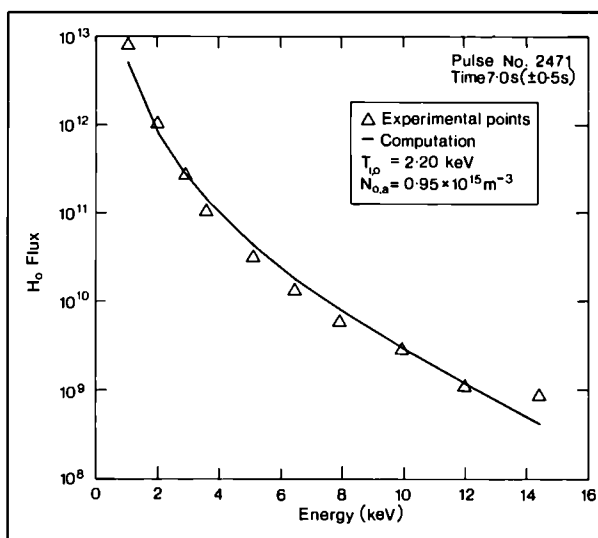


Fig. 146: Comparison between the experimental spectrum (triangles) and the computed one (Pulse No.2471, $t=7s$)

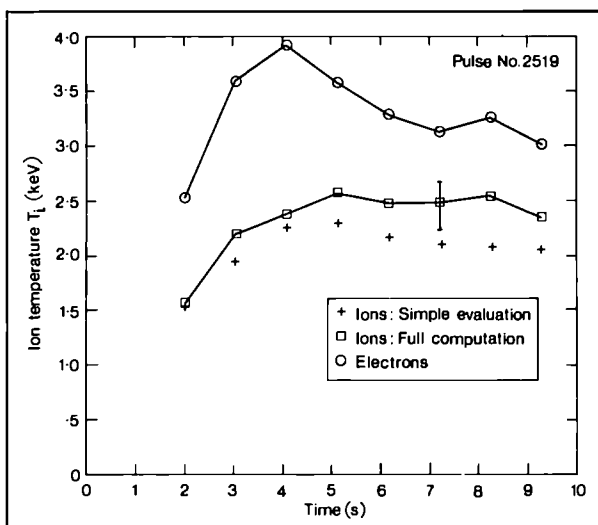


Fig. 147: Peak values of T_e and T_i versus time for Pulse No.2519 in deuterium

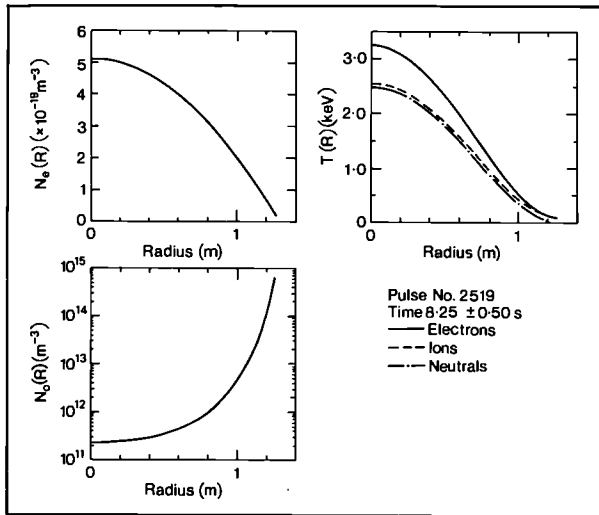


Fig. 148: T_e , T_i and n_e profiles used in the computations (Pulse No.2519) and computed neutral density profile $n_o(r)$ at $t=7s$

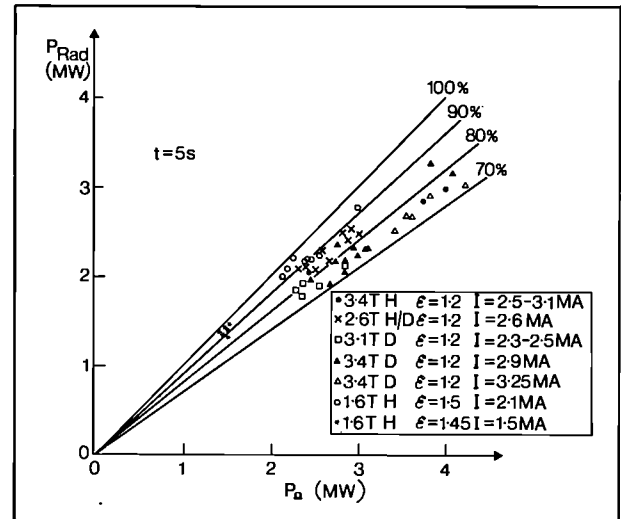


Fig. 151: Radiated power and ohmic input power for the flat-top of various discharges

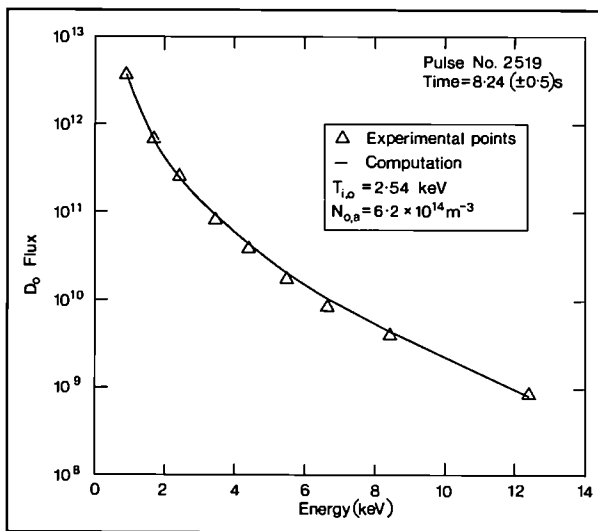


Fig. 149: Comparison between the experimental spectrum (triangles) and the computed one (Pulse no.2519, $t=7s$)

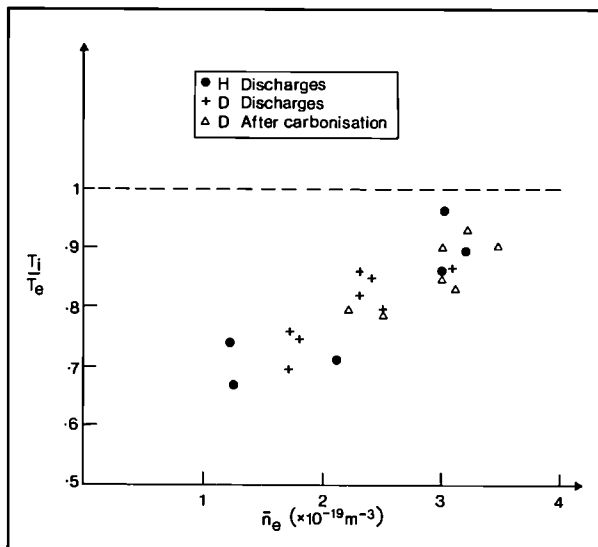


Fig.150: Ratio T_i/T_e versus density for a number of pulses

range and a rapid transition to 100% radiated power when the density limit is approached.

Measured profiles of the chord-averaged intensities were Abel inverted to give local emissivities using a simple variation to the standard method which assumes constant emissivity on nested circles. In this case, a set of nested ellipses with one common centre and constant ellipticity is assumed. The characteristics of these ellipses are taken from the shape of the outermost flux surface as determined from magnetic measurements. While this procedure is a good approximation to the actual flux surfaces at present, later additional heating and D-shaped plasmas will require a more general approach. A code which solves the inversion problem for an arbitrary set of nested surfaces was written and installed on the IBM computer. The nested surfaces of assumed equal emissivity are taken from another code which outputs the nested flux surfaces as determined from magnetic measurements, physical restraints, and the condition of magnetic equilibrium. As was expected, this code and the simpler one assuming nested ellipses agree well for present plasmas.

Fig.152 shows an example of an inversion using the IBM code. The upper part of the figure gives the measured intensities from all three cameras. The vertical camera data and the lower horizontal camera data are transformed into the viewing frame of the upper horizontal camera and thus can be drawn over the same coordinate which is the viewing angle of the upper horizontal camera. The plasma centre is normalised to a viewing angle of 0 rad. The lower part of the figure gives the result of the inversion, the local plasma radiation profile. The profile is hollow which is typical for JET discharges and the central radiation being less than 10kW/m^3 is an insignificant fraction only of the central ohmic heating (70kW/m^3).

Generally, lines of equal emissivity closely follow the plasma flux surfaces for discharges well below the density limit. In the vicinity of the density limit, strong

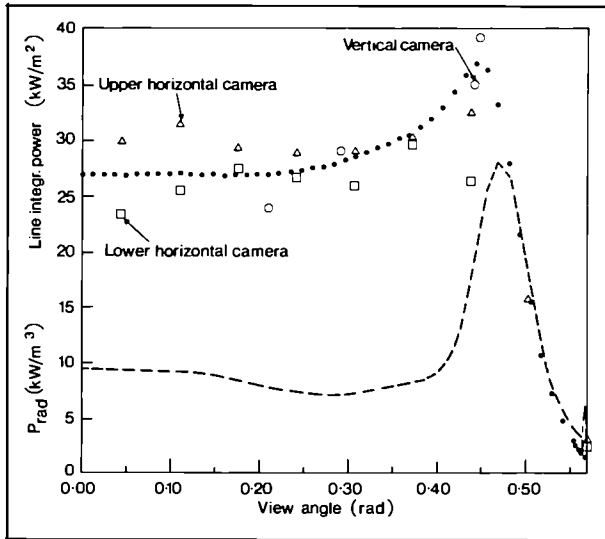


Fig.152: Measured intensities and inverted profile for Pulse No.3049. Circles indicate vertical camera data, triangles upper horizontal camera data, and squares lower horizontal camera data

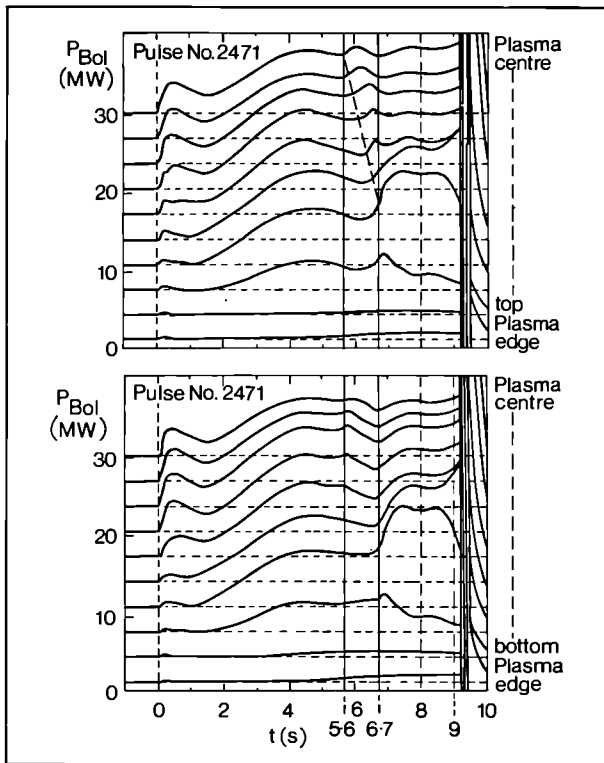


Fig.153: Bolometer signals for all channels of the two horizontal cameras showing up/down asymmetries

deviations sometimes occur. Fig.153 shows an example of the measured intensity of the 20 channels of both horizontal cameras. Up to $t=5.6s$, the upper half profile and the lower half profile agree well, but after this a strongly radiating 'blob' of plasma develops at the plasma edge, initially near the equatorial plane at the plasma inside. This blob then spreads upward (but not downward) along the plasma periphery until the whole plasma is surrounded by a strongly radiating mantle. At this stage, the plasma radiates away 120% of the ohmic

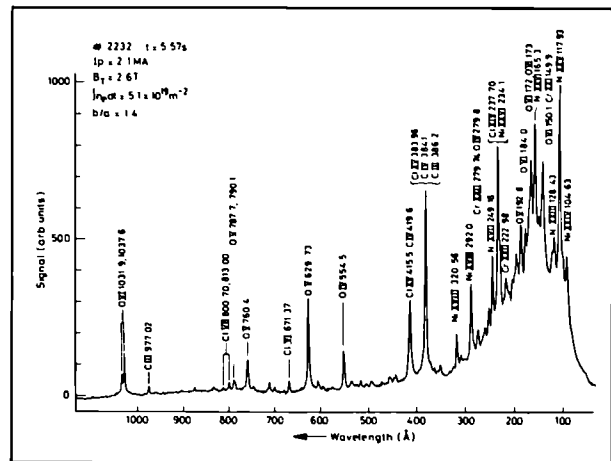


Fig.154: Spectrum in the region 10-100nm (100-1100 Å) for a medium-density plasma. The main emission lines are indicated (Wavelengths are marked in Å)

input power. After $t=8.5s$, the plasma starts to shrink in size and terminates disruptively.

VUV Broadband Spectroscopy (KT2)

(B. Denne, N.C. Hawkes+, M. Mansfield, N.J. Peacock+, A. Ravestein, J.L. Martin)
+ EURATOM-UKAEA Association, Culham Laboratory, U.K.

The spectral emission in the wavelength region 10-170nm is routinely monitored by the VUV broadband spectrometer (KT2). The spectrometer is normally operated using the grating with higher resolution (450 lines/mm, resolution $\sim 0.1-0.2nm$) of the two available, which limits the region observed to 10-110nm.

For a first sensitivity calibration of the spectrometer, Fonck's results [2] served as a guideline. The relative system response curve was modified slightly according to the observed relative intensities of hydrogen and oxygen lines. The absolute calibration is based on the $H_{\alpha}-L_{\beta}$ branching ratio. Usually, the VUV instrument was used in survey mode, i.e. recording about 70 complete spectra during a plasma discharge. These were taken in 16ms intervals during the break-down phase of the pulse and at 600ms intervals subsequently. In polychromator mode, the intensity of six spectral lines can be followed throughout the entire JET pulse, with 1.5ms time resolution.

Following operation on JET, the VUV survey spectrometer was installed on the ASDEX tokamak, in collaboration with EURATOM-IPP Association, Garching, F.R.G., to study charge exchange excited lines during neutral beam injection. The intensity ratios of these lines are well established theoretically allowing a relative sensitivity calibration of the instrument [3]. A preliminary analysis of the respective results essentially confirms Fonck's calibration curve.

As an example of JET data obtained, a spectrum during the flat-top of Pulse No.2232 (June 1984) is shown in Fig.154. (The plasma parameters relate to conditions

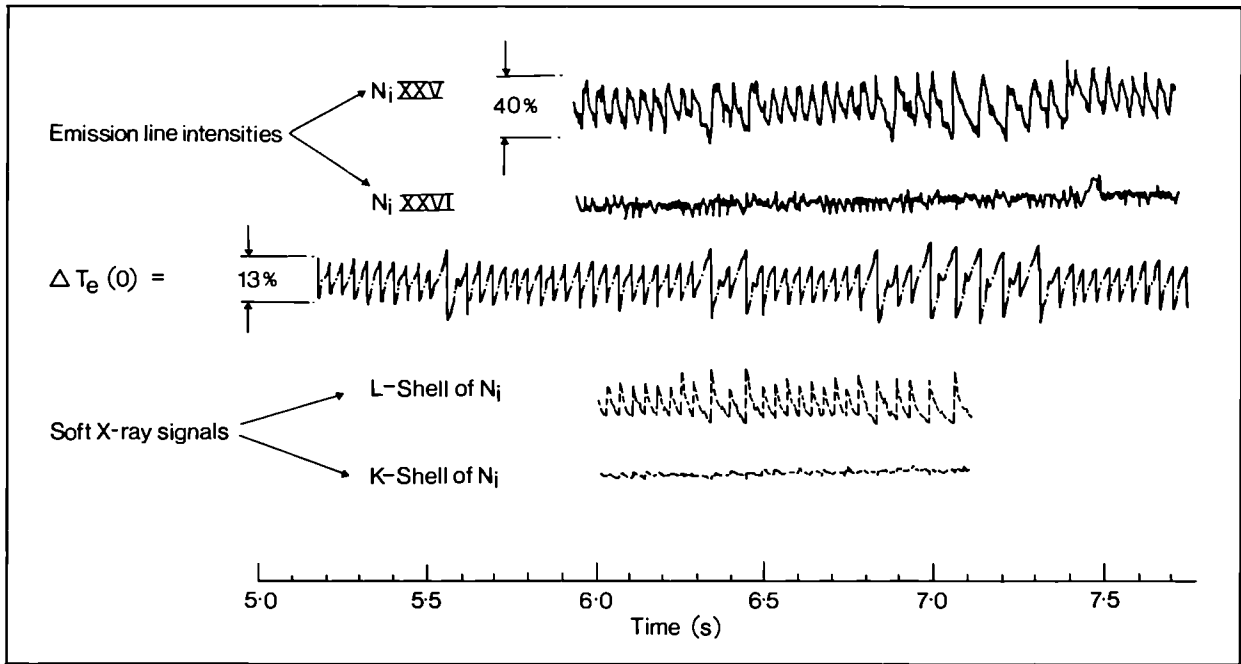


Fig.158: Sawtooth pattern observed by different JET diagnostics

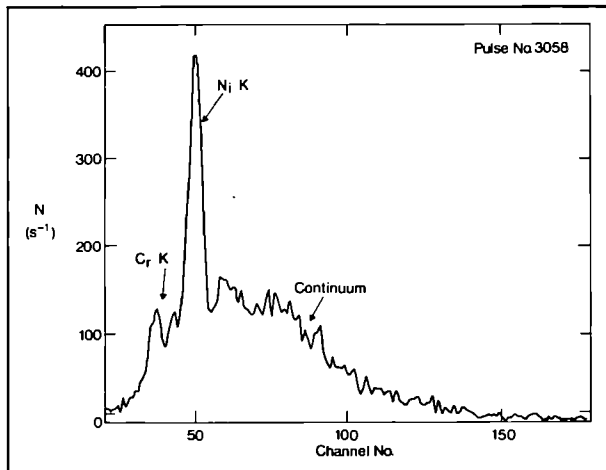


Fig.159: Example of measured X-ray Spectra

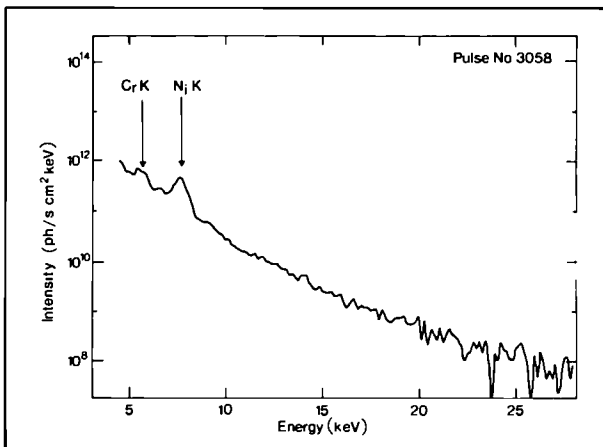


Fig.160: Semi-logarithmic plot of X-ray data

X-Ray Pulse Height Analysis

(R. Gill, E. Källne and G. Decker+, G. Braithwaite)
+ EURATOM-IPP Association, IPP Garching, F.R.G.

A single channel (horizontal central chord) X-ray detector has been mounted on Octant No.2 to observe the X-ray pulse height spectrum between 4-100keV. The X-ray detector consists of a mercury iodide crystal with preamplifier mounted directly at the torus looking through a 200 μm Be window. The line-of-sight has been defined with a dual set of fixed apertures (0.05 and 0.03cm) with a 60cm air path between. The flux at the detector was also controlled with an extra aluminium filter directly in front of the detector. The system was calibrated with a range of radioactive sources from 4 to 30keV and found to have a linear energy calibration. The efficiency of the detectors was tested with calibrated radioactive sources and found to agree with predicted values to within 20%. The resolution of the detectors was ±500eV at 6keV.

An example of the measured X-ray spectra is displayed in Fig.159. The characteristic Ni K and Cr K emission peaks are superimposed on the continuum spectrum. In Fig.160, the X-ray spectrum is displayed on a semi-log plot where the energy calibration of the instrument has been included and the data has been corrected for transmission in the Be foils and air path between the plasma source and the detector. The continuum slope measured between 10 and 20keV yields an electron temperature value of 3.2keV. The flux of X-rays at the detector has allowed time resolved measurements of the electron temperature during the plasma discharge. Comparisons have been made with the other electron temperature diagnostics on JET, the ECE measurements and the Thomson scattering and good agreement has been obtained.

Fig.161 shows a comparison of the ECE electron temperatures with the T_e obtained from the X-ray

spectrum. The analysis assumes parabolic radial profiles for the electron temperature and density. Good agreement is found, although there is a tendency for the X-ray continuum measurements to yield lower temperature values for the high current, high temperature shots. A few examples of non-thermal tails have also been observed.

The nickel impurity concentrations have been deduced from the line emission spectra at 7.7keV. The nickel line emission is found to increase steadily at the beginning of the pulse and to stay constant or to decrease during the flat-top and the decay of the pulse. Nickel concentrations have been deduced during the flat top of the pulse by accounting for the absolute intensity of the full area under the peak in Fig.159 and assuming the emission to be composed of $n=1$ to $n=2$ transitions in He-like nickel, using best values of available excitation rates. The concentrations of nickel were deduced thereafter by accounting for the relative abundance of H- and He- like nickel using a transport code. The nickel concentrations were also calculated from the line to continuum ratios using Z_{eff} values from the visible bremsstrahlung radiation. The nickel concentrations were found to be low for most operations of JET and were found to decrease rapidly with electron density. A comparison of nickel concentrations deduced from the VUV spectroscopy and the pulse height analysis is described later in the Report.

Impurity Analysis in Ohmically Heated JET Plasmas

(K.H. Behringer, J. Bonnerue, A. Bulliard, P.G. Carolan*, B. Denne, G. Decker+, W. Engelhardt, M.J. Forrest*, R. Gill, N. Gottardi, N.C. Hawkes*, E. Källne, H. Krause+, G. Magyar, M. Mansfield, J-L Martin, F. Mast+, P. Morgan, N.J. Peacock*, A. Ravestein, M.F. Stamp, H.P. Summers).

+ EURATOM-IPP Association, IPP-Garching, F.R.G.

* EURATOM-UKAEA Association, Culham Laboratory, U.K.

Visible Spectroscopy

As described in the 1983 JET Progress Report, signals of H_{α} and continuum radiation at 523.5nm are used to derive the hydrogen influx from walls and limiters, and to measure the plasma effective ion charge, Z_{eff} . For the latter analysis, Maxwell averaged Gaunt factors were calculated in a hydrogenic approximation as a function of temperature and ion charge, in agreement with Karzas and Latter [4].

Impurity lines in the visible spectrum were monitored routinely, during 1984 operation, and have been used to locate impurity sources in the torus and to derive impurity influxes into the plasma. The methods applied are essentially the same as described in the 1983 JET Progress Report, although knowledge of atomic data in this field has improved considerably. In 1984, the main emphasis was on interpretation of the VUV spectra obtained from the newly installed survey spectrometer.

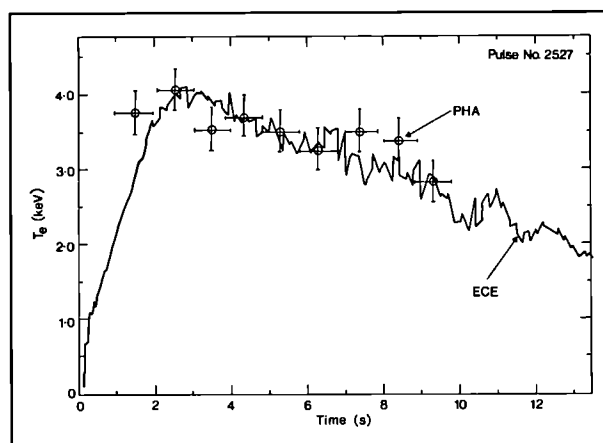


Fig.161: Comparison of ECE electron temperatures with those obtained from X-Ray measurements

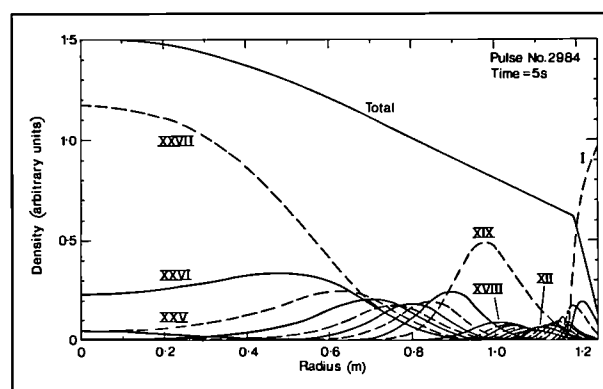


Fig.162: Radial distributions of nickel ground state densities as calculated by the impurity transport code

Analysis of VUV Spectra

To interpret the measured spectral line intensities in terms of impurity concentrations, line excitation rates and ionisation balance must be calculated from atomic physics models using measured plasma parameters for the respective discharges. Impurity transport modifies the ionisation equilibrium particularly at the plasma edge (i.e. the region of steep gradients), and is responsible for the radial profile shape of the total ion densities. In the present analysis, a numerical code [5] is used to describe the impurity behaviour, which solves, in cylindrical co-ordinates, the coupled set of time-dependent continuity equations for the individual ionisation stages of a particular element, taking account of ionisation, recombination and diffusion processes. The code calculates the radial distributions of ground state densities, as well as emission shells and line-of-sight integrals of selected lines for comparison with the respective experimental results. It also gives local and global radiation losses caused by line emission. The code has been set up to compute the time dependence of the above quantities after impurity injection or for changing plasma parameters. However, at present, only the stationary solution is being used for impurity analysis, during the stationary conditions of current and density

flat-top. The results presented were obtained between 4.4s and 6.8s in the pulse.

For the interpretation of JET spectra, the T_e profiles from ECE diagnostics were used in the code. Electron density profiles were taken from fixed-frequency relectometer measurements, except for the last few pulses of the 1984 operation period, when profiles from the multi-channel DCN interferometer became available. Conditions at the plasma boundary were estimated from an interpolation of ECE and Langmuir probe measurements. Fall-off length of density and temperature in the scrape-off layer were modelled to fit the probe data. An example of the calculated ground state distributions of nickel for Pulse No.2984, at 5s, is shown in Fig.162.

Rate Coefficients and Radiation Data

The ionisation rate coefficients are calculated as proposed by Lotz [6]. For the Na-like ions, where inner-shell ionisation is known to be important, correction factors to the Lotz formula have been calculated for the relevant temperature range and are implemented in the code. Inner shell ionisation enhances the total rate coefficients by a factor of two for Na-like chlorine and by a factor of three for Na-like nickel ions. Radiative recombination is treated in the usual way by applying the hydrogen formula and introducing effective quantum numbers. For dielectronic recombination, the Burgess prescription [7] with modifications by Merts et al [8] has been used. A density dependence of the latter rate coefficient has been adopted as suggested in [9]. For calculating individual resonance line radiation of one and two electron systems, a survey of the existing theories has been undertaken [10] and interpolation routines have been established. In order to calculate the total power emitted by line radiation, two effective resonance lines have been defined for each ionisation stage to account for $\Delta n=0$ and $\Delta n \neq 0$ transitions. For this purpose processed data sets are used based on f -values from Wiese et al [11,12] for light impurities and for chlorine, and from Fuhr et al [13] for nickel. An attempt has been made to fill in gaps by interpolation along the isoelectronic sequence. Line radiation is calculated according to a van Regemorter type formula [14], the Gaunt factors being taken from Mewe [15]. In the case of optically forbidden lines, the f -values of the allowed lines are used and the Gaunt factors are taken again from Mewe's prescription. The resonance line data for allowed transitions are also used for calculating the dielectronic recombination rate coefficients. Systematic improvement of the atomic rate data base is in progress.

Transport Coefficients

The fluxes of all elements and ionisation stages Γ_k are described by the sum of an anomalous spreading term and a convective term

$$\Gamma_k = -D \frac{\partial n_k}{\partial r} + V_D n_k \quad (1)$$

The anomalous diffusion coefficient D and the drift velocity V_D are probably a function of plasma parameters, but are assumed to be constant in the present analysis. In Eq.(1), n_k is the number density of a particular species. Due to an accidental impurity injection (Fig.157), evidence exists that the spreading coefficient D in JET is similar to that in other tokamaks, i.e. about $0.6 \text{ m}^2/\text{s}$. However, the magnitude of the corresponding drift velocity V_D , determining the radial profile shape of impurity densities, is not known, though a rough estimate is possible by analysing different ionisation stages of heavy impurities. In the past, the drift velocity was assumed to be given by [16]

$$V_D = -2Dr/a^2 \dots \quad (2)$$

resulting in moderately peaked radial profiles similar to those measured for electron densities. In the transport code, used for interpreting the JET VUV spectra, this same expression has been adopted.

The problems associated with the uncertainties of the transport model are of a different nature for the light and for the heavy impurities. At the present electron temperatures in JET, metal lines are observed in the VUV spectrum, emitted from the inner half radius of the plasma, where corona ionization equilibrium is expected to hold. Therefore, information on the metal content should be quite reliable from the transport viewpoint. Light impurities radiate only at the plasma edge, where both the electron density and temperature are poorly known. Then, the transport model must be used, in order to calculate the concentrations in the plasma interior. Due to these problems, the light impurity results at the plasma centre have large error bars.

Consistency of Analysis

The most important spectral lines, which have been used more or less routinely for analysis, are shown in Table XIV.

By means of the impurity transport code, the respective impurity densities in the plasma centre are calculated from line-of-sight integrals of these line intensities. The second transition, listed for two-electron systems of light impurity ions, is used to measure the metastable state population, which is particularly important for O V and Cl VI. The results for different ionisation stages of the same element are within about a factor of two (i.e. the expected error limits of calibration and excitation models). In the case of nickel, where ionisation stages are observed radiating within the inner half radius and right at the boundary, the radial profile assumed in the code is confirmed within the same uncertainty margin.

In all cases checked, calculations of the total radiation losses based on measured impurity densities are consistent with the bolometer results (i.e. the total radiated power). This is not surprising, since the strongest lines contributing to the bolometer signals are observed in the region of the present VUV instrument anyway and the impurity densities are derived from

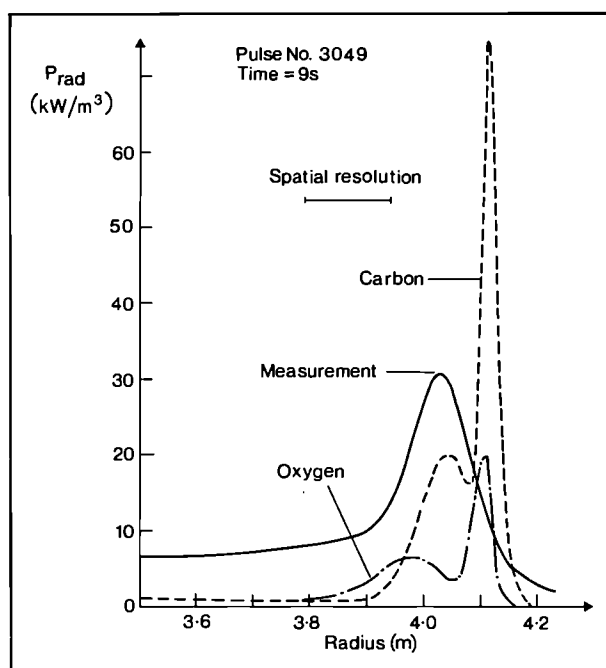


Fig.163: Part of the Abel inverted bolometer profile versus major radius. The limiters are at 4.11m. Calculated emission shells of carbon (3%) and oxygen (1%) are shown for comparison.

these particular lines. It is more difficult to compare measured and calculated radiation profiles. Examples of the code calculations are shown in Fig. 163, together with the Abel-inverted bolometer data. The local emission due to line radiation is shown computed for 1%O and 3%C, and for the respective discharge parameters. The spatial resolution of the bolometer (15cm in the respective midplanes) is not sufficient to resolve the individual shells. Taking into account spatial averaging, the height of the measured profile is in reasonable agreement with calculations. Its position is displaced by about 5cm, a value within the measurement error limits.

The Z_{eff} values derived from the measured impurity concentrations usually agree well with those derived from visible Bremsstrahlung, but sometimes differ as much as 1.5. Under normal conditions, this discrepancy cannot be explained by the uncertainties of the metal concentrations, as these hardly contribute to Z_{eff} . It must be attributed to light impurity results, which are less reliable, since these are only obtained for the plasma edge. Erroneous radial profiles in the code or insufficient knowledge of the plasma edge parameters may easily change the light impurity results by a factor of two, whilst their ratio is expected to be more accurate. Due to the usual consistency of the different ionisation stages of nickel, the second argument is thought to apply. In either case, a method of proceeding is to scale these numbers to explain the measured Z_{eff} or at least to be within the error limits of the Bremsstrahlung data. Unfortunately, for the period reported, the latter are disputable, too, because of the limited knowledge of density profiles, in addition to the usual uncertainties of intensity calibration and temperature measurements. This means that the

TABLE XIV
Most important impurity lines in analysis of the JET VUV spectrum

C III	97.70nm	+ C III	45.96nm
C IV	31.24nm		
O IV	55.43nm	+ O IV	62.51nm
O V	62.97nm	+ O V	76.03nm
O VI	103.19nm		
Cl VI	67.14nm	+ Cl VI	55.20nm
Cl VII	80.07nm		
Cl XIV	23.77nm	(+ Cl XIV	28.63nm)
Cl XV	38.40nm	(blended with CIV)	
Ni XII	432.12nm	(visible spectrum)	
Ni XVIII	29.20nm		
Ni XXV	11.80nm	(=30% correction due to NI XXII and Ni XXIV lines)	
Ni XXVI	16.54nm		
Cr XXII	22.30nm		
Fe XVI	33.54nm		
Mo XXXII	12.78nm		

spectroscopic results, usually being within ± 1 of the Z_{eff} values from Bremsstrahlung, are within the error limits of the latter anyway. Therefore, the light impurity densities presented are as derived from the code analysis, but it must be realised that the results have some uncertainties.

RESULTS

Important Impurities and Trends

Due to the presence of carbon limiters, carbon has always been an important impurity in JET. The carbon concentration in the plasma was 2-3% n_e , consistently throughout the operation period. The limiters are a main source of carbon influx, but the vessel walls are about equally important, in particular, when the plasma elongation is high and the boundary approaches top and bottom of the vacuum vessel. The carbon influx is a steep function of electron density, just as the hydrogen flux, but is almost insensitive to the plasma current, I_p . This means that the respective production mechanisms, hardly depend on temperature, but on the number of recycling hydrogen ions.

The oxygen level in JET has been much more variable and reflects the cleanliness of the vacuum vessel. Judging from the respective influxes, the torus walls are more effective oxygen sources than the limiter surfaces. Just as, in the case of carbon, oxygen production is not correlated with plasma current, but with electron density, n_e . However, since impurity shielding improves with n_e , the concentrations of both carbon and oxygen are weak functions of density for a particular experimental

campaign. The lowest levels of oxygen were achieved at the end of 1983 period, after extensive glow discharge cleaning, and in September 1984, after repetitive wall carbonisation.

Strong lines of chlorine were observed in the visible spectra during the JET start-up phase, but their significance was only realised when the first VUV spectra became available, and the usual resonance lines could be analysed. According to the latter results, several per cent of chlorine must have contaminated the first JET plasmas. Chlorine is thought to have been introduced into the torus by washing with a detergent. The chlorine level has decreased significantly in the course of operation and as a consequence of cleaning procedures. However, it is still an important impurity. In cases of strong plasma-wall interaction (e.g. high elongation or density limit studies), the chlorine fraction in the plasma is appreciable, and the VUV spectra may even be dominated by Cl lines.

Significant amounts of wall material, nickel, chromium and iron were found in the plasma particularly at low electron densities before carbonisation. The carbon limiters had already been identified in 1983 as the main source of these metal impurities. As confirmed by a post-mortem limiter surface analysis, these had been coated by wall material either during glow discharge cleaning or normal tokamak operation. Arcing and disruptions may play a significant role, too, melting and evaporating large amounts of metal. Molybdenum was found both in the plasma and on the limiter surfaces. It was deposited on the graphite tiles by accident during manufacture. However, it has always represented a minor fraction of the metals and has become less important during the operation period. Metal fluxes and metal densities increase with plasma current and decrease with electron density, a behaviour which had been observed before and which was detailed in the 1983 JET Progress Report. Furthermore, an inverse relationship was found to exist between metals and low-Z impurities, as has been observed in other tokamaks [17]. This behaviour may be explained by the sensitivity of metal sputtering rates to the plasma edge temperature.

The trends of light and heavy impurities, described above, lead to the usual steep decrease of Z_{eff} tends to be a rather weak function of n_e . In the first case, the radiative power losses, P_{rad} , are fairly constant, since the increase of n_e is compensated by a decrease of metal number densities. However, the radiation depends strongly on plasma current (1983 results). At high densities, metal impurities become insignificant and P_{rad} increases, usually up to 100% P_{Ω} at the density limit.

Impurity Behaviour prior to May 1983

During March-May 1984, VUV spectroscopy was only available during the last few days. On the other hand, the variety of different modes of machine operation made it impossible to carry out a similar analysis, as that in 1983, though the usual visible signals (i.e. O IV, C III and Ni XII) were recorded routinely. Judging from these data, metals remained fairly constant for comparable pulses.

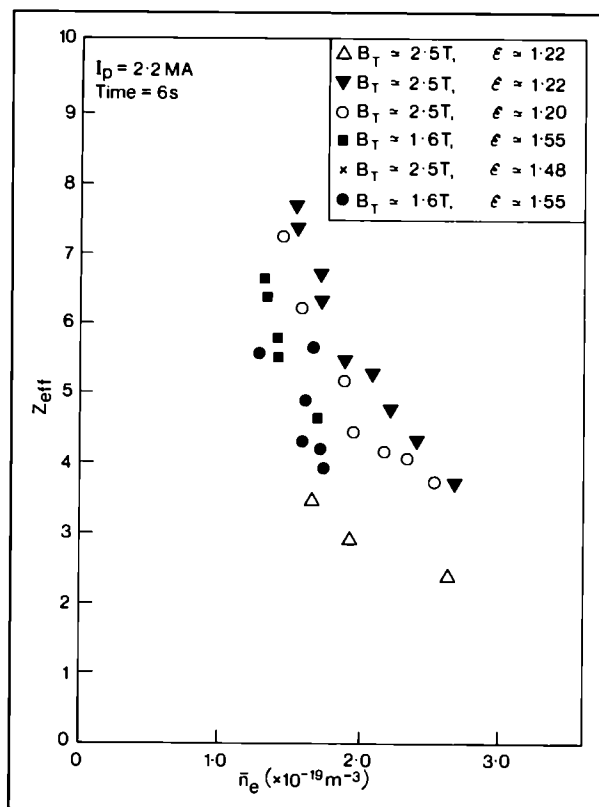


Fig.164: Z_{eff} versus n for several experimental campaigns. Open triangles are for December 1983, and Spring 1984 are other symbols. Higher Z_{eff} values belong to earlier operation periods

The carbon wall influx from top and bottom of the vessel increased considerably for vertically elongated plasmas generated during this period. The oxygen situation deteriorated somewhat during Spring operation. However, these observations could not explain the high values of Z_{eff} found particularly at the beginning of March 1984. A summary of Z_{eff} data from several experimental campaigns is shown in Fig.164, including some of the 1983 results. The measured Z_{eff} values did show the usual tendency to decrease with n_e , and the values were decreasing gradually in the course of operation, but never quite reached the lower 1983 results. A high fraction of radiation power (80-100% P_{Ω}) and flat radiation profiles confirmed that the plasmas were metal-dominated, as in December 1983. For a unknown reason, the pulses with lower toroidal field and with lower q radiated a larger fraction of the input power, usually close to 100% P_{Ω} .

When the first VUV spectra became available, it was realised that chlorine was an important impurity in JET, thought to have been introduced by the detergent used for washing. Since the torus had been washed again before March operation, a possible explanation for the high values of Z_{eff} may be a high chlorine contamination (up to 1.5% n_e would have been required), which reduced gradually in operation. However, there is no measurements to prove this hypothesis.

A detailed analysis of VUV spectra is available for Pulse No.2050, which is comparable to the 1983 plasmas

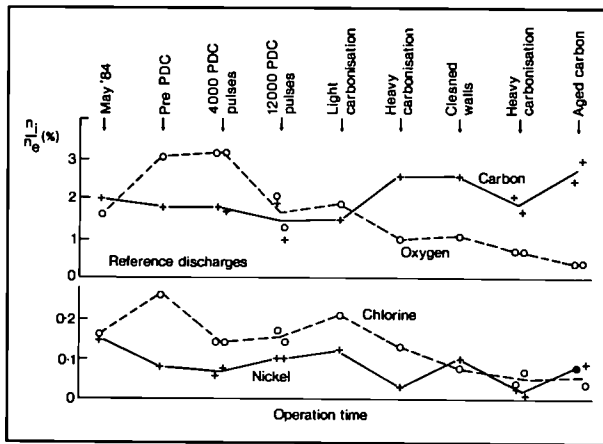


Fig. 165: Impurity levels derived from VUV spectroscopy for reference pulses during the period May-September 1984. The results demonstrate the consequences of PDC and carbonisation

(as well as to the later reference discharges to be discussed in the next sections). It had the parameters: $I_p = 2.3\text{MA}$, $n_e = 1.6 \times 10^{19}\text{m}^{-3}$, $B = 2.6\text{T}$, $\epsilon = 1.4$. The respective results for the metals are close to those claimed for the 1983 plasmas (i.e. a total metal content of about 0.2% (0.2%) and a ratio of Ni:Cr:Mo: of 9:1:0.5 (7:1:1). Iron was about 4% of the total metal content. The straightforward results for oxygen and carbon were 1.6% and 2% respectively. This meant that the carbon level was in good agreement with the 1983 result (2%), while the oxygen may have been somewhat underestimated (0.5%), though it had probably increased by a factor x2 in March-May operation. The chlorine fraction of Pulse No.2050 was found to be 0.16%. The respective values of impurity concentrations are marked on the left-hand side of Fig.165 as starting points for trends throughout the remaining operation time.

PDC Period

After four commissioning weeks, June and part of July operation was devoted to the assessment of the effectiveness of Pulse Discharge Cleaning (PDC). Glow discharge cleaning, used routinely previously was abandoned during this period in order not to confuse the PDC results. A total of 12000 PDC discharges was carried out, mostly in the Taylor mode $p < 10^{-5}$ mbar H_2 , $I_p = 30\text{-}40\text{kA}$, $B_T = 0.15\text{T}$, $t = 0.1\text{s}$, but some in the high power mode ($I_p = 400\text{kA}$, $t = 0.6\text{s}$). In order to study the plasma response, the parameters of a reference discharge were defined ($I_p = 2\text{MA}$, $b/a = 1.4$, $B_T = 2.5\text{T}$, $n_e = 2 \times 10^{19}\text{m}^{-3}$, which was repeated throughout the following operational periods and allowed an easy comparison of the plasma achieved. The development of impurities will be described referring to the data in Fig.165. However, it must be borne in mind, that only a few examples are being discussed, which are considered as representative. Even comparing pulses with the same gross parameters, the scatter in results is $\sim 20\%$.

The reference discharges before PDC showed an increase in oxygen and a respective reduction in metal

impurities compared to the May situation. After four week of commissioning, that is probably not surprising. However, the Cl level increased significantly too. After about 4000 PDC pulses, oxygen, carbon and nickel were effectively unchanged while the chlorine showed a reduction of about a factor x2. After 12000 pulses, there was some effect on oxygen, accompanied by an increase in metal concentration. Carbon and chlorine remained constant. These differences, which are all not dramatic, are essentially in agreement with the respective influxes of oxygen, chlorine and nickel. There was a change in the ratio of Ni:Cr:Mo, i.e. more chromium and less molybdenum were found after PDC, but again, the differences only minor. The total radiated power hardly changed during the PDC period and was about 80% \dot{P}_Ω . At the end of the PDC assessment, Z_{eff} was still about 5 for the parameters of the reference discharges. All together, 12000 PDC pulses seem not sufficient to have a major impact on the impurity situation in JET.

For the pre-PDC pulses, the following impurity influxes from the CII, CIII, OII, OIV and CrI signals were estimated:

$$\begin{aligned} \phi_c/\phi_H &= 0.20; \phi_{\text{WALL}}/\phi_{\text{LIMITER}} = 1 \\ \phi_O/\phi_H &= 0.15; \phi_{\text{WALL}}/\phi_{\text{LIMITER}} = 2 \\ \phi_{\text{METAL}}/\phi_H &= 0.02; \phi_{\text{WALL}}/\phi_{\text{LIMITER}} = 0.1 \end{aligned}$$

The limiter fluxes of carbon and metals are similar to those during 1983 operation. However, it was realised that, at the stage, the carbon wall production was similar to that on the limiters. For oxygen, influxes were higher than 1983 and the walls seemed to play a dominant role.

Reference Discharges after Carbonisation

After a period of high density and deuterium operation (see next sections), light and heavy carbonisations of the vacuum vessel were carried out to remove oxygen and chlorine, and to assess the influence of an all-carbon wall on plasma behaviour and metal contamination. After three commissioning weeks, less than one monolayer of carbon was deposited on the vessel walls and removed again before tokamak operation (light carbonisation). The impurity situation was then much the same as after PDC (see Fig.165), except that the chlorine recovered again after the break in operation.

During heavy carbonisation [18], about 50 monolayers of carbon were deposited on walls and limiters. This procedure affected plasma performance: Z_{eff} dropped, at least initially, the radiated power reduced to about 50% \dot{P}_Ω at moderate densities, and consequently, the carbon limiters heated up to as high as 1500C.

From the spectroscopic viewpoint, the main differences were a strong reduction in metals and an increase in carbon. The bolometer profiles became hollow and the central radiation was very low. Metals returned considerably after a weekend of glow discharge cleaning, and even after ageing of the carbon layer for two days. Oxygen and, in particular, chlorine declined gradually during the last weeks of operation, but not as a consequence of specific action taken. The conclusions drawn from the VUV spectra are well confirmed by the

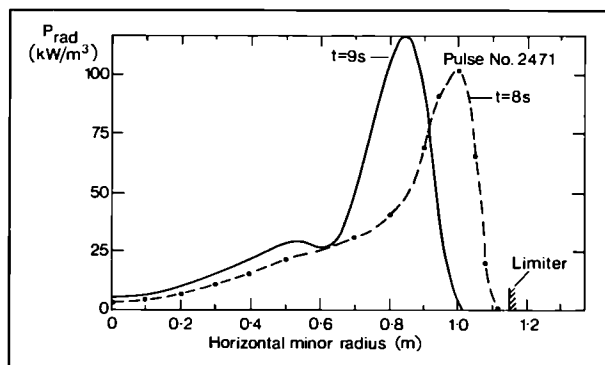


Fig. 166: Abel inverted bolometer results demonstrating the existence of a radiation mantle. It leads to a shrinking of the plasma radius and a disruption at 9.2s

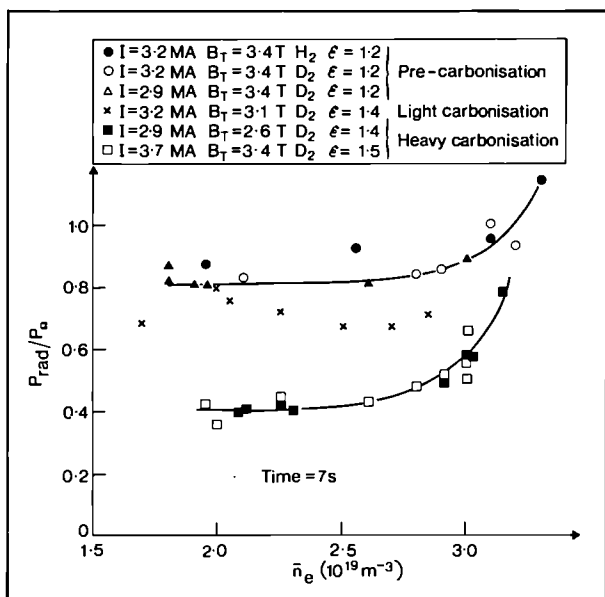


Fig. 167: Fraction of radiation power as a function of electron density before and after carbonisation

respective impurity influxes and Ni XII signals. The higher carbon level is due to an increased influx from the carbon limiters. The observed reduction of metal influxes from the limiters confirms the present idea, that metal depositions on the carbon limiter had been responsible for the metals problem.

When the limiter reached high temperatures at the end of the flat-top period of some pulses, a sudden increase in metal influx was observed, attributed to metal evaporation. It seems that due to this process the limiters were better conditioned throughout the remaining operational period, and metal influxes and densities never returned to such a high value as previously. It should be noted that during these limiter temperature excursions, the carbon influx (as derived from C II signals), followed the electron density in the usual way. There was no indication of the existence of chemical sputtering [19] expected to occur around carbon surface temperatures of 900C. On the other hand, the high carbon yield ($10\% \phi_H$) could be indicative of a temperature independent-chemical release mechanism.

Although carbonisation had the favourable effect of reducing metals and lowering the radiated power in the plasma centre, there was a problem of a high concentration of carbon in the plasma leading to a dilution of the working gas. Furthermore, disregarding the pulses immediately after fresh carbonisation, the values of Z_{eff} were again up in the range 4-5.

High Density Discharges

At the beginning of August, the toroidal field and plasma current were increased at moderate plasma elongation ($\epsilon = 1.2$). Then, average electron densities of about $3 \times 10^{19} \text{m}^{-3}$ were achieved in both hydrogen and deuterium at $I_p = 3 \text{MA}$, $B_T = 3.4 \text{T}$. Later on, similarly high densities were achieved at lower toroidal fields and lower currents, but at an elongation of $\epsilon = 1.4$. The consequences of carbonisation on high density plasmas were studied for different plasma currents (2.8-3.5MA), elongations (1.2-1.4) and toroidal fields (2.6-3.4T). Nevertheless, these discharges behaved quite similarly in many respects, though there was some scatter in individual results.

At high density and a significant level of light impurities, edge radiation cools the plasma boundary and reduces the production of metal impurities. Therefore, the metal concentration of such discharges was very low throughout, even before carbonisation. If the density is pushed even further the plasma may eventually detach completely from the limiter and shrink, as is demonstrated by the bolometer profiles of Fig. 166 for the later phase of Pulse No.2471. Before carbonisation, the level of oxygen and carbon could have been as high as 4%, but, there may be some problems in analysing the VUV signals because of poloidal asymmetries. After carbonisation, oxygen was reduced and the carbon stayed at about 2.5%, very similar to Fig. 165, but the analysis is not consistent in all details with that of the reference pulses. A consistent result was that chlorine showed a tendency to reduce and reached the very low level of 0.05% at the end of September operation. For high density pulses after carbonisation, typical impurity concentrations were 1%O, 2.5%C, 0.05%Cl and 0.015% metals, resulting in a Z_{eff} value of about 2.6. During the August-September operation, no significant changes in impurity levels was observed when changing the working gas from hydrogen to deuterium.

Radiation and Z_{eff}

The reference pulses after light carbonisation still radiated about 90% P_{Ω} . It was only after heavy carbonisation that the radiation levels for moderate densities ($= 2 \times 10^{19} \text{m}^{-3}$) reduced to 50% and even 40% after repetitive carbon deposition. Judging from spectroscopic results, this reduction was due to lower concentrations of oxygen and chlorine. The metals do play a role but, when these recovered significantly after removing the carbon layer, the increase in radiated power was only moderate, i.e. from 40% to 60% P_{Ω} .

For higher electron densities, the fraction of radiated power increased both before and after carbonisation. In

the latter case, however, it increased from a much lower level. This behaviour is demonstrated in Fig. 167. Going from low to high densities, the radiation in the plasma centre dropped from about 100 kW/m^3 to almost zero, while the edge radiation increased. JET high density discharges are obviously light impurity dominated and, after carbonisation, oxygen and carbon contribute about equal amounts to the total radiation.

Fig. 168 shows the measured values of Z_{eff} before and after carbonisation as a function of the ratio of electron density to current density, a presentation which accounts for the increase of Z_{eff} with current. Generally, the pulses with carbon have somewhat lower Z_{eff} values, accounted for by a reduction in oxygen and chlorine. The diagram also shows that higher electron densities have been achieved at a given current. The lowest Z_{eff} values in Fig. 168 are between two and three.

The nickel concentrations after carbonisation deduced from the X-ray spectra are shown in Fig. 169 as a function of line average density, \bar{n}_e . The trend of a decreasing nickel concentration with increasing \bar{n}_e is in agreement with data obtained from the VUV spectroscopy. The respective results are also shown in Fig. 169. The different methods give consistent values within the 30-40% error bars, although the values deduced from the pulse height spectra have a tendency to be lower by about 50% than those deduced from the VUV spectra.

Summary

During the first operational period in 1984, the impurity situation (as indicated by Z_{eff} and radiated power) showed a decline on 1983. The reason for this behaviour is not clear, since the levels found for the essential impurities (i.e. C, O, Ni) agreed very well with the 1983 results. However, chlorine was not monitored and only received attention when the first VUV spectrometer was installed at the end of May and strong Cl lines were observed in the VUV spectrum. The torus had been washed again before the 1984 operation; therefore, a high fraction of chlorine may well be responsible for the early 1984 results. The plasmas became cleaner gradually in the course of operation, although the oxygen level was increasing.

The following period of PDC assessment was expected to reduce light impurities and possible metals due to lower light impurity sputtering rates. However, the PDC campaign made little impact on the plasma impurities. Oxygen and chlorine concentrations were somewhat lower after PDC, but the metals had increased instead and there were only minor improvements in Z_{eff} and P_{rad} .

High density operation at high toroidal fields and plasma currents resulted in oxygen dominated plasmas with strong edge cooling and much reduced metal content. Poloidal asymmetries were observed in the radiation and sometimes a radiation mantle formed and led to a shrinking of the plasma radius.

By means of heavy carbonisation, metals were reduced, even at lower electron densities, and without high edge radiation. In the process of depositing and

removing carbon, both oxygen and chlorine reduced, leading to quite clean plasmas with radiation levels between 40% P_{Ω} (at moderate densities) and 80% P_{Ω} (close to the density limit). A drawback of carbonisation is the high percentage of carbon present in the plasma. At Z_{eff} values around 3, about 40% of the plasma electrons originate from impurities.

Generally, it was observed that light impurity concentrations hardly depended on plasma current or

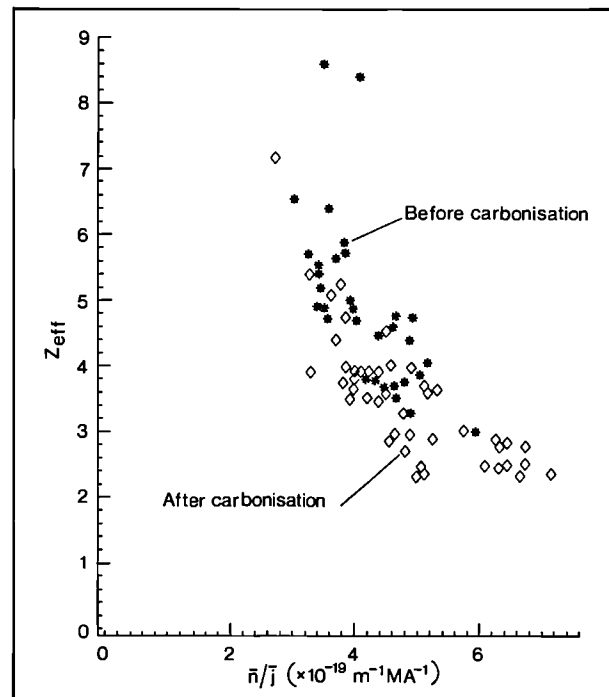


Fig. 168: Values of Z_{eff} before and after carbonisation;

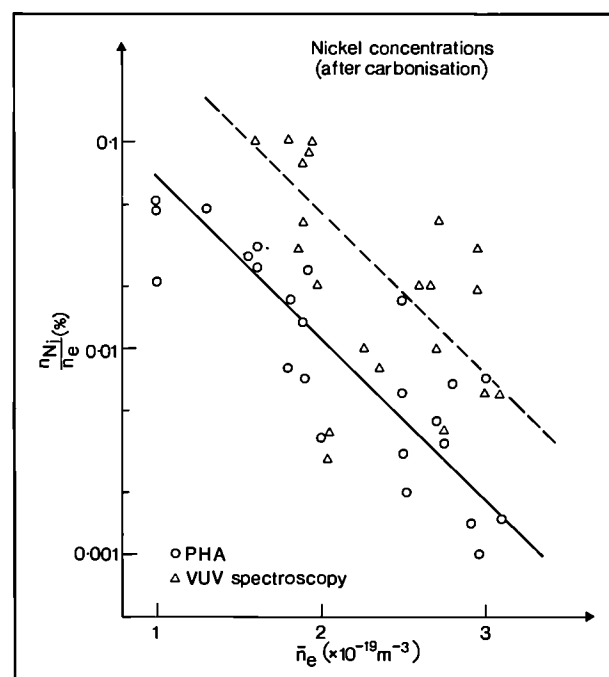


Fig. 169: Nickel concentrations derived from provisional PHA and from spectroscopy as a function of electron density.

electron density. Metals increased with current and decreased with n_e . An inverse relationship was found to exist between metals and low-Z impurities.

Typical impurity levels at the end of the 1984 operation were 1%O, 2.5%C, 0.05%Cl and 0.015% metals resulting in a Z_{eff} value of 2.6. According to code calculations, oxygen and carbon are responsible for the measured radiation losses and contribute about equal amounts. By means of longer operation and repetitive carbonisation, the oxygen level should be further reduced. This should allow higher electron densities and lead to very acceptable impurity levels, even if the carbon fraction remains in the range of a few percent.

References

- [1] B. Lipschultz, B. La Bombard, E.S. Marmar, M.M. Pickrell, J.L. Terry, R. Watterson, S.M. Wolfe, Nucl. Fusion 24, 977 (1984)
- [2] R.J. Fonck, A.T. Ramsey, R.V. Yelle, Appl. Opt. 21, 2115 (1982)
- [3] R.C. Isler, R.A. Langley, Appl. Optics 24, 254(9185)
- [4] W.J. Karzas, R. Latter, Astrophys. J. Suppl. No.55, 6, 167(1961)
- [5] K. Lackner, K. Behringer, W. Engelhardt, R. Wunderlich, Z. Naturforsch. 37a, 931,938 (1982)
- [6] W. Lotz, Lab. Reports IPP 1/62 (1967) and IPP 1/76 (1968), Garching, Germany
- [7] A. Burges, astrophys. J. 141, 1588 (1968)
- [8] A.L. Merts, R.D. Cowan, N.J. Magee, Los Alamos Scientific Laboratory Report LA-6220-Ms (1976)
- [9] D.E. Post, R.V. Jensen, C.B. Tarter, W.H. Grasberger, W.A. Lokke, Atomic Data and Nuclear Data Tables 20, 397 (1977)
- [10] H. Gordon, H.P. Summers, The Calculation of the Spectral Line Emission from Plasmas II, Culham Laboratory Report 1985 (in print)
- [11] W.L. Wiese, M.W. Smith, B.M. Glennon, National Bureau of Standards Report NSRDS-NBS4 (1966)
- [12] W.L. Wiese, M.W. Smith, B.M. Miles, National Bureau of Standards Report NSRDS-NBS 22 (1969)
- [13] J.R. Fuhr, G.A. Martin, W.L. Wiese, S.M. Younger, J. Phys. Chem. Ref. Data 10, 305 (1981)
- [14] H. Van Regermorter, Astrophys. J. 136, 906 (1962)
- [15] R. Mewe, Astron. Astrophys. 20, 215 (1972)
- [16] K. Behringer, W. Engelhardt, G. Fussmann, ASDEX-Team, Proc. IAEA Techn. Comm. Meeting on Divertors and Impurity Control Garching 1981, 42.
- [17] E. Hinnov, S. Suckewer, K. Bol, R.J. Hawryluk, J. Hosea, E. Merservey, Plasma Phys. 20, 723-734 (1978)
- [18] F. Waelbroeck, TEXTOR Team, J. Nucl. Mat. 121 378(1984) and private communications
- [19] J. Roth, Sputtering by Particle Bombardment II, Topics in Applied Physics Vol.52, p.91, Springer Verlag, Berlin, New York, Tokyo, 1983.

Theory Division

(Division Head: D.F. Duchs)

Theory Division is responsible for the prediction of JET performance by computer simulation, the interpretation of JET data and the application of analytic plasma theory to gain an understanding of JET physics. In addition, the Division assists in execution of the programme and in making proposals for future experiments, in collaboration with Experimental Divisions 1 and 2, the Physics Operations Group and the Operations and Development Department.

In comparison with the activities of 'traditional' plasma physics Theory Divisions, it is appropriate for a project such as JET that the tasks of a Theory Division are extended towards application and directed towards more specific development.

The central task of the Division consists in providing a quantitative theoretical model of tokamak plasmas, gauged in particular by JET data. The long term objective is to include in this model all essential quantitative plasma physics knowledge gained from JET (and other tokamaks) data, at least, through empirical description. It is preferable to have many mechanisms in the models understood theoretically in terms of basic physics principles.

The Division's 1984 research activities can be subdivided into the following subjects:

1. Data Banks (and computing hardware);
2. Data Management Software;
3. Code Libraries (Interpretation and Prediction);
4. Data Interpretation;
5. Modelling of JET Plasmas;
6. Comparisons of Model Results and Measurements;
7. Predictive Computations;
8. Analytic Plasma Theory;
9. Development of Methods.

Within the Division, these subjects are the responsibility of three groups; the Interpretation Group; Prediction Group; and Analytic Theory Group. The nature of these subjects require extensive cooperation and overlap with other Divisions, and to some extent also between the Groups.

A considerable amount of theoretical work has also been carried out through contracts, as follows:

Article 14-Contracts with Associations

Impurity diffusion package	IPP Garching, FRG
Neutral Beam heating	IPP Garching, FRG
MHD stability	UKAEA Culham, UK
Particle slowing-down	UKAEA Culham, UK
1 ½-dim transport code with free boundary	ENEA Bologna, Italy
Electron Cyclotron Emission	CNR Milano, Italy
Non-thermal ECE spectra	FOM Jutphaas, Netherlands
Plasma boundary identification	CEA Fontenay-aux-Roses, France
Global wave ICRF heating	CRPP Lausanne, Switzerland

Other Contracts

Autoionization	AERE Harwell, UK/ Queen's Univ. Belfast, N.Ireland
Charge exchange	AERE Harwell, UK
Atomic physics and plasma transport	Oxford University, UK.

On staffing, the ceiling for JET Posts had already been reached in 1983. The number of contract scientific programmers (for the whole Project) could, however, be increased from 6 to a maximum of 12.

The Division has hosted the following visitors, during the year:

As Associated Staff members: Dr. W. Feneberg (IPP, FRG); Prof. D. Pfirsch (IPP, FRG); Prof. E. Rebhan (IPP, FRG); Dr. A. Samain (CEA Fontenay-aux-Roses, France) and Dr. K. Thomsen (Riso/, Denmark).

As 'Visiting Scientists': Prof. B. Coppi (MIT, USA); Dr. W. Houlberg (ORNL, USA) and Prof. R. Zelazny (Institute for Nuclear Studies, Otwock-Swierk, Poland) made valuable contributions to the JET theoretical programme.

Under other arrangements (Fellowships, etc.), the Division had the benefit of being joined by Mr. P. Ashman, Dr. H. Hamnen, Ms. L. Lauro-Taroni, Ms. M. Lorentz-Gottardi, Ms. D. Sealey and Dr. F. Tibone.

The Divisions progress is described under the following subject activities.

1. Data Banks (and computing hardware)

The bank of raw data (JET Pulse Files) has been created by the Experimental Divisions and CODAS, and most of the evaluated data has been produced by Experimental Divisions and the Interpretation Group.

PPF and TRANSPORT Banks

(M. Brusati, J.P. Christiansen, J.G. Cordey, O.N. Gottardi, E. Lazzaro, R.T. Ross)

The Interpretation Group has been responsible for the setting-up and running of several data processing codes (see below), and for maintaining the storage of the processed data. Data from about 750 plasma pulses comprising approximately 630 Mbytes of processed data have been stored for pulses up to the end of 1984. The basic magnetics and line averaged density data are stored for all pulses, data from the FAST equilibrium code are stored for all pulses with a plasma current above 1 MA, (about 65% of 1984 pulses) and the results from ECE measurements and related calculations (e.g. confinement time, Z_{eff}) are stored for all successful flat-top shots.

Various high level summary data banks have been established. These include a short summary of each plasma shot, in the Diary bank, and a more complete set of data for good 'flat top' shots in the TRANSPORT bank. A more complete SURVEY bank is also being developed. At present, these data are held under the SAS data file system.

Technical Data Bank

(M. Brusati, A. Galway, D. Sealey)

A Technical Data Bank (TDB) for JET is being developed containing information of the machine hardware, such as diagnostics, coils, additional heating systems, etc. However, this is a long term project. At present, the TDB contains graphical and printed information on six of the major diagnostic systems.

IBM Computing Support

(J. Davis)

The use of the IBM and CRAY Harwell computers continues to increase. Currently, there are 147 IBM users from JET and the hardware available on the JET site has been expanded to accommodate this increased usage. The system comprises 20 colour graphics terminals and 44 non-graphics terminals controlled by 4 cluster controllers. Four Versatec printer plotters are available for printed or graphical output. In addition, there is an IBM5285 microcomputer with floppy disc unit, which facilitates the transfer of programs between the local NORD system and the IBM mainframe computer. Future developments planned, include the installation of a Laser Printer for graphics and other output, the use of some intelligent terminals (IBM3270-PC/GX) and a further 10 graphics terminals.

2. Data Management Software

Considerable effort has been spent in developing and adapting software for efficient storage, retrieval, display and monitoring the large JET data banks. Until now, the JET developed PPF storage/retrieval system has dealt well with most requirements, as did the display facilities and various specifically written directories. In addition, the SAS (Statistical Analysis System) package has been

adapted to JET needs and has been used widely for data evaluation.

To cope with future large data volumes, with manpower shortage, and with further requests for such items as data security and data processing speed, a number of commercially available database management systems have been screened and tested, and in December 1984 the DBMS NOMAD2 was purchased. It is intended that all the existing smaller ones should be merged into this system.

JET Pulse File Management

(M.G. Pacco, E. Springmann)

964 JET Pulse Files (ca. 2.2 GBytes) were produced during 1984. These are stored on 22 private MSS volumes and backed up on 13 tapes. Altogether, there are now 1601 JET Pulse Files (JPFs) produced in 1983 and 1984 (ca. 2.9 GBytes) stored on 29 private MSS volumes and backed up on 17 tapes. The JPF directory records their location. The data amount is expected to increase even more rapidly in 1985, so that an archiving procedure is being developed.

Data Processing and Data Display on the IBM

(R.T. Ross, A. Galway, B. Keegan)

A series of programs for the processing and display of data derived from the measurements from the JET diagnostics has been established on the IBM. The raw data from each shot, stored on the JET Pulse File (JPF), is transmitted to the Harwell IBM3085 central computer within a few minutes of the shot being completed. The processing of various diagnostic data (in particular the magnetics data) is initiated automatically and depending on the quality of the shot subsequent analyses programs are executed (for example the full magnetic analysis using the FAST code) and a set of characteristic traces are sent to a hard copy unit in the Experimental Control Room. Following an assessment of these data, a further series of analyses can be invoked to process the ECE and Neutral Particle Analyser (NPA) data, and run the second stage kinetic confinement analysis program CONKIN and finally produce a further set of plots.

Each of these programs writes data to a Processed Physics File (PPF). The PPF system has been significantly enhanced over the last 12 months. In particular the system of independent standardised files has been united into a data base system by the introduction of a directory facility which controls all the access and cataloguing of these files.

Processed data for all plasma shots is now stored on the PPF system and is easily available for display or input to other programs on the IBM or CRAY1A computers. Access to the raw data on the JPF has been simplified for many of the diagnostics by the introduction of a generalised access package GETDAT developed on the Nord system by C. Best (ED1) and subsequently installed on the IBM.

A general display facility, JETDSP, is available on the IBM. This can display any data stored on the PPF system

from any shot, together with any raw data signals from the JPF data that can be accessed with the GETDAT package. The system gives the choice of various layouts of plots, with interactive zoom and pan facilities.

Processed Pulse File Management

(B. Hodge, M.G. Pacco)

The number of PPFs increased rapidly in 1984 and it was necessary to write utilities to extend and compress the PPF directory.

Interactive System for JET/SAS Data Bases

(T. Cox, M.G. Pacco, E. Springmann)

SAS (Statistical Analysis System), a data retrieval and manipulation system already available on the IBM system at Harwell, was provisionally selected to store the first 'high level' data bases set up on the IBM system. These databases consist of tables of parameters which characterise the JET pulses. At present there are two: DIARY, which contains small amounts of information on every plasma shot, and TRANSPORT, which contains data from shots used in transport studies.

An interactive system was designed for use by persons unfamiliar with SAS. It allows the user to display and print the data bases, select subsets, add new variables, plot variables against each other, overlay curves, save and print selected pictures.

Study and Evaluation of Data Base Management Systems

(M.G. Pacco, E. Springmann)

The SAS system is too limited and inflexible to manage the large physics data bases, which should be made available on JET. Therefore it was decided to investigate whether commercially available Data Base Management Systems could be used for JET purposes.

According to requirements, a shortlist of possible systems was set up. This included: ADABAS, BCS/RIM, IBM DB2, FOCUS, MODEL 204, NOMAD2, ORACLE, RAMIS II, and RAPPORT. The study of these systems showed that none had been designed to optimise the use of scientific/engineering data. Nevertheless, two seemed to possess sufficient features to be suitable for JET; these were MODEL 204 and NOMAD2.

Both systems were tested at JET. To perform meaningful tests, a database consisting of two files was designed: the first file contained scalar parameters characterising the JET pulse, the second one contained physical quantities as functions of time characterised by pulse number and diagnostic name. Real JET data was loaded into the databases.

User-friendly menus were written for both systems to use interactively the data bases (selection of pulses, addition of new fields, modification of values, display of data, plot of functions). The same functions were also needed using a FORTRAN program. Therefore, a FORTRAN interface to access the data bases was written. Both tests were successful, i.e. both systems

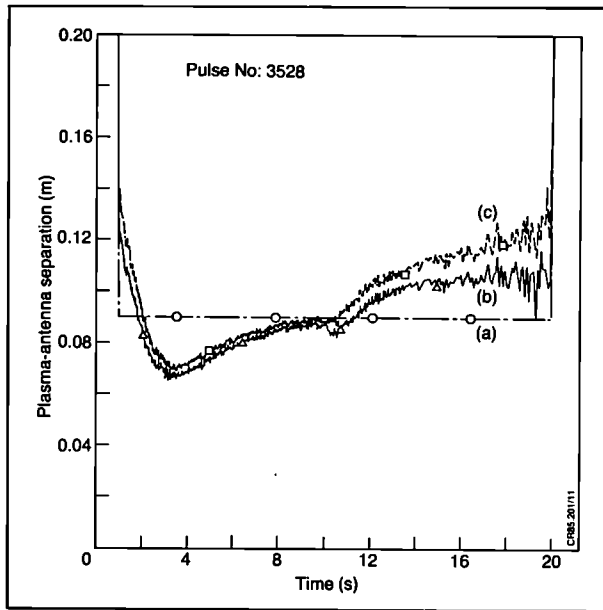


Fig.170 Pulse No. 3528: Plasma-antenna distance as a function of time (a) at antenna centre ($Z=0$); (b) bottom of antenna; and (c) top of antenna.

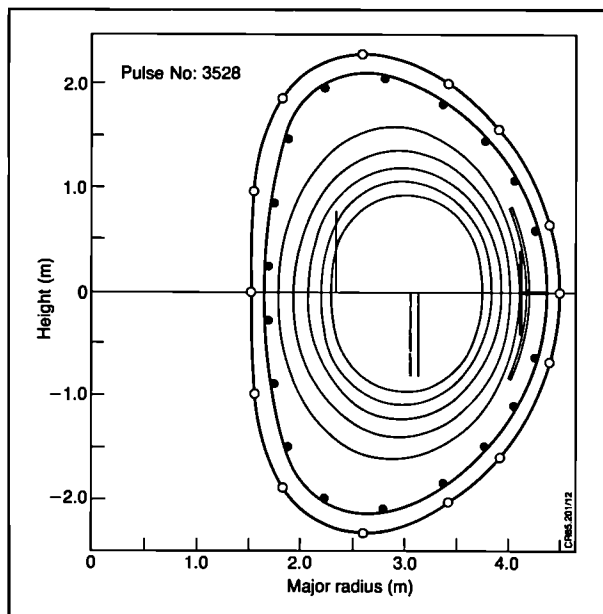


Fig.171 Surfaces of constant P.S.I. on plasma cross-section (Pulse No. 3528).

could manage JET data and satisfy most requirements.

MODEL 204 offers a more flexible data file structure. NOMAD2 provides a better handling of floating point arrays and a user-friendly user language. However, in view of its lower price, NOMAD2 was purchased.

3. Code Libraries

For most diagnostics, programs for first level data evaluation have been developed for the local NORD computers. With increasing refinement and consequently increasing demand for computing power, and with

decreasing availability of the CODAS computers for data evaluation, the codes had to be transcribed to or even rewritten for the mainframe IBM and CRAY computers.

A systematically maintained collection of codes, the JET Interpretation Code Library, has been started. Proper documentation is expected soon; then the library will be made available to JET personnel. A similar collection for predictive codes, the JET Prediction Code Library, is planned for 1985.

Intershot Analysis on the NORD EC Computer

(J.P. Christiansen, K. Thomsen, E.M. Jones, J. McDonald, A. McPhail, S. Cooper, P. Lallia)

Extensive timing-performance tests have been undertaken on the NORD version of the intershot analysis code FAST which gives a preliminary analysis of magnetic data. As a result of these tests, modifications were made to both the computer and the code which significantly increased the speed of this analysis so that the first results are now available (about 80-100s after the data arrives at the EC computer).

Recently three new features have been added to FAST to assist with the intershot interpretation of ICRH data. These are:

- i) the matching of plasma shape to the antenna wave pattern. To assess how well these are matched the normal distance from the antenna screen to the plasma surface is calculated as a function of time. An example of the output for a typical shot is shown in Fig.170 where distance from the bottom, middle and top of the antenna is given versus time. For this particular shot the optimum matching would occur between 8s and 10s, when the plasma shape matches that of the antenna;
- ii) The position of the various resonance and cut-off lines. The position of these, together with the shape of the antenna, are presented as in Fig.171;
- iii) Absorption indicators for the minority heating scenario. The indicators are a first attempt to estimate that fraction of the total power that is coupled to the electrons and minority ions. An example showing the time behaviour of these absorption indicators is given in Fig.172. (The theory behind the indicators has been carried out in collaboration with Drs. Brambilla and Lallia).

Intershot Analysis on the Harwell IBM

(J.P. Christiansen)

During 1984, all plasma pulses with $I_p > 1\text{MA}$ (455 pulses) have been analysed by the intershot analysis program FAST. Each of the 62 physics quantities calculated by FAST contains 1000 values at discrete time intervals during the JET pulse; a time interval is typically 10ms. These 62 quantities are stored in the JET data bank of PPF files and are retrieved for subsequent analysis, e.g. either display or processing, on a regular basis.

The results from FAST are used by the ECE program and the global confinement program CONKIN.

Global Confinement Intershots

(J.P. Christiansen, J.G. Cordey)

The data from the neutron yield monitors (KN1), the visible Bremsstrahlung, H_{α} emission (KS3), and ECE temperature data (processed) are analysed by a global confinement program CONKIN. During 1984, all plasma pulses with $I_p > 1\text{MA}$ and ECE data have been analysed. Each of 24 physics quantities calculated by CONKIN contains 1000 values at the same time intervals as that of FAST. These 24 physics quantities are also stored in the JET data bank of PPF files. Fig.173 shows a few of these parameters versus time for a typical shot.

Installation of Diagnostic Codes on the IBM System

(M. Brusati, A. Galway)

During 1984, two codes were installed on the IBM system to provide the first stage of data reduction for the Electron Cyclotron Emission (ECE) and the Neutral Particle Analyser (NPA) diagnostics. In both cases, the running of the codes is performed via CLIST commands

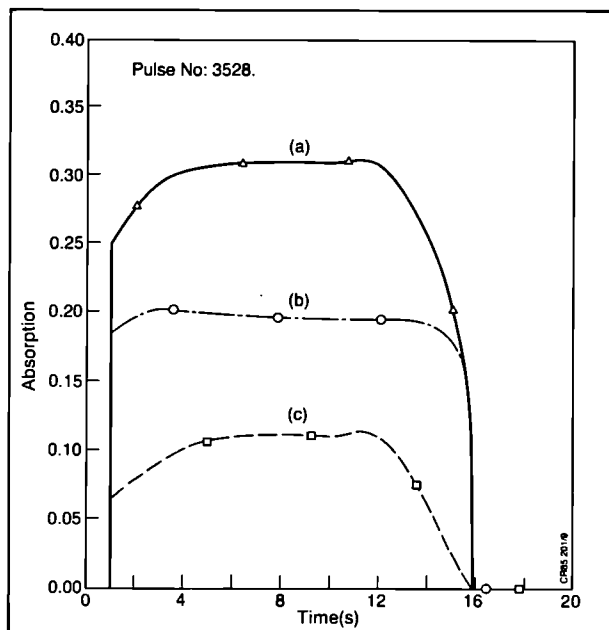


Fig.172 Absorption Indicators: (a) total power absorption; (b) electron power absorption; and (c) minority power absorption.

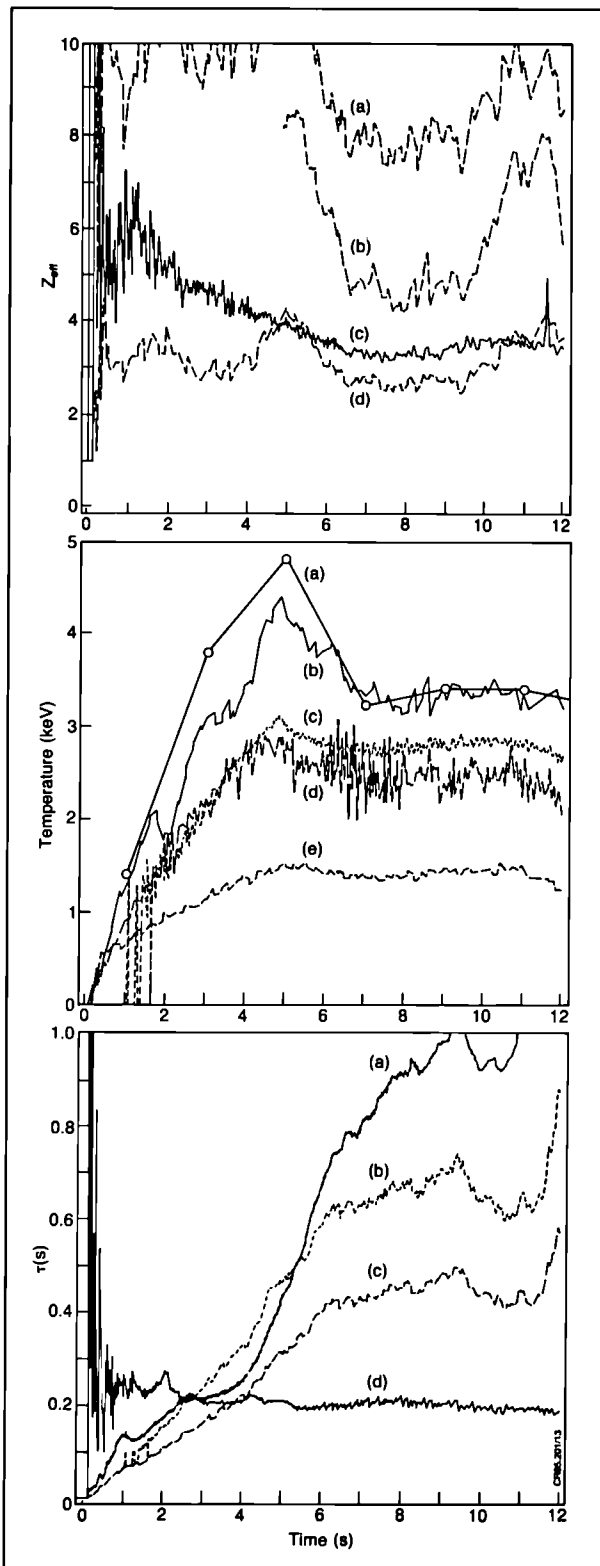
Fig.173 Pulse No. 3050:

- (i) Z_{eff} versus time: (a) Spitzer resistivity; (b) Axial; (c) Bremsstrahlung; (d) Neoclassical resistivity;
- (ii) Temperature versus time: (a) Thomson scattering electron temperature; (b) Axial electron temperature (ECE); (c) Axial ion temperature; (d) Deuteron ion temperature (NPA); (e) volume average electron temperature (ECE);
- (iii) Confinement time versus time: (a) electron particle confinement time; (b) kinetic confinement time; (c) MHD confinement time; (d) Edge particle confinement time.

in an user-friendly manner. The results of the analysis (ECE spectra, T_e profile, fast neutral fluxes and T_i time evolution) are filed automatically in the JET PPF database system.

4. Data Interpretation

In addition to the actual data interpretation, a great deal of effort has been spent in direct data validation and consistency checks of data from various diagnostics.



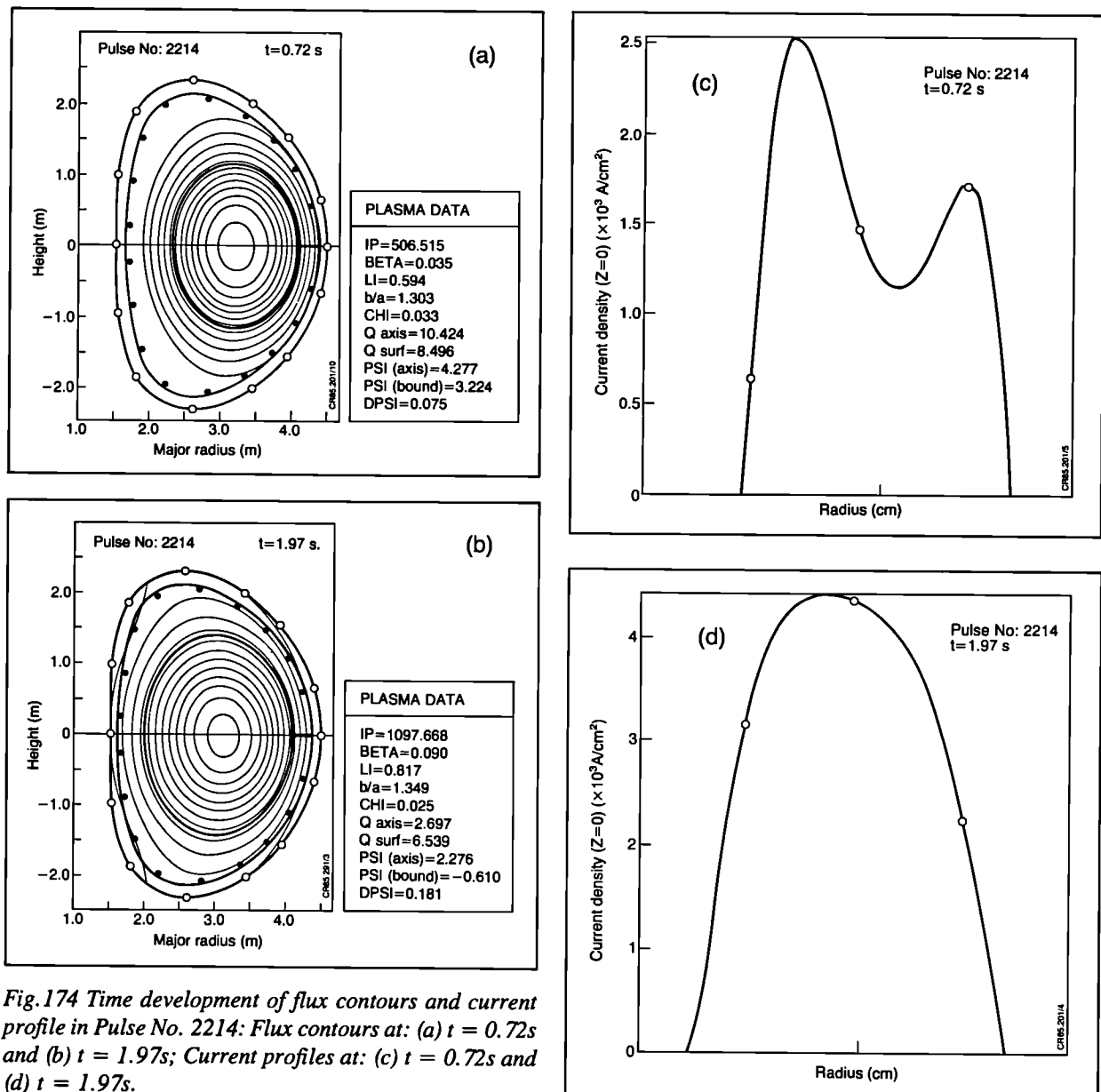


Fig.174 Time development of flux contours and current profile in Pulse No. 2214: Flux contours at: (a) $t = 0.72$ s and (b) $t = 1.97$ s; Current profiles at: (c) $t = 0.72$ s and (d) $t = 1.97$ s.

Analysis of Magnetic Measurements

(J.P. Christiansen, J.G. Cordey, E. Lazzaro)

The magnetic data from the magnetic loops (KC1) and (KC2) has been analysed by IDENTB and FAST5 in an extensive series of calculations on a few JET pulses of different plasma shapes. Investigations have shown that plasma shape and safety factor q deduced by the two analysis methods differ by 1-2%. A comparison between the plasma beta β_{MHD} calculated from the MHD magnetic analysis by IDENTB and FAST5 and the β estimated from other JET diagnostics shows a systematic difference: $\beta_{\text{MHD}} < \beta$ is found for all plasma shapes, the discrepancy increases with increasing circularity of the plasma shape.

Linear and non-linear error analysis methods have been applied to the analysis of magnetic measurements. For an assumed relative error of 2% on the magnetic

data, the following estimates of accuracy are found (Pulse No. 1353):

- Plasma width : 1.14 ± 0.019 m
- Plasma height : 1.72 ± 0.037 m
- Safety factor : 5.41 ± 0.226
- Plasma inductance : 1.15 ± 0.023 mH
- Plasma beta : 0.17 ± 0.014 .

Equilibrium Identification During Current Fast Rise

(E. Lazzaro, in collaboration with R. Gruber of EURATOM-Suisse Association, CRPP Lausanne, Switzerland, and J. Blum of EURATOM-CEA Association, CEA Fontenay-aux-Roses, France)

The identification of MHD equilibria during the current rise poses special problems due to skin effects in the plasma eddy currents in the tokamak vessel. A

preliminary study carried out with two magnetic identification codes (IDENTB and JETEQU) showed that in JET the early evolution of the current density is very often decoupled from that of the electron temperature. It is possible to have hollow (skin) current profiles associated with peaked temperature profiles, and often a very fast anomalous peaking of the current channel is related to observed MHD activity. From analysis, it appeared that to obtain a proper identification of the inner characteristics of the plasma equilibrium, such as the value of internal inductance (β_i), poloidal beta (β_p) and safety factor on axis ($q(0)$) compatible with the appearance of MHD activity ($m=1$ sawteeth, $m>2$ tearing modes), it was necessary to modify the physical constraints under which the 'optimal' solution of the Grad-Shafranov equation is found. A new magnetic identification code was designed and subsequently constructed by J. Blum (IDENTC). This code allows identification of hollow current profiles and the fitting of internal pressure profiles, if available from the ECE and interferometer diagnostic. An example of the time development of the current profile and flux contours from this new code is given in Fig.174.

Observation of Formation of a Magnetic Separatrix Inside the Vessel

(E. Lazzaro, F. Alladio*, F. Crisanti*, A. Tanga)
 *EURATOM-ENEA Association, ENEA Frascati, Italy.

The terminal stage of many JET discharges feature divertor-like configurations with two magnetic stagnation points. This phenomena is related to an increase of β_p and the special permeability distribution of the JET iron core during that stage. Analysis of the behaviour of the iron core and of the shaping poloidal field coils has been undertaken, to extend this performance to higher plasma currents.

Model for the Analysis of MHD Helical Perturbations

(E. Lazzaro, F. Alladio*, F. Crisanti*)
 *EURATOM-ENEA Association, ENEA Frascati, Italy.

A complete magnetic data analysis in tokamaks should include an accurate reconstruction of the axisymmetric flux structure and also information on the island structures produced by resistive tearing modes. The objectives of a tearing mode identification code are the evaluation of island location, width and rotation, for a mode of chosen helicity (m,n). A theoretical model has been developed which links the measurable MHD fluctuation signals to the tearing mode instability parameter $\Delta'(0)$, in the proper non-circular, toroidal geometry of JET. A code has been produced and used to analyse a number of disruptive discharges, a typical result is shown in Fig.175. The results show that the $m=2$ island rotation generally stops just before the final burst of the disruption.

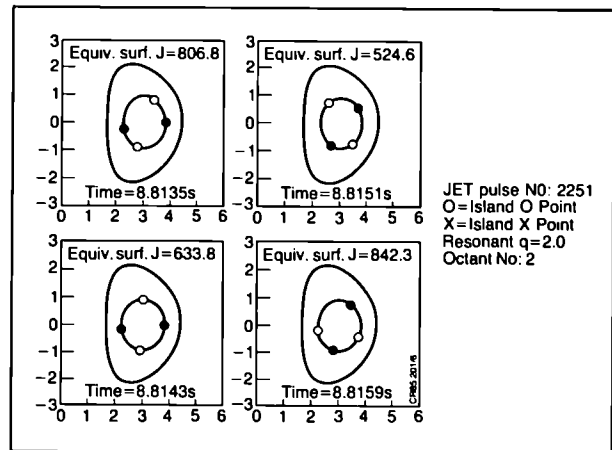


Fig.175 Rotation of $m = 2$ magnetic island in Pulse No. 2251, shown at times: (a) $t = 8.8135s$; (b) $t = 8.8143s$; (c) $t = 8.8151s$; and (d) $t = 8.8159s$.

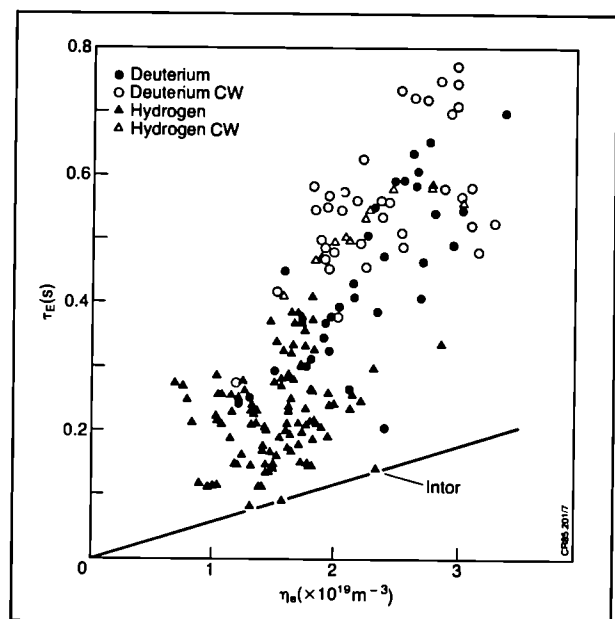


Fig.176 Global energy confinement time, τ_E , versus density, showing pulses taken in both deuterium and hydrogen plasmas and with and without carbon walls (CW).

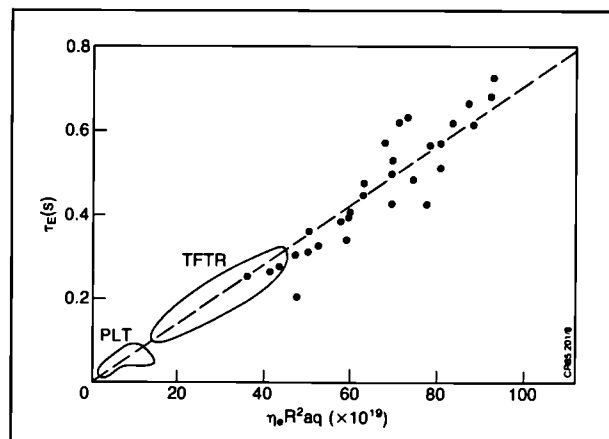


Fig.177 Global energy confinement time, τ_E , versus scaling law $n_e R^2 a q$. Results for PLT and TFTR are shown for comparison.

Global Energy and Confinement

(J.G. Cordey, J.P. Christiansen)

The global energy confinement properties of JET have been examined through the various phases of operation, during 1984. A high level data bank (TRANSPORT) has been set up to contain the data which is all extracted at the end of the current flat-top, when the plasma is close to steady state. The data is stored under the data management system SAS which is used to manipulate and display the data.

The global energy confinement time, τ_E , is found to increase initially with density (Fig.176) as in many other experiments. At the highest densities, there was some evidence of saturation of τ_E which was identified as due to an increase in radiated power with density. In Fig.176 the energy confinement time in deuterium is about 20% higher than in hydrogen, and that confinement was marginally improved after wall carbonisation.

In an attempt to determine the scaling of the energy confinement with plasma parameters, regression analyses have been completed using several combinations of basic parameters. Due to the rather limited range of parameter variation and the usual problem of the interdependence of parameters, it was not possible to obtain a precise conclusion. The best fit found so far was $\tau_E \propto nq$ (q is the cylindrical safety factor); which fits with data from smaller experiments if an R^2a dependence on plasma dimensions is assumed, as shown in Fig.177.

Local Transport Analysis

(M. Brusati, A. Galway, D. Sealey, P. Ashman)

The interpretation code JICS has been used extensively to obtain information on the power balance of ions and electrons for a variety of JET ohmic plasmas. It was found that the electron balance was dominated by heat transport in the plasma core, while for regions beyond the location where $q=2$ these were dominated by radiation. Radiation losses were responsible for the saturation of confinement with density. The ion balance was dominated by conduction up to the plasma periphery and convection only became significant close by the plasma boundary.

Further studies were undertaken to identify local transport coefficients. It was found that, in the MHD stable region $1 < q < 2$, the electron heat diffusivity, χ_e , was well represented by the scaling law:

$$\chi_e = 3 \times 10^{19} n_e^{-1/2}$$

for different toroidal field strengths ($2T < B_T < 3.4T$) and current levels ($1.8MA < I_p < 3MA$).

Sawtooth Oscillations

(T.E. Stringer)

The periodicity of sawteeth on soft X-ray and ECE signals has been compared with predictions. The periods observed before 1984, which varied from 30ms to 60ms agreed fairly well with the McGuire and Robinson predictions. More recent pulses have not shown the full

increase in period predicted for the higher density and temperature.

The temperature perturbation around the $q=1$ surface, associated with the sawtooth reconnection, diffuses outwards with time. At distant points, it appears as a temperature pulse, whose arrival time depends on the electron thermal diffusivity. The Soft X-Ray (SXR) signal is at present measured only along a central chord, so the pulse propagation must be studied using other effects. Identifying the periodic increase in H_α signal with the arrival of the temperature pulse at the plasma edge, a value is deduced for the effective electron thermal diffusivity, which is about twice that derived from energy confinement. In an attempt to explain this discrepancy, the influence of several effects such as impurity radiation on the pulse propagation has been studied.

The energy balance equations describing the increase in the electron and ion axial temperatures during the sawtooth recovery phase can be used to evaluate various parameters. Immediately after reconnection the temperature profiles are flattened, and the thermal conduction loss is relatively small. Energy balance is then used to derive Z_{eff} on axis. The resulting value is typically about 30% less than the global value deduced from Bremsstrahlung. An estimate of the electron thermal diffusivity on axis can be made from the change in dT_e/dt during a recovery phase, obtained from the ECE signal.

Vertical Instability

(J.A. Wesson, H. Niedermeyer)

The vertical instability of the JET plasma has been analysed. Using the measured electric and magnetic fields the force on the plasma has been calculated, allowing a determination of the force on the vacuum vessel. For Pulse No.1947, this force had a maximum value of $\sim 250t$.

Current Formation

(J.A. Wesson, M.F. Nave)

The experimental observation of a narrow current channel early in the discharge (when $q = 11$) has been explained in terms of a theoretical model based on a radiation instability. This instability allows current to form around the axis without skin current formation.

5. Modelling of JET Plasmas

The Prediction Group is largely responsible for this central task within JET Theory Division. Both the geometry of JET and the plasma phenomena necessitate up-dating of existing and development of new code packages.

Main Plasma Transport Codes

(E. Springmann, A. Taroni, F. Tibone, M. Watkins)

The 1.5D version of ICARUS for a non-circular plasma with prescribed boundary has been improved mainly by including updated auxiliary heating packages. In particular, a new package allows an evaluation on non-

circular flux surfaces of the power deposition profiles for ICRF heating. It is based on simple approximated expressions for the positions and width of the deposition layer and a semi-analytical treatment of the Fokker-Planck equation to evaluate the fractions of the input power given to ions and electrons.

A new version of the BOTTO transport code, (developed under Article 14 contract with EURATOM-ENEA Association, ENEA Bologna, Italy), has been implemented and tested on the CRAY computer. It can take into account up to three hydrogenic species and four impurities in coronal equilibrium. The free boundary equilibrium package for the 1.5D version of this code has also been installed and tested. It allows the computation of free boundary equilibria with prescribed arbitrary profiles of pressure and safety factor.

Anomalous Transport Models for Plasmas with Vigorous Auxiliary Heating

(B. Coppi*, P. Stubberfield, A. Taroni, F. Tibone, M. Watkins)

*Massachusetts Institute of Technology, Cambridge, Massachusetts, USA.

No really satisfactory theory explains the degradation of confinement in tokamaks in the presence of additional heating, but it is generally accepted that local electron energy transport increases. Starting from this consideration, a few models proposed to enhance the electron thermal conductivity above the values for pure ohmic heating have been implemented in JET transport codes. In particular, the package relating enhanced transport to ballooning modes has been improved and a model based on the so-called profile consistency constraint (proposed by B. Coppi), has been introduced.

A new version of the ion mixing mode anomalous transport term in the ion temperature equation has also been considered, in view of its possible importance in auxiliary heated plasmas.

Sawtooth Activity

(A. Taroni, F. Tibone)

A new package for the simulation of this activity has been produced taking into account, in addition to the basic Kadomtsev's model previously available, the more refined models of Pareil-Pereverzev and Pfeiffer. These models deal with the possible presence of more than one resonating surface ($q = 1$) and can reproduce double or giant sawteeth.

Impurity Transport and Related Atomic Physics

(A. van Maanen-Abels, D. Muir, A. Taroni, M.L. Watkins)

The very fast and fully vectorised non-coronal impurity transport code IMPUDI, (developed at EURATOM-IPP Association, Garching, F.R.G. under Article 14 contract) has been installed, tested, extended to non-circular flux surfaces in the case of anomalous transport and coupled to the 1.5D version of ICARUS. An improved version of another impurity code, BITC,

(developed at EURATOM-ENEA Association, ENEA, Bologna, Italy, under Article 14 contract) has also been implemented and modified to take full advantage of vectorization on the CRAY computer. The two codes have been extensively cross-checked and this work provided the basis for the development of a new atomic physics package for non-coronal impurity calculations. This package now replaces the original ones in both codes.

Edge Plasma

(W. Feneberg*, R. Simonini, A. Taroni)

*EURATOM-IPP Association, IPP, Garching, F.R.G.

Transport code ICARUS includes a zero-dimensional model of flow parallel to magnetic field in the edge plasma allowing a first estimate of the main sources (through sputtering) and sinks (through cross field and parallel flows) in this region. More accurate estimates, even within the frame of this simple and fast model, would be possible by calibrating it against the results of more refined codes. A first step in this direction has been accomplished with the development of a 1D package solving the conservation equation, in the fluid approximation, along the field lines in the limiter region. This package is now being coupled with a similar 1D solver for the equations across the field lines aiming to a 2D fluid code for the plasma in the vicinity of a limiter. The fluid model considered so far has been developed by W. Feneberg. Extension to other models should be straightforward.

ICRF Heating

(W. Core, H. Hamnen, T. Hellsten)

A series of tests have been performed using the Brambilla ray tracing code, which is a code for wave propagation in slab geometry and different packages solving the Fokker-Planck equation under different simplifying assumptions. The purpose of these tests has been to determine the level of accuracy achievable in a package that is sufficiently economic in computer time to be coupled to a transport code. As a result of these tests a simple model has been chosen and included in ICARUS to treat ICRF heating, at least until the experimental results reveal in which direction the model should be improved.

Pellet Injection Studies

(W.A. Houlberg*, M. Watkins)

*EURATOM-IPP Association, IPP Garching, FRG

The Milora-Foster model for pellet ablation including the effects of multi-electron energy groups, fast ions associated with neutral beam injection and alpha power heating has been installed and tested on the JET computing system. Used as a stand-alone code with specified plasma profiles appropriate to present and later phases of JET operation, it shows that pellet diameters up to 8mm injected with speeds in the range 5-10km/s would be required for density control, between the $q=1$ and $q=2$ surfaces, for plasmas with peak electron densities of 10^{20}m^{-3} at peak temperatures of 10keV.

6. Comparisons of Model Results with Measurements

Running models of actual JET discharges not only provide a validation of the model assumptions, but also serves as a means to check consistency of the measured sets of data.

Simulation of Ohmic Discharges in JET

(A. van Maanen-Abels, D. Muir, P. Stubberfield, A. Taroni, F. Tibone, M. Watkins)

JET discharges throughout the ohmic phase have been simulated using JET codes for main plasma and impurity transport. From this campaign of computations, it has been shown that simulations of the JET ohmic plasma, consistent with experimental results, are now possible within the frame of models available in the codes. These models evolved as new or more accurate diagnostics became available and further refinements are expected in the future. In spite of many uncertainties, the existing models provide a sufficiently reliable background for reasonable predictions of JET results, in future phases of operation.

Simulations confirm that the anomalous transport of electron energy in ohmic discharges is described, within the accuracy of the experimental data, by most of the

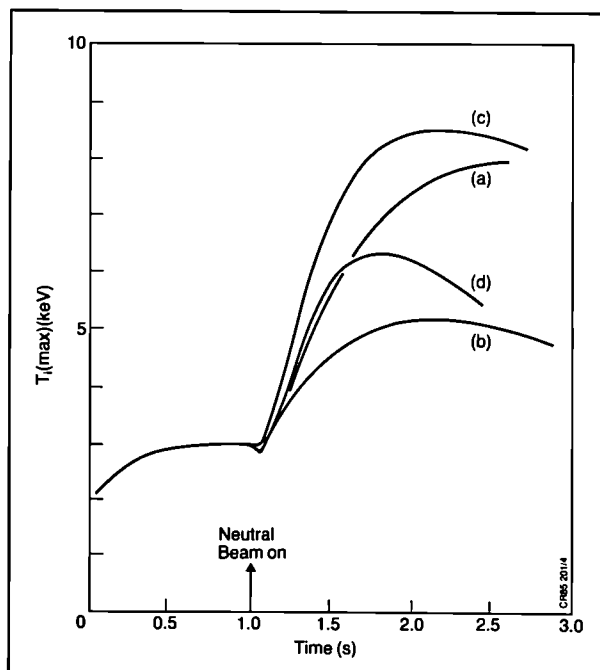


Fig.178 Predicted time variation of the central ion temperature for the first neutral injection box, assuming:

- (a) Hydrogen injection at 80kV, ohmic electron transport losses
- (b) Hydrogen injection at 80kV, electron transport losses enhanced by a factor of 2 over ohmic levels
- (c) Deuterium injection at 80kV, ohmic electron transport losses
- (d) Deuterium injection at 80kV, electron transport losses enhanced by a factor of 2 over ohmic levels.

commonly used transport coefficients, provided that these are reduced by factors 2 to 3. The Coppi-Mazzucato-Gruber coefficient seems to be an exception, as it does not need modification or it must be increased (up to 40% in last D-D discharges). The reason that it has not been possible to define in a satisfactory way the complete functional dependence of χ_e is mainly related to the presence of a high level of impurities and, to a certain extent, to the lack of measurements of the ion temperature (T_i) profile.

The available measurements of T_i at the centre of the discharge are best simulated with an ion thermal diffusion coefficient larger by a factor 3-4 than the neoclassical value (Chang-Hinton expression). Preliminary results show that the ion mixing mode anomalous coefficient is a possible candidate to explain this enhanced transport.

The influence of sawtooth activity and impurity radiation on the global confinement time has been assessed and found consistent with the experimental results. The mixtures of light and metal impurities required in the codes for a reasonable simulation of the experiments have been found in reasonable agreement with the experimental values of Z_{eff} and concentrations of impurities. The effects of the impurities have been studied both in the coronal and the non-coronal approximation, the latter by means of the stand-alone impurity code IMPUDI. New packages for the atomic physics data have been used. The best agreement with experimental results has been found when the anomalous fluxes of particles in the transport equations have the same diffusion coefficient ($D = \chi_e/4$) but different inward velocities for different species.

The models of impurity production implemented in ICARUS seem to be consistent with the measured influxes. They show the important role played by sputtering by impurities, such as carbon and oxygen, in addition to the sputtering by hydrogenic ions and atoms. Finally, it must be pointed out that the latest and more accurate experimental evaluations of Z_{eff} seem to be consistent with the neoclassical expression for the resistivity, while previous estimates were more consistent with the Spitzer model.

7. Predictive Computations

Future Phases of JET Operation

(P. Stubberfield, M. Watkins)

The plasma models developed for ohmic operation have been used as the basis for studying specific aspects of the approach to operation at full planned power in a deuterium-tritium plasma in JET. These studies include comparing various modes of neutral beam injection and ion cyclotron resonance heating, the effect of various models for the degradation of confinement with additional heating, and the resultant neutron yields to be expected from deuterium plasmas prior to the introduction of tritium.

Neutral Beam Injection Heating Studies

(P. Stubberfield, M. Watkins)

Transport calculations based on the reference ohmic model indicate that for an ohmic plasma similar to that obtained in JET Pulse No. 3050 together with up to 10MW of neutral hydrogen injection at 80keV (15MW total injected power, including the fractional energy components) substantial increases in the ion temperature are expected (11keV for 10MW injected power and 8keV for 5MW injected power, see Fig.178). This arises as appreciable direct heating of the ions occur, and these are only weakly coupled to the less confined electrons, since at the high electron temperatures achieved in the ohmic plasmas, the energy equipartition times are long.

Since all the neutral beam particles injected are retained in the discharge (100% recycling assumed), the mean density increases. The energy confinement time follows, since the reference ohmic model assumes this to be dominated by electron thermal losses that scale with density according to the ALCATOR-INTOR law ($\tau_E \propto n_e$). Results are shown in Fig.178, in which this apparent benefit is discounted by using χ_e obtained for the ohmic steady state of JET Pulse No. 3050 with an additional enhancement factor of two for the subsequent beam heating phase. In this case, the central ion temperature falls to 5.6keV and the global energy confinement time falls from 0.7s to 0.5s in going from the ohmic plasma to the injection heated plasma. Even if application of 'profile consistency' constrains the electron temperature to its ohmic value, the ion temperature still increases with neutral injection heating. However, if the confinement was determined by ion losses, there could be substantial degradation in the performance.

The short-term benefits in plasma performance, that might occur if deuterium injection at 80keV was used to heat the plasma, have been recognised for some time. With the best models presently available, the improved performance arises not only from the increased power levels assumed to be injected into the plasma but also from the more direct heating of the ions as the injected energy/nucleon is decreased.

However, it should be noted that as the plasma density increases and heating of the plasma centre becomes less effective, the usefulness of long pulse heating with deuterium at 80keV would be limited, unless effective density control were available.

Neutron Yields from Deuterium Plasmas

(M. Watkins)

The relative importance of neutrons produced by thermal and beam-plasma interactions is strongly dependent on the plasma density and ion temperature, and to a lesser extent on the electron temperature and the energy/nucleon of the injected neutrals. Transport calculations based on the reference ohmic model and enhanced electron thermal transport with 10MW of neutral deuterium injection at 160keV (15MW total injected power, including the fractional energy

components) indicate a maximum ion temperature of 9keV at a peak electron density of $5.3 \times 10^{19} \text{m}^{-3}$ and $Z_{\text{eff}} = 2.4$, when thermal and beam-plasma processes contribute equally to the total neutron yield of 10^{16}ns^{-1} .

In the approach to this level of heating, 5MW and 10MW of hydrogen injection at 80keV will be used, when only low yields of thermal neutrons will be encountered in deuterium plasmas. However, should the injection of deuterium at 80keV be considered, it is appropriate to consider the attendant neutron yields in view of the higher deuterium densities and temperatures expected.

Results of calculations indicate that only with low additional heating power levels (5MW) and enhanced thermal transport are the ion density and temperature kept sufficiently low for the beam-plasma neutron yield to exceed the thermal yield. As the injection power increases (or as the temperature increases with a more optimistic transport model), the thermal yields increase more rapidly than the beam-plasma yields.

Ion Cyclotron Heating Studies

(P.M. Stubberfield, M.L. Watkins)

Transport calculations based on the reference ohmic model, enhanced electron thermal transport and up to 3MW of ICRF power modelled using the package referred to earlier, indicate peak ion temperatures of $\sim 4.2 \text{keV}$ if the zone between the helium minority cyclotron layer and the ion-ion hybrid layer is assumed to be heated uniformly. Higher temperatures ($\sim 5.6 \text{keV}$) are predicted if focussing of the radiofrequency power heats this zone uniformly 0.86m above and below the horizontal mid-plane.

Approach to Ignition

(M.L. Watkins)

Transport calculations based on the reference ohmic model, enhanced electron thermal transport, 10MW of neutral deuterium injection and 15MW of ICRF into a deuterium-tritium plasma with the present levels of low Z impurities, indicate that high temperatures, but not necessarily high levels of alpha power, are readily achievable.

Assuming that better plasma purity and higher plasma densities can be achieved in ohmic operation, conditions close to ignition are achieved with the above transport model, but ignition with the additional heating power switched off is only achieved with a more optimistic transport model, comparable to that determined for ohmic plasmas.

8. Analytic Plasma Theory

With limited man-power, plasma theory cannot be covered completely. Therefore, current disruption, ICRH absorption, transport and flow processes, and particle confinement and heating have been selected as topics for special efforts. Work on the last topic has not yet started.

Theory of Marfes

(T.E. Stringer)

These toroidally symmetric bands of enhanced radiation are frequently observed in higher density pulses in JET. A large decrease in temperature in the marfe region must be balanced by a corresponding increase in density. The conditions for such an equilibrium have been studied in a simplified model. The predictions are compared with detailed measurements made in Alcator C, where marfes were first identified. Qualitative agreement is found. Thermal conduction along the field lines seems insufficient to completely balance the measured radiation from the marfe. Some local increase in perpendicular conduction, possibly due to the observed enhanced fluctuation level, is needed.

Theory for ICRF Heating in JET

(T. Hellsten)

The wide frequency regime covered by the RF-generators (25-55MHz) provides a large number of possible heating scenarios. The quality of these scenarios can be very different in terms of damping, energy transfer to background species, presence of high energy tails, etc. To find optimal heating scenarios, and to interpret experimental results, theories and models are being developed to calculate power deposition and interaction between RF-waves and the plasma.

Wave Propagation in a Slab Geometry

(K. Appert*, T. Hellsten, J. Vaclavik*, L. Villard*)

*EURATOM-Suisse Association, CRPP, Lausanne, Switzerland.

A new type of heating scenario, the so-called harmonic minority heating, has been proposed. Studies of wave propagation and absorption have been made with a one-dimensional global finite element code which treats the mode conversion of the fast magneto-acoustic wave into a kinetic wave, as well as coupling between the fast wave and the antenna, in a self consistent manner. Ion cyclotron absorption by the second harmonic resonance of He-3 or hydrogen in a deuterium plasma is found to be strong if the minority concentration exceeds a threshold value such that interaction between the magneto-acoustic wave and the ion-Bernstein wave occurs. An advantage of these scenarios is that they should decrease the amount of RF-energy absorbed by the α -particles.

2-D Ion Cyclotron Resonance Code - LION

(K. Appert*, R. Gruber*, T. Hellsten, J. Vaclavik*, L. Villard*)

*EURATOM-Suisse Association, CRPP, Lausanne, Switzerland

Wavelengths comparable to the characteristic dimensions of the plasma as well as strong reflection makes ray tracing calculations of power deposition questionable. A two-dimensional global finite element code has been developed under an Article 14 contract with EURATOM-Suisse Association, CRPP, Lausanne,

Switzerland. The code describes the fast magneto-acoustic wave, as well as the slow wave corresponding to the finite frequency generalisation of the shear Alfvén wave. Ion heating is provided by the electric field component rotating in the same direction as the ions near the cyclotron resonance.

Studies of the Evolution of the Resonant Ion Distribution Functions During RF Heating

(W.G.F. Core, H. Hamnen, T. Hellsten)

Semi-analytic models for the determination of the steady state and time dependent behaviour of resonant ion distributions in a tokamak under the influence of ICRF heating have been developed. These procedures have been used to make preliminary studies of the heating process and to obtain, from measurements of charge exchange and neutron spectra, the power deposition within the plasma volume and the efficiency of the RF schemes.

Under an Article 14 contract, further analytic studies in collaboration with the Chalmers University of Technology, Gothenburg, Sweden are currently in progress (Anderson, D., Eriksson, L., Lisak, M. and Pekkari, L.)

A collaboration has been set up with CRPP, Lausanne, Switzerland (Appert, K. and Succi, S.) to develop numerical codes to study the evolution of the ion distribution function in more detail. For this purpose, the two-dimensional time dependent finite element code 'BACCHUS' has been installed at JET and modified to include the bounced averaged Rosenbluth collision and quasilinear RF diffusion operators. Using this code trapped particle effects have been investigated and possible current drive systems for JET have been examined.

Disruption Analysis

(J.A. Wesson, M.F. Nave)

An analysis has been made of the disruption behaviour in JET. All discharges in 1983 and 1984 have been studied and the density limit established. A theoretical model based on radiative losses leading to disconnection and plasma contraction seems to be consistent with the observed trajectories in the Hugill diagram.

Tearing Mode Catalogue

(J.A. Wesson, M.F. Nave)

Numerical calculations of the properties of tearing modes have been made for a wide range of current configurations. The linear stability properties, including the effect of a conducting wall, were calculated, together with the saturated island size.

 β Limit Scaling

(J.A. Wesson)

An analytic calculation of the β limit scaling has reproduced the scaling law obtained numerically by previous workers.

β Limit - Murakami Limit

(J.A. Wesson, M.F. Nave)

Calculations have been made of the α -particle heating for a D-T plasma in JET as a function of β and the Murakami parameter. The associated confinement times for ignition were also calculated.

Non-Linear Tearing and Kink Modes

(J.A. Wesson, L. Taroni)

The amplitude of saturated islands and the surface deformation resulting from saturated ideal MHD kink modes have been calculated in the quasi-linear, large aspect-ratio approximation.

Current Penetration

(J.A. Wesson, M. Lorentz)

A programme of non-linear simulations of double tearing modes and current penetration has been started.

Reactor Costs

(J.A. Wesson, J.P. Freidberg)

A simple analytic model was developed to investigate the question of the minimum required β and minimum cost for a tokamak reactor. The results show the dependence of the required β on the wall loading and the importance of the aspect ratio in choosing relevant physics experiments.

Equilibria with Plasma Flows

(R. Zelazny)

In the framework of possible optimisation and identification studies of JET, the problem of stationary flows has been studied. The importance of flows in the presence of neutral-beam and RF auxiliary heating has been discussed, taking into account JET conditions.

Internal and Major Disruptions

(A. Samain**)

**EURATOM-Association CEA, Fontenay-aux-Roses, France

The reconnection process during internal disruptions has been studied using energy balance arguments and a variational formulation of the nonlinear equations. It is difficult to explain the very rapid rate of change observed

during the collapse. Analysis has also been undertaken on the Rebut-Hugon theory, in which magnetic island growth due to thermal instability leads to a major disruption.

9. Development of Methods

A small and necessary effort, within the responsibility of the Analytic Theory Group, has been devoted to modifying and developing appropriate mathematical methods for JET requirements.

Generalised Abel Inversion

(N. Gottardi)

A method of generalised Abel inversion has been developed and tested on the experimental data from the three multichannel bolometers. The flux surface geometry from IDENTB is used to combine the data from the three cameras and at low densities it is found that a consistent Abel inverted profile can be obtained. However, at high densities there is a strong up-down asymmetry in the data coming from the two horizontal cameras indicating the presence of Marfes. This means that the surfaces of constant emissivity do not coincide with the flux surfaces. In this situation, a new tomographic approach using the bolometer data alone is required and this is being developed.

Scaling Law Systematics

(D. Pfirsch*, D.F. Duchs)

*EURATOM - IPP Association, Garching, F.R.G.

Statistical implications of empirical scaling laws in the form of power products obtained by linear regression have been analysed. The sensitivity of the error against a change of exponents is described by a 'sensitivity factor', and the uncertainty of predictions by a 'range of prediction factors'. The sometimes small value of the former (and a corresponding large value of the latter) are related to the existence of inner relations in the basic statistical material. A procedure for identifying such inner relations has been outlined. In addition, the consequences of discarding variables, in particular of eliminating inner relations, have been investigated. These methods have been exemplified by considering scaling laws for the energy confinement time of ohmically heated tokamak plasmas.

Appendix 1

Task Agreements 1984

<i>Title</i>	<i>Associations</i>	<i>Duration of Agreement</i>	<i>Present Status</i>
RF HEATING DIVISION DETAILED CALCULATION OF THE QUADRUPOLE VERSION OF THE A ₁ ANTENNA	EUR-ERM (ERM 1)	March–April 1984	Completed
ICRF CURRENT DRIVE EFFECTS – Asymmetric heating of minority species ions, Absorption of fast magnetosonic waves by TTMP of suprathermal electrons, ICRF enhancement of beam driven currents	EUR–UKAEA CULHAM LABORATORY (CUL/TA6)	November 1984–October 1985	a method has been chosen a code is being developed
RF ANTENNA DEVELOPMENT, TESTING, COMMISSIONING AND OPERATION	EUR–CEA FAR (FAR/TA2)	Sept 1984–Aug 1986	a contract for additional Test Bed equipment is placed. The Test Bed has been moved from FAR to JET
ICRH HEATING – operation of ICRH antennae, The evaluation of the heating performance and the comparison to theoretical expectations,	EUR–CEA (FAR/TA3/ GREN/TA1)	Sept 1984–Sept 1986	Since January 1985, FAR. Staff have been participating actively in analysis of results already obtained.
ICRH HEATING – Coupling calculations of ICRH antennae, Calculations of the power deposition profile by the method of ray tracing, Experiments with a complete ICRH system on the Textor Tokamak	The theory of RF current drive. EUR–ERM/KMS (ERM2)	1 Feb 1985–30 Sept 1986	Agreement just established
SCIENTIFIC DEPARTMENT PLASMA START-UP, SHAPE AND POSITION CONTROL	EUR–IPP, FRG	July 1984–July 1984	Completed – (One man joined JET for one year to work on this subject.)
DISRUPTION PHENOMENA – DETECTION AND PREVENTION	EUR–ENEA CREF	Sept 1983–August 1984	Completed (2 man-months 1983; 9 man-months 1984.)
EXPERIMENTAL DIVISION 1 PHYSICS OF SHAPED CROSS-SECTIONS	CULHAM CUL/TA4	March 1983–May 1985	Work continuing, and task agreement will be extended.
EDGE PLASMAS & PLASMA SURFACE INTERACTIONS	CULHAM CUL/TA2	June 1983–May 1986	Work proceeding
PLASMA WALL INTERACTIONS	GARCHING IPP/TS2	January 1984–December 1986	Work proceeding
MHD ACTIVITY, DISRUPTION AND RF WAVEFIELDS, EDGE PLASMAS UNDER INTENSE RF FIELDS.	LAUSANNE CRPP/TA1	March 1984–March 1986	Work proceeding
NEUTRON PRODUCTION, RELATED PHYSICS AND ASSOCIATED DIAGNOSTICS	SWEDEN SERC/TA1	January 1984–December 1986	Work proceeding
PLASMA SURFACE INTERACTIONS	SWEDEN SERC/TA2	July 1984–June 1987	Work proceeding

continued overleaf

EXPERIMENTAL DIVISION 2			
BULK IMPURITY PHYSICS	EUR-IPP	08.02.83 –	Bolometer arrays installed and and operating (See text for details.)
IMPURITY RELATED DIAGNOSTICS	FRG	08.02.86	
IMPURITY ANALYSIS	EUR-UKAEA CULHAM LABORATORY	01.02.83 – 01.06.85	Construction of impurity survey VUV Spectrometer. (See text for details.)
SPECTROSCOPIC MEASUREMENTS: THEIR INTERPRETATION AND IMPURITY EFFECTS ANALYSIS	EUR-CEA FAR	July '84 – July '85	Construction and operation of VUV spectrometers. (See text for details.)
PHYSICS OF ION AND ELECTRON ENERGY TRANSPORT AND RELATED DIAGNOSTICS	EUR-ENEA CREF	October '83 – unlimited	Construction, installation and operation of Neutral Particles Analyser (NPA). (See text for details.)
PHYSICS OF NEUTRAL BEAM HEATING OPTIMISATION	EUR-UKAEA CULHAM LABORATORY	01.07.83 – 01.07.86	Part 1 completed 1983 (See JET-PR1). Part 2: Interpretation of ion velocity distribution. Evaluation of charge-exchange diagnostics. Work proceeding.

Appendix 2

Articles, Reports and Conference Papers published, 1984

1. Manufacture of beam sources and neutralisers for JET neutral injection.
Altmann, H.
Fusion Technology 13th Symp., Varese, 24-28 September 1984, Oxford, Pergamon, 1984.
Vol.1, pp.579-585.
2. The neutral injector auxiliary power supply system in JET: design, manufacture and tests.
Basile, G.L., Ciscato, D., Dobbing, J.A., Mondino, P.L.
Fusion Technology 13th Symp., Varese, 24-28 September 1984, Oxford, Pergamon, 1984.
Vol.2, pp.835-842.
3. RF tests on JET first stage antenna system.
Beaumont, B., Arbez, J., Brugnetti, R., Franklin, A., Hanley, E., Jacquinet, J., Kaye, A., Plancovaline, J., Speziale, A., Walker, C.
Fusion Technology 13th Symp., Varese, 24-28 September 1984, Oxford, Pergamon, 1984.
Vol.1, pp.599-604.
4. Impurity concentrations and fluxes in the joint JET-ISX-B beryllium limiter experiment.
Behringer, K., Källne, E., Morgan, P., Peacock, N.J., Isler, R.C., Neidlich, R.V.
American Physical Society, Bulletin.
Series 2, vol.,29 no.8 October 1984,
(Abstracts of the 26th Ann. Mtg. Div. Plasma Phys., Amer. Phys. Soc., Boston, 29 October - 2 November 1984)
Paper 9T 11.
5. Impurity studies and transport code modelling of JET plasmas.
Behringer, K.H., Bonnerue, J., Bulliard, A., Carolan, P.G., Decker, G., Denne, B., Düchs, D.F., Ehrenberg, J., Engelhardt, W.W., Forrest, M.J., Gill, R., Gondhalekar, A., Hawkes, N.C., Källne, G.E., Krause, H., Magyar, G., Martin, J.L., Mast, F., McCracken, G.M., Morgan, P., Muir, D., O'Rourke, J., Peacock, N.J., Ravestein, A., Stamp, M.F., Stubberfield, P.M., Taroni, A., van Maanen-Abels, A., Watkins, M.L.
Plasma Physics and Controlled Nuclear Fusion Research, 10th Int. Conf. London, 12-19 September 1984, Volume 1., Vienna, IAEA, 1985, pp.291-300.
6. Physics Performance of the Joint European Torus.
Bickerton, R.J.
Plasma Physics and Controlled Fusion, vol.26 no.12A December 1984, (11th Annual Conf. Plasma Physics Group of the Inst. of Physics, 27-29 June 1984, Selwyn College, Cambridge, Invited Papers). pp.1355-1365.
7. Physics Performance of the Joint European Torus.
Bickerton R.J.
Joint European Torus JET, 1984.
12p.
Report JET-P(84)02.
8. The central interlock and safety system of JET.
Bombi, F., Nijman, J., Van Montfoort, J.
Fusion Technology 13th Symp., Varese, 24-29 September 1984, Oxford, Pergamon, 1984.
Vol.2, pp.1133-1139.
9. Integrated control and data acquisition of experimental facilities.
Bombi, F.
Computing in Accelerator Design and Operation. Europhysics Conf., held in Berlin, 20-23 September 1983, Edited by Busse, W., and Zelazny, R., Springer-Verlag, 1984, pp.311-315.
10. The gas introduction system of JET.
Boschi, A., Dietz, K.J., Rebut, P.H.
Fusion Technology 13th Symp., Varese, 24-28 September 1984,
Oxford, Pergamon, 1984.
Vol.1, pp.247-254.
11. JET ICRF antenna coupling and real-time impedance matching.
Bosia, G., Jacquinet, J., Lallia, P.P., Rebut, P.H., Sand F., Schmid, M., Wade, T.
Heating in Toroidal Plasmas 4th Int. Symp., organised by the International School of Plasma Physics, Rome, 21-28 March 1984, 2 volumes.
Perugia, Monotypia Franchi, 1984. ppl445-450.
12. Analysis of magnetic measurements in tokamaks.
Brusati, M., Christiansen, J.P., Cordey, J.G., Jarrett, K., Lazzaro, E., Ross, R.T.

- Computer Physics Reports.
Vol.1 no. 7 and 8 August/September 1984.
(Computational problems in the calculation of magnetohydrodynamic (MHD) equilibria, Procs. of the 2nd Workshop (Review papers) Wildhaus, Switzerland, 12-14 September 1983).
pp.345-372.
13. Commissioning and early operation of the power supply and protection system for the extraction grid of the JET neutral injectors.
Claesen, R., Dobbing, J.A., Hartline, R., Egerszegi, L., Hrabal, D., Mondino, P.L., Tournesac, B.
Fusion Technology 13th Symp., Varese, 24-28 September 1984, Oxford, Pergamon, 1984. Vol.2, pp.829-834.
 14. Measurement of emission in the ion cyclotron frequency range for ohmic and ICRH discharges in TFR.
Clark, W.H.M., TFR Group.
Heating in Toroidal Plasmas 4th Int. Symp., organised by the International School of Plasma Physics, Rome, 21-28 March 1984, 2 volumes. Perugia, Monotypia Franchi, 1984.
pp.385-391.
 15. A review of non-inductive current drive theory.
Cordey, J.G.
Plasma Physics and Controlled Fusion, 11th European Conference 5-9 September 1983, Aachen, Invited Papers.
Vol.26 no.1A January 1984.
pp.123-132.
 16. A review of current drive by fast ion injection (Invited).
Cordey, J.G.
Non-inductive Current Drive in Tokamaks. IAEA Technical Committee Meeting, held at Culham Laboratory, 18-21 April 1983. Edited by D.F.H. Start.
2 Vols, Abingdon, Culham Laboratory. 1984. CLM-CD (1983).
pp.1-10.
 17. Trapping and thermalization of fast ions.
Cordey, J.G.
Applied atomic collision physics, volume 2 - plasmas.
Barnett, C.F., and Harrison, M.F.A., editors.
Orlando, Academic Press, 1984.
pp.327-338.
 18. Particle and energy confinement in ohmically heated JET plasmas.
Cordey, J.G., Bartlett, D.V., Bickerton, R.J., Bracco, G., Brusati, M., Campbell, D.J., Christiansen, J.P., Corti, S., Costley, A.E., de Kock, L., Fessey, J., Gadeberg, M., Gibson, A., Gill, R.D., Gottardi, N., Gondhalekar, A., Gowers, C.W., Hubbard, A., Hugenholtz, C.A., Jarvis, O.N., Krause, H., Lazzaro, E., Lomas, P.J., Mast, F.K., Morgan, P.D., Nielsen, P., Noll, P., Pick, M., Prentice, R., Ross, R.T., Sadler, G., Schuller, F., Stamp, M.F., Summers, D., Tanga, A., Thomas, P.R., Tonetti, G., van Belle, P., Zanza, V.
Plasma Physics and Controlled Nuclear Fusion Research, 10th Int. Conf., London, 12-19 September 1984, Volume 1.
Vienna, IAEA, 1985.
pp.167-177.
 19. Collection, review and adaption for NET needs of plasma modelling codes.
De Barbieri, O., Dücks, D.F., and others.
Next European Torus, 1984.
133p.
Report NET 32.
EUR XII 324/32.
 20. Start-up and initial operation of JET.
Dietz, K.J., Bartlett, D., Baumel, G., Behringer, K., Bertolini, E., Best, Bickerton, R.J., Bombi, F., Boschi, A., Browne, M.L., Brusati, M., Bulliard, A., Campbell, D., Carolan, P.J., Clausing, R., Christiansen, J., Chuilon, P., Cordey, J.G., Costley, A., de Kock, L., Dücks, D.F., Duesing, G., Emery, R.K.F., Engelhardt, W.W., Eriksson, T., Forrest, M.J., Froger, C., Fullard, K., Gibson, A., Gill, R., Gondhalekar, A., Gowers, C., Green, B.J., Hemmerich, J., Huart, M., Hugenholtz, C.A., Huguet, M., Jarvis, O.N., Jensen, B.E., Krause, H., Kupschus, P., Last, J., Lazzaro, E., McCracken, G.M., Magyar, G., Mast, F.K., Mead, M., Mondino, P.L., Morgan, P., Morris, A.W., Nickesson, L., Niedermeyer, H., Noll, P., Paillere J., Peacock, N.J., Pick, M., Raymond, C., Rebut, P.H., Ross, R., Sadler, G., Schmidt, V., Schuller, F.C., Sonnenberg, K., Stamp, M.F., Steed, C.A., Stella, A., Stott, P.E., Summers, D., Tanga, A., Thomas, P.R., Usselmann, E., van Belle, P., van der Beken, H., van Montfoort, J.E., Waelbroeck, F., Wesson, J.A., Winkel, T., Winter, J., Zwart, J.
Journal of Nuclear Materials
vol.128 129 December 1984 (Proc. 6th Int. Conf. on Plasma Surface Interactions in Controlled Fusion Devices, Nagoya, Japan, 14-18 May 1984).
pp.10-18.
 21. JET neutral beam injection system, construction and component tests.
Duesing, G.
Joint European Torus. 1984.
16p.
Invited paper at the 13th Symp. on Fusion Technology, Varese (September 1984).
 22. Construction, operation and enhancement of JET.
Duesing, G., Dietz, K.J.
Joint European Torus, 1984.
21p.
Report JET-P(84)04

- Invited paper presented at the 31st National Symp. of the American Vacuum Society, Reno, December 1984.
23. JET neutral beam injection system, construction and component tests.
Duesing, G.
Joint European Torus, 1984.
16p.
Report JET-P(84)07.
 24. JET neutral beam injection system, construction and components tests.
Duesing, G.
Fusion Technology 13th Symp., Varese, 24-28 September 1984.
Oxford, Pergamon, 1984.
Vol.1, pp.59-75.
 25. The Joint JET-ISX-B beryllium limiter experiment.
Edmonds, P.H. Mioduszewski, P.K., Dietz, J., Watson, R., Smith, M.
American Physical Society, Bulletin. Series 2. vol. 29 no.8 October 1984.
(Abstracts of the 26th Ann. Mtg. Div. Plasma Phys., Amer. Phys. Soc., Boston, 29 October - 2 November 1984).
Paper 7F 9.
 26. Power load and limiter considerations in JET.
Engelhardt, W.
Heating in Toroidal Plasmas 4th Int. Symp., organised by the International School of Plasma Physics, Rome, 21-28 March 1984, 2 volumes.
Perugia, Monotypia Frachi, 1984.
p.1371.
 27. Operation and control of the JET poloidal field power supply system.
Eriksson, T., Corbyn, D.B., Huart, M., Marchese, V., Mondino, P.L., Raymond, C.
Fusion Technology 13th Symp., Varese, 24-28 September 1984.
Oxford, Pergamon, 1984.
Vol.1, pp.571-578.
 29. Resistively heated plasmas in JET - characteristics and implications.
Gibson, A.
Joint European Torus, 1984.
28p.
Report JET-P(84)01.
Invited paper presented at the Int. Conf. on Plasma Physics, Lausanne, June 1984.
 30. Resistively heated plasmas in JET, characteristics and implications.
Gibson, A.
Int. Conf. on Plasma Physica, Lausanne, 27 June - 3 July 1984.
Invited papers, 2 Vols. 1984. Brussels, EEC, pp.13-38.
 31. Energy containment time scaling in tokamak H-modes.
Gill, R.D.,
Plasma Physics and Controlled Fusion. Vol.26 no.4 April 1984.
pp.683-687.
 32. Soft X-ray measurements on JET.
Gill, R.D., Decker, G., Kallne, E., Krause, H., O'Rourke, J.O. Stringer, T.E.
American Physical Society, Bulletin. Series 2, vol.29 no.8 October 1984.
(Abstracts of the 26th Ann. Mtg. Div. Plasma Phys., Amer. Phys. Soc., Boston, 29 October - 2 November 1984),
Paper 5T 19.
 33. Real-time plasma fault protection system for JET.
Gondhalekar, A., Lomas, P., Noll, P., Reed, K., Schüller, F.C.
Fusion Technology 13th Symp., Varese, 24-28 September 1984.
Oxford, Pergamon, 1984.
Vol.2, pp.1661-1665.
 34. Real-time plasma fault protection system for JET.
Gondhalekar, A., Lomas, P., Noll, P., Reed, K., Schüller, F.C., Cooper, D., Stabler, A., Stork, D.
American Physical Society, Bulletin. Series 2, vol.29 no.8 October 1984.
(Abstracts of the 26th Ann. Mtg. Div. Plasma Phys., Amer. Phys. Soc., Boston, 29 October - 2 November 1984)
Paper 5T 21
 35. The state of controlled thermonuclear fusion research.
Green, B.J.,
The Nuclear Engineer
vol.25 no.5 September/October 1984 pp.186-190.
 36. The Scientific programme of the Joint European Torus, JET.
Green, B.J.
Physikalische Blatter, vol.40, no.3, 1984.
pp.70-72.
In German.
 37. Controlled nuclear fusion, Inexhaustible energy from Plasma.
Green, B.J.
Umschau, vol.84, no.25/26, 1984.
pp.770-773.
In German.
 38. Ripple-induced radial diffusion of fast ions in tokamaks.
Hamnen, H., Anderson, D., Lisak, M., Core, W.G.F.
Physica Scripta.
vol.30 no.5 November 1983.
pp.346-349.
 39. Optimisation of the proton fraction in the JET ion sources.
Holmes, A.J.T., Green, T.S., Martin, A.R., Hemsworth, R.S., Thompson, E.

- Heating in Toroidal Plasmas 4th Int. Symp., organised by the International School of Plasma Physics, Rome, 21-28 March 1984, 2 volumes. Perugia, Monotypia Franchi, 1984. pp.1065-1072.
40. Commissioning of the JET flywheel-generator-converter systems.
Huart, M.
Fusion Technology 13th Symp., Varese, 24-28 September 1984.
Oxford, Pergamon, 1984.
Vol.2, pp.851-858.
 41. Commissioning and operation of JET.
Huguet, M.
Transactions of the American Nuclear Society, vol.46 June 1984, (Annual Meeting, New Orleans, 3-7 June 1984) pp.182-183
 42. Papers presented to the Institution of Mechanical Engineers Seminar on the JET Project (5 papers).
Main Authors: Huguet, M.; Last, J.R.; Walravens, M.; Huart, M., and Sonnerup; L., Haage, R.
Joint European Torus, JET, 1984. Report JET-P(84)12.
 43. Assembly and commissioning of the JET magnets.
Huguet, M., Last, J.R., Pochelon, R., Booth, J.A., Cacaut, D., Pratt, A.P.
Magnet Technology 8th Int. Conf. held in Grenoble, 5-9 September 1983. Journal de Physique, vol.45, Colloquia 1. 1984.
pp.C1-121 - C1-124.
 44. Assembly, commissioning and first operation of JET.
Huguet, M.
Joint European Torus, JET, 1984.
9p.
Report JET-P(84)03.
 45. Present status of commissioning and operation of JET.
Huguet, M., and others.
Fusion Technology 13th Symp., Varese, 24-28 September 1984.
Oxford, Pergamon, 1984.
Vol.1, pp.91-103.
 46. Overview of RF heating studies in tokamaks after the Aachen conference.
Jacquinot, J.
INTOR. International Tokamak Reactor Phase IIA.
European contributions to the 8th Workshop-meeting, Brussels, EEC, January 1984.
Group B, part 1, pp.1.1-1.10.
 47. Summary talk on RF heating workshop.
Jacquinot, J.,
INTOR. International Tokamak Reactor Phase IIA.
European contributions to the 8th Workshop-Meeting, Brussels, EEC, January 1984.
Group B, part 2, pp.2.1-2.11.
 48. The JET ICRF antenna system.
Jacquinot, J., Arbez, J., Beaumont, B., Hanley, E., Kaye, A., Lallia, P., Plancoulaine, J., Sand, F., Walker, C.
Heating in Toroidal Plasmas 4th Int. Symp., organised by the Int. School of Plasma Physics, Rome, 21-28 March 1984, 2 volumes.
Perugia, Monotypia Franchi, 1984.
pp.1244-1251.
 49. Matching the JET ICRF antenna.
Jacquinot, J.
Joint European Torus, JET, 1984.
27p.
Report JET IR(84)01.
 50. Control, data acquisition and analysis for the JET neutral injection testbed.
Jones, T.T.C., Brennan, P.R., Rodgers, M.E., Stork, D., Young, +I.D.
Fusion Technology 13th Symp., Varese, 24-28 September 1984.
Oxford, Pergamon, 1984.
Vol.2, pp.1125-1132.
 51. Observation of Recombination population of $n=2$ excited states of $Ar(16+)$ in tokamak plasmas.
Källne, E., Källne, J., and others.
Phys. Rev. Lett. 52 2245-2248 (1984)
 52. The JET ICRF antennae systems: description and testbed results.
Kaye, A., Arbez, J., Beaumont, B., Franklin, A., Hanley, E., Jacquinot, J., Panissie, H., Plancoulaine, J., Walker, C.
Fusion Technology 13th Symp., Varese, 24-28 September 1984.
Oxford, Pergamon, 1984.
Vol.1, pp.669-674.
 53. Possible ICRF heating modes of operation in non active JET plasma.
Lallia, P.P., Clark, W.H.M., Jacquinot, J., Sand, F.
Heating in Toroidal Plasmas 4th Int. Symp., organised by the International School of Plasma Physics, Rome, 21-28 March 1984, 2 volumes.
Perugia, Monotypia Franchi, 1984.
pp.393-398.
 54. The JET Nuclear Fusion Project:
Maple, J.H.C.
Joint European Torus, JET 1984.
Report JET-P(84)10.
 55. The JET power supplies: a Review after one year of operation.
Mondino, P.L.
Fusion Technology 13th Symp., Varese, 24-28 September 1984.
Oxford, Pergamon, 1984.
Vol.1, pp.119-131.
 56. The JET Power Supplies: A Review after one year of Operation:
Mondino, P.L.
Joint European Torus, JET, 1984.
Report JET-P(84)06.

57. The use of optical fibre in a high-radiation environment to monitor H alpha light from the JET tokamak.
Morgan, P.D., Magyar, G.
Optical Fibres in Adverse Environments, vol.404, 1984.
pp.126-131.
58. Particle balance, recycling and density control in JET discharges.
Morgan, P.D., Boschi, A., Gowers, C.W., Hugenholtz, C.A., Tanga, A.
American Physical Society, Bulletin. Series.
vol.29 no.8 october 1984.
(Abstracts of the 26th Ann. Mtg. Div. Plasma Phys., Amer. Phys. Soc., Boston, 29 October - 2 November 1984).
Paper 3F 9.
59. Charge-changing collisions in the JET neutral injection bending magnets.
Nielsen, B.R., and others.
Vacuum.
(Proc. 3rd Int. Conf. on Low Energy Ion Beams 28-31 March 1983, Loughborough University of Technology).
vol.34 no.1&2 January-February 1984.
pp.37-40.
60. The single point Thomson scattering system at JET.
Nielsen, P., Gadeberg, M., Prentice, R.
American Physical Society, Bulletin.
Vol.29 no.8 October 1984.
(Abstracts of the 26th Ann. Mtg. Div. Plasma Phys., Amer. Phys. Soc., Boston, 29 October-2 November 1984)
Paper 5T18.
61. The JET plasma position and current control system.
Noll, P.
INTOR. International Tokamak Reactor. Phase IIA.
European contributions to the 8th Workshop-Meeting.
Brussels, EEC. January 1984.
Group C, 12pp.
62. The JET plasma position and current control system.
Noll, P., Browne, M., Huart, M., Piacentini, I., Santagiustina, A., Watkins, J.R.
Joint European Torus, JET. 1984.
8p. Report JET-P(84)08.
63. The JET plasma position and current control system.
Noll, P., Browne, M., Huart, M., Piacentini, I., Santagiustina, A., Watkins, J.R.
Fusion Technology 13th Symposium, Varese, 24-28 September 1984.
Oxford, Pergamon, 1984.
Vol.1, pp.503-509.
64. The JET cryopump system and its cryolines for neutral injection.
Obert, W., Duesing, G., Kussel, E., Kupschus, P., Mayaux, C., Rebut, P.H., Santos, H.
Fusion Technology 13th Symposium, Varese, 24-28 September 1984.
Oxford, pergamon, 1984.
Vol.1, pp.311-318.
65. Vacuum measurement and control for the Joint European Torus (JET) project.
Parrix, M., May, P.L., Usselman, E., Daser, W., Dietz, K.J.
Vakkum Technik.
Vol.33 no.2 March 1984
pp.52-55.
In German, English Abstract.
66. Vacuum ultra-violet line intensities from JET.
Peacock, N.J., Hawkes, N.C., Behringer, K.H., Denne, B., Griffin, W.G.
American Physical Society, Bulletin. Series 2
vol.29 no.8 October 1984
(Abstracts of the 26th Ann. Mtg. Div. Plasma Phys., Amer. Phys. Soc., Boston, 29 October - 2 November 1984)
Paper 5T 20.
67. Limiter viewing on JET.
Pick, M.A., Summers, D.
Journal of Nuclear Materials
vol.128 & 129 December 1984
(Proc.6th Int. Conf. on Plasma Surface Interactions in Controlled Fusion Devices, Nagoya, 14-18 May 1984).
pp.440-444.
68. The role of metal-hydrogen systems in fusion research.
Pick, M.A.
Journal of the Less-Common Metals, 103, 1984,
pp.5-17.
Paper presented at the Int. Symp. on the Properties and Applications of Metal Hydrides IV, Eilat, 9-13 April 1984.
69. JET: something new under the sun.
Poffé, J-P., Sand, F.
Europe 84
no.6 June 1984
pp.116-17.
70. Status and programme of JET.
Rebut, P.H., Green, B.J.
Plasma Physics and Controlled Fusion
11th European Conference 5-9 September 1983, Aachen. Invited papers.
vol.26 no.1A January 1984
pp.1-10.
71. JET Progress Report.
Rebut, P.H.,
Heating in Toroidal Plasmas 4th Int. Symp., organised by the International School of Plasma Physics, Rome, 21-28 March 1984, 2 volumes.

- Perugia, Monotypia Franchi, 1984.
pp.991-1011.
72. First experiments in JET.
Rebut, P.H., Bartlett, D.V., Baumel, G., Behringer, K., Behrisch, R., Bertolini, E., Best, C., Bickerton, R.J., Bombi, F., Bonnerue, J.L., Boschi, A., Bracco, G., Browne, M.L., Brusati, M., Bulliard, A., Campbell, D.J., Carolan, P.G., Christiansen, J., Chuilon, P., Cordey, J.G., Corti, S., Costley, A.E., Decker, G., de Kock, L., Dietz, K.J., Düchs, D.F., Duesing, G., Emery, R.K.F., Engelhardt, W.W., Eriksson, T., Fessey, J., Forrest, M.J., Froger, C., Fullard, K., Gadeberg, M., Gibson, A., Gill, R., Gondhalekar, A., Gowers, C., Green, B.J., Grosso, G., Hawkes, N.C., Hemmerich, J., Huart, M., Hubbard, A., Hugenholtz, C.A., Huguët, M., Jarvis, O.N., Jensen, B.E., Jones, E.M., Källne, G.E., Källne, J.C., Krause, H., Kupschus, P., Last, J.R., Lazzaro, E., Lomas, P., McCracken, G.M., Magyar, G., Mast, F.K., Mead, M., Mondino, P.L., Morgan, P., Morris, A.W., Nickesson, L., Niedermeyer, H., Nielsen, P., Noll, P., Paillere, J., Peacock, N.J., Pick, M., Poffé, J.P., Prentice, R., Raymond, C., Robinson, D.C., Ross, R., Sadler, G., Saffert, J., Schmidt, V., Schueller, F.C., Sonnenberg, K., Stamp, M.F., Steed, C.A., Stella, A., Stott, P.E., Summers, D., Tanga, A., Thomas, P.R., Tonetti, G., Usselman, E., van Belle, P., van der Beken, H., van Montfoort, J.E., Watkins, M.L., Wesson, J.A., Winkel, T., Zanza, V., Zwart, J.
Plasma Physics and Controlled Nuclear Fusion Research, 10th Int. Conf., London, 12-19 September 1984, Volume 1, Vienna, IAEA. 1985. pp.11-27.
 73. First JET results and its prospects.
Rebut, P.H.
Euratom, Joint European Torus JET, 1984.
12p.
Report JET-P(84)11.
 74. RF properties of the JET antennae.
Sand, F., Arbez, J., Jacquinet, J., Lallia, P.P., Theilhaber, K.
Heating in Toroidal Plasmas 4th int. Symp., organised by the International School of Plasma Physics, Rome, 21-28 March 1984, 2 volumes.
Perugia, Monotypia Franchi, 1984. pp.1121-1127.
 75. Fokker-Planck calculations for JET ICRF heating scenarios.
Scharer, J., Jacquinet, J., Sand, F.
Int. Conf. on Plasma Physics, Lausanne, 27 June - 3 July 1984.
Contributed papers, 2 volumes.
Lausanne CRPP, 1984.
Paper P5-5.
 76. Fokker-Planck calculations for JET ICRF fusion heating scenarios.
Scharer, J., Jacquinet, J., Lallia, P., Sand, F.
American Physical Society, Bulletin Series 2.
Vol.29 no.8 October 1984.
(Abstracts of the 26th Ann. Mtg. Div. Plasma Phys., Amer. Phys. Soc., Boston, 29 October - 2 November 1984).
Paper 3F 12.
 77. Fokker-Planck calculations for JET ICRF heating scenarios.
Scharer, J., Jacquinet, J., Lallia, P., Sand, F.
Heating in Toroidal Plasmas 4th Int. Symp., organised by the Int. School of Plasma Physics, Rome, 21-28 March 1984, 2 volumes.
Perugia, Monotypia Franchi, 1984.
pp.427-432.
 78. Operational aspects of disruptions in JET.
Schueller, F.C., Wesson, J., Noll, P., Thomas, P., Cordey, J.G., Christiansen, J., Lazzaro, E.
American Physical Society, Bulletin Series 2.
Vol.29 no.8 October 1984
(Abstracts of the 6th Ann. Mtg. Div. Plasma Phys., Amer. Phys. Soc., Boston, 29 October - 2 November 1984).
Paper 3F 10.
 79. MESHJET. A mesh generation package for finite element MHD equilibrium codes at JET.
Springmann, E., Taroni, A.
Joint European Torus, JET, 1984.
35p.
Report JET-R(84)01.
 80. Observation of high beta effects during plasma termination in JET.
Tanga, A., Alladio, F., Crisanti, F., Lazzaro, E.
American Physical Society, Bulletin.
vol.29 no.8 October 1984.
(Abstracts of the 26th Ann. Mtg. Div. Plasma Phys., Amer. Phys. Soc., Boston, 29 October - 2 November 1984).
Paper 3F11.
 81. Global particle balance and recycling in first JET discharges.
Tanga, A., Gowers, C.W., Hugenholtz, C.A., Morgan, P., Schueller, F.C.
Joint European Torus, JET, 1984.
10p.
Report JET-P(84)09.
 82. Thermal energy confinement scaling in PDX limiter discharges.
Thomas, P., and others.
Nuclear Fusion.
vol.24 no.10 October 1984.
pp.1303-1334.
 83. Results from ohmic heating experiments in JET.
Thomas, P.R.
American Physical Society, Bulletin Series 2.
vol.29 no.8 October 1984.

- (Abstracts of the 26th Ann. Mtg. Div. Plasma Phys., Amer. Phys. Soc., Boston, 29 October - 2 November 1984).
Paper 1A 2.
84. MHD behaviour and discharge optimization in JET.
Thomas, P.R., Wesson, J.W., Alladio, F., Bartlett, D., Behringer, K., Bickerton, R.J., Brusati, M., Campbell, D.J., Christiansen, J.P., Cordey, J.G., Costley, A.E., Crisanti, F., de Kock, L., Dietz, K.J., Dupperex, P.A., Engelhardt, W.W., Gibson, A., Gill, R.D., Gottardi, N., Gowers, C.W., Green, B.J., Hemmerich, J.L., Hugenholtz, C.A., Huguet, M., Keller, R., Krause, H., Last, J., Lazzaro, E., Mast, F.K., Morgan, P., Morris, A.W., Niedermeyer, H., Noll, P., Pick, M., Pochelon, A., Rebut, P.H., Robinson, D.C., Ross, R.T., Sadler, G., Schueller, F.C., Stringer, T.E., Summers, D., Tanga, A., Tonetti, G., van Belle, P.
Plasma Physics and Controlled Nuclear Fusion Research, 10th Int. Conf., London, 12-19 September 1984. volume 1.
Vienna, IAEA, 1985.
pp.353-361.
85. The JET magnetic diagnostic.
Tonetti, G., de Kock, L., Morris, A.W., Todd, T., Robinson, D., Fessey, J., Stevens, A., Wilson, D., Cordey, J.G., Christiansen, J., Ross, R., Pochelon, A., Duperrex, P.A., Alladio, F., Wesson, J., Crisanti, F.
American Physical Society, Bulletin.
Series 2.
vol.29 no.8 October 1984.
(Abstracts of the 26th Ann. Mtg. Div. Plasma Phys., Amer. Phys. Soc., Boston, 29 October - 2 November 1984).
Paper 5T 17.
86. Vacuum system and wall conditioning in JET.
Usselmann, E., Dietz, K.J., Hemmerich, H., Schueller, F.C., Tanga, A.
Fusion Technology 13th Symp., Varese, 24-28 September 1984.
Oxford, Pergamon, 1984.
vol.1, pp.105-117.
87. JET ICRF power plant.
Wade, T., Anderson, R., Bosia, G., Schmid, M.
Fusion Technology 13th Symp., Varese, 24-28 September 1984.
Oxford Pergamon, 1984. Vol.1, pp.727-732.
88. Impurity control studies in JET.
Watkins, M.L., Abels-Van Maanen, A.E.P.M., Düchs, D.F.
Journal of Nuclear Materials.
vol.121 May 1984.
(Procs. Symposium on Energy Removal and Particle Control in Fusion Devices, Princeton, 26-29 July 1983).
pp.429-434.
89. The JET Project and the European Fusion Research Programme.
Wüster, H-O.
Energy Options 4th Int. Conf: The role of alternatives in the world energy scene, held in London, 3-6 April 1984.
London, IEE. 1984.
p.349.
IEE Conference Publication 233.
90. The JET Project and the European Fusion Research Programme.
Wüster, H-O.
The Nuclear Engineer.
vol.25 no.3 May/June 1984.
pp.87-90.
91. The Joint European Torus.
Wüster, H-O, Maple, J.H.C.
Culham Laboratory.
Nuclear Europe.
no.12 December 1984.
pp.11-14.
92. JET magnet coil instrumentation.
Zwart, J.W., Keane, D.V., Thomsen, F.
Fusion Technology, 13th Symp., Varese, 24-28 September 1984.
Oxford, Pergamon, 1984. Vol.2, pp.1119-1124.
93. Annual Report, 1983.
Abingdon, JET Joint Undertaking, June 1984.
55p. (Kind, P.J.D., O'Hara, G.W., Eds)
94. JET Joint Undertaking Progress Report 1983.
Abingdon, EURATOM JET Joint Undertaking, 1984. (Keen, B.E., Kupschus, P.: Eds)
134p.
EUR 9472 EUR-JET-PRI.
95. JET papers presented at Int. Atomic Energy Agency 10th Int. Conf. on Plasma Physics and Controlled Nuclear Fusion Research, London, 12-19 September 1984.
EURATOM, Joint European Torus, JET, 1984.
Report JET-P(84)05.

